A physiological, microbial and transcriptomic study of peduncle necking in cut *Rosa hybrida*

A thesis submitted to the University of London for the degree of Doctor of Philosophy

Bianca Lear

Supervised by

Dr. Tony Stead (RHUL) &

Prof. Hilary Rogers (Cardiff University)

School of Biological Sciences

Royal Holloway, University of London

2020

Declaration of Authorship

I, Bianca Lear, hereby declare that this thesis and the work presented in it is entirely my own. Where I have consulted the work of others, this is always clearly stated.

Signed: Bianca Lear

Date: 20/03/2020

Abstract

Roses are one of the UKs most popular cut flower in terms of sales per stem. However, bent-neck or necking is a phenomenon often seen in cut roses, whereby the flower head droops due to a bending of the peduncle resulting in reduced vase life and postharvest loss. Necking is thought to be caused either by an air embolism or an accumulation of microorganisms at or within the stem end, blocking the xylem vessels and preventing water uptake. Although the association between bacteria and necking has been widely studied, little is known about the prevalence and impact of fungal species. Susceptibility to necking also varies between cultivars and it is unknown if there are any molecular mechanisms involved with this process. In this study, the number of bacterial and fungi present on cut Rosa hybrida stems has been analysed using petrifilm culture plates, and the species identified by 16S and ITS sequenced regions respectively. A transcriptome analysis of three stages of peduncle necking (Straight, <90° and >90°) in the necking susceptible *Rosa hybrida* cultivar H30 has also been carried out using next generation sequencing. Differential expression analysis with DESeq2 identified over 3,500 genes significantly expressed in full necking (>90°) compared to straight control peduncles (p adjust <0.05). Analysis of the differentially expressed genes has highlighted many processes and pathways associated with the necking, providing a greater understanding of this phenomenon as well as potential targets for further research.

Acknowledgements

Firstly, I would like to thank my supervisors, Tony Stead and Hilary Rogers for their continued help and support throughout the project. Including an added thank you to Hilary for her hospitality while working in Cardiff and Bedford. Thank you to my advisor Paul Devlin and my industrial supervisors Keith Richardson, Rebecca Crompton and Jason Allen, for their knowledge and guidance. Also, to Tara Wheeler for her invaluable support with all things flower related. I would also like to thank BBSRC and Flamingo flowers for funding this project.

I would like to acknowledge and thank Angela Marchbank for her work in completing the RNA sequencing and both Robert Andrews and Katherine Tansey for providing training on Unix script and use of the ARCCA (Cardiff University). I would also like to acknowledge the help of Anton Page and Catherine Griffiths at the Biomedical Imaging Unit (Southampton) for producing the sections of rose peduncles for light microscopy and for assisting with the scanning electron microscopy work. Also, thank you to Dudu tech for the use of their equipment and laboratory space during field work in Kenya.

I am grateful for the support and advice provided by my fellow PhD students, Shaoli Das Gupta, George Skinner, Stacey Vincent, Francesca Baylis, Sebastien Lambertucci and post doc Emily Bailes. With a special thank you to Lauren Edwards, Kate Orman and Matthew Casey for taking me under their wing and for all the advice and encouragement since. And to Louise Montgomery, Giles Grange and Tara O'Neil, for their support during my final year.

I would also like to extend my gratitude to members of the department who go above and beyond and have helped throughout my time as a PhD student, including Tracey Jeffreys, Michelle Jux, Lyn Samways and Pauline Baker. Also, to Heather MacDonald (UWE), who encouraged me to apply in the first place.

Finally, I am extremely grateful for the support provided by my family and by Julie. Thank you for always welcoming me home and for all the rationale discussions, hot meals and general family madness. And to my partner Ethan, for being there through it all and for believing in me even when I didn't.

Table of contents

List of figures

List of tables

List of Abbreviations

ANOVA	**An**alysis **o**f **va**riance
BLAST	**B**asic **L**ocal **A**lignment **S**earch **T**ool
cfu	**C**olony **f**orming **u**nits
CTAB	**C**etyl **T**rimethyl **A**mmonium **B**romide
cv.	**C**ultivar
DRR	**D**Nase **r**emoval **r**eagent
DW	**D**ry **w**eight
EDTA	**E**thylene**d**iamine**t**etraacetic **a**cid
FAA	**F**ormaldehyde – **A**cetic acid - **A**lcohol
FC	**F**old **c**hange
FDR	**F**alse **d**iscovery **r**ate
FW	**F**resh **w**eight
gDNA	**G**enomic **D**eoxyribo**n**ucleic **a**cid
GO	**G**ene **o**ntology
ITS	**I**nternal **t**ranscribed **s**pacer region
KEGG	**K**yoto **E**ncyclopedia of **G**enes and **G**enomes
LB	**L**uria **B**ertani (Broth)
LM	**L**ight **m**icroscopy
ME	**M**alt **e**xtract (Broth)
MS	**M**id **s**tem
NCBI	**N**ational **C**entre for **B**iotechnology **I**nformation
PAGE	**P**arametric **a**nalysis of **g**ene set **e**nrichment
PVP	**P**oly**v**inyl**p**yrrolidone
qPCR	**q**uantitative **P**olymerase **c**hain **r**eaction
rDNA	**r**ibosomal **d**eoxyribo**n**ucleic **a**cid
RFW	**R**elative **f**resh **w**eight
RNA seq.	**R**ibo**n**ucleic **a**cid **seq**uencing
RO H2O	**R**everse **o**smosis **H2O** (water)
rpm	**R**evolutions **p**er **m**inute
RT	**R**oom **t**emperature
SE	**S**tem **e**nd
SEA	**S**ingular **e**nrichment **a**nalysis
SEM	**S**canning **e**lectron **m**icroscopy
Str	**Str**aight
TBE	**T**ris-**B**orate-**E**DTA
TFs	**T**ranscription **f**actor**s**
YM	**Y**east and **m**ould (Petrifilm)

Chapter 1 Introduction

1.1 General overview

Roses have been of significant cultural importance worldwide for centuries, with their first use as ornamental cut flowers dating back to early Roman, Greek and Persian civilisations. Their symbolism and popularity continues today with roses successfully topping the UK cut flower market in terms of sales per stem; out competing other UK favourites such as tulips, chrysanthemums, gerberas, lillies, freesias and alstromeria (Bendahmane et al., 2013; Hanks, 2015). Roses therefore represent a highly valuable product for the cut flower industry, with the UK fresh cut flower and indoor plant market currently estimated to be worth around £2.2 billion and cut flowers making up almost 78% of this total value (Flowers and Plants Association, 2015). However, despite being of great cultural importance worldwide and being consistently successful within the market, roses often die prematurely during their cut life (Bendahmane et al., 2013). This not only causes dissatisfaction for the consumer but is also a wider problem faced within the industry, resulting in both waste and monetary losses.

Since energy prices have risen over the past decade, the production costs associated with heating and lighting greenhouses within the UK or the Netherlands are currently not as economically viable as they once were; unless energy saving initiatives have been implemented to save on cost (Williams, 2007). Growth of roses for the cut flower market has therefore gradually moved overseas to equatorial countries such as Kenya, Tanzania, Ecuador and Columbia; where year-round production is possible due to naturally ambient conditions and where labour is abundant and less costly (Wilson, 2015). Despite the need for shipping and air freight to transport the cut roses to market, energy consumption and CO2 emissions are thought to be reduced with growth in equatorial countries. As Dutch greenhouse emissions have been estimated to be six times higher than that of Kenyan rose farms based on the production of 12,000 cut rose stems, according to a report by Williams (2007). Kenya is currently the lead exporter of rose cut flowers to the European Union, with 70% of roses in the UK market supplied by Kenyan rose farms; with most Kenyan rose farms located around Lake Naivasha, at the foot of Mount Kenya where average annual air temperatures are 17.1 °C (Mumia, 2016; Wilson, 2015; Climate-Data.org, 2020).

Farms are also situated further up Mt. Kenya for higher altitudes, resulting in preferential growing conditions of roses with larger blooms and longer stems which may be sold at a premium price. Due to their abundance in the UK cut flower market, Kenyan grown roses are the focus of this study.

Roses or *Rosa* species belong to the family Rosaceae, a major angiosperm family estimated to be composed of 2,500 species, including important crop plants such as apples, cherries, raspberries and strawberries. The genus Rosa itself is made up of around 100 species of woody plants, with alternate and pinnately compound leaves, oval leaflets with serrated margins and usually feature variously shaped prickles on their stems (Britannica Acadamic, 2015a, 2015b). Primarily, roses are native to the temperate regions of the northern hemisphere and were first used as ornamentals. However, the modern day rose cultivars known as *Rosa hybrida* did not begin to exist until the 14th century when the native Chinese roses, including *Rosa chinensis*, the original cultivar for recurrent blooming, were brought across to Europe and extensively hybridised with the European and the Middle-Eastern roses (Bendahmane et al., 2013).

Wild roses such as *Rosa virginiana (Figure 1A)* native to eastern North America typically feature five petals organised as regular polypetalous corollas, unlike the ornamental *R.hybrida* varieties which have been selected though hybridisation to become the more familiar double-flowered form with numerous petals *(Figure 1B)*; some of which are stamens, mutated in favour of additional petals. This double-flowered trait of the modern rose however means very few varieties are naturally pollinated by insects in the way the wild types are to produce a berry-like fruit known as a hip, due to the petals remaining too tightly whorled for insects to gain necessary access to the reproductive organs (Bendahmane et al., 2013; Dubois et al., 2010).

Figure 1. Contrast in typical flower form between a wild rose and a hybrid rose bred for ornamental purposes. A, Wild rose Rosa virginiana, five petals in a simple flower arrangement *(Gardinia.net, 2020). B, Hybrid rose* Rosa hybrida, *double-flowered with numerous petals.*

Despite this apparent wide genetic origin, of the 200 species that existed, only 8-20 species are likely to have contributed to the modern day *R. hybrida* cultivars; with the majority having strong genetic similarity to *R. chinensis*, due to backcrossing in the generation of new varieties (Bendahmane et al., 2013; Martin et al., 2001). Modern day varieties are selected for a number of reasons including appearance factors such as colour, bloom size, stem length and number of petals, as well as a number of economic factors including ease of growth, yield and recurrent blooming, disease resistance and vase life (Martin et al., 2001).

The vase life of a cut flower refers to the amount of time (days) a flower remains of acceptable ornamental value after being placed in a vase (Fanourakis et al., 2013). The end of vase life (termination) of a cut rose may occur due to several factors including visible infection (e.g. by *botrytis cinerea*), colour change of the petals, wilting or bending of the peduncle (van Meeteren et al., 2015). Of these symptoms, bending of the peduncle, referred to as ‘bent neck’ or ‘necking’ is the cause of interest within this study. As stems exhibiting water stress symptoms including necking and wilting are often the first to be deemed terminated, making it a primary cause of reduced vase life for cut roses (Robinson et al., 2007; de Witte & van Doorn, 1988; Woltering & Paillart, 2018).

Necking of rose stems is thought to be a consequence of vascular occlusion (blockage), resulting in reduced water uptake in the stem (Bleeksma & van Doorn, 2003; de Witte & van Doorn, 1988; van Doorn, 1997; Damunupola & Joyce,

2008). Vascular occlusions can be caused solely by air embolisms, introduced through cutting the stem, or also by microbial cells. Microbial occlusions are generally associated with bacteria, whereby an accumulation of bacterial colonies at the stem end or in the vase water cause a blockage of the xylem and result in an embolism within the stem. Reduced water uptake in the stem due to an air embolism or microbial occlusion disrupts the water relations within the stem, resulting in bending of the peduncle (Bleeksma & van Doorn, 2003; Damunupola & Joyce, 2008).

Although the association between microbial contamination and necking is widely accepted, there is still considerable variation in occurrence between rose cultivars and in individual stems (Bleeksma & van Doorn, 2003). Current knowledge on the causes of reduced vase life and factors affecting the occurrence of necking in cut roses, including variances in rose physiology, microbial contamination, biocidal treatments and the potential role of molecular mechanisms will therefore be covered.

1.2 Physiological aspects of necking

1.2.1 Growth conditions

Relative air humidity during growth has been found to effect the vase life of some rose cultivars; with the cultivar Pink Prophyta shown to have a reduced vase life of up to an 80 % when grown at a high relative air humidity of 95 %, in comparison to a moderate relative humidity of 60 % due to a low evaporative demand (Fanourakis et al., 2012). This reduction in vase life is thought to be due to stomata remaining more open when grown at high humidity compared to moderate humidity, resulting in a higher rate of transpiration and increased water loss. Therefore, making the cut flower much more susceptible to wilting and necking in the event of a vascular occlusion or reduced water uptake (Fanourakis et al., 2012). Increases in relative air humidity may occur during cold, wet (winter) seasons or potentially due to dense rose canopies (Fanourakis et al., 2015). Increased day length with supplemental lighting can increase duration of stomatal opening post-harvest, also leading to an increase in water loss and a shorter vase life of 4- 47 % depending on cultivar (Slootweg & van Meeteren, 1991; Mortensen

& Gislerød, 1999; Fanourakis et al., 2015). However, supplemental lighting practices are not known to be practiced on Kenyan rose farms, therefore day length is unlikely to be a contributing factor for Kenyan grown roses.

1.2.2 Post-harvest conditions

Roses are currently packed dry and leave Kenya via regular flights direct from Nairobi airport to various UK destinations. From here they are transported to storage warehouses to be sorted, bunched and rehydrated before being distributed out to stores where they may be purchased by consumers. The journey and time spent before the in store and consumer stage is of vital importance to ensure the best quality is supplied and guaranteed to the customer, as any days added on during transportation will result in fewer days of consumer enjoyment and satisfaction. However, the minimum amount of time between harvest in Kenya and purchase by the consumer is approximately 8 days (*Figure 2*). Roses are then expected to last a further 7 days in order to meet vase life guarantees. Careful handling during this post-harvest phase can dramatically impact resulting vase life and the occurrence of necking.

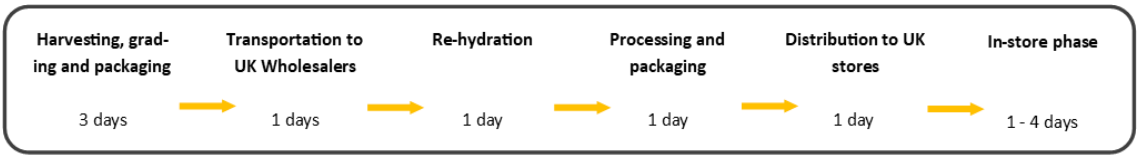

Figure 2. Outline of the Kenyan supply chain, from harvest to consumer. Amount of time at each stage is the expected duration and may be longer depending on season and demand.

Dry storage of roses is necessary for air freight and has been shown to limit the amount of bacterial growth within the stems and increased vase life compared to wet storage (van Doorn & de Witte, 1991b). During storage, roses should optimally be kept below 5°C and as close to 0°C as possible to both reduce the rate of respiration of the flowering stems and the amount of microbial growth on and within the cut surface of the stem (van Doorn & de Witte, 1991b; Zagory, 1999; Reid, 2001). Temperature fluctuations during air freight are therefore a major cause of reduced vase life, with boxes of roses often left out in the sun prior to being loaded onto the planes; increasing temperatures within the stack

(Zagory, 1999). Increased temperatures during dry transport can lead to increased losses in fresh weight and reduced stomatal function, both of which may lead to increased water stress and be detrimental to flower longevity (Cevallos & Reid, 2001). Although increased temperatures are detrimental to cut roses during dry storage, cut roses may also be negatively affected by long term cold storage. As some cultivars can similarly loose stomatal functionality following extended periods of cold storage (Woltering & Paillart, 2018). However, long term cold storage is often necessary surrounding peak seasons such as Valentines day and Mothers day in order for wholesalers to provide enough stock to meet increased demands.

'Pregnant' boxes due to roses being packed too tightly for transportation and a lack of careful handling of flowers throughout the supply chain are both potential sources of physical damage to cut rose flowers (Staby, 2015). Mechanical stress can also be incurred by vibrations during transportation, with the amount of damage and reductions to vase life shown to be cultivar dependent (Pouri et al., 2017). Cutting, de-leafing or physical processes postharvest that cause wounding can all result in air embolisms within the stem and therefore an increased occurrence of necking and water stress symptoms (van Doorn & Perik, 1990). Wounding can also increase the production and release of plant hormones such as ethylene and polyphenols which have a further negative impact on vase life (Woltering, 1987). The use of a blunt blades during the supply chain has been shown to reduce the life of fresh cut produce (Zagory, 1999). Regular blade changes or sharpening of blades used to cut rose stems can therefore reduce physical damage to cut roses and potentially increase vase life. However, practices such as thorn removal are still likely to be highly detrimental due to causing damage to the whole stem length rather than just the stem end. Wounded plant tissue often also leads to increased growth of opportunistic microorganisms which can also negatively impact vase life and occurrence of necking (Woltering, 1987; Zagory, 1999).

1.2.3 Peduncle architecture

Peduncles are located between the receptacle and the upper most internode of an inflorescence stem (Andre, 2003). As shown in *Figure 3* peduncles do not

contain secondary conductive tissue (secondary xylem or phloem), with secondary conductive tissue ending at the transition point between the stem and the peduncle, defined by an abscission zone (*Figure 4*). Primary xylem also change in morphology across the abscission zone, causing a point of reduced hydraulic conductance in inflorescence stems (Andre, 2003; Chimonidou, 2003). Reduced hydraulic conductance across the abscission zone is thought to induce cavitation in the peduncle, limiting water flow to the flower head in times of water stress in order to reduce water loss and maintain water supply to the main axis of the plant (Chimonidou, 2003; Darlington & Dixon, 1991). Due to a lack of secondary growth, the peduncle is also less lignified than the rest of the stem and is therefore a point of reduced strength (Parups & Voisy, 1976)

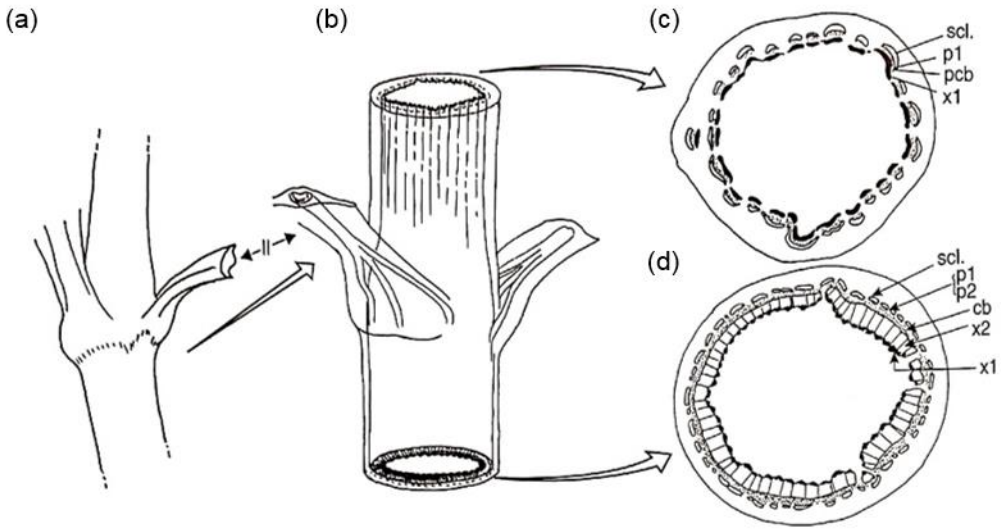

Figure 3. Rose peduncle anatomy. The floral peduncle (a,b) and transverse sections of the peduncle (c) and the stem under the last leaves (d). II, last leaves; scl., pericyclic sclerenchyma; p1, primary phloem; p2, secondary phloem; pcb, procambium; cb, cambium; x1, primary xylem; x2, secondary xylem. Figure adapted from André, (2003)

Figure 4. Abscission zone (AZ) between stem (ST) and peduncle (PD). Figure reproduced from Chimonidou, (2003).

Rose stems are harvested between stage one and two of bud development, depending on cultivar and retailer specifications (*Figure 5*). Flowers are cut at these stages to prevent petal damage during transport and are not cut at an earlier stage as this can result in improper flower development and a lack of opening post-harvest (van Doorn, 1997). However, peduncle development and strength coincide with flower bud development, therefore harvesting of stems at an earlier stage can also result in reduced strength and increased incidence of peduncle bending (Zieslin et al., 1989).

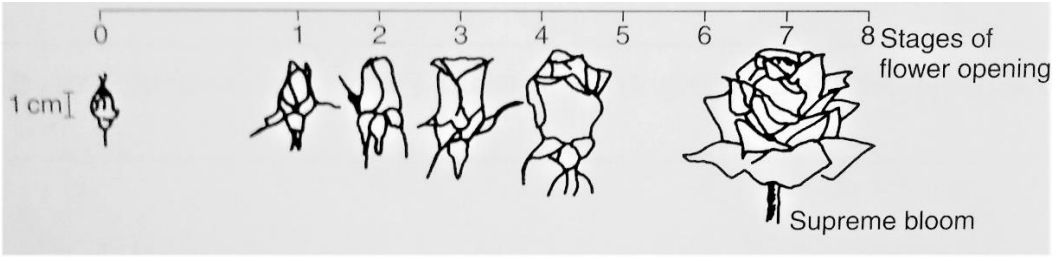

Figure 5. Stages of R. hybrida *flower opening and development. Adapted from Berkholst, (1980).*

1.3 Microbial load and the effect on cut rose vase life

1.3.1 Bacteria and fungi

Bacterial contamination is currently thought to be the main source of vase water contamination and a major cause of reduced vase life amongst cut flowers; thought to affect not only roses but also Carnations, Delphinium, Alstromeria and Orchids to name a few (van Doorn et al., 1995; Song et al., 1995; Jowkar, 2015; Rahman et al., 2014). Arnold (1930) is thought to be one of the first to associate a reduction of water uptake in cut flowers with a potential bacterial blockage (van Doorn, 1997). Many studies since have determined the amount of contamination needed to cause such an effect, however recorded amounts range from 10^5 colony forming units (cfu) mL^{-1} (Zagory & Reid, 1986; Laird et al., 2005) to usually between 10^7 cfu mL^{-1} and 10^8 cfu mL^{-1} (Put & Jansen, 1989; Clerkx et al., 1989; Bleeksma & van Doorn, 2003; van Doorn et al., 1986).

Species of bacteria currently identified from the stem ends and vase water of cut roses include those listed in *Table 1* (Put, 1990; de Witte & van Doorn, 1988; van Doorn et al., 1991a). *Bacilllus* and *Enterobacter* species are thought to be the predominant bacteria on freshly harvested rose stems (Put & Jansen, 1989). However, *Pseudomonas* species are often found to soon become the most prevalent genera in vase water due to their high reproductive rate within the vase environment (Put & Jansen, 1989), with *Pseudomonas* populations accounting for 74% of the total bacterial population on day one, and increasing to 83% by day seven. In contrast, populations of *Enterobacter* species have been shown to decrease from 8% on day one to undetectable by day seven (van Doorn et al., 1991a). Due to their prevalence, many papers have carried out studies using single *Pseudomonas* species and have monitored specific effects such as the occurrence of embolisms in the stems (Bleeksma & van Doorn, 2003; Robinson et al., 2007).

Table 1. Bacterial species identified from cut cv. 'Sonia' roses during vase life

	Put (1990)	de Witte & van Doorn (1988)	van Doorn *et al.* (1991)
Gram-negative rods			
Aeromonas species	-	-	+
Acinetobacter species	-	-	+
Alcaligens species	+	+	+
Citrobacter freundii	+	-	+
Citrobacter amalonaticus	+	-	-
Enterobacter:			
E. agglomerans	+	-	+
E. cloacae	+	-	-
Flavobacterium species	+	-	+
Pseudomonas:			
P. aeruginosa	-	+	+
P. cepacia	-	+	+
P. fluorescens	+	-	+
P. maltophilia	+	+	+
P. mendocina	-	-	+
P. pikettii	-	-	+
P. putida	+	+	+
P. putrefaciens	+	-	-
P. stutzeri	-	+	+
P. vesicularis	-	+	+
Gram-positive rods			
Bacillus:			+
B. cereus	+	-	*
B. licheniformis	+	-	*
B. polymyxa	+	-	*
B. subtilis	+	-	*
Corynebacteria	+	-	-

Although all fresh produce is covered in a characteristic mix of bacteria and fungi, only a few studies have focused on the prevalence and impact of fungi on cut roses compared to bacteria (Zagory, 1999). Yet, it has been found by Zagory and Reid (1986) that an unidentified yeast isolated from the vase water of a carnation had the greatest mean reduction in vase life of cv. 'Cara Mia' roses, compared to three *Pseudomonas* species. The unidentified yeast species was even found have a greater effect on vase life at 10^3 cfu ml^{-1} compared to a *Pseudomonas* species at 10^6 cfu ml^{-1}.

Put (1990) and Muñoz et al. (2019) have both identified species of fungi from the vase water of cut rose flowers, however little cross over was found between the two studies (Table 2). This is likely due to one study having been conducted on roses grown in the Netherlands and one on roses grown in Colombia, with sampling taken following transport by sea freight. The difference in species found therefore highlights the need for a study specifically on the microflora associated with Kenyan grown roses, to further understand the factors associated with necking in Kenyan grown commercial varieties.

Table 2. Fungal species identified from cut roses

Fungal *(Genus / species)*	Put (1990)	Munoz et al. (2019)
Alternaria alternata	-	+
Aspergillus brasiliensis	-	+
Bipolaris sorokiniana (Formerly *Drechslera)*	+	-
Botrytis:		
B. cinerea	+	+
*B. species**	+	-
*Candida species**	+	-
Cladosporium cladosporioides	+	+
*Diplodia species**	-	+
Epicoccum nigrum	-	+
Fusarium:		
F. oxysporum	+	-
F. solani	+	-
Mucor hiemalis	+	-
Penicillium:		
P. brevicompactum	+	-
P. purpurgenum	+	-
P. citrinum	-	+
Rhizopus:		
R. stolonifer	+	-
*R. species**	+	-
Rhodotorula rubra	+	-
Saccharomyces	+	-
Trichoderma pseudokoningii	+	-
Verticillium brevicompactum	+	-

Scanning electron microcopy studies have shown microbial growth to be primarily on the cut surface of the stem end and reduce water uptake by blocking the xylem vessel entrances (Put & Clerkx, 1988). Microbial cells have also been found to enter the vascular tissue and travel up the stem, however the number of microbial cells found greatly reduces with distance from the cut surface. Infiltration ability is dependent on the size and shape of the cells as well as the width and length of the xylem vessels, with distance thought to be restricted to the maximum length of any cut vessel (Put & van der Meyden 1988).

1.3.2 Extracellular polysaccharides and debris

Heat-inactivated bacterial cells have been shown to evidently reduce vase life but with a lesser effect than viable cells, suggesting that the size and shape of the microbial cells and vascular plugging is not the sole cause of decreased water conductivity in the stem segments of the roses (Put & Jansen, 1989). Many bacterial species are also known to produce a ‘slime’ made up of extracellular polysaccharides; these are thought to aid with the adhesion of bacteria to xylem vessels, seen as a layer of amorphous material, but may also be secreted into the surrounding medium and reduce conductance (Van Doorn et al, 1990). Put and Rombouts (1989) found that the addition of these microbial polysaccharides above a molecular weight of 10 000 into the vase water resulted in the total blockage of the xylem vessels causing necking to occur within 24 hrs. Low hydraulic conductance in cut rose stems has also been induced by the addition (1-10 g per litre) of protein (ovalbumin) with a size of 50 kD. Addition of any globular molecule over 50 kD was therefore hypothesized to potentially cause blockages in the pores of vessel walls and therefore may result in necking (van Doorn, 1989). Lysed particles of bacterial cells have also been shown to reduce hydraulic conductance to a greater extent than non-lysed bacteria (van Doorn & de Witte, 1991a). Thus, the effects are thought to be physical rather than due to a biological interaction between bacterium and plant.

1.3.3 Sources of microbial load

The bacterial and fungal species identified in Table 1 and Table 2 may be naturally prevalent on the rose stems themselves, or introduced onto the stem or into the vase water environment from other sources throughout the supply chain such as cutting or de-leafing equipment, holding containers (i.e. bucket or vase), tap water, other cut flowers or from human contact (Florack et al., 1996; van Doorn & de Witte, 1997). In order to reduce the occurrence of necking, care should therefore be taken throughout the supply chain to minimise the microbial load associated with the cut flower. As indicated previously, poor temperature management and increased wounding can also both lead to increased microbial growth on the stem (Cevallos & Reid, 2001; Woltering 1987).

1.3.4 Antimicrobial solutions

The main flower food companies currently operating in the European market include Chrysal, Floralife and Vaselife. Each of these companies have a range of products specific for each of the stages throughout the supply chain, from grower to consumer in order to control microbial growth and increase cut flower longevity. Hydration solutions primarily used following harvest or after periods of dry storage (i.e. following long distance transportation), would normally contain a biocide, a buffer to adjust (lower) pH and a wetting agent (surfactant) to increase water uptake and hydrate the cut flower more effectively. Flower foods on the other hand also have the addition of a sugar to maintain and replenish the carbohydrate content of the cut flower for increased vase life (Nell et al., 2006). Flower foods composition varies depending on the supply chain stage. Low-dose flower foods called holding solutions are added to holding containers (buckets) at the end of cut flower production lines for transport and use within supermarkets. Whereas full-dose flower foods are supplied to consumers in the form of the flower food sachets, usually attached to bunches for home use within the vase water (Nell et al., 2006).

Silver nitrate, silver thiosulphate, aluminium sulphate and hydroxyquinoline have all been used commercially in preservative formulations due to their antimicrobial activity (Thwala et al., 2013; van Doorn et al., 1990a; van Doorn, 1997). However,

many of these treatments may be persistent and hazardous to the environment due to their heavy metal content (Damunupola & Joyce, 2008). More environmentally friendly options include citric acid as an acidifier and sodium hypochlorite as a chlorinating agent (Jowkar, 2015). Chemical alternatives such as antibacterial peptides have also been studied, including peptides cecropin B, hordothionin and tachyplesin I. These have all shown promising results in reducing bacterial counts in rose vase life trials, with Tachyplesin I shown to be highly toxic to a range of bacteria and Cecropin B and hordothionin both found to inhibit the growth of bacteria, with an additive antibacterial effect when applied together (Florack et al., 1996). The antimicrobial properties of essential oils are also well known and extracts from *Mentha pulegium*, *Jatropha curcas*, *Psidium guajava* and *Andrographis paniculata* have been tested as potential vase water biocides with some promising results (Hashemabadi et al., 2014; Rahman et al., 2014). An essential oil biocidal product derived from species in the Lamiaceae (mint) family including thyme is also currently in the patenting process and has been shown to reduce *botrytis cinerea* infection in cut roses. If approved this product may also have potential applications in reducing the microbial load on flower stems prior to and during vase life (Gianfagna et al., 2015).

Although it can be hypothesised that a decrease in microbial load will reduce the occurrence of necking, this is often not stated and studies such as Florack et al. (1996) and van Doorn and Perik (1990) do not conclude if the biocide being studied effectively increases vase life as well as reducing contamination. This is important as often if the biocide is potent enough to have an effect on the microorganisms present, may also have a phytotoxic effect on the living cut flower; therefore even if all contamination is eliminated from the vase water, the vase life may not be extended due to other symptoms of senescence (Damunupola & Joyce, 2008). For example, a low pH of 3.0 can reduce bacterial replication and growth and may also inhibit the enzymes involved in the deposition of lignin and suberin at the cut surface that are thought to cause reduced hydraulic conductance (van Doorn & Perik, 1990). However, a low pH will also likely inhibit other cellular processes and can cause a discolouration of the petals and a lack of floral development due to a change in vacuolar pH, therefore resulting in an overall reduced vase life (Bendahmane et al., 2013).

1.4 Molecular mechanisms involved in the necking process?

Although necking is generally associated with a reduced water uptake, it is unknown if any molecular mechanisms are involved with the necking process. RNA sequencing provides a snapshot view of the presence and quantity of RNA within a sample and can be used to analyse differences in gene expression. As necking is thought to be water stress related, genes associated with water stress may be up-regulated within the peduncle during necking. Stress responses such as water stress can also induce senescence, therefore it may be hypothesised that senescence related gene may also be found within the peduncle.

1.5 Summary

Despite the use of biocides to reduce microbial load, necking continues to occur post-harvest and cause significant post-harvest losses for industry. For industry relevant data, more needs to be known about roses produced in the Kenya as so far most studies have been conducted in the Netherlands, on roses grown in the Netherlands. Little is therefore known about the microbial load associated with roses produced through the Kenya supply chain or the necking susceptibility of Kenyan grown cultivars.

Although much research has focused on the microbial and physiological aspects of necking, it still also remains unclear if there are any molecular processes associated with the phenomenon.

1.6 Aims

1) To identify potential differences in susceptibility to peduncle necking in Kenyan grown *Rosa hybrida* cultivars.
2) To study the possible physiological factors contributing to the necking phenomenon in Kenyan grown cut *Rosa hybrida* stems.
3) To determine the prevalence of fungi on *Rosa hybrida* stems throughout the cut flower supply chain and their potential role in the vase water environment.

4) To explore the potential molecular mechanisms underlying necking in *Rosa hybrida* stems through the use of next generation sequencing.

Chapter 2 General Methods

2.1 Flower material

All *Rosa hybrida* stems used in this project were provided by Flamingo Flower Ltd. Stems were grown at an altitude of 2000 m on commercial flower farms in Naivasha, 47 miles North West of Nairobi (Kenya) with an average annual air temperature of 17 °C ± 1.4 °C dependent on month due to the equatorial location (Climate-Data.org, 2020). Roses were grown under polythene greenhouses, in raised beds for controlled watering and fertilisation (*Figure 6*).

Figure 6. Image of Rosa hybrida cv. Fuchsiana greenhouse in Naivasha, Kenya

2.1.1 Harvest and transport to UK

Harvested stems were bunched and packed on site and transported dry via refrigerated lorry to Nairobi International Airport for air freight transport to the UK. Stems were then collected from the Flamingo Flowers warehouse in Sandy and transported dry to RHUL.

2.1.2 Storage and handling

Upon arrival at RHUL, all stems were cut using a razor blade, removing the bottom 2 cm and placed in buckets containing 2 litres of tap water. Buckets were sprayed with Distel disinfectant (1:10), rinsed and then washed with washing up liquid prior to use. Any foliage showing obvious damage or sitting below the water line was removed. Bunches were separated into buckets by cultivar and kept in the dark at 5˚C overnight to re-hydrate. After re-hydration, stems were re-cut using a razor blade to 47 cm in length and any foliage on the lower 20 cm of each stem was removed. Razor blades were wiped clean with Distel disinfectant (1:10) between stems to prevent microbial contamination.

2.2 Vase life conditions

Vase conditions varied depending on experiment, with stems either being placed in 1 litre of tap water in clear glass vases as bunches (10 stems) or individually in 100ml of tap water in clear glass milk bottles. In addition to tap water, commercial rose flower food (Chrysal) at the manufacturers recommended concentration or a 2% sucrose solution (w/v) were used for vase water conditions, both made up just prior to use with tap water. A 2% sucrose solution was used for experimentation due to being in-line with the final concentration of flower food solutions, minus the biocidal chemicals and other variable additives dependent on brand and product (personal communication, Tony Stead). Stems were kept at a constant temperature of 21 ˚C for the duration of vase life, with a 12 hr light cycle of 15-20 µmol m^{-2} sec^{-1} from cool white fluorescent tubes. Vases were arranged on benches in a completely randomised design and re-ordered every few days to reduce the effect of placement within the vase life room.

2.2.1 Determination of vase life termination factors

Vase-life was determined as the time from being placed in the vase until a termination factor was reached. Termination factors included: bending of the peduncle, petal abscission, visible infection, visible colour change (blueing or browning) and wilting. A visual guide to the terminating factors is shown below (*Figure 7*).

Figure 7. Terminating factors of vase life. a) Necking, ≥90˚; b) visible infection on ≥ one whole petal; c) visible colour change, shown as blueing in example and d) petal wilting.

2.3 Enumeration of bacteria and fungi by dry medium culture plate method

Dry medium culture plates are a compact and convenient plating method for counting microorganisms compared to conventional agar plates. They consist of nutrients and a cold-water-soluble gelling agent which forms a gel plate with the addition of a water sample. The 3M Petrifilm dry medium plates were used, as they contain an additional activity indicator dye for improved counting, and due to their efficiency and ease of use by industry (T. Wheeler, Flamingo Horticulture pers com., 2016). Enumeration via Petrifilm plates are an accepted alternative to standard agar plating methods and have been shown to be as sensitive when compared (Nero et al., 2006; Kudaka et al., 2010) and have so far been awarded the Official Methods of Analysis (OMA) for food (#997.02).

2.3.1 Collection and preparation of sample material

Water and stem samples were collected in sterile 15 ml Falcon tubes. Water samples (2 ml) were collected using a 1000 µl pipette and sterile pipette tips and

2 cm stem samples were cut using a Distel (1:10) disinfected razor blade. The stem samples were immersed in 4 ml of autoclaved physiological saline (0.85 % NaCl), adjusted to pH 7.4 with HCl or NaOH. Tubes were then pulse vortexed for 10 seconds, mixed via inversion and left to incubate for 15 minutes at RT. Samples collected from different methods were either used neat or diluted using autoclaved physiological saline, pH 7.4 through a 1/10 serial dilution series (dilution dependent on sample type).

2.3.2 Aerobic and Yeast and Mould (YM) Petrifilm plating and incubation

The Petrifilm aerobic count plates (3M) and the Petrifilm yeast and mould (YM) count plates (3M) were prepared following the manufacturer's guidelines. The sample (1000 µl) was transferred to the centre of the bottom film, covered with the top film and then evenly spread using the provided plate spreader (*Figure 8*). Aerobic plates were incubated at 25 °C for 2-3 days and the YM plates were incubated at 21 °C for 5 days. All plates were left to firm for 5 minutes after preparation, before being placed into stacks of no more than 15 for incubation.

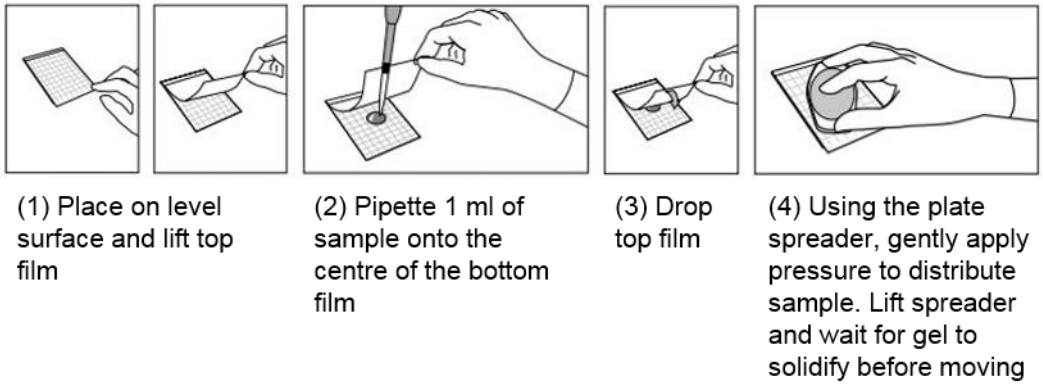

Figure 8. Petrifilm inoculation guide. (Adapted from the 3M Petrifilm interpretation guide, 2017)

2.3.3 Analysis of Aerobic and YM Petrifilms

The aerobic Petrifilms contain a red tetrazolium indicator to facilitate enumeration, and all red colonies were counted regardless of size and intensity as described in the manufacturer's instructions and interpretation guide. For

colony counts exceeding 300, two representative squares (1 cm^2) of the 20 cm^2 growth area were counted, averaged and multiplied by 20 to provide an estimated plate count. Plates were deemed too numerous to count (TNTC) when the whole growth area appeared red or pink in colour or a red ring of small colonies could be seen around the perimeter of the growth area, indicating a higher dilution was needed. A few species of bacteria can re-liquefy the gelling agent in the plates, if this occurred, an estimated count was taken using unaffected squares when possible.

YM Petrifilms contain a blue phosphatase indicator dye to aid counting, and antibiotics to prevent the growth of bacterial colonies. Colony counts for YM Petrifilms were determined using the manufacturer's interpretation guide, with yeast and mould differentiated using the characteristic guide (*Table 3*).

Table 3. Yeast and mould colony characteristics

Yeast	**Mould**
Small colonies	Large colonies
Colonies have defined edges	Colonies have diffuse edges
Pink-tan to blue-green in colour	Variable colour
Colonies appear raised	Colonies appear flat
Colonies have uniform colour	Colonies have a dark centre

(Table adapted from the 3M Petrifilm Product Instructions for Yeast and Mold Count Plate, issue date 09-2015)

Plates were observed at day 3 and day 5 to prevent mis-interpretation due to fast growing colonies. For counts exceeding 150, two 1 cm squares of the 30 cm^2 growth area were counted, averaged and multiplied by 30 to provide an estimated plate count. YM Petrifilms were deemed TNTC when the whole growth area appeared blue-green in colour or when an accurate count could not be achieved.

Both the aerobic and YM Petrifilm counts were carried out using a Wild Heerbrugg M8 (Switzerland) observation microscope with 1x or 2.6x magnification, and a Schott KL 1500-T (Germany) fibre optic gooseneck external light source.

2.4 RNA extraction

High quality RNA is necessary for successful use in sensitive downstream processes such as reverse transcription polymerase chain reaction (RT-PCR) and RNA sequencing (RNA-seq). *Rosa hybrida* however, are recalcitrant woody plants, therefore the isolation of pure RNA is made more difficult due to high amounts of polyphenols and polysaccharides; which are known to bind to and co-precipitate with the RNA, causing large amounts of contamination in the final extracts (Moazzam Jazi et al., 2015; Dash, 2013). Quick, silicon column-based methods are preferable due to their efficiency, however they provided inadequate quantity and quality RNA from rose tissue. A protocol based on the extraction method devised by Moazzam Jazi et al. (2015) was therefore used, with a buffer modified from Chang et al. (1993).

2.4.1 Extraction buffer

The RNA extraction buffer composed of 100 mM Tris-HCl (pH 8.0), 25 mM EDTA (pH 8.0), 2 M NaCl, 2 % CTAB (w/v), 2 % PVP (w/v) and 4 % β-mercaptoethanol (added just prior to use). Made up to volume with autoclaved reverse osmosis water (RO H20). (Moazzam Jazi et al., 2015)

2.4.2 Protocol

Roughly 200 mg of plant material was ground to a fine powder using liquid nitrogen and an autoclaved pestle and mortar. For each sample, 50 mg of ground plant material was transferred into 2.5 ml Eppendorf tubes containing 1 ml of buffer and homogenised using a vortex for 40 seconds. Samples were incubated for 35 minutes at 65 ˚C in a dry bath and mixed by inverting every 7 minutes. Following incubation, 1 ml of chloroform:isoamylalcohol (24:1) was added, mixed by inverting and incubated at RT for 15 minutes with gentle shaking. Samples were centrifuged at 5500 g for 20 minutes in a cooled microcentrifuge set to 4 ˚C.

The supernatant was transferred to a new tube and a second extraction with chloroform:isoamylalcohol (24:1) was performed. After transferring the supernatant to a new tube once more, equal volumes of 5 M NaCl and chilled isopropanol were added and mixed by inverting. The samples were then chilled at -20 ˚C for at least 2 hours, or alternatively at -80 ˚C for between 30 and 40 minutes or overnight at 4 ˚C. The samples were then centrifuged at 17000 g for 35 minutes at 4 ˚C and without disrupting the pellet, the supernatant was removed and discarded. The pellet was re-suspended in 125 µl of autoclaved RO H2O and 30 µl of 12 M LiCl added before once more either being chilled at -20 ˚C for at least 2 hours, or alternatively at -80 ˚C for between 30 and 40 minutes or overnight at 4 ˚C. The samples were centrifuged at 12000g for 15 minutes at 4 ˚C, followed by the removal of the supernatant. The remaining pellet was washed with 5 M NaCl, vortexed for 15 to 30 seconds and centrifuged at 15000 g for 10 minutes at 4 ˚C. The supernatant was once more removed and the pellet washed in chilled 70 % ethanol (volume dependant on size of pellet), vortexed for 15 to 30 seconds and centrifuged for a final time at 15000 g for 10 minutes at 4 ˚C. The pellet was then left to air dry for 5 to 10 minutes before being re-suspended in 40 µl of RNase free water.

2.4.3 Quality control

RNA samples were analysed using a Nanodrop spectrophotometer (Thermo Scientific, Wilmington, USA) to determine the purity and quantity of the extraction. The absorbance of 2 µl of extract was measured at 260 nm for nucleic acids, with an A260/280 nm ratio and an A260/230 of over 2 and 1.8 respectively indicating a pure RNA sample, free from protein and organic contamination. A concentration over 50 ng/µL was also required for downstream processes.

2.5 Statistical analysis

All statistical analysis was completed using R software v3.6.1 (R Core Team, 2019) with R studio v1.2.5001 (RStudio Team, 2019) unless otherwise stated. Using R packages dplyr v0.8.3 (Wickham et al., 2019), car v3.0-6 (Fox & Weisberg, 2019), ggpubr v0.2.3 (Kassambara, 2019), lme4 v1.1-23 (Bates et al.,

2015), lmerTest v3.1-2 (Kuznetsova et al., 2017) and ordinal v2019-12-10 (Christensen, 2019). Data was assessed for normality both visually with a histogram and qqplot, and statistically with a Shapiro-Wilk test for normality ($p>0.05$). ANOVA analysis were further assessed visually with a homogeneity of variance plot (residuals versus fits plot) and with a normality plot of residuals and statistically with a Levene's test for homogeneity ($p>0.05$) and a Shapiro-Wilk test of residuals ($p>0.05$) to ensure assumptions were met. Homogeneity in variance was also assessed prior to un-paired two sample t-tests using an F test ($p>0.05$).

Chapter 3 Physiological factors contributing to necking in cut *Rosa hybrida*

3.1 Introduction

Cut roses bought in the UK and the Netherlands are often supplied with a vase life guarantee of seven days from purchase date (Innovative fresh, 2017). However, cut roses may become visually unattractive and die prematurely within this period due to a number of terminating factors including wilting, browning or blueing of the petals, petal abscission, visible infection or bending of the peduncle (necking) (Put & Jansen, 1989). Necking is thought to be caused by an air embolism or a microbial blockage of the xylem, preventing water uptake and is a number one cause of postharvest loss for cut roses. Terminating factors associated with water stress including wilting and necking of the peduncle are also often the first to appear during vase life and are therefore a huge issue for the cut flower industry (Robinson et al., 2007; de Witte & van Doorn, 1988; Woltering & Paillart, 2018). However, vase life and occurrence of terminating factors such as necking varies amongst *Rosa hybrida* cultivars and is affected by a number of environmental factors and post-harvest conditions (Fanourakis et al., 2013).

Physiological factors affecting the vase life of *R. hybrida* cultivars and occurrence of necking have previously been covered in *Section 1.2* and include variations in pre- and post- harvest conditions such as light, air humidity, temperature, nutrition, CO_2 and post-harvest handling (Fanourakis et al., 2013). Many of which affect stomatal function and therefore water relations in the stem post-harvest. Water balance i.e. the amount of water being uptaken by the stem in relation to the amount lost via transpiration, is an important factor in determining vase life and the occurrence of necking (Graf et al, 2009; Matsushima et al., 2010). Although dry storage is necessary for air freight transport and has been shown to be beneficial for longer periods of storage compared to wet storage in terms of vase life. Dry storage of stems can result in a loss of fresh weight and altered water up-take ability upon rehydration (Ahmad et al., 2012).

In order to study necking, susceptible and non- susceptible cultivars were identified. A comparative vase life study of Kenyan grown *R. hybrida* cultivars was therefore conducted to identify suitable cultivars for further study. Due to the differential effects of growing conditions on vase life and necking, all cultivars

selected were supplied by the same farm in Kenya. Rehydration ability and water balance were also analysed in relation to vase life and termination factors and will be discussed.

Water balance as well as the development of vascular bundles, thickness of the epidermis and cell wall structure and composition all contribute to stem strength in *Rosa hybrida* cut flowers (Chabbert et al., 1993; Graf et al., 2006; Matsushima et al., 2012; Matsushima et al., 2010; Zamski et al., 1991). Cultivar variation in susceptibility to necking is thought to be related to differences in mechanical stem strength, with increased mechanical strength shown to increase resistance to peduncle necking. Disruptions to water balance during vase life and loss of turgor pressure in the peduncle results in a reliance on stem architecture to remain in an upright position; peduncle lignification, number of phloem fibres and presence of interfascicular cambium have all been found to vary in relation to peduncle strength (Zamski et al., 1991; Chabbert et al., 1993). Factors which increase mechanical strength can also help maintain water balance, with thickness of the epidermal layer or cuticle thought to both increase structural support and reduce transpiration (Matsushima et al., 2010). Differences in these factors has been shown to naturally vary between cultivars but they are also dependent on stem tissue development, with stem developmental stage shown to vary between cultivars at the point of harvest (Matsushima et al., 2010; Graf et al., 2006; Matsushima et al., 2012). Stem strength was therefore analysed in both a necking susceptible and a necking resistant *R. hybrida* cultivar chosen for further study. A two-point cantilever bend test to assess bending strength of the peduncles was employed (Shah et al., 2017). As stem strength is closely related to the water status of the peduncle, relative water contents of stems at three stages of necking was also compared to determine if there is an identifiable relationship between water content and the occurrence of necking.

As variations in stem architecture have been found to relate to peduncle strength, microscopical analysis of *R. hybrida* peduncles has previously focused on differences in stem structure between *R. hybrida* cultivars of differing susceptibility to necking. Including the use of synchrotron X-ray computed tomography (SXCT) to study stem micro anatomy (Herppich et al., 2015).

However, it is believed that no previous studies have analysed *R. hybrida* peduncles exhibiting the necking process. Microscopy analysis of peduncles at distinct stages of necking was therefore completed to analyse potential differences in anatomy between necking and straight (control) peduncles of the same cultivar.

3.2 Methods

3.2.1 Preliminary Rosa hybrida *cultivar comparison of water uptake, termination factors and suitability for further study*

3.2.1.1 Flower material and vase set up

Three (10 stem) bunches of *Rosa hybrida* cv. Akito, Furiosa, Fuchsiana, H30, Topsun and Tropical Amazon (*Figure 9*) were grown and transported as described in *Section 2.1.1.* Stems were individually labelled upon arrival at RHUL, and then processed as described in *2.1.2.*

Figure 9. Rosa hybrida *cultivars. Images from www.rosaprima.com, www.flowerflow.com and www.flowerweb.com.*

Vase life conditions were as described in *2.2*. However, bunches were split at random, with eight stems from each bunch placed together in glass vases and the remaining two stems from each bunch placed individually in glass milk bottles, with 1 litre and 100 ml of tap water respectively. All individually held stems, totalling six for each cultivar, had all bar the uppermost five leaflets (comprising one compound leaf) removed to reduce differences in transpiration between the stems. The individual bottles were also sealed with parafilm to limit evaporation, with a small hole cut for the stem to be easily inserted and removed. A vase with one litre of tap water, and two milk bottles with 100ml of water sealed with parafilm and a small hole cut into the top, but with no flower stems acted as vase and individual controls respectively.

3.2.1.2 Re-hydration ability and water uptake of cut Rosa hybrida cultivars

All stems were weighed upon arrival (following initial stem end removal) and after re-hydration (prior to secondary stem end and leaf removal) to determine re-hydration ability. Rehydration was calculated in terms of relative fresh weight (RFW) using *Equation 1,* where W_t was the weight of the stem (in g) following re-hydration and W_{t-0} was the weight of the stem (g) on arrival (t= day 0) (He et al., 2006).

Equation 1

$$RFW\ (\%) = \left(\frac{W_t}{W_{t=0}}\right) * 100$$

All individually held stems and their holding containers were weighed on a daily basis over the 14 day period to determine water balance of the stems. Water balance was calculated by taking water loss from water uptake, with water loss and water uptake calculated as shown in *Equation 2* and *Equation 3*. Where St is the weight of the vase and vase water and Ct is the weight of the vase, vase water and stem (g) at day (t), with St_{-1} and Ct_{-1} indicating the weight (g) recorded on the previous day (i.e day -1) (He et al., 2006; Lü et al., 2010).

Equation 2

$$Water\ uptake\ (g\ stem^{-1}day^{-1}) = St_{-1} - S_t$$

Equation 3

$$Water\ loss\ (g\ stem^{-1}day^{-1}) = Ct_{-1} - C_t$$

3.2.1.3 Vase life termination factors of the cut Rosa hybrida cultivars

Flower quality was assessed daily over the 14 day period, with terminating factors determined as outlined in *2.2.1*. Both the day of termination and the terminating

factor were individually recorded for each stem. An estimated vase life of 15 days was given to any remaining viable stems at the end of the 14 day vase life period.

3.2.1.4 Statistical analysis

Vase life and relative fresh weight (RFW) data for bunched stems were analysed with one-way ANOVA's to determine the effect of cultivar on the average length of vase life (days) and the effect of cultivar on RFW. Tukey post hoc tests were then used for multiple comparison of means to determine significance difference between cultivars. Stem data were averaged to produce vase (bunch) values prior to ANOVA analysis.

Vase life data for individual stems did not meet assumptions of normality (Shapiro-Wilk $p < 0.05$). The effect of cultivar on the average length of vase life (days) for individual stems was therefore assessed with a non-parametric Kruskal-Wallis test, followed by Wilcoxon tests with Benjamini-Hochberg correction for multiple comparisons to determine statistical differences between cultivars.

The effects of cultivar and day (of vase life) on the water balance of stems was analysed with a linear mixed effects model also known as a repeated measures ANOVA using the R package lme4 (Bates et al., 2015) and lmerTest (Kuznetsova et al., 2017). Where repeated measures were included for each stem due to testing over multiple days. Multiple pairwise Wilcoxon tests with Benjamini-Hochberg correction were then carried out to determine significant differences in water balance between the cultivars for each individual day. Non-parametric tests were used for further analysis as water balance data for each individual day did not always meet assumptions of normality (Shapiro-Wilk, $p < 0.05$).

3.2.2 Stem strength analysis of Rosa hybrida *cultivars H30 and Fuchsiana*

Stem flex was used as an indicator of stem strength and was measured by adding a weight to the peduncle, just below the flower head and the degrees of bending measured. Stem flex of *Rosa hybrida* cultivars H30 and Fuchsiana were compared, with flower material harvested and transported as described in *2.1*.

Measurements were taken following re-hydration with all leaves removed from the stems just prior to use.

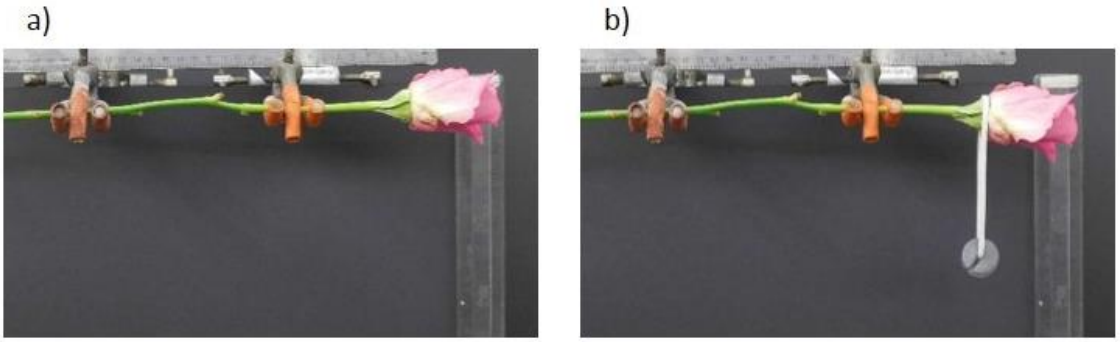

Figure 10. Stem flex of Rosa hybrida *peduncles. a) without weight, b) with weight, difference in angle between two images calculated with ImageJ.*

Stems were mounted horizontally using two burette holders at fixed points, one 7 cm below the flower head and one 22 cm below the flower head. Images were taken before and after the addition of a 30 g weight (total 31.9 g including attachment) (*Figure 10*), and the change in angle calculated using the ImageJ 'measure' tool (Schneider et al., 2012). Measurements were taken with the flower head attached and after removal of the flower head, on both a 0˚ and 180˚ rotation of the stem with a total of 15 stems analysed for each cultivar.

3.2.2.1 Water content of Fuchsiana and H30 flower heads

To determine water content (%), fresh weights (FW) of the flower heads were taken immediately upon removal from the stem and placed in pre-weighed paper envelopes. Flower heads were dried in a 50 °C drying cabinet until completely dry and no change in weight could be recorded. Dry weights (DW) were taken following removal from the drying cabinet, once samples had returned to room temperature. All weights were taken to the nearest mg. Water content was then calculated with respect to fresh weight using *Equation 4*

Equation 4

$$Water\ content\ (\%) = \left(\frac{FW - DW}{FW}\right) * 100$$

3.2.2.2 Statistical analysis

Statistical differences between the *Rosa hybrida* cultivars Fuchsiana and H30 for stem flex (flower head attached and unattached) and flower head fresh weight were calculated using un-paired t-tests ($p<0.05$). The effect of the flower head being attached or unattached on the degree of stem flex was assessed using paired two sample t-tests for each cultivar separately.

Flower head relative water content (RWC) data did not meet the assumptions of normality (Shapiro-Wilk $p <0.05$), therefore statistical difference between the RWC for each of the cultivars was assessed with a non-parametric Wilcoxon tests.

3.2.3 Evaluation of the relative fresh weights of cut Rosa hybrida *H30 and Fuchsiana flower stems at defined stages of induced necking*

Flower material was harvested, transported and processed as described in *2.1*. H30 and Fuchsiana cut *Rosa hybrida* flower stems (30 of each) were held individually in 100 mL of 2 % (w/v) sucrose solution. To induce necking, cultured *Pseudomonas fluorescens* bacterial colonies were added to the vase water to produce a final vase water concentration of 5×10^4 colony forming units (cfu). *P. fluorescence* cultures were stored, grown and processed as described in *4.2.5.*

3.2.3.1 Relative fresh weight of each necking stage

All stems were weighed to the nearest mg just prior to being placed in vases (following rehydration and stem end removal). Straight (control) stems and stems at <90° and $\geq$90° necking stages (as defined in *Figure 11*) were then harvested and weighted on days 3 and 5 of vase life as necking occurred. Percentage relative fresh weight (RFW %) for each necking stage was calculated using *Equation 1,* where W_t was the weight of the stem (g) at harvest and $W_{t=0}$ was the weight of the stem (g) at the start of vase life.

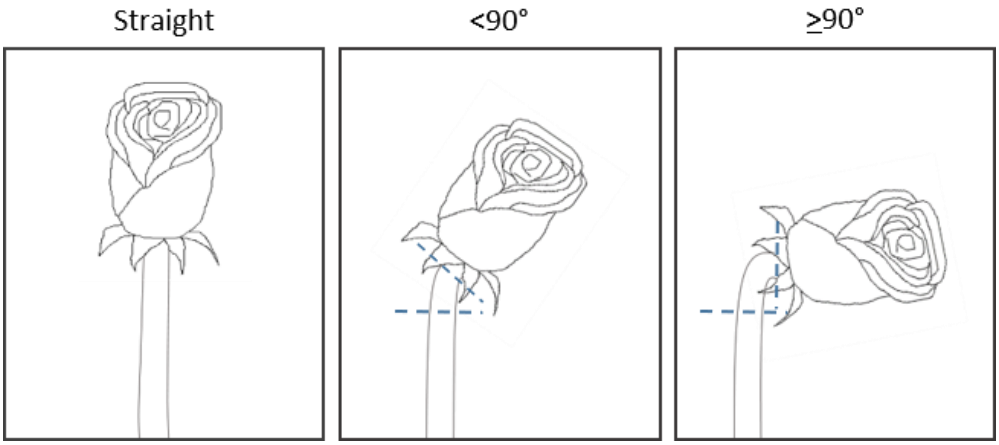

Figure 11. Stages of necking in cut Rosa hybrida *flower stems*

3.2.3.2 Statistical analysis

Statistical difference was calculated with a two-way ANOVA (un-balanced model) and a Tukey post-hoc test, with both cultivar and necking stage as factors. An unbalanced model was used due to the different number of stems collected for each cultivar and stage (*Table 4*).

Table 4. Number of stems at each necking stage collected for RFW analysis

Cultivar	**Necking stage**		
	Str	**<90**	**>90**
Fuchsiana	6	8	6
H30	10	3	15
Total	**16**	**11**	**21**

3.2.4 Microscopy analysis of Rosa hybrida *cv. H30 induced necking peduncles (Transverse sections)*

To determine the sampling area for microscopy, images of (H30) necking peduncles from previous vase life experiments were analysed using ImageJ (Schneider et al., 2012). Measurements of the average peduncle length, the initial point at which necking occurs and the mid-point in bending of the peduncle were taken in mm from just below the flower head.

3.2.4.1 Flower material

Bunches of H30 were harvested, transported and processed as described in *2.1*. Stems were held individually in 100 mL of 2 % (w/v) sucrose solution. To induce necking, cultured *Pseudomonas fluorescens* bacterial colonies were added to the vase water to produce a final vase water concentration of 5 x 10^4 colony forming units (cfu). *P. fluorescens* cultures were stored, grown and processed as described in *4.2.5.*

3.2.4.2 Fixation

Peduncle sections (1 cm) for straight, <90° and >90° necking stages were cut using a sterile razor blade and placed immediately in a standard FAA fixative solution of 50 % ethanol, 10 % formalin, 5 % glacial acetic acid, 35 % water (v/v) (Ruzin, 1999). Samples were fixed overnight at 5˚C and stored at 5 ˚C until use. After initial fixation, the fixative solution was replaced with fresh fixative to prevent oxidation/saturation, as seen by a colour change of the solution. Samples of each necking stage for light microscopy (LM) and scanning electron microscopy (SEM) were harvested on the same day of vase life to reduce any potential influences of time or flower age.

3.2.4.3 Light microscopy (LM)

Following fixation, peduncle samples (straight, <90° and >90°) were first rinsed in buffer and then dehydrated in graded ethanol at concentrations of 30; 50; 70; 95 % and absolute ethanol for a duration of an hour each, with an additional overnight dehydration step in absolute ethanol. Peduncles were then transferred to acetonitrile for one hour, followed by infiltration with a 50:50 acetonitrile/ Spurr resin mixture for 24 hours. Peduncles were then infiltrated with 100 % Spurr resin for an initial six-hour period, followed by an overnight infiltration and a further six-hour infiltration, both with fresh 100 % Spurr resin. Samples were then embedded in Spurr resin and polymerised at 60 °C. Once embedded, thin 500 nm transverse sections were cut using a microtome and stained with toluidine blue. Prepared slides were then scanned using an Olympus BX51 microscope with an Olympus CC12 colour microscope camera and an Olympus dotSlide automated scanner using a 40x objective for image analysis.

These steps were performed by Catherine Griffiths at the Biomedical Imaging Unit (Southampton).

3.2.4.4 Scanning electron microscopy (SEM)

Straight and >90° peduncle samples were cut into 1 mm transverse sections using a razor blade and mounted uncoated onto specimen stubs. A FEI Quanta 250 scanning electron microscope was used (Biomedical imaging unit, Southampton), with 10 kV accelerating voltage, 8.7 mm working distance (WD) and low vacuum mode 60 Pa chamber pressure. The microscope was also equipped with a field emission gun, secondary electron and concentric ring backscatter detectors and beam deceleration.

3.3 Results

3.3.1 Comparison of Rosa hybrida *cultivars Akito, Furiosa, Fuchsiana, H30, Top Sun and Tropical Amazon and suitability for further study*

In the cultivar comparison vase life study, cultivar was found to have a significant effect on relative fresh weight (RFW) following rehydration ($F_{5, 12} = 5.00$, $p < 0.05$), with *Rosa hybrida* cultivars Akito and Furiosa shown to have significantly higher mean RFWs following rehydration than H30 (*Figure 12; Appendix 1.2.1.1; p <0.05*). Cultivar was also shown to have a significant effect on the vase life of bunched stems ($F_{5, 12} = 22.07$, $p < 0.001$), with H30 and Akito found to have significantly shorter vase lives than all the other cultivars tested with mean vase lives of 7.6 and 5.3 days respectively (*p <0.05; Figure 13; Appendix 1.2.1.1*).

For the individually held rose stems, a significant interaction was found between day of vase life and cultivar in terms of mean water balance ($F_{20, 137} = 2.30$, $p < 0.01$). In general, a positive water balance was seen for stems of all cultivars at day one. However, the mean water balance of Tropical Amazon stems on day one was found to be significantly higher than all the other cultivars ($p < 0.05$; *Figure 14; Appendix 1.2.1.1*). Only the mean water balance of Fuchsiana was positive on day two of vase life, with Fuchsiana stems found to have a significantly higher mean water balance than Akito, Furiosa, H30 and Tropical Amazon on both day

two and three of vase life ($p < 0.05$). Tropical Amazon had a significantly lower mean water balance than Akito as well as Fuchsiana on day three of vase life ($p < 0.05$; *Figure 14; Appendix 1.2.1.1*). No cultivars showed significant difference in water balance on day four or five of vase life, with all cultivars showing an overall reduction in water balance between day one and day four, followed by an increase water balance at day five to near neutral. Water balance data was not analysed beyond day five due to the number of terminated stems beyond this point in vase life.

Cultivar was also found to have a significant effect on the vase life of individually held stems (X^2 (5, N = 36) = 16.87, $p < 0.01$), with Furiosa and Fuchsiana both found to have significantly longer vase lives than H30 ($p < 0.05$; *Figure 15*). However, no significant difference in vase life was found between the other cultivars tested for individually held stems ($p > 0.05$; *Figure 15; Appendix 1.2.1.1*).

All of the stems held individually and in bunches for both H30 and Akito (minus those damaged in transit) were terminated due to water stress associated factors (necking and wilting) as seen in *Figure 16* and *Figure 17*. The majority of Topsun stems were also terminated due to water stress associated factors, however in this case only petal wilting was seen. Fuchsiana stems all terminated due to a change in petal colour, including both blueing and browning of petals. No stems were terminated due to necking for cultivars Fuchsiana, Topsun or Tropical Amazon during the observed 14 day vase life period (*Figure 16*).

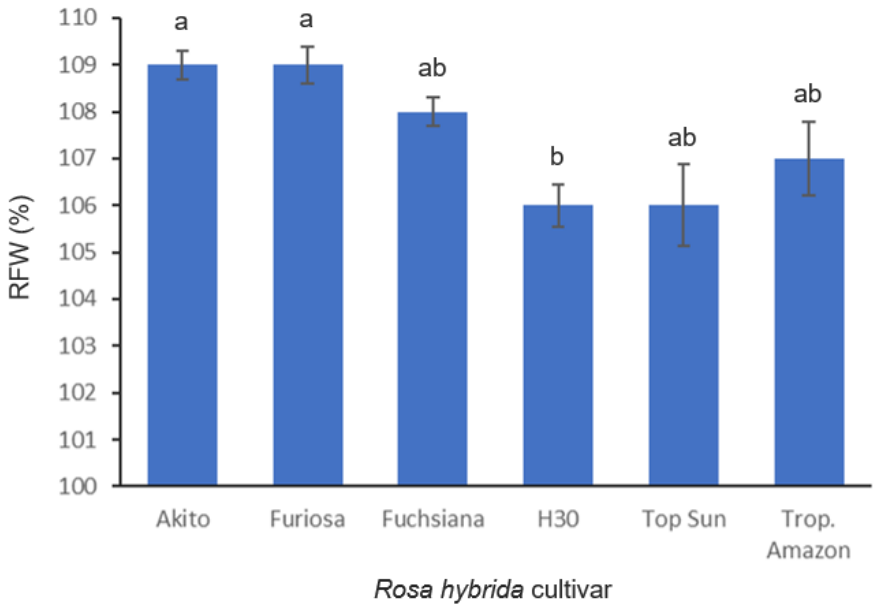

Figure 12. Mean relative fresh weight following rehydration in each Rosa hybrida cultivar. Significance difference in RFW between cultivars was calculated using an ANOVA test with a Tukey post-hoc test for multiple comparisons of means. Cultivars with no significant difference in RFW are shown with the same letter (p <0.05). Bars represent standard error of the mean. RFW, relative fresh weight. n=24

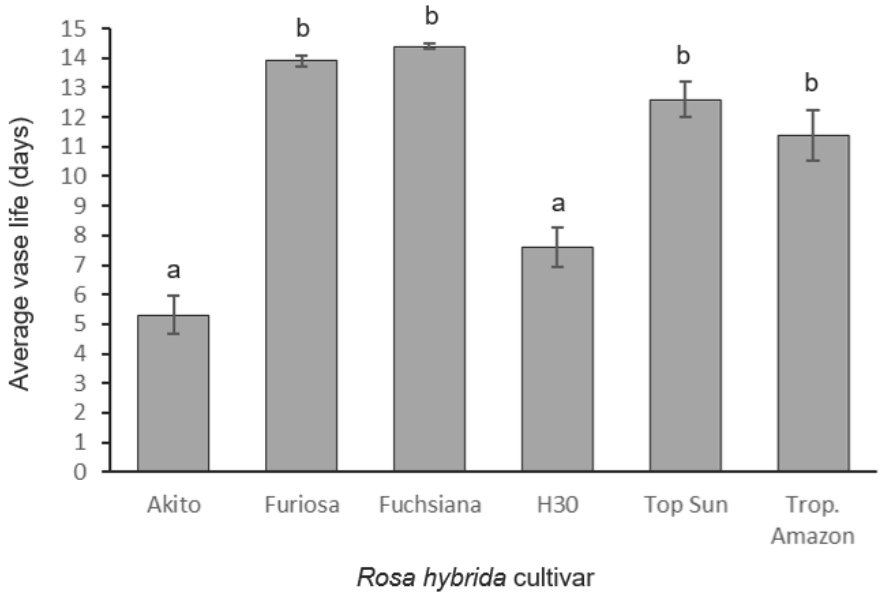

Figure 13. Average vase life of each Rosa hybrida *cultivar. Significance difference in vase life between cultivars was calculated using an ANOVA test with a Tukey post-hoc test for multiple comparison of means. Cultivars with no significant difference in vase life are shown with the same letter (p <0.05). Bars represent standard error of the mean. n= 24*

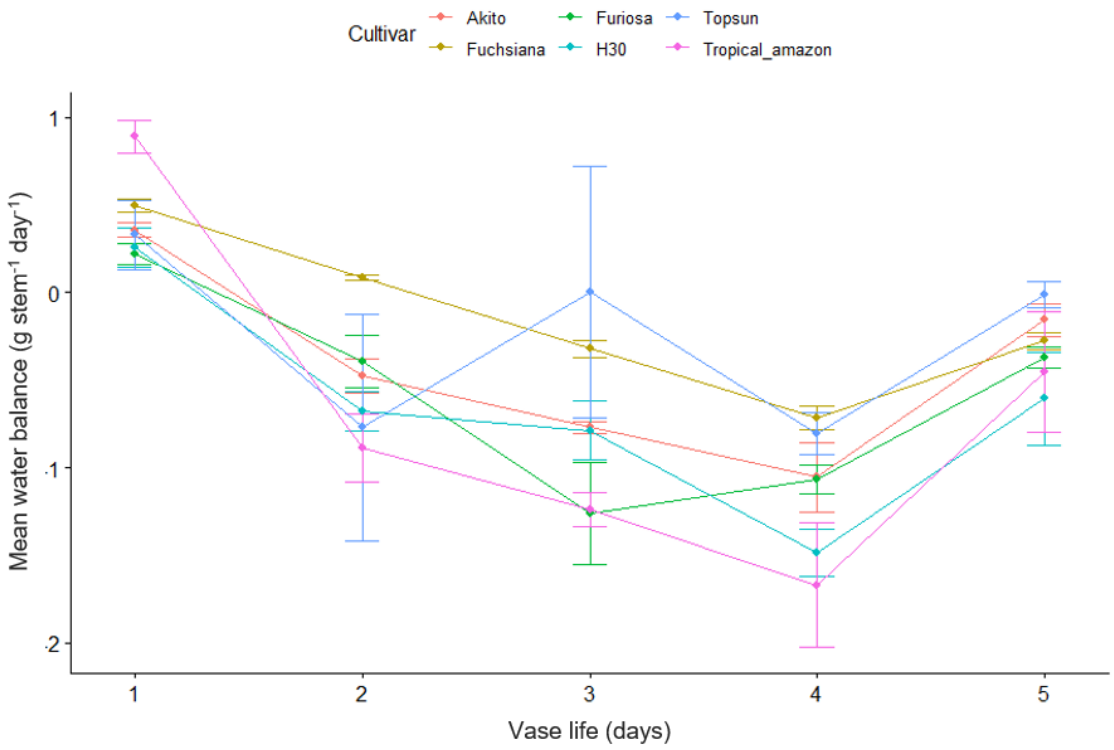

Figure 14. Comparison of the mean water balance of Rosa hybrida *cultivars for the first 5 days of vase life. Data from terminated stems was not included from the point of termination. Bars represent standard error of the mean.*

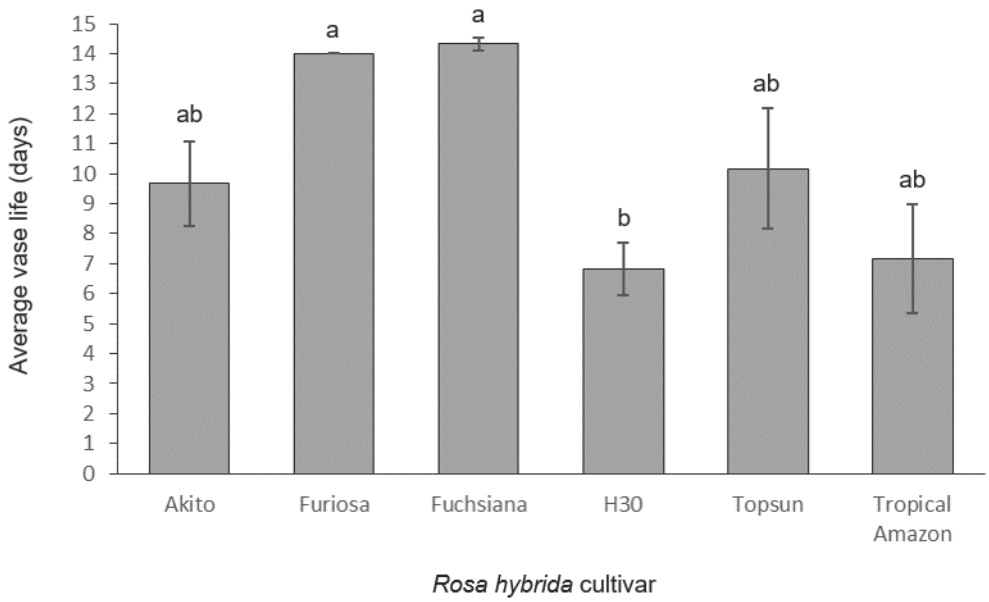

Figure 15. Mean vase life for individually held roses. Significance difference in vase life between cultivars was calculated using a Wilcoxon signed rank test with Benjamini-Hochberg correction for multiple comparisons. Cultivars with no significant difference in vase life are shown with the same letter (p <0.05). Bars represent standard error of the mean. n=6

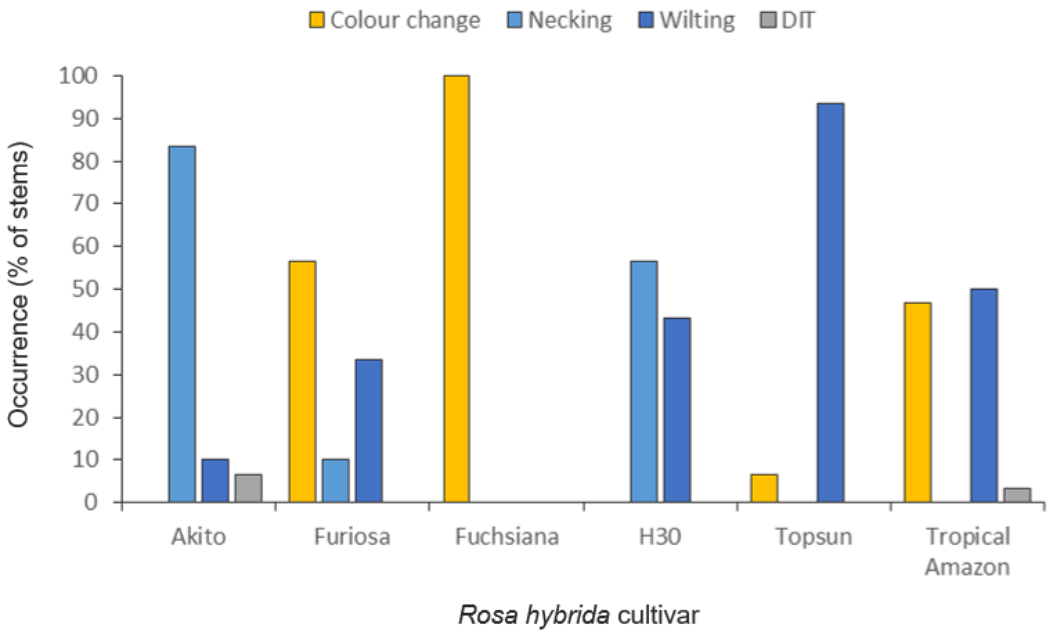

Figure 16. Terminating factors of vase life for each Rosa hybrida *cultivar. Colour change includes both blueing and browning of petals; DIT, damaged in transit. n=30*

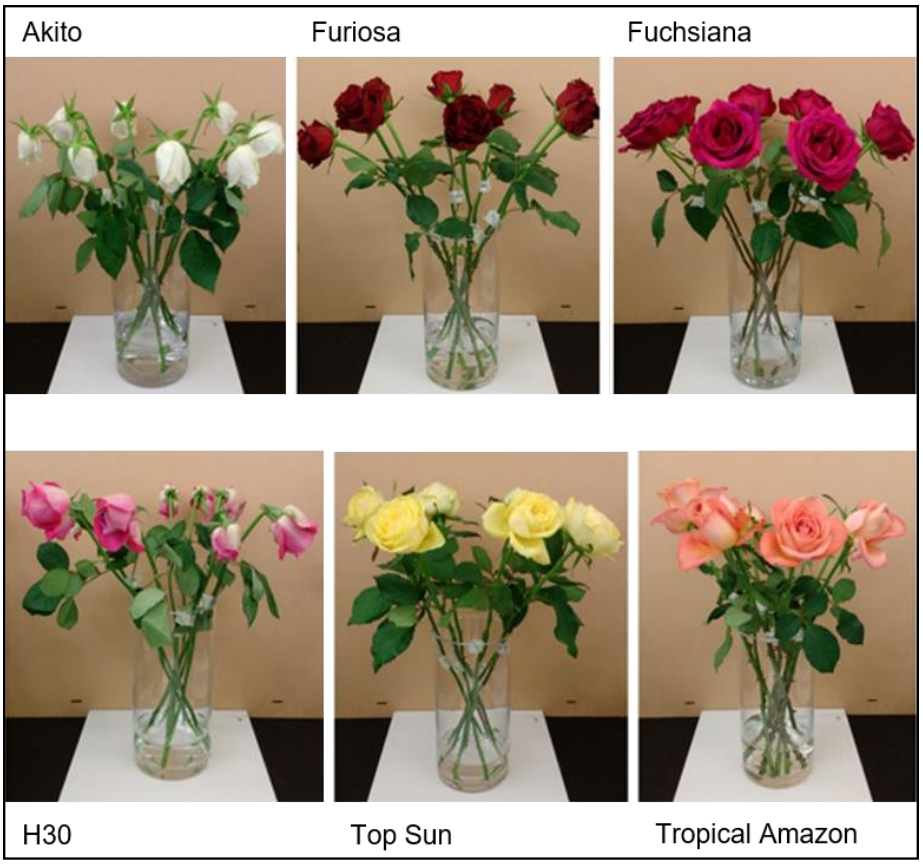

Figure 17. Comparison of cultivars at day 9 of vase life. Images are representative of the vase condition and termination factors seen at this time point.

3.3.2 Stem strength analysis of Rosa hybrida *cultivars H30 and Fuchsiana*

Significant difference in stem flex was found between the two cultivars, with H30 stems flexing significantly less than Fuchsiana stems with the addition of a weight (flower head attached $t_{28} = 5.46$, $p < 0.05$ and detached $t_{28} = 4.11$, $p < 0.05$; *Figure 18*). Significance between the stem flex achieved with the flower head attached compared to not-attached was also determined with a paired t-test, with significant difference seen for H30 but not for Fuchsiana stems (H30 $t_{14} = 2.40$, $p < 0.05$ and Fuchsiana $t_{14} = 1.14$, $p > 0.05$; as shown by asterisks *Figure 18*). Although no significant difference was seen between the fresh head weight of each cultivar ($t_{28} = -0.486$, $p > 0.05$; *Figure 19*), H30 was found to have a significantly higher percentage water content than Fuchsiana with a mean water content of 87.9 % ($W_{28} = 0$, $p < 0.05$; *Figure 20*).

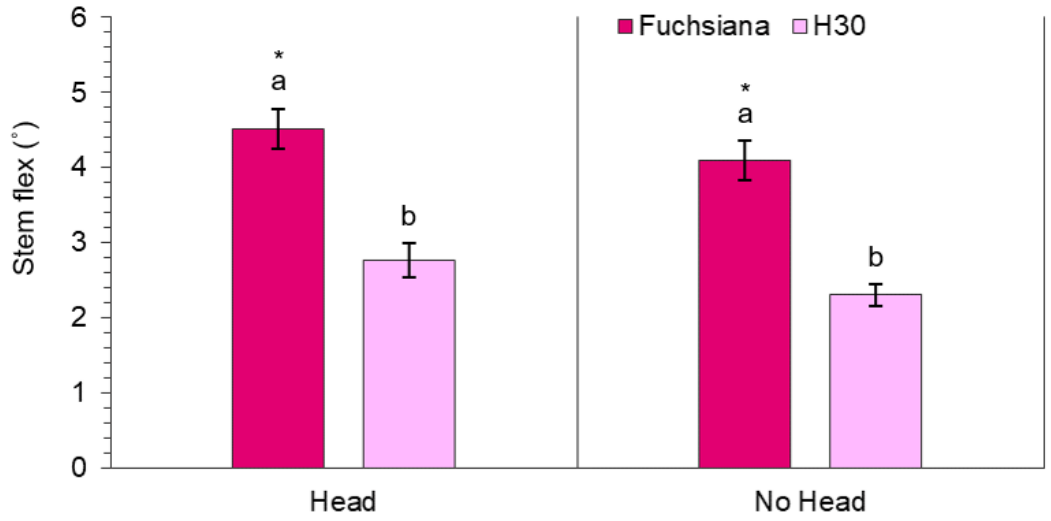

Figure 18. Degrees of stem flex for H30 and Fuchsiana with and without the flower head attached. Significance between cultivars was measured with an unpaired t-test, p<0.05. n= 15

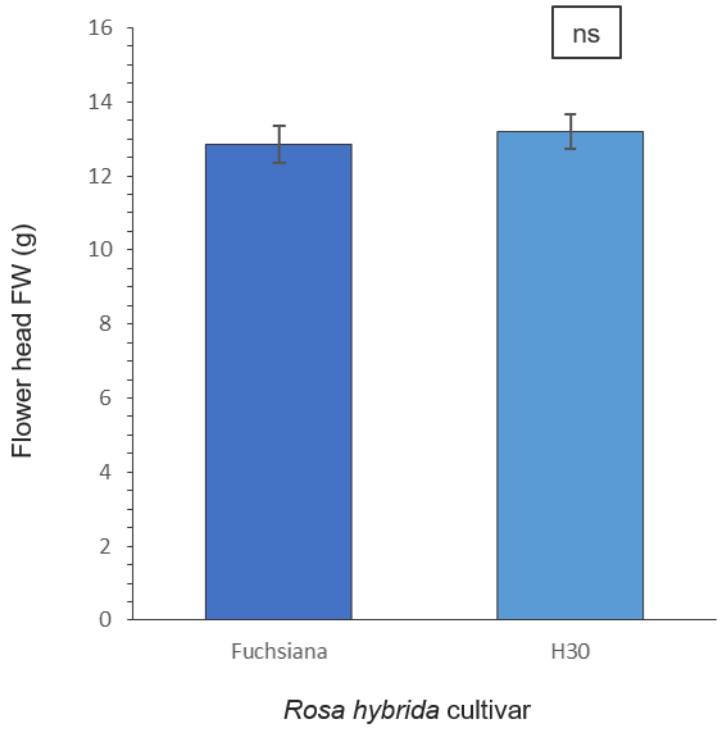

Figure 19. Fresh weight of the flower heads of H30 and Fuchsiana cut Rosa hybrida *flowers. No significant difference (ns) was found between the cultivars with an unpaired two-sample t-test (p <0.05), n= 15. FW, fresh weight.*

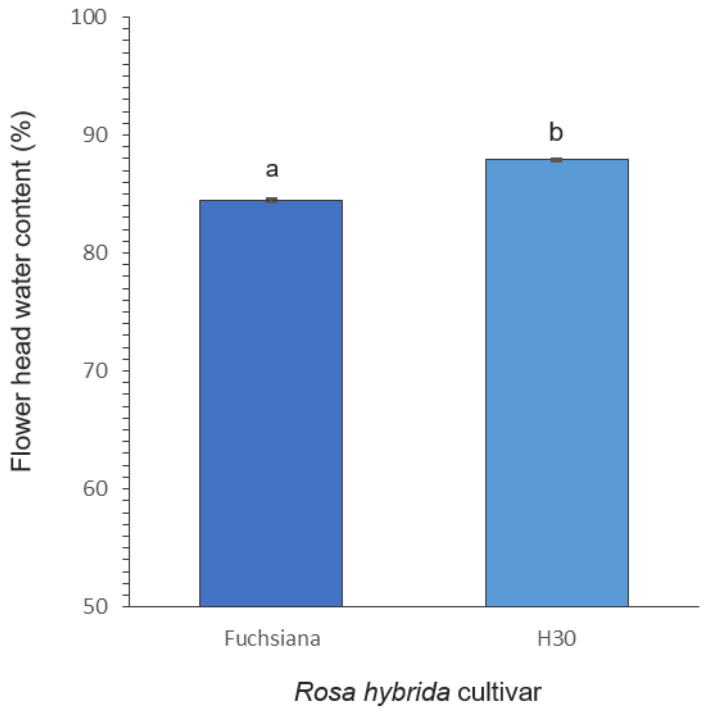

Figure 20. Water content of flower heads of H30 and Fuchsiana cut Rosa hybrida flowers. Significance between cultivars was calculated with an unpaired two-sample Wilcoxon test (p <0.05), n= 15.

3.3.3 Relative fresh weights of flower stems at each necking stage for Rosa hybrida *cultivars H30 and Fuchsiana*

Addition of *Pseudomonas fluorescens* cultures to the vase water induced necking in both H30 and Fuchsiana flower stems by day 5 (addition of *P. fluorescence* further discussed in Chapter 4. Analysis of relative fresh weight (RFW) at each stage of necking for H30 and Fuchsiana was conducted with a two-way ANOVA, using an un-balanced model due to the different number of stems collected for each cultivar and stage (*3.2.3.2; Table 4*). No significant interaction was found between necking stage and cultivar in terms of RFW ($F_{2, 42} = 0.62$, $p > 0.05$), with no significant difference found between the mean RFW of H30 and Fuchsiana at each necking stage (*Figure 21A; Appendix 1.2.1.2*). However, necking stage alone was found to have a significant effect on RFW ($F_{2, 42} = 16.57$, $p < 0.001$), with significant difference seen in RFW at each necking stage for H30 and Fuchsiana stems combined ($p < 0.05$; *Figure 21B; Appendix 1.2.1.2*).

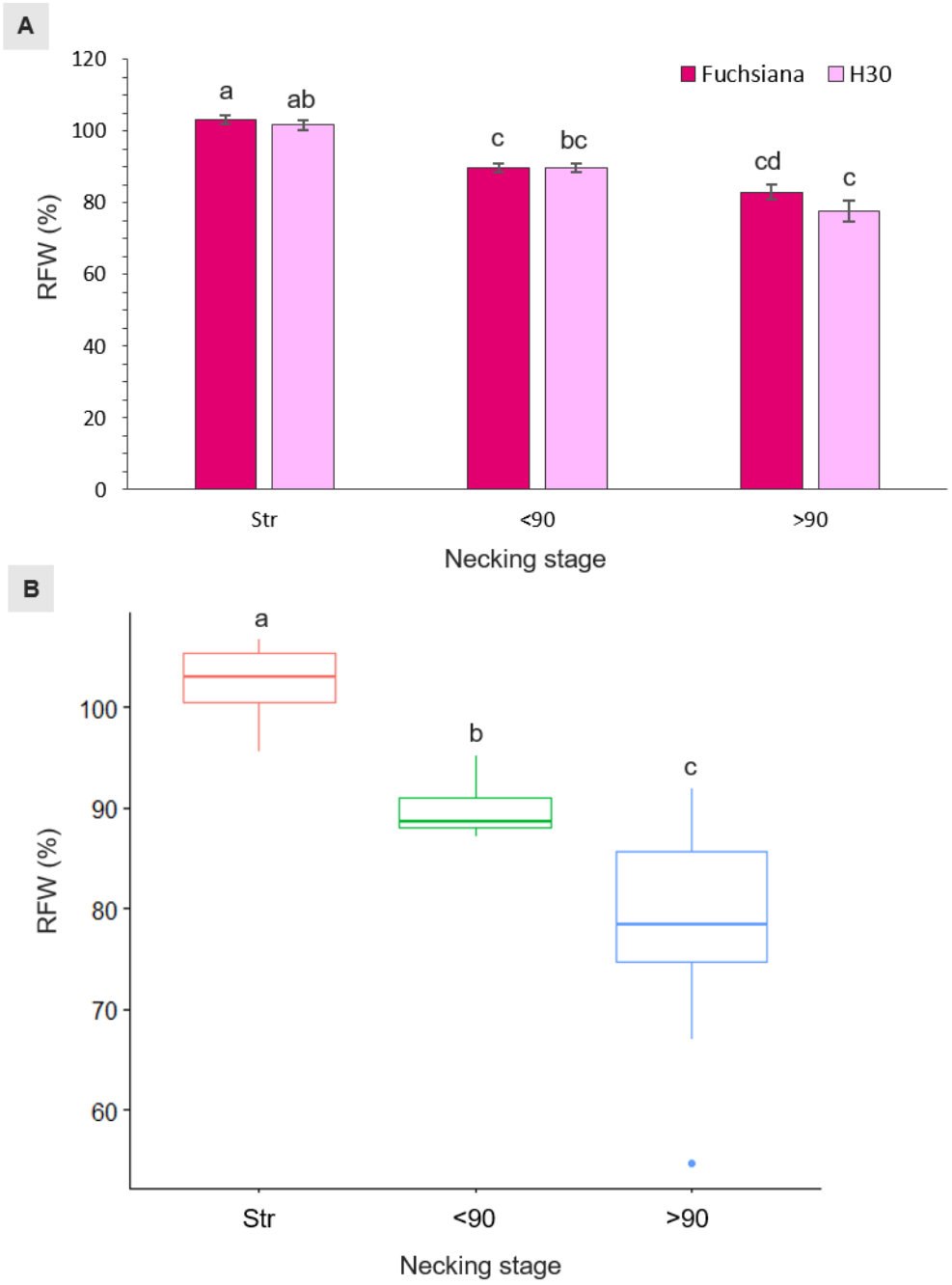

Figure 21. Relative fresh weights of H30 and Fuchsiana flower stems at three necking stages (Straight, <90° and >90°). A, RFW separated by cultivar for each necking stage; B, combined relative fresh weights (RFW) of H30 and Fuchsiana for each necking stage. Statistical analysis was completed using a two-way ANOVA (un-balanced model), with a Tukey post-hoc test.

3.3.4 Microscopy analysis of Rosa hybrida cv. H30 necking peduncles

Analysis of necking peduncles with ImageJ identified the average peduncle to be 97.8 mm in length (± 2.2 mm SE) and the mid-point of the bend in a necking peduncle to be on average 19.7 mm (± 1.2 mm SE) below the flower head (*Figure 22*). Transverse sections of the predicted mid-point in necking were therefore taken ~20 mm below the flower head for straight and <90 where this could not easily be identified.

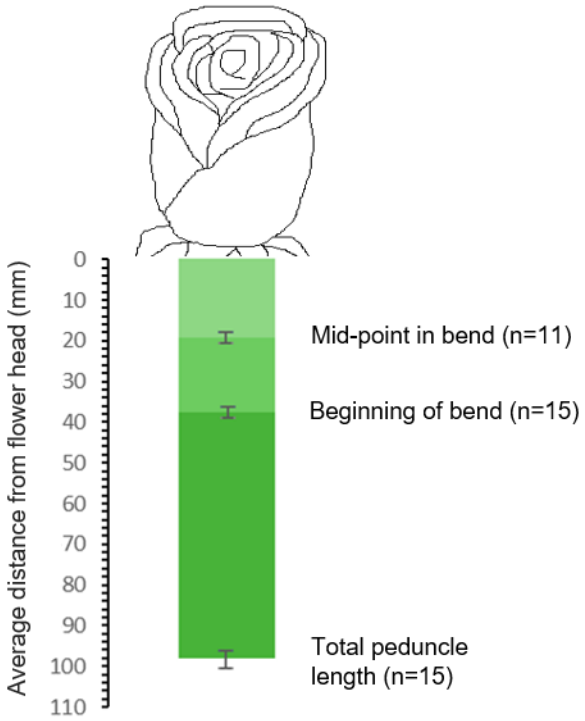

Figure 22. Average peduncle length and points of necking in H30. Distance was measured from the base of the flower head in mm; bars represent standard error. n= 11-15 as indicated.

The light microscopy sections of necking peduncles show shrinkage of the pith as necking progresses (*Figure 23 A-C*). Along with an undulation of the epidermis, clearly seen between >90° and straight peduncles (*Figure 23 D&E*). Shrinkage of the pith can also be seen in the scanning electron microscopy (SEM) images, with greater contrast shown here between the straight and >90 sections due to the more advanced >90° necking peduncle analysed (*Figure 24*).

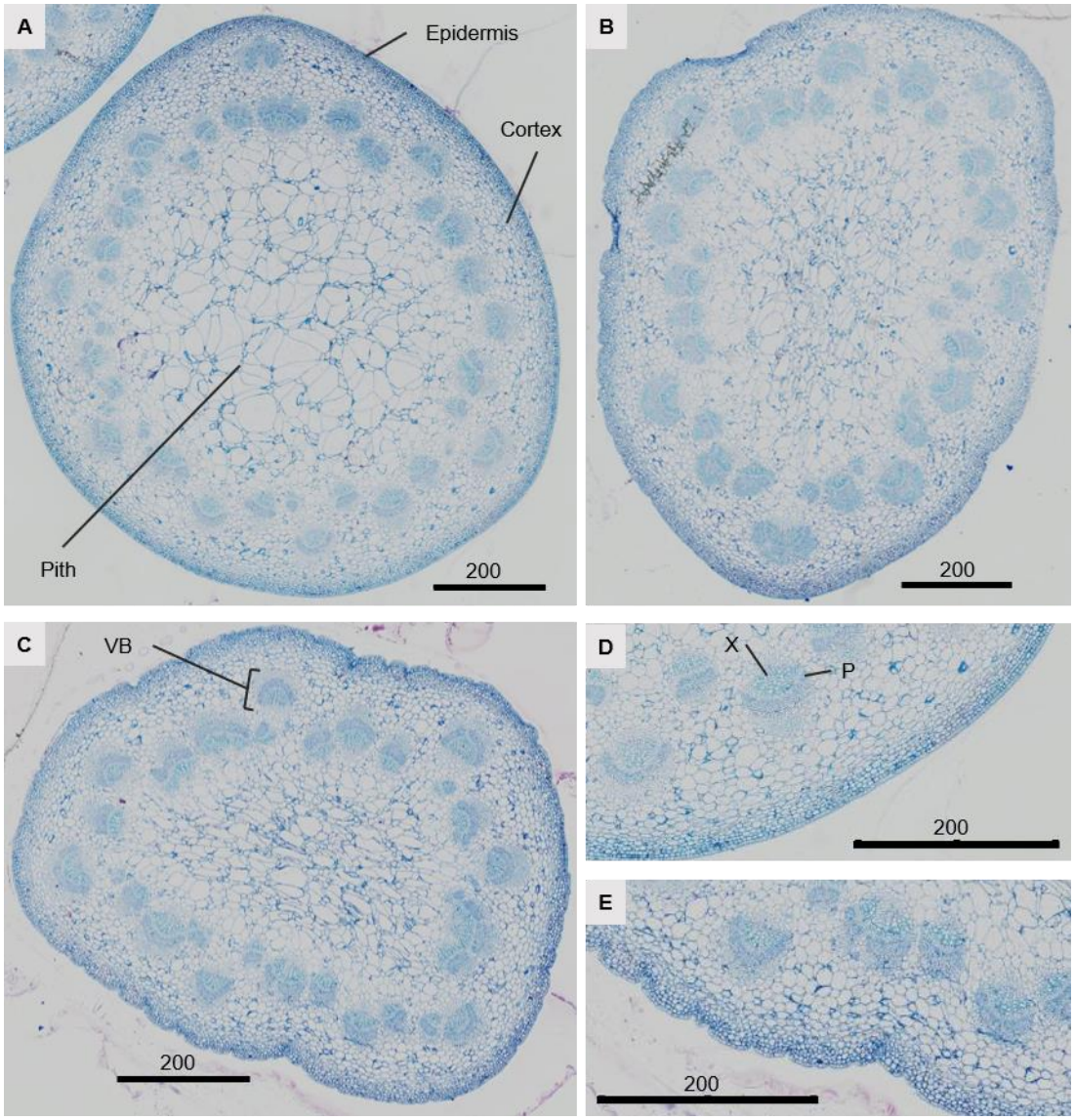

Figure 23. Transverse sections of Rosa hybrida *cv. H30 peduncles at three necking stages. Straight (A), <90˚ (B) and >90˚ (C). D and E show the epidermis of straight and >90° peduncles respectively. Light microscopy stained with toluidine blue. VB, vascular bundles; X, xylem; P, phloem. Slides prepared and images taken by the Biomedical Imaging Unit (Southampton) with a dotSlide scanner at 40x magnification.*

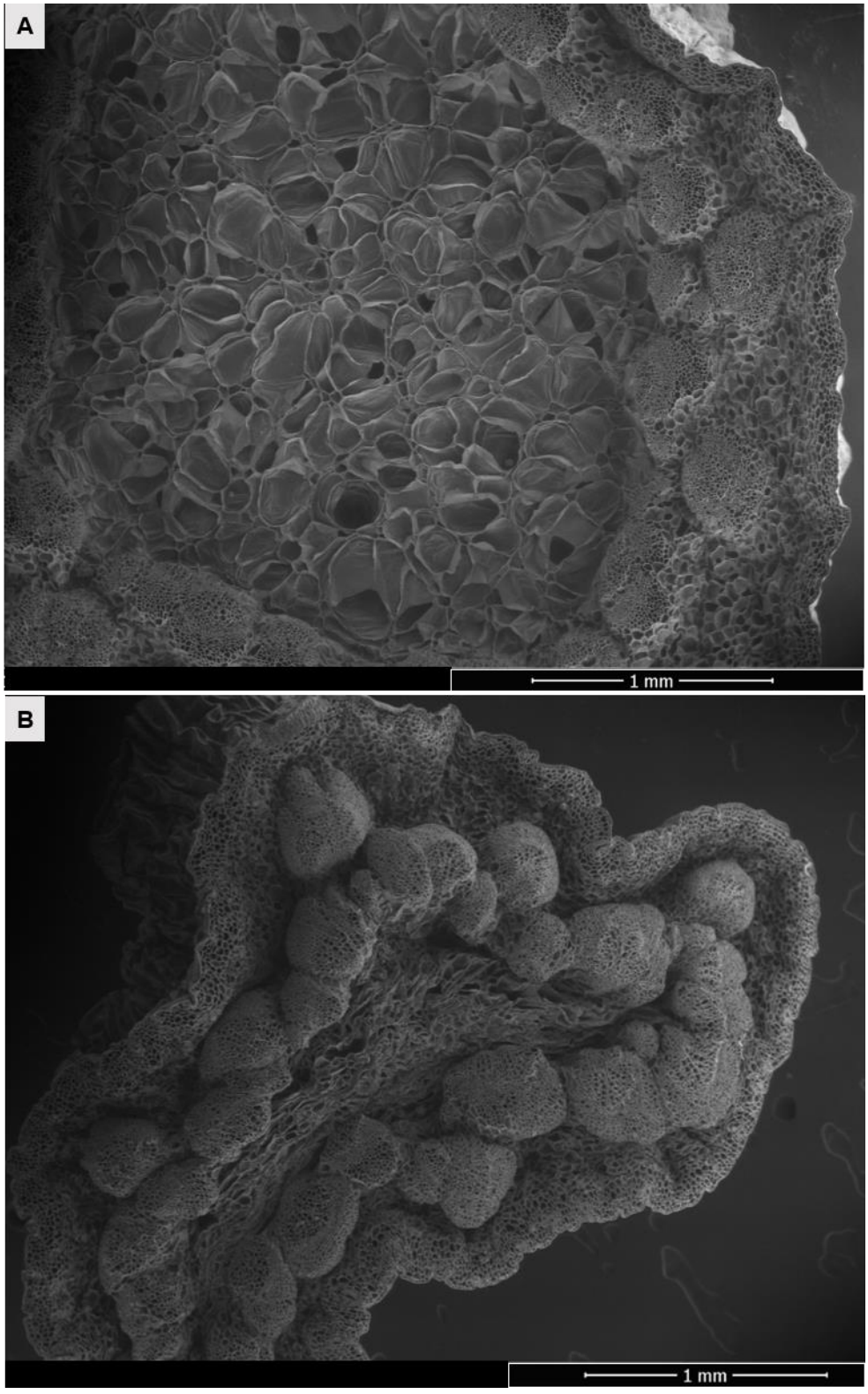

Figure 24. Electron microscopy images. Straight (A), >90˚ (B). Images were collected with a dwell time of 45 µs (amount of time the beam will collect data at each pixel). 50x magnification.

3.4 Discussion

3.4.1 Preliminary comparison of Kenyan Rosa hybrida *cultivars and their suitability for further study*

The *Rosa hybrida* cultivars Akito, Furiosa, Fuchsiana, H30, Top Sun and Tropical Amazon (*Figure 9*) were selected as potential cultivars for study due to their popular use by industry in straight line bunches and bouquets and for their previous use in industry vase life trials (T. Wheeler, Flamingo Horticulture pers com., 2016). All cultivars tested were grown in Kenya and transported dry via air freight to the UK. Dry storage is necessary for long distance transport via air freight however dry storage can reduce fresh weight and alter water uptake ability upon rehydration (Ahmad et al., 2012). *R.hybrida* cultivars are known to respond differentially to dry storage in relation to re-hydration rate following periods of desiccation potentially having an effect on overall vase life (Fanourakis et al., 2013). In this study significant differences were found in re-hydration ability of the cultivars, with Akito and Furiosa showing a significantly greater increase in fresh weight following rehydration than H30 (*Figure 12*). This was partially reflected in the average vase life seen, with Furiosa having a significantly longer vase life than H30, suggesting that H30 stems did not sufficiently re-hydrate following dry storage and consequently terminated due to water stress associated factors (*Figure 13*). However, this same trend was not seen for Akito, with Akito having one of the highest percentage increases in fresh weight following rehydration but the shortest significant vase life of all the cultivars tested, with all stems terminating due to water stress associated factors (*Figure 12; Figure 13; Figure 16).* One possible reason for this is differences in fresh weight upon arrival. As although all the stems were transported together, it is unknown how desiccated the stems were upon arrival and if this varied between cultivar. Matsushima et al. (2010) found Akito to have an underdeveloped epidermal layer which was hypothesised to allow for increased transpiration and water loss from the stem. Hence, in this study Akito may have lost more fresh weight during dry storage compared to the other cultivars and therefore had a lower initial fresh weight from which the rehydration ability was calculated relative to.

For individually held rose stems a mixed result was also found in terms of water balance and vase life. Fuchsiana was found to be more efficient at maintaining a positive water balance than all the other cultivars for day two and three of vase life (excluding Topsun) and had one of the longest mean vase lives, with no stems terminating due to water stress associated factors (*Figure 14; Figure 15; Figure 16*). However, Furiosa did not have a significantly better water balance than any of the other cultivars on any of the days analysed, yet Furiosa had a significantly longer vase life than H30. Therefore, water balance alone was not found to explain the differences in vase life seen. Interestingly, all cultivars showed an increase in water balance between day four and five and could indicate a potential stomatal response for all cultivars at this point in vase life. As changes in stomatal functionality can reduce water loss by transpiration and therefore improve water relations within the stem.

In terms of suitability for further study, Akito showed the highest levels of necking of the cultivars tested and has been used as a necking susceptible or short vase life cultivar in many studies (Graf et al., 2006; Pompodakis et al., 2010; Matsushima et al., 2010; Matsushima et al., 2012; Macnish et al., 2010; Spinarova & Hendriks, 2007; Woltering & Paillart, 2018). However, Akito was not chosen for further analysis due to being phased out of main production in Kenya. With the majority of rose bushes on the Kenyan farms coming to the end of their 7 year rotation and due to be replaced by a new white cultivar (*Figure 16*; K. Richardson, Flamingo Horticulture pers com., 2016). H30 was therefore selected as the necking susceptible cultivar for further study, alongside Fuchsiana as the less susceptible cultivar due to showing no necking or water stress terminating factors during standard vase life conditions (*Figure 16*).

3.4.2 Stem strength analysis of H30 and Fuchsiana

Stem strength and susceptibility to necking have previously been found to negatively correlate, with cultivars less susceptible to necking showing increased stem strength compared to more susceptible cultivars (Zamski et al., 1991; Chabbert et al., 1993; Graf et al., 2006). However, the opposite was found in this study, with the necking susceptible *R. hybrida* cultivar H30 showing increased

stem strength compared to the less susceptible cultivar Fuchsiana (*Figure 18*). This difference in stem strength however may be attributed to the difference in water content seen between the two cultivars (*Figure 20).* As turgor pressure provides structural support to the peduncle tissue and H30 was found to have a significantly increased water balance compared to Fuchsiana (Beauzamy et al., 2014; Graf et al., 2006). Although no significant difference in flower head fresh weight was seen between the two cultivars, only H30 also showed significantly less stem flex following head removal. This suggests that H30 is more affected by relative flower head weight than Fuchsiana and may contribute to the increase in susceptibility to necking for H30. However, it may be hypothesised that differences in necking susceptibility between H30 and Fuchsiana may be more closely associated with variations in water relations and fresh weight than stem architecture and mechanical strength. As H30 has been shown to have a significantly reduced water balance compared to Fuchsiana on day two and three of vase life (*Figure 14*). A negative water balance results in a reduction in water content within the flower stem therefore H30 would have seen a larger decrease in water content than Fuchsiana during the first few days of vase life. Potentially resulting in a loss of turgor pressure and stem strength and hence may explain the increased occurrence of necking in H30 stems (*Figure 16*).

3.4.3 Relative fresh weights of Rosa hybrida flower stems at different stages of necking

In this study necking was found to occur at significantly different percentage relative fresh weights and clearly associates occurrence of necking to water relations in cut *R. hybrida* flower stems. The fact that no significant difference was found between H30 and Fuchsiana in relative fresh weight at each stage of necking is in line with the hypothesis made in *3.4.2* that differences in necking susceptibility between H30 and Fuchsiana are associated with water relations rather than mechanical strength. As increased mechanical strength is thought to provide increased resistance to bending following reductions in water content, yet the same extent of necking occurred for each cultivar at the same relative fresh weight suggesting no significant differences in mechanical strength (Graf et al., 2006; Chabbert et al., 1993). However, as this study was based on relative fresh

weights it assumes that the two cultivars had similar water contents at the start of the experiment and therefore would need to be verified using calculated water contents for each cultivar (Equation 4).

3.4.4 Microscopy analysis of Rosa hybrida *cv. H30 necking peduncles*

In this study transverse sections of straight (control) and necking peduncle tissue of *R. hybrida* cultivar H30 were analysed by both light and scanning electron microscopy and identified undulation of the epidermis and shrinkage of the pith in >90° necking peduncles compared to control stems (*Figure 23; Figure 24*). The collapse of cells within the pith and concurrent shrinkage indicates loss of osmotic balance and turgor pressure in the pith of >90° necking peduncles. This is in line with the overall reduction in water content seen for necking peduncles in *Figure 21B* and with a previous study by Matshushima et al. (2010) which identified a loss of water content in peduncle parenchyma tissue of *Rosa hybrida* cultivars Akito, Milva and Red Giant with cold neutron radiography following short term drought stress.

3.5 Conclusions

Termination factors were found to vary between cultivars despite the same transport and growth conditions as found in previous studies. Of the cultivars analysed, H30 and Fuchsiana were selected as necking susceptible and necking resistant cultivars for further study. Stem strength analysis of these two cultivars, was found to be inconclusive due to differences in water content and therefore turgor pressure. However, analysis of relative fresh weights identified significant differences between the three necking stages under the outlined experimental conditions. As the data was relative, it would be interesting to see if this trend is also seen in terms of water content.

Chapter 4 Microbial audit of the *Rosa hybrida* supply chain and identification of stem end micro-organisms

4.1 Introduction

Necking and reduced vase life of cut roses is thought to be caused by a microbial occlusion of the stem, preventing water uptake. However, most studies have primarily focused on the effect of bacterial load in relation to vase life and necking (de Witte & van Doorn, 1988; van Doorn & de Witte, 1991a; van Doorn & de Witte, 1991b; van Doorn & de Witte, 1997; Put & van Meyden, 1988; Robinson et al., 2007; van Doorn, 1995; Laird et al., 2005; van Doorn et al., 1989; Bleeksma & van Doorn, 2003; van Doorn et al., 1990b), with only a few studies having also focused on the potential effect of fungi (Li et al., 2015; Put, 1990; Put & Clerkx, 1988; Zagory & Reid, 1986; Put & Conway, 1986; van Doorn et al., 1991). This is likely because fungal species have previously been found to be less prevalent in the vase water and on the stems of roses than bacteria (Li et al., 2015; van Doorn et al., 1991; van Doorn, 1989; Put & Clerkx, 1988) and it has been hypothesised that fungi therefore have a lesser role in causing stem blockages or no effect on vase life (van Doorn et al., 1991).

Contrary to this, Zagory & Reid (1986) found an unidentified yeast to cause the largest reduction in vase life of cv. Cara Mia rose stems compared to three *Pseudomonas* species, with two of the *Pseudomonas* species showing no significant effect on vase life. Despite all microbial additions being added at a vase water concentration of 10^6 per mL and all microorganisms being of similar size and shape. Put & Clerkx, (1988) also found that the fungal mycelium of *Fusarium oxysporum* were able to plug xylem vessels of cv. Sonia roses more readily than the singular microbial cells of *Bacillus polymayxa*, *Pseudomonas putida* and *Kluveromyces marxianus* and the microcondida of *Fusarium oxysporum*. This highlights the potential impact of fungi on necking and the importance of the species of microorganisms present.

Put, 1990 has so far carried out the most extensive analysis of microorganisms associated with cut roses and identified 15 bacteria and 16 fungi from the stem ends and vase water of *Rosa hybrida* cultivar Sonia. Studies which have identified microorganisms isolated from cut roses have done so by traditional techniques (Put, 1990; Zagory & Reid, 1986; Put & Jansen, 1989; van Doorn et al., 1991).

However, PCR amplification and sequencing of the variable regions within the 16S ribosomal RNA (rRNA) gene and the internally transcribed spacer (ITS) are now commonly used for studying prokaryotes and eukaryotic microbes respectively and allow for precise species level taxonomic identification (Turner et al., 2013). The use of sequencing techniques was previously limited by the number of available reference sequences. However, this is a continually growing resource with 20, 461 bacterial and 11, 252 fungal species entries currently available through NCBI for 16S ribosomal RNA and ITS targeted loci searches (correct of March, 2020).

Aside from the studies by Zagory & Reid (1986) and Put (1988) previously mentioned, the effect of isolated species added to the vase water of cut *R. hybrida* flowers have primarily focused on the addition of bacteria. In particular the addition of *Pseudomonas* species (Robinson et al., 2007; Laird et al., 2005; Put & Meyden,1988; van Doorn & de Witte, 1991a; Put & Jansen, 1989). However, results of these studies have generally been reported in terms of the overall impact on vase life, rather than the occurrence of necking.

In order to determine the prevalence of fungi on Kenyan grown roses, fungal counts have been conducted through-out stages of the supply chain. Identification of bacterial and fungal species associated with Kenyan grown roses has also been determined by colony PCR and sequencing methods. As the focus of this study is necking, the effect of the bacterium *Pseudomonas fluorescens* as well as the effect of two fungal species (a yeast and a filamentous fungus) added to the vase water of cut *R. hybrida* cultivars was assessed, with results reported in terms of the incidence of necking rather than in terms of general vase life.

4.2 Methods

4.2.1 Fungal Petrifilm audit of the Kenyan supply chain

Stem sections from the bottom 2 cm of stem (stem end) and 2 cm sections from 30 cm below the flower head (mid-stem) were collected from three points in the Kenyan supply chain as described in *Table 5* for *Rosa hybrida* cultivars H30 and Fuchsiana. Stem sections were cut using a razor blade, with both the cutting tile and blade sterilised with ethanol (absolute) between sections. Stem sections were placed in individual sterile Falcon tubes and transported in a cool bag to the laboratory at Dudu tech within 2 hours of collection. Stem sections were then suspended in 4 mL of autoclaved saline solution (un-buffered 0.85 % NaCl) and plated neat onto Yeast and Mould (YM) Petrifilms (3M) as described in 2.3. Plates were incubated and counted as described in 2.3.3 using an observation microscope provided by Dudu tech.

Table 5. Stages in the Kenyan supply chain

Stage	Description
Harvest	Flower stems were harvested in the greenhouses and brought to the packhouse in post-harvest solution. Stem sections were taken following arrival to the central packhouse.
Cold Store	Following harvest, stems lengths were graded and leaves were stripped from the bottom half of the stems. Flower stems were then placed in buckets of postharvest solution and transferred to the cold store. Stem sections were taken after cold storage of 24 hrs.
Processing	Following cold storage, stems were re-cut and arranged into bunches. Stem sections were taken from the end of the processing line, prior to being packed into boxes for transport to the UK.

H30 and Fuchsiana mid stem and stem end sections were collected from a replicate of three stems on each day of collection (collection period; *Table 6*) for each stage of the Kenyan supply chain (*Table 5*). Stems were sampled at random

at each identified stage of the supply chain, i.e. stems selected at the harvest stage were not followed through and re-sampled at each subsequent stage. Due to limitations in availability, only Fuchsiana stem end sections were sampled on collection day 4 at the cold storage stage (Table *6*). H30 and Fuchsiana stem end and mid stem sections were only collected on one day (day 3) for the processing stage and did not have replicate collections due to production timings (Table *6*).

Table 6. Collection periods of mid stem and stem end sections

	Collection period (day)			
Stage	1	2	3	4
Harvest	MS, SE	MS, SE	-	SE
Cold Store	MS, SE	MS, SE	-	SE *
Processing	-	-	MS, SE	-

**Only Fuchsiana stem ends were collected on collection day 4 for the Cold store stage. SE, Stem ends; MS, Mid stem sections*

4.2.1.1 Statistical analysis

Mid stem and stem end fungal count data did not meet assumptions of normality (Shapiro-Wilk, $p < 0.05$) and were therefore analysed non-parametrically. Differences in fungal counts between H30 and Fuchsiana cultivars for each stage of the supply chain were determined with Wilcoxon tests for both mid stem and stem end sections. Fungal counts for each of the supply chain stages (Harvest, Cold store and Processing; H30 and Fuchsiana data combined) were then analysed using Kruskall-Wallis tests for mid stem and stem end sections separately, followed by pairwise Wilcoxon tests with Benjamini-Hochberg correction for multiple analysis to determine between stage differences. As mid stem and stem end sections were taken from the same flower stems, differences between the fungal counts of mid stem and stem end sections for each supply chain stage were analysed with paired Wilcoxon tests (H30 and Fuchsiana data combined).

4.2.2 Comparison of fungal colony counts on the stem ends of Rosa hybrida cultivars Fuchsiana and H30 on arrival in the UK

Flower stems were harvested and transported as described in 2.1. On arrival at RHUL (prior to rehydration), 2 cm stem sections were taken from the bottom of the flower stems and prepared for Petrifilm plating as described in 2.3.1. YM Petrifilms were plated, incubated and analysed as described in 2.3. YM Petrifilms were taken for stem end sections of Fuchsiana and H30 flower stems in January 2018 and January 2019. For the 2018 collection, 2 stems were chosen at random from five bunches of each cultivar, for a total of 10 stem-end sections for each cultivar. For the 2019 collection, 3 stems were chosen at random from six bunches of each cultivar, for a total of 18 stem-end sections for each cultivar.

4.2.2.1 Statistical analysis

Stem end fungal count data did not meet assumptions of normality (Shapiro-Wilk, $p < 0.05$) and was therefore analysed using non-parametric tests. Stem end fungal counts for *Rosa hybrida* cultivars H30 and Fuchsiana were compared with Wilcoxon tests for both 2018 and 2019 separately. Difference between the stem end fungal counts on arrival in the UK between years 2018 and 2019 for (H30 and Fuchsiana cultivars combined) was also determined with a Wilcoxon test.

4.2.3 Comparison of fungal and aerobic colony counts on the stem ends of Rosa hybrida cultivar H30 on arrival in the UK and after re-hydration

Rosa hybrida cv. H30 flower stems were harvested and transported as described in 2.1. On arrival at RHUL (prior to rehydration), 2 cm stem sections were taken from the bottom of the flower stems and prepared for Petrifilm plating as described in 2.3. Flower stems were then rehydrated for 24 hrs at 5°C as described in 2.1, with 2cm stem end sections also taken after this rehydration period. All aerobic and YM Petrifilms were plated, incubated and analysed as described in 2.3.

4.2.3.1 Statistical analysis

Fungal (YM) counts and bacterial (Aerobic) Petrifilm count data did not meet assumptions of normality (Shapiro-Wilk, $p < 0.05$) and was therefore analysed using non-parametric tests. As YM and Aerobic Petrifilm plates were both sampled from the same stem end sections and from the same stems at each time point, Wilcoxon matched-pairs tests were used to compare YM and Aerobic counts at the arrival and rehydration time points (for both within and between comparisons).

4.2.4 Identification of fungi and bacteria by colony PCR

Bacteria and fungi from the stem-ends and vase water of *Rosa hybrida* cultivars H30 and Fuchsiana were grown on aerobic and YM Petrifilms, with plates prepared and incubated as described in 2.3. Microbial samples were collected from multiple vase life experiments and time points. Plates were prepared from stem ends on arrival in the UK, following re-hydration and at day 1, 7 and 14 of vase life, as well as from vase water on day 14 of vase life. All flower material was harvested and transported as described in 2.1.

4.2.4.1 Growth and preparation

Luria-Bertani (LB) and Malt Extract (ME) broth (Sigma) were made up as 2 % agar plates (100 x 15 mm petri dishes) following manufacturers guidelines. Colonies were isolated from aerobic and YM Petrifilms and transferred to 2 % LB agar or 2 % ME agar plates respectively using a sterile toothpick. Plates were sealed with parafilm and inverted during incubation. Bacterial 2 % LB agar plates were incubated for 2-3 days and fungal 2% ME agar plates incubated for >4 days, both at RT (~ 21 ˚C). ME agar plates were routinely monitored during the incubation period, with colonies sub-sampled onto fresh 2 % ME agar plates when necessary to prevent overgrowth of fast-growing colonies.

Following incubation, established colonies were sampled from the outer growing edge using a sterile toothpick and placed into a sterile 500 µl micro centrifuge tube containing 100 µl of RNase free water. Using the toothpick as a micro pestle, colonies were broken down and mixed with the water to create a suspension.

This colony-water suspension was used directly for PCR or stored at -20 °C until use.

4.2.4.2 Colony PCR

A 50 µl polymerase chain reaction (PCR) was performed using a Flexigene thermo cycler (Techne) with 2 µl of 10 µM forward primer, 2 µl of 10 µM reverse primer, 21 µl of PCRBIO Taq Mix Red (PCRBiosystems) and 21 µl of colony-water suspension (0). PCRBio Taq Mix Red contains Taq DNA polymerase, 6 mM MgCl2, 2 mM dNTPs, as well as 'enhancers', 'stabilisers' and a red tracking dye for electrophoresis. The PCRBio Taq mix Red was used due to the robust buffer composition, capable of amplifying target sequences from colonies without a prior DNA extraction step.

For fungal identification, the nuclear ribosomal internal transcribed spacer (ITS) region was targeted for amplification using fungal specific universal primers ITS1-F (CTTGGTCATTTAGAGGAAGTAA) and ITS4 (TCCTCCGCTTATTGATA TGC). The ITS1-F and ITS4 primer pair amplifies both variable ITS regions, the internal transcribed spacer region 1 (ITS-1) and the internal transcribed spacer region 2 (ITS-2), with targets for the conserved 18S rRNA and 28S rRNA genes respectively (*Figure 25;* Gardes & Bruns, 1993). ITS1-F and ITS4 produce an expected amplicon size of approximately 400 - 900 bp dependent on fungal species. Bacterial 16S rDNA was amplified for bacterial identification, using the 63f (5'-CAGGCCTAACAC ATGCAAGTC-3') and 1492r (5'-GGCTACCTTGTTACGACT T-3') primer pair. Primers 63f and 1492r amplify variable regions 1-9 and have an expected amplicon size of ~ 1400 bp (*Figure 26*).

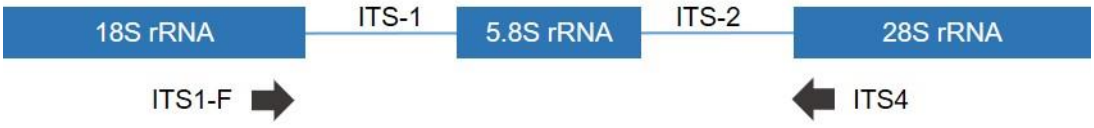

Figure 25. ITS1-F and ITS4 primer annealing sites on fungal rDNA

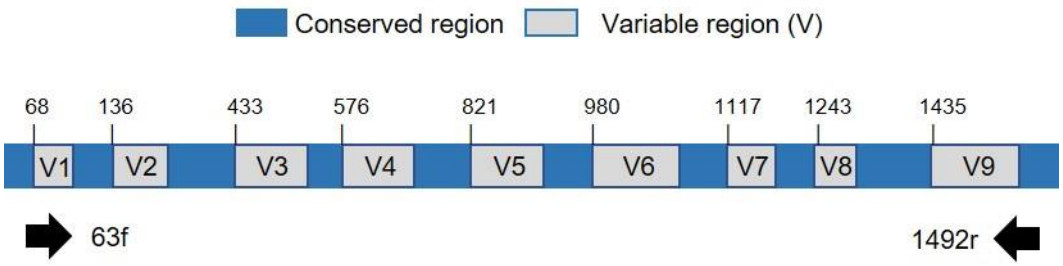

Figure 26. Bacterial 16S rDNA primer annealing sites for primers 63f and 1492r

Colony PCR cycle conditions included an initial 1 min denaturation and enzyme activation step at 95 ˚C, followed by 35 cycles of 15 sec at 95 ˚C denaturation, 15 sec annealing at 55 ˚C for fungal or 50 ˚C for bacterial, and an 8 sec extension at 72 ˚C. PCR products were then held at 4 ˚C after completion of the programme.

4.2.4.3 Gel electrophoresis and sequencing of PCR product

PCR products were loaded directly onto a 1 % agarose gel made up with 1 x Tris-Borate-EDTA (TBE) buffer and stained with (1 µL per 10 mL) SYBR Safe DNA gel stain (Invitrogen). Samples were run alongside the molecular weight marker, Hyperladder 50bp (Bioline) for reference. All PCR amplicons showing a single, clear band of between 400 – 900 bp (fungal) or approximately 1400 bp (bacterial) in length were purified using the Wizard SV Gel and PCR Clean-up System (Promega), following the manufacturer's purification by centrifugation protocol. If significant well contamination or primer dimer could be seen on the electrophoresis gel, then 700 µl of 80 % Ethanol was substituted for the Membrane wash solution in the first wash step, as recommended in the Wizard SV Gel and PCR clean-up System Technical Bulletin.

Purified amplicons were then quantified using a Nanodrop spectrophotometer before being sent for sequencing using Mix2Seq tubes (Eurofins genomics). Mix2Seq tubes were prepared following the manufacturer's guidelines with the purified DNA concentration adjusted with RNAse free water (concentration dependent on amplicon size) and pre-mixed with the appropriate forward primer (ITS1-F or 63f).

4.2.4.4 Identification of sequences using Blastn

Sequences were uploaded onto the National Center for Biotechnology Information (NCBI) website, within the Nucleotide Basic Local Alignment Search Tool (BLASTn) suite for targeted loci and searched against the ITS database for fungal sequences, or the 16S ribosomal RNA sequences database (Bacteria and Archaea) for bacterial sequences. Uncultured and environmental sequences were excluded and the megablast algorithm was used to find highly similar sequences. Output was limited to a maximum of 10 target sequences per entry sequence. For ITS and 16S rRNA sequences, a 97 % and a 99 % identity cut off were used for species level identification respectively (Blaalid et al., 2013; Janda & Abbott, 2007). Both ITS and 16S rRNA sequences which were below the species level identity threshold but had ≥95 % identity were recorded to a genus level (Yarza et al., 2014). A BIT score threshold of >200 was also applied to all sequences.

4.2.5 Addition of three concentrations of the bacteria Pseudomonas fluorescens *to the vase water of* Rosa hybrida *cultivars H30 and Fuchsiana*

Rosa hybrida cv. H30 and Fuchsiana flower stems were harvested, transported and processed as described in 2.1. Following re-hydration, stems were placed in individual vases (1 stem per vase) with a total of 10 stems of each cultivar per vase water condition. Vase water conditions included three different concentrations of *Pseudomonas fluorescens* cultures in 100 mL of 2 % sucrose solution and 100 mL of 2 % sucrose solution with no microbial addition as the vase water control.

Pseudomonas fluorescens cultures were transferred from frozen glycerol stocks, to 2 % LB broth and incubated for 24 hours at 28 ˚C, shaken at 200 rpm. Following incubation, cultures were spun at 500 x g (RCF) for 10 mins in a chilled centrifuge. The growing medium was then carefully poured off and the sediment microbial cells re-suspended in a 2 % sucrose solution. The liquid culture was initially counted using a haemocytometer, before being adjusted and added to the vase water for three incremental 10-fold concentrations of 1.9×10^5, 1.9×10^6 and 1.9

x 10^7 (cfu per mL). Final inoculation colony counts were determined by aerobic Petrifilm analysis through a serial dilution in physiological saline as described in 2.3.

The number of stems at each necking stage (Straight, <90° and >90°) were recorded for each vase water treatment on day 3 of vase life.

4.2.5.1 Statistical analysis

A Cumulative Link Model (CLM) using the R package ordinal v2019.12-10 (Christensen, 2019) was used to analyse the necking stages of stems within each of the vase water conditions. A CLM is a form of ordinal generalised link model used when one of the dependent variables has a ranked order, i.e. necking stage Straight is less than necking stage <90°, which is less than necking stage >90°. A default logit link function was used for a proportional odds model due to the proportional nature of the data. Interaction and statistical significance were determined by removing terms sequentially and with an analysis of deviance (type II) test. Significance of the vase water conditions on each of *Rosa hybrida* cultivars was further tested independently with Kruskall-Wallis tests and pairwise Wilcoxon tests with Benjamini-Hochberg correction for multiple comparisons. Non-parametric tests were used for analysis due to the necking data being ordinal and therefore unsuitable for analysis with conventional parametric tests.

4.2.6 Addition of bacteria and fungi to the vase water of Rosa hybrida *cultivars H30 and Fuchsiana*

Rosa hybrida cv. H30 and Fuchsiana flower stems were harvested, transported and processed as described in 2.1. Following re-hydration, stems were placed in individual vases (1 stem per vase) with a total of 10 stems of each cultivar per vase water condition. Bacterial and fungal additions were prepared as described below (*4.2.6.1; 4.2.6.2*), with 100 mL of 2 % sucrose solution with no microbial addition as the control condition. The number of stems at each necking stage (Straight, <90° and >90°) were recorded for each vase water treatment on day 4 of vase life.

4.2.6.1 Bacterial vase water addition

Pseudomonas fluorescens (bacterial) cultures were transferred from frozen glycerol stocks and were grown as described in 4.2.5. Re-suspended *P. fluorescens* cultures were added to individual vases containing 2 % sucrose solution for a total volume of 100 mL at a vase water concentration of 8.3×10^6 (cfu per mL)

4.2.6.2 Fungal vase water additions (yeast and mould)

Papilotrema flavescens and *Neocosmospora rublicola* fungal cultures were isolated from the stem end and vase water of *Rosa hybrida* cv. H30 respectively on YM Petrifilms (2.3) and were identified as described in 4.2.4. *P. flavescens* (formerly *Crytococcus flavescens*) is a basidiomycota-yeast and was chosen for its growth as a yeast in culture. The fungal ascomycete species *N. rublicola* was chosen its fast growth and as a representative filamentous fungi. *P. flavescens* and *N. rublicola* will further be referred to as yeast and mould species respectively for distinction between the two growth habits.

Papiliotrema flavescens cultures were grown on 2% malt extract (ME) agar at room temperature (RT) and transferred to 2 % ME broth using a sterile plastic inoculation loop. *P.flavescens* cultures were then grown and prepared as previously described (*4.2.5*). Re-suspended *P. flavescens* cultures were added to individual vases containing 2 % sucrose solution for a total volume of 100 mL at a vase water concentration of 3.4×10^5 (cfu per mL).

Neocosmospora rublicola cultures were grown on 2% ME agar plates at room RT. A 2 mm core was taken from the outer growing edge of the hyphae using a unicore punch (GE Healthcare; sterilised with absolute ethanol) and added directly to the individual vases containing 100 mL of 2 % sucrose solution for an initial vase water concentration of 1.1×10^5 (cfu per mL).

Control vases, with no flower stems were set up for each vase water condition. Water samples (1 mL) were collected from each of the vase water controls at the start of the experiment, serially diluted with physiological saline and plated on aerobic and YM Petrifilms to determine initial vase water colony counts (2.3).

4.2.6.3 Statistical analysis

Data was analysed as previously described in section *4.2.5.1*.

4.3 Results

4.3.1 Fungal Petrifilm audit of the Kenyan supply chain

No significant difference was found between the mid stem fungal colony counts of Fuchsiana and H30 at each stage of the supply chain, or between Fuchsiana and H30 stem end sections at each stage of the supply chain ($p > 0.05$; Table *7*). By combining the count data for both H30 and Fuchsiana, stage of supply chain was found to have a significant effect on the fungal colony counts found for mid stem ($X^2_{2, N = 30} = 14.77$, $p < 0.001$) and stem end ($X^2_{2, N = 39} = 22.06$, $p < 0.001$) sections. For the stem end sections, fungal colony counts were found to increase at each stage of the supply chain, with significant difference found between harvest, cold store and processing stages ($p < 0.05$; *Figure 27*). Although mid stem fungal colony counts found only found to be statistically higher during the processing stage of the supply chain, compared to fungal colony counts found at harvest and following cold storage ($p < 0.05$; *Appendix 1.2.2.1*) a similar trend could be seen for both mid stem and stem end colony counts at each stage of the Kenyan supply chain (Figure 27). However, stem end sections were found to have a significantly greater number of fungal colonies at each stage compared to mid stem sections ($p < 0.05$; *Figure 28; Appendix 1.2.2.1*).

Table 7. Comparison of fungal counts for H30 and Fuchsiana stem sections

	Mid Stem	Stem end
Harvest	W = 28, p >0.05	W= 18, p >0.05
Cold store	W = 26, p >0.05	W = 38, p >0.05
Processing	W = 5, p >0.05	W = 5, p >0.05

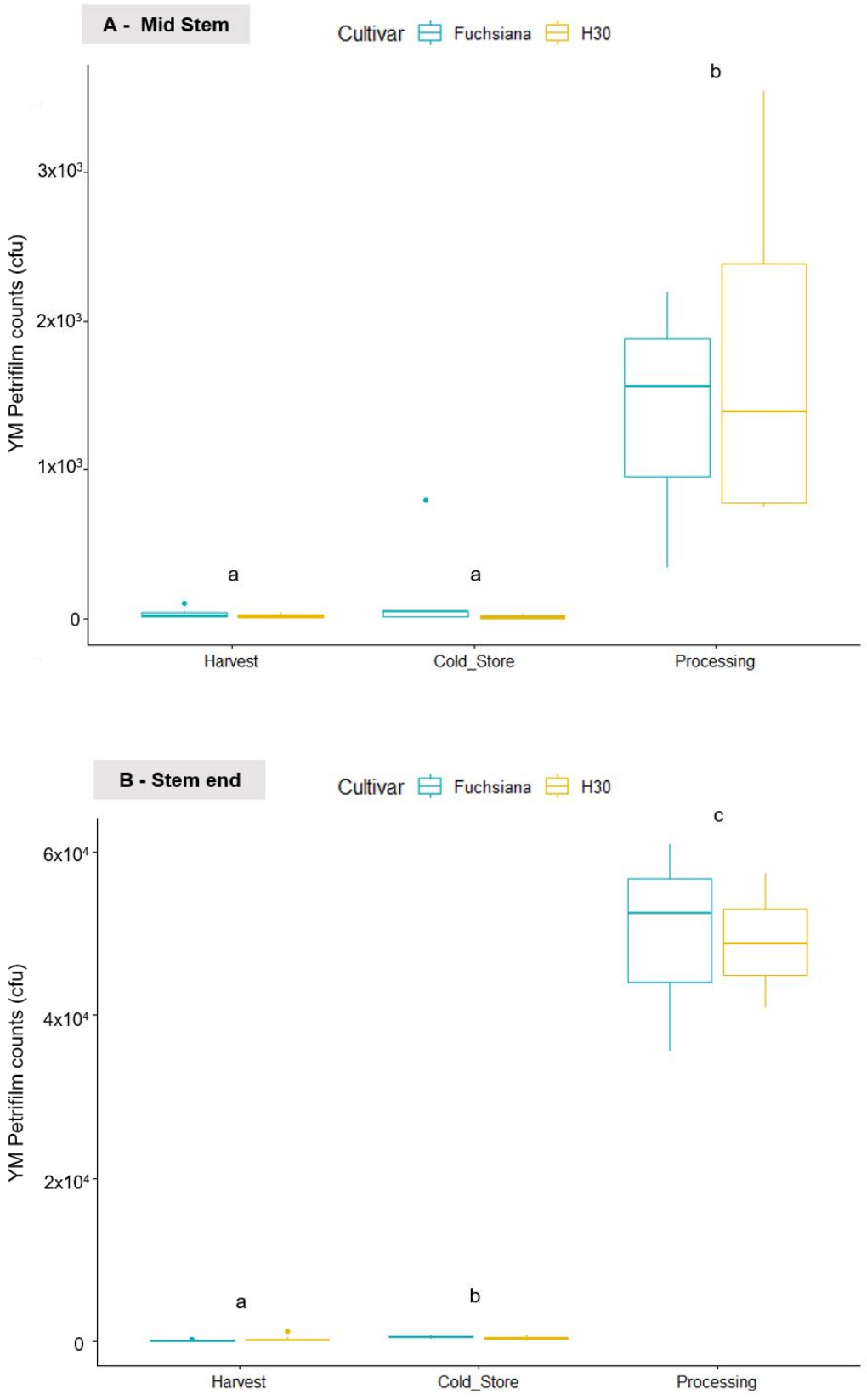

Figure 27. Fungal colony counts for each cultivar at different stages of the Kenyan supply chain. A, mid-stem sections; B, stem end sections. Statistical difference between the stages was determined by a Kruskal-Wallis non-parametric test followed by a pairwise Wilcoxon test ($p < 0.05$). Stages with the same letter are not significantly different. Cfu, colony forming units. (n= 3 – 9 stems of each cultivar dependent on stage, see Table 6*)*

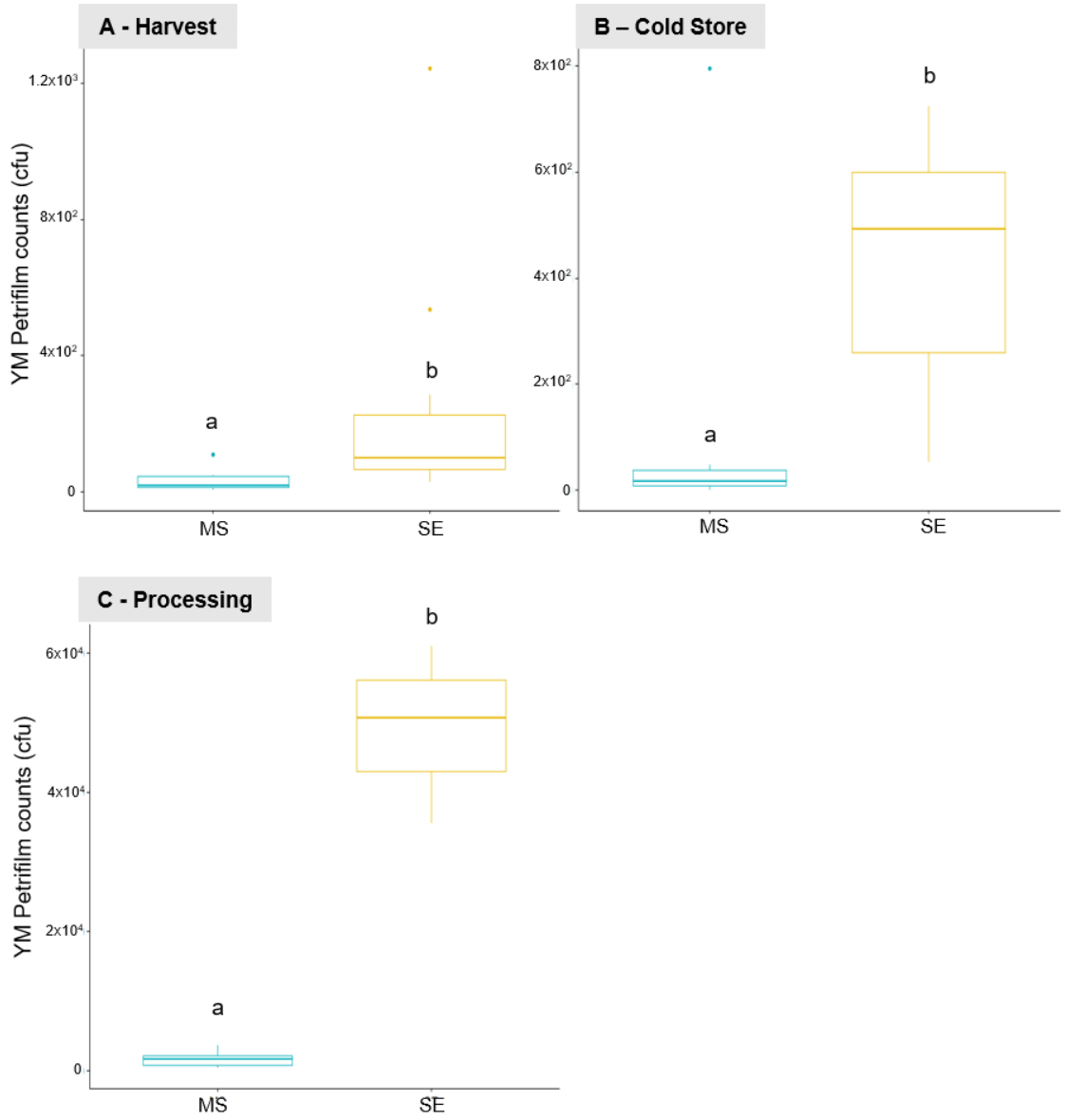

Figure 28. Fungal colony counts for mid-stem and stem-end sections Boxplot A, B and C represent fungal counts taken for stem sections at harvest, cold store and processing stages respectively. MS, mid stem; SE, stem end. Statistical difference between the YM colony counts on mid stem and stem end sections was calculated with paired Wilcoxon tests (p <0.05). Stem sections with the same letter are not significantly different. n=12 for harvest and cold store, n=6 for processing

4.3.2 Comparison of fungal colony counts on the stem ends of Rosa hybrida *cultivars Fuchsiana and H30 on arrival in the UK*

No significant difference was found between the fungal colony counts of Fuchsiana and H30 on arrival at RHUL for either of the 2018 (W= 36.5, p >0.05) or 2019 collections (W = 215.5, p >0.05; *Figure 29*). Overall fungal colony counts

between the two collection periods (2018 and 2019) were also not significantly different (W = 268.5, p >0.05).

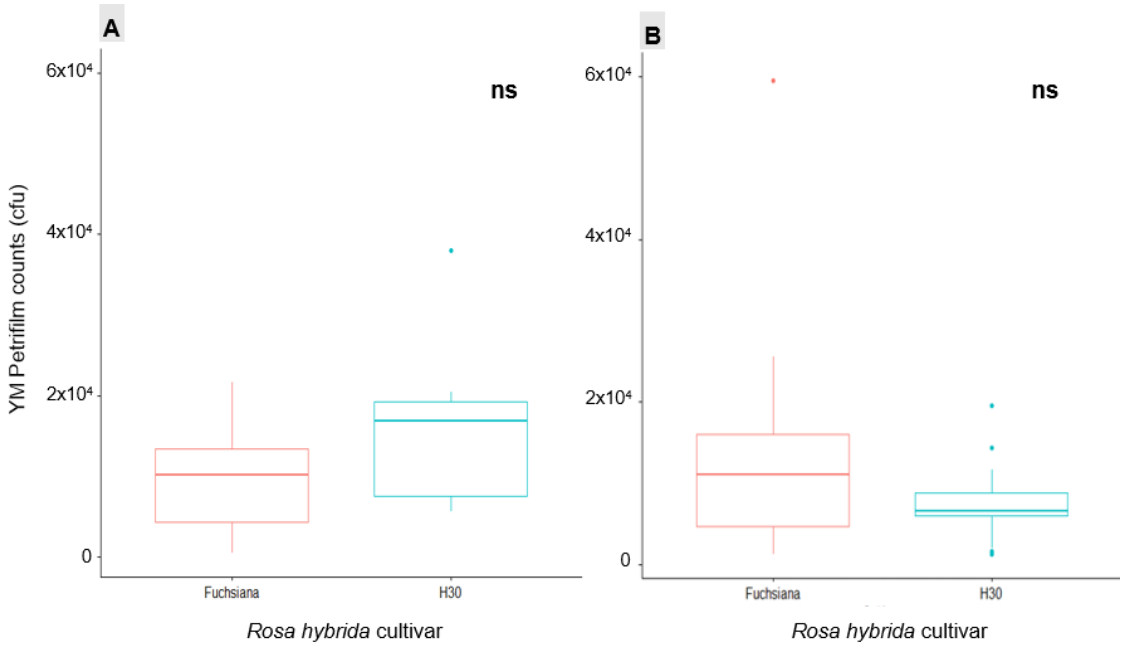

Figure 29. Fungal colony counts from Fuchsiana and H30 stem ends prior to rehydration. Boxplot A is data from January 2018 and boxplot B is data from January 2019. No significant difference (ns) was found with a non-parametric Wilcoxon test. n = 10 (2018); n= 18 (2019).

4.3.3 Comparison of fungal and aerobic colony counts on the stem ends of Rosa hybrida *cultivar H30 on arrival in the UK and after re-hydration*

No significant difference was found between aerobic (bacterial) and YM (fungal) colony counts on H30 stem ends at arrival (V= 22, p >0.05; *Figure 30A*). However, aerobic colony counts were found to be significantly higher than YM colony counts following re-hydration (V = 65, p <0.05; *Figure 30B)*. Aerobic and YM colony counts on the stem ends of H30 significantly reduced following re-hydration compared to on arrival (V = 66, p <0.05; *Figure 31*), with both aerobic and YM colony counts falling from a mean count of 32,000 on arrival to 2,400 and 300 respectively following rehydration (all to 2 significant figures).

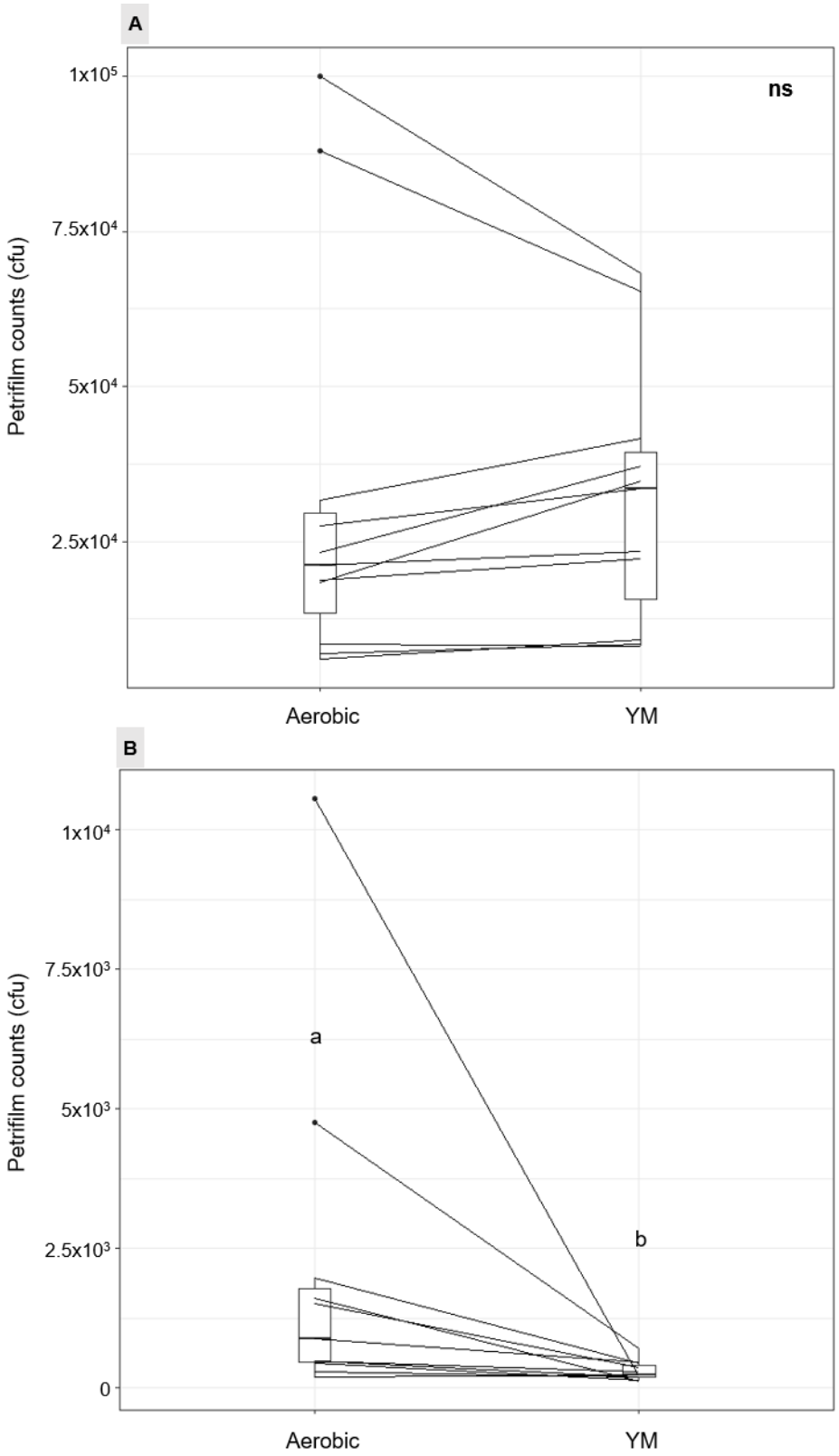

Figure 30. Bacterial and fungal colony counts of stem-end section at arrival to the UK and following rehydration. Paired boxplot A shows aerobic (bacterial) and YM (fungal) colony counts on arrival, and boxplot B shows counts following rehydration. Lines connect paired counts taken from the same stem end sections. Significant difference was calculated with a Wilcoxon matched-pairs test ($p < 0.05$), with significance between groups shown by differing letters and no significance shown by an 'ns'. n= 11.

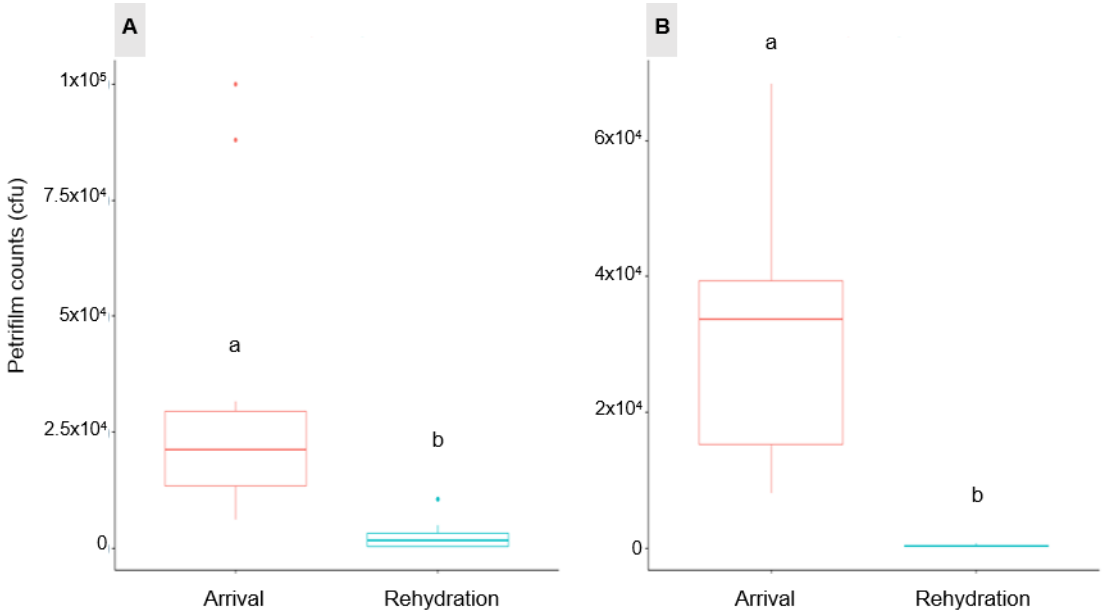

Figure 31. Colony counts on the stem-ends of Rosa hybrida *cv. H30 at arrival to the UK and following rehydration. Boxplot A shows aerobic (bacterial) colony counts and boxplot B shows YM (fungal) colony counts. Significant difference was calculated with a Wilcoxon matched pairs test (p <0.05), with significance between groups shown by differing letters. n= 11.*

4.3.4 Identification of fungi and bacteria by colony PCR

A total of 30 species of fungi were identified from the stem ends and vase water of *Rosa hybrida* cultivars Fuchsiana and H30 using ITS primers ITS1-F and ITS4, with species spanning 20 genera and 14 families of fungi (Table 8; Table 9). Comparatively fewer bacterial than fungal species were identified, with a total of 24 bacterial species identified using the amplified 16S rDNA 63f and 1492r primer region. Of these identified species only three were classified as gram-positive, with the majority of species found to be gram-negative (Table *10*; Table *11*). *Pseudomonas* made up the largest genera of gram-negative bacteria, with nine different species identified from stem ends and vase water of *Rosa hybrida* cultivars H30 and Fuchsiana. Pseudomonadaceae and Enterobacteriaceae families were found to have the largest number of identified species, with nine species identified from seven different genera in the family Enterobacteriaceae (Table 10).

Table 8. Identified fungal species (yeasts)

Family	**Genus/ species** (Closest match in database)
Bulleribasidiaceae	
	Vishniacozyma:
	V. carnescens
	*V. species **
Debaryomycetaceae	
	Debaryomyces prosopidis
Filobasidiaceae	
	Filobasidium magnum
Saccharomycetaceae	
	Candida:
	C. saitoana
	*C. species **
	Hyphopichia burtonii
	Kazachstania exigua
	Zygotorulaspora florentina
Sporidiobolaceae	
	Rhodotorula:
	R. babjevae
	R. diobovata
	*R. species **
Tremellaceae	
	Holtermanniella festucosa
	Papiliotrema:
	P. flavescens
	P. laurentii
Wickerhamomycetaceae	
	Wickerhamomyces anomalus

*sequences were not identified beyond genus level

Table 9. Identified fungal species (filamentous fungi)

Family	**Genus / species** (Closest match in database)
Cordycipitaceae	
	Beauveria bassiana
Cystobasidiaceae	
	Cystobasidium slooffiae
Davidiellaceae	
	Cladosporium
	C. colombiae
	C. cycadicola
	C. macrocarpum
	C. pini-ponderosae
	C. puyae
Nectriaceae	
	Neocosmospora rubicola
Plectosphaerellaceae	
	Gibellulopsis:
	G. nigrescens
	G. piscis
	G. simonii
Trichocomaceae	
	Paecilomyces hepiali
	Penicillium:
	P. kongii
	P. rubens
	P. salami
Trichosporonaceae	
	Apiotrichum dehoogii
	Cutaneotrichosporon dermatis

Table 10. Identified bacterial gram-negative rods

Family	**Genus / species** (Closest match in database)
Burkholderiaceae	
	Burkholderia vietnamiensis
Enterobacteriaceae	
	Citrobacter:
	C. youngae
	Kluyvera intermedia
	Pantoea:
	P. agglomerans
	P. ananatis
	Rahnella:
	R. aquatilis
	R. woolbedingensis
	Raoultella planticola
	Rouxiella chamberiensis
	Serratia quinivorans
Moraxellaceae	
	Acinetobacter:
	A. johnsonii
	A. lactucae
Pseudomonadaceae	
	Pseudomonas:
	P. azotoformans
	P. helmanticensis
	P. koreensis
	P. lactis
	P. lutea
	P. marginalis
	P. putida
	P. tolassii
	P. trivalis

Table 11. Identified bacteria gram-positive rods

Family	**Genus / species** (Closest match in database)
Bacillaceae	
	Bacillus:
	B. licheniformis
Leuconostocaceae	
	Weissella soli
Microbacteriaceae	
	Microbacterium proteolycticum

4.3.5 Addition of three concentrations of Pseudomonas fluorescens *to the vase water of H30 and Fuchsiana*

A cumulative link model (CLM) of the data found both vase water condition ($X^2_{3, N= 80}$ = 40.35, p <0.05) and cultivar ($X^2_{1, N= 80}$ = 42.05, p <0.05) to have a significant effect on the necking stages of stems at day four of vase life. Indicating significant difference between the response of H30 and Fuchsiana stems to the *Pseudomonas fluorescens* vase water additions.

The addition of *P. fluorescens* at an initial vase water concentration of 1.9 x 10^6 (cfu) or above was found to significantly increase the incidence of necking (including stages <90° and >90°) in the *Rosa hybrida* cultivar H30 compared to the sucrose control at day 4 of vase life ($F_{3, 38}$ = 19.36, p < 0.05; *Figure 32B*). Necking was also seen to be significantly induced by the addition of *P. fluorescens* cultures in the *R. hybrida* cultivar Fuchsiana by day 4 of vase life, but

only with an initial vase water concentration of 1.9 x 10^7 (cfu) ($F_{3, 38} = 15.72$, $p < 0.05$; *Figure 32A; Appendix 1.2.2.2*).

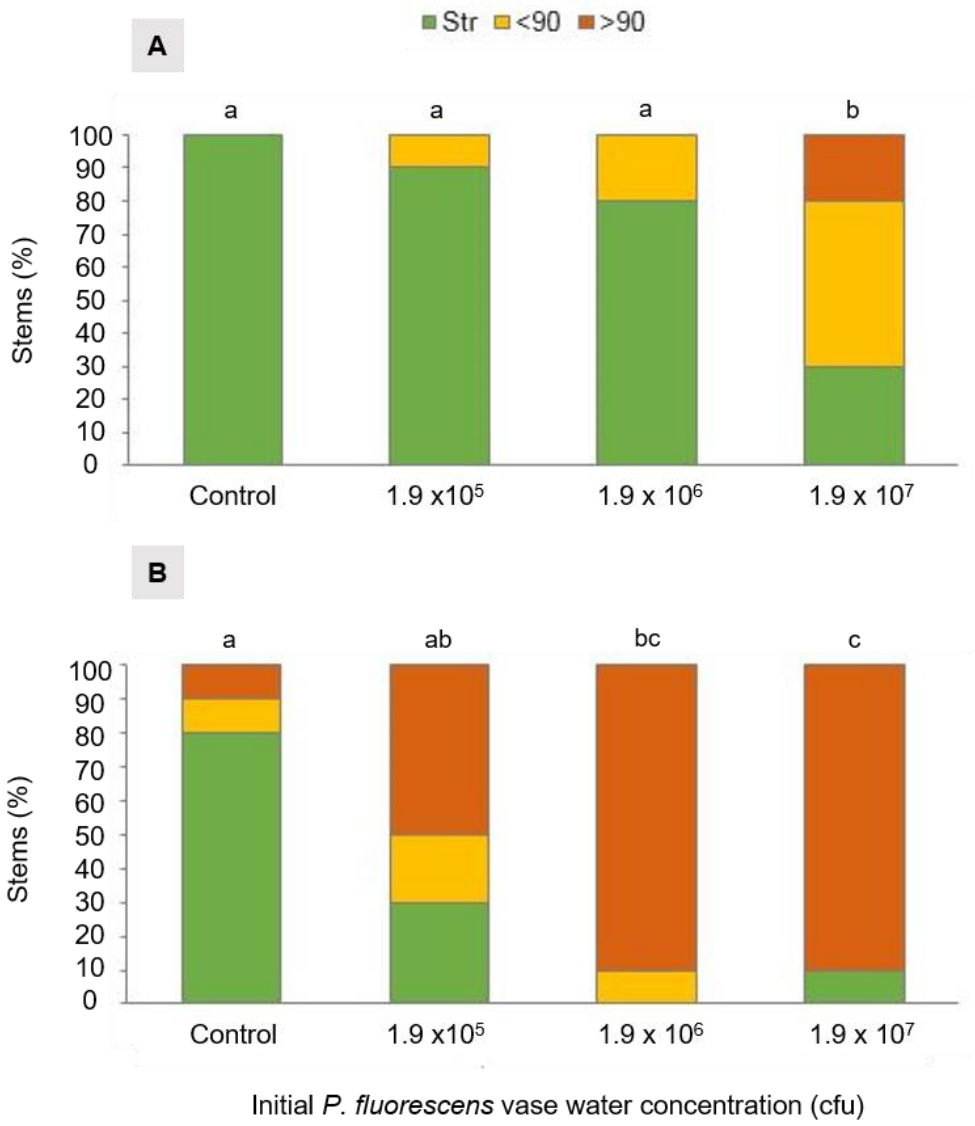

Figure 32. Incidence of necking stages at day 4 of vase life for each P. fluorescens vase water concentration. A, Fuschiana; B, H30. Str, straight stems with no bending; <90°, bending of less than 90°; >90°, bending of equal to or more than 90°. Statistical difference between the vase water concentrations was determined by a Wilcoxon test with Benjamini-Hochberg correction for multiple comparisons (p <0.05). Concentrations with the same letter show no significant difference in the number of stems at each stage (Str, <90°, >90°). Cfu, colony forming units. n=10 stems

4.3.6 Addition of bacterial and fungal species to the vase water of H30 and Fuchsiana

A cumulative link model (CLM) of the bacterial and fungal addition data for H30 and Fuchsiana also showed both vase water condition ($X^2_{3, N= 80}$ = 46.34, p <0.05) and cultivar ($X^2_{1, N= 80}$ = 29.87, p <0.05) to be significant factors affecting the necking stage of stems on day 3 of vase life. Indicating significant difference between the response of H30 and Fuchsiana stems to vase water additions, with H30 stems more likely to show increased stages of necking than Fuchsiana stems at day 3 of vase life as seen by the positive shift in letent distributions (+ 2.97 σ* scale units) for H30 stems relative to Fuchsiana.

Due to different initial concentrations, the different microbial additions cannot be directly compared, with *Pseudmonas fluroescens*, *Neocosmospora rubicola* and *Papilotrema flavescens* added at initial vase water concentrations of 8.3 x 10^6, 1.1 x10^5 and 3.4 x10^5 cfu per mL respectively. However, the addition of *Neocosmospora rubicola* (mould), *Papilotrema flavescens* (yeast) and *Pseudomonas fluorescens* (bacteria) all significantly increased the incidence of necking in *Rosa hybrida* cultivar H30 compared to the sucrose control ($F_{3, 38}$ = 32.85, *p* <0.05). Whereas, in cv. Fuchsiana, necking was only found to be signifcantly induced by *Pseudmonas fluorescens* ($F_{3, 38}$ = 27.17, *p* < 0.05, *Figure 33, Appendix 1.2.2.3*).

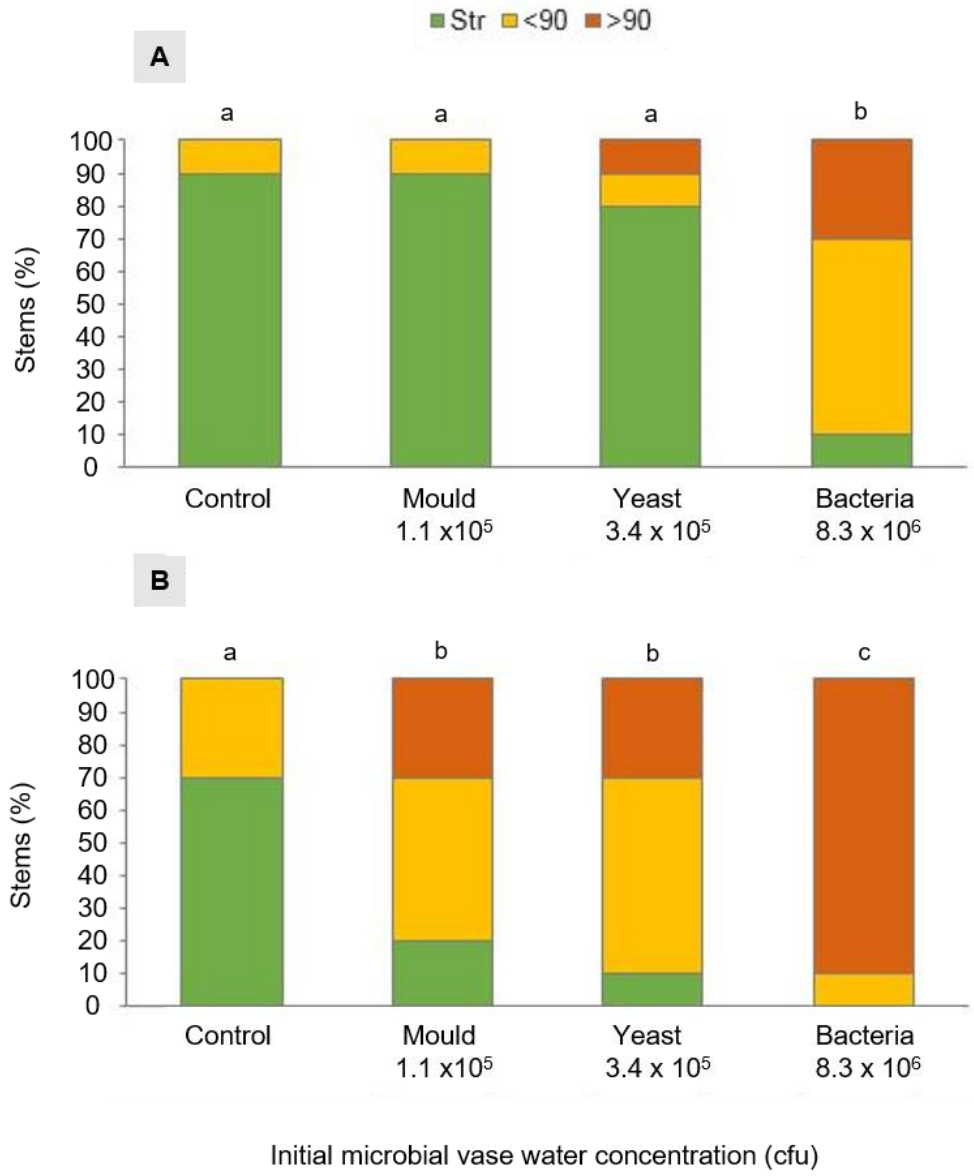

Figure 33. Incidence of necking at day 3 for each microbial vase water addition. A, Fuchsiana; B, H30. Mould, Neocosmospora rubicola*; Yeast,* Papilotrema flavescens*; Bacteria,* Pseudomonas florescens*. Str, Straight stems with no bending; <90°, stem bending of less than 90˚; >90° = stem bending equal to or more than 90°. Statistical difference between the vase water additions was determined by a Wilcoxon test with Benjamini-Hochberg correction for multiple comparisons (p <0.05). Vase water conditions with the same letter are not significantly different. Cfu, colony forming units.*

4.4 Discussion

4.4.1 Fungal colony counts of the Kenyan supply chain

Analysis of the Kenyan supply chain identified the presence of fungi at each of the three stages analysed for both Rosa hybrida cv. H30 and Fuchsiana (Table *5*; *Figure 27*). However, colony counts were found to be much higher at the processing stage where stems were arranged into bunches for dry transport to the UK (*Figure 28)*. This suggests that handling practices at the processing stage incur an increased amount of microbial contamination. Cutting equipment is known to be a potential source of introduced contamination (Laird et al., 2005; van Doorn & de Witte, 1997) and may have resulted in the increased number of fungi on the stem ends following processing, as stems were re-cut to a uniform length during bunching. However, as both the mid and stem end sections showed a significant increase in fungal counts at the processing stage (*Figure 27*), contaminated cutting equipment is unlikely to have been the sole source as this would only have affected the stem end. An increase in fungal counts on the mid stem sections may therefore be due to the handling of stems (i.e. with contaminated gloves), further leaf or thorn removal with contaminated equipment or due to placement on contaminated benches. However, fungal counts on these potential sources were not analysed and would need to be determined in further work.

Damaged or wounded tissue is a better substrate for the growth of opportunistic microorganisms (Zagory, 1999). Leaf removal and de-thorning practices prior to cold storage may therefore result in increased microbial growth on the stem during the processing stage where temperatures are warmer (for an improved working conditions of the processing staff) and is another possible explanation for the increased number of fungi seen following processing.

The difference in counts between the mid stem and stem end sections found at each stage of the supply chain may also be attributed to the presence of an exposed layer of damaged tissue at the cut surface of the stem end, where bacteria and fungi have been shown to rapidly accumulate (*Figure 28;* Put & Clerkx, 1988; van Doorn et al., 1991; Clerkx et al., 1989; Put et al., 2001). Fewer

microbial cells have also been found inside the xylem vessels of cut roses at increasing heights between the stem end and the flower head due to the limited infiltration ability of microorganisms to travel up the stem (Put & Clerkx, 1988; van Doorn et al, 1991; Put & van Meyden, 1988).

4.4.2 Fungal colony counts on arrival in the UK for cv. H30 and Fuchsiana

No differences in fungal counts were seen between the two cultivars H30 and Fuchsiana upon arrival in the UK (*Figure 29*). This indicates that there was no preferential growth of fungi on either cultivar when subjected to the same processing practices and supply chain variables (i.e. temperatures during transport to UK).

4.4.3 Fungal and aerobic colony counts on stem ends of cv. H30 on arrival and following rehydration

In this study, bacterial and fungal counts on cv. H30 were found to decrease in number between arrival in the UK and following rehydration with a 92 % and 99 % reduction in counts respectively (*Figure 31*). However, the numbers shown for rehydration represent counts from a 'new' stem end section, as initial stem ends were removed upon arrival (and used for arrival counts). In the Kenyan supply chain, mid stem sections had consistently lower fungal counts than stem end sections (*Figure 28*). This may explain the reduced number of bacteria and fungi following rehydration as rehydration stem sections were technically taken from a higher point up the stem than at arrival. The exposed cut surface of the rehydrated stem end was also cut with a sterile razor blade and therefore may have had a lower number of introduced microorganisms onto the cut surface than the original (arrival) stem end section. Additionally, placement of the flower stems in water for rehydration may have led to a proportion of microbial cells being washed into the solution, resulting in a reduced microbial load on the stem end.

Put & Clerkx, (1988) found that *Bacillus* and *Pseudomonas* cells adhered to the xylem vessel walls of cv. Sonia rose stems, but both *Fusarium* microconidia and *Kluyveromyces* cells were unattached. The higher number of bacteria than fungi found in this study following re-hydration may therefore be due to the adherent

capacity of bacterial cells compared to fungi (yeasts and conidia), meaning more fungal cells may have been washed off upon placement in water than bacterial cells (*Figure 30*).

Previous studies which reported fungal counts found fungi to be less prevalent or present in very low numbers in the vase water or on the stem ends of cut roses during vase life compared to bacteria (Li et al., 2015; Put & Clerkx, 1988; van Doorn et al., 1991). The proportionally lower number of fungi compared to bacteria following rehydration is therefore somewhat consistent with data from literature, as fungal counts would have been lower than bacterial counts on entering the vase (*Figure 30*).

However, reported figures for microbial counts have all derived from stems harvested and taken directly to the lab for vase life studies, were they have often been treated aseptically (de Witte & van Doorn, 1988; Li et al., 2015; Put & Clerkx, 1988; van Doorn et al., 1991). These figures are therefore unlikely to be representative of actual bacterial and fungal numbers present on the stems received by consumers. As large numbers of microbial contamination may be introduced at the UK rehydration, processing and supermarket stages which were not tested in this study.

4.4.4 Identification of fungi and bacteria by colony PCR

Many *Pseudomonas* species have previously been identified by Put (1990), van Doorn et al. (1991) and de Witte & van Doorn (1988) and are thought to be the predominant genera associated with cut roses. Although only the Pseudomonas species *P. putida* was found in common with these studies, a large number of *Pseudomonas* species were also isolated from Kenyan grown *R. hybrida* stems (Table *10*; *Figure 34*). Isolation of *Citrobacter* and *Pantoea* species is also in line with previous research, however both *Citrobacter youngae* and *Pantoea anatis* are thought to be novel to this study (Put, 1990; van Doorn et al., 1991). Although previously found by Put (1990), de Witte and van Doorn (1988) and van Doorn (1991), no *Aeromonas*, *Alcaligens*, *Enterobacter* (excluding what is now known as *Pantoea*), *Flavobacterium* or *Corynebacteria* species were identified. However, bacteria in the genera *Burkholderia, Kluyvera, Rahnella, Raoultella*,

Rouxiella, Serratia, Microbacterium and *Weissella* were identified in this study and are not thought to have previously been isolated from cut *R.hybrida* flower stems (Table *10*; Table *11*; *Figure 34*).

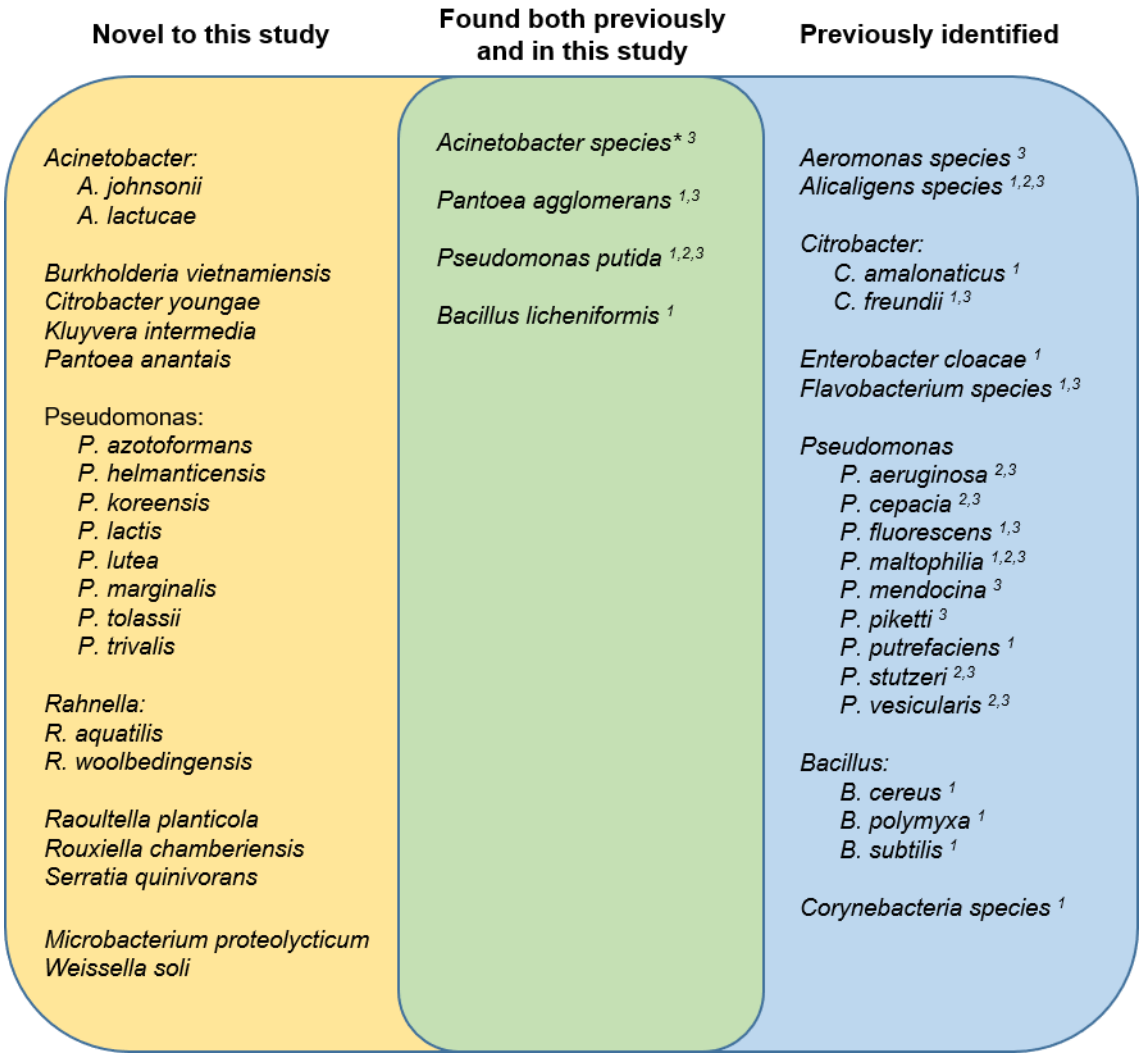

Figure 34. Comparison of bacteria identified in this study compared to those identified previously by Put (1990)[1], de Witte & van Doorn (1988)[2] and van Doorn et al. (1991)[3].

Fungal species from the genera *Candida, Cladosporium, Penicillium and Rhodotorula* were found in this study as well as by Put (1990) and Muñoz et al. (2019). However, this is thought to be the first study to report findings of *Vishniacozyma, Debaryomyces, Filobasidium, Hyphopichia, Kazachstania, Zygotorulaspora, Holtermanniella, Papilotrema, Wickerhamomyces, Beauveria, Cystobasidium, Neocosmospora*, *Gibellulopsis*, *Paecilomyces*, *Apiotrichum* and *Cutaneotrichosporon* species associated with cut rose stems (Table 8; Table 9).

Differences in species and genera of bacteria and fungi found are likely to be due to different growing conditions and due to natural variances in microflora, as cited studies were either based on roses grown in The Netherlands (Put, 1990; van Doorn et al., 1991; de Witte & van Doorn, 1988) or in Colombia (Muñoz et al., 2019) rather than in Kenya. Many Kenyan rose farms have also recently adopted an integrated pest management (IPM) approach to control insect pests and microbial pathogens, in a movement away from widespread spraying of produce with insecticides and fungicides (Gacheri et al., 2015). The entomopathogenic fungus *Beauveria bassiana* is a biocontrol against rose insect pests including rose aphid (*Macrosiphum rosae*), thrips and whiteflies and is a listed product supplied by Kenyan IPM company Dudutech (BEAUVITECH® WP) (Sayed et al., 2019; Gao et al., 2012; Wraight et al., 2000). *B. bassiana* may therefore have been identified from Kenyan grown rose stems due to its use on roses as a biocontrol agent rather than due to natural occurrence (Table *9*).

Many species isolated in this study including *Wickerhamomyces anomalus* (formerly *Saccharomyces anomalus*, Hansenula anomala and Pichia anomala), *Pantoea agglomerans* (formerly *Erwinia herbicola*), *Burkholderia vietnamiensis*, *Bacilius licheniformis* and *Candida saitoana* are known to have antibacterial or antifungal activity and have been used to control the growth of plant pathogenic species (Passoth et al., 2006; Fredlund et al., 2002; Özaktan & Bora, 2004; Compant et al., 2008; Govender et al., 2005; Arras et al., 2006). These species may therefore have potential biocontrol applications post-harvest in controlling microbial growth on cut *R. hybrida* stem ends and could be an interesting avenue for further research. However, their potential to cause xylem occlusions and infiltration abilities would also need to be considered.

Although sequencing techniques were adopted to identify the bacterial and fungal species, identification of micro-organisms in this study still relied on initial plating of cultures. Plating requires the microorganisms to grow on a culture media, however it is thought that the majority (99.5 – 99.9 %) of soil bacteria cannot be isolated and cultured in vitro (Torsvik et al., 1990; Turner et al., 2013). The isolated cultures may therefore only account for a very small proportion of total microorganisms present and an entirely molecular approach such as microbiome

sequencing (metagenomics) may be worth exploring in further study, to provide a broader view of the microbial diversity associated with cut rose stems (Turner et al., 2013). In particular, it would be interesting to analyse potential differences in the microbiome of *R. hybrida* stems exhibiting necking compared to straight (control) stems and also between necking susceptible and necking tolerant cultivars.

4.4.5 Addition of microorganisms to vase water of cv. H30 and Fuchsiana

The vase life of cut roses is known to naturally vary between cultivars under sterile conditions as well as in response to bacteria in the vase water, with some cultivars more affected than others (Laird et al., 2005). In this study, the addition of *Pseudomonas fluorescens* at different initial concentrations differentially induced necking between two cultivars of *R. hybrida*, with cv. H30 showing full >90° necking in 90 % of stems by day 4 of vase life following the addition of 1.9 x 10^6 cfu per mL *P. fluorescens*. In contrast, cv. Fuchsiana roses only showed <90° necking in 20 % of stems at day 4 of vase life under the same conditions. However, the addition of *P. fluorescens* at 1.9 x 10^7 did increase the occurrence of necking stages <90° and >90° in Fuchsiana rose stems compared to controls. This highlights that poor control of microbial numbers in the supply chain will have a greater effect on the occurrence of necking in necking susceptible cultivars such as H30, however, necking tolerant cultivars will also terminate prematurely due to necking at increased levels. Reduced contamination in the supply chain is therefore vital to reduce post-harvest waste and reduced vase life for consumers.

Addition of the fungal species *Neocomospora rubicola* and *Papilotrema flavescens* to the vase water of cv. H30, even at a lower colony count (compared to bacteria) also increased the incidence of necking stages (<90° and >90°) compared to controls by day 3 of vase life. Therefore, even if fungi occur at lower levels on the stem ends and in the vase water of cut rose stems, they are still likely to significantly increase the occurrence of necking in necking susceptible cultivars and have a cumulative effect with bacterial numbers. Determination of microbial counts on the stem end should therefore be considered in terms of bacteria and fungi and not just bacteria.

4.5 Conclusions

Fungi were identified on rose stems at each stage of the Kenyan supply chain and were not significantly different from bacterial numbers on arrival in the UK. However, as found with other studies, numbers of fungi at the start of vase life are likely to be lower than bacteria based on colony counts following rehydration. For the necking susceptible cultivar H30, both a yeast and a filamentous fungus at 10^5 cfu per ml were found to induce necking and cause premature termination of stems. This highlights the importance of maintaining both low bacterial and fungal levels.

As the two cultivars H30 and Fuchsiana were not found to have differing microbial counts on arrival in the UK and showed varying responses to the microbial additions, necking susceptibility between the two cultivars is unlikely to be due to differences in the number of microorganisms on the stem end. However, it is currently unknown if different microbial species are associated with each of the cultivars and if species composition affects the occurrence of necking within cultivars. As colony PCR and sequence identification of microbial species still requires culturing methods, microbiome sequencing is recommended for further analysis of stem end microflora.

Chapter 5 A transcriptome analysis of peduncle necking in cut *Rosa hybrida* cultivar 'H30'

Part of this chapter has been published and is appended to this thesis:
Lear, B.G.A., Marchbank, A., Kent, N.A., Tansey, K.E., Andrews, R., Devlin, P.F., Rogers, H.J. & Stead, A.D. (2019). De novo transcriptome analysis of peduncle necking in cut *Rosa hybrida* cultivar 'H30'. *Acta Horticulturae*. 1263, 351-358. https://doi.org/10.17660/ActaHortic.2019.1263.46

5.1 Introduction

RNA-sequencing provides a snap-shot view of the presence and quantity of RNA in a sample with the direct sequencing of transcripts. RNA-sequencing by next generation sequencing (NGS) is now a widely adopted method for transcriptomic studies, with trends moving away from the use of microarrays where expression analysis requires prior knowledge of genome sequences (Wang et al., 2009). *De novo* assembly of RNA sequences allows for transcriptomic studies to be carried out on non-model organisms as they do not require a reference genome. *De novo* assembly programmes such as Trinity use a multi-step process with de Bruijn graph analysis to build full-length transcripts from a sample of raw sequenced reads (Grabherr et al., 2011). Koning-Boucoiran et al. (2015) used Trinity to successfully develop a *de novo* rose transcriptome and SNP array using *Rosa hybrida* petals, whole flowers and young leaves from 12 garden rose cultivars and stressed leaves from *Rosa multiflora*. Another extensive *de novo* transcriptomic study has also been carried out for *Rosa chinensis* focusing on a mixture 13 different rose tissues under varying abiotic and biotic stress conditions (Dubois et al., 2012). However, no studies have currently been published on peduncle tissue undergoing necking and it is unknown if there are any molecular mechanisms involved in this process.

Roses belong to the Rosaceae, a large family including many important crop plants such as apple, peach and strawberry. An increase in Rosaceae genomic research over the past 14 years has meant that there are currently genomes available for seven genera, all of which are available on the 'Genome Database for Rosaceae' (GDR), an integrated web resource for Rosaceae genomics and genetic research (Jung et al., 2004; Jung et al., 2014). The diploid woodland strawberry (*Fragaria vesca*) genome was the closest related species available for rose studies (Shulaev et al., 2011). However, the *Rosa chinensis* cv. 'Old Blush' genome has recently been published and has expanded the prospects for rose research (Hibrand Saint-Oyant et al., 2018; Raymond et al., 2018).

Rosa chinensis cv. 'Old Blush' originated in China over a thousand years ago and was brought to Europe and North America in the eighteenth century. This diploid variety is thought to be a common ancestor to many of the modern tetraploid

commercial roses, contributing the recurrent flowering and ‘tea’ fragrance traits of the hybrid tea varieties (Martin et al., 2001). ‘Old Blush’ is an easily propagated diploid garden rose cultivar of high ornamental value with double flowers and pink petals and has therefore been chosen as the model for rose breeding and genetics. Sequencing of a high-quality rose genome has added a new resource to the 44 ornamental genomes now currently available (Chen et al., 2019) and has already provided insights into floral colour and scent pathways (Raymond et al., 2018). Release of the genome has also enabled genome guided transcriptomic studies to be possible. Use of a reference genome provides greater information for the arrangement of reads and generally out-performs *de novo* assembly methods (Hayer et al., 2015). However, no transcriptome studies have so far assessed the benefits of a genome guided alignment to the new *Rosa* genome over a *de novo* assembly for *Rosa hybrida* sequencing data.

A *de novo* transcriptome as well as an alignment to the *Rosa chinensis* reference genome have therefore both been carried out for *Rosa hybrida* cv. H30 rose peduncles at three stages of necking and will be discussed.

5.2 Methods

5.2.1 Plant material

Rosa hybrida cv. H30 stems were grown, transported and processed as described in 2.1. Stems were arranged in bunches of 10 and placed in clean vases containing 1 litre of tap water, plus a sachet of commercial flower food (Chrysal clear *Rosa*, Chrysal) and were held in standard experimental conditions for the duration of the experiment. For each stage of necking (Straight, <90˚, ≥90˚), 2cm stem sections were cut using a sterile razor blade and flash frozen in liquid nitrogen (*Figure 35*). Samples were taken within 5-7 days of being placed in a vase, as the necking stages appeared and were stored at -80˚C until RNA extraction. Straight (control) peduncles were sampled at each time point to account for any variability in the collection period. Vase life and sampling for replicate 1 was carried out in November 2015, with replicates 2 and 3 carried out in October the following year.

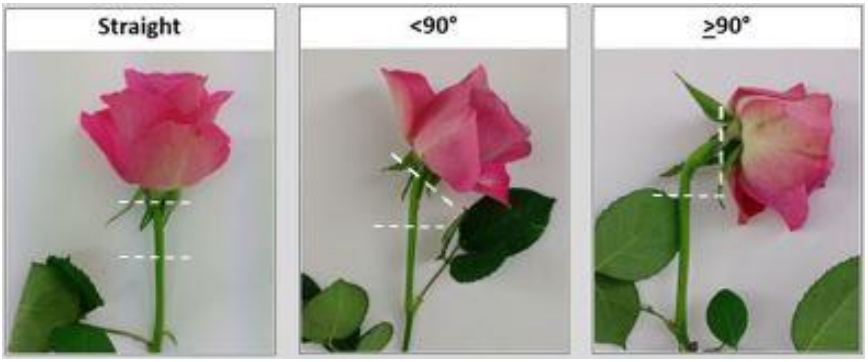

Figure 35. Stages of necking sampled for RNA sequencing. For each of the three stages (Straight, <90˚, ≥90˚), 2 cm stem sections were cut ~1 cm below the flower head as indicated by the dashed white lines.

5.2.2 RNA extraction

Samples were ground to a fine powder in liquid nitrogen using an autoclaved pestle and mortar. For each stage, three peduncle sections were ground to produce one pooled sample (*Figure 36*). This was repeated for each of the three replicates (1, 2, 3) to form nine pooled samples.

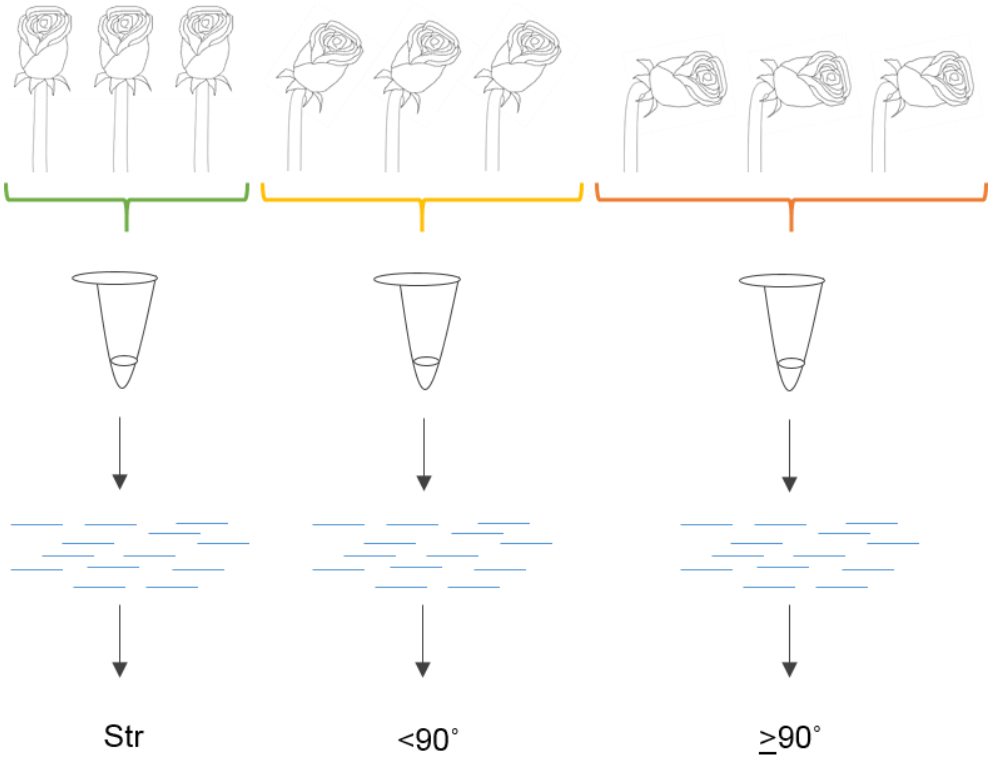

Figure 36. RNA extraction and sequencing of pooled samples. Diagram is representative of one replicate; this process was repeated three times to produce a total of 9 sequenced samples.

Total RNA was extracted from each sample using the RNA extraction method devised by Moazzam Jazi et al. (2015), adapted for use with 1.5 mL microcentrifuge tubes as described in 2.4.

5.2.3 Genomic DNA removal

Genomic DNA (gDNA) contamination was removed from the RNA samples using the RapidOut DNA removal kit (Thermo Scientific) following the standard protocol. DNase buffer with $MgCl_2$ (1 µL of 10X), and 0.5 µL of RNase free DNase I were added to 1 µg of RNA and adjusted to a total volume of 10 µL with nuclease-free water in 1.5 mL RNase free microcentrifuge tubes. Samples were vortexed briefly to mix and left to incubate at 37 ˚C for 30 mins to allow for cleavage and degradation of any gDNA present. To each tube, 1 µL of DNase Removal Reagent (DRR) was added and left to incubate at RT for 2 mins with gentle vortexing to re-suspend the DRR every 40 secs. Following incubation, samples were centrifuged at 1000 x g for 1 min to pellet the DRR, and the

supernatant carefully transferred to new RNase free microcentrifuge tubes. All samples were then checked on a 1 % agarose gel made up with 1 x Tris-Borate-EDTA (TBE) buffer and stained with (1 µL per 10 mL) SYBR Safe DNA gel stain (Invitrogen) to verify successful gDNA removal. RNA quality and yield were measured with a Nanodrop spectrophotometer as described in 2.4.3.

5.2.4 RNA sequencing

All samples were quality tested using a Qubit fluorometer and then sequenced using an Illumina NovaSeq 5000 to produce paired-end reads for each sample. These steps, as well as the library preparation, were completed by Angela Marchbank in the Genomics Research Hub, School of Biosciences at Cardiff University.

5.2.5 De novo *transcriptome assembly*

Bioinformatic analysis was carried out using the Advanced Research Computing at Cardiff (ARCCA), a supercomputer running Unix. This was accessed remotely using MobaXterm Personal Edition v10.2 (Mobatek, 2008), with Unix scripts written and edited using Notepad++ v7.3.3 (Ho, 2017). Files were uploaded to the server and managed using the FTP software FileZilla Client v3.34.0 (Kosse, 2018).

The quality of the raw paired-end reads was assessed using the quality control tool FastQC v0.11.2 (Andrews, 2014). Forward and reverse reads from each sample were then assembled into a reference transcriptome using the Trinity software package v2.3.2 with default settings (Grabherr et al., 2011). Prior to assembly, Trimmomatic v0.35 was run as part of the Trinity pipeline to remove low quality reads and bases from the data, using default settings with a 4 bp sliding window trimmer (min. score of 5) and a minimum read length of 25 bp (Bolger et al., 2014). Reads were then sequentially passed through the three modules of the Trinity pipeline: Inchworm, Chrysalis and Butterfly (*Figure 37*).

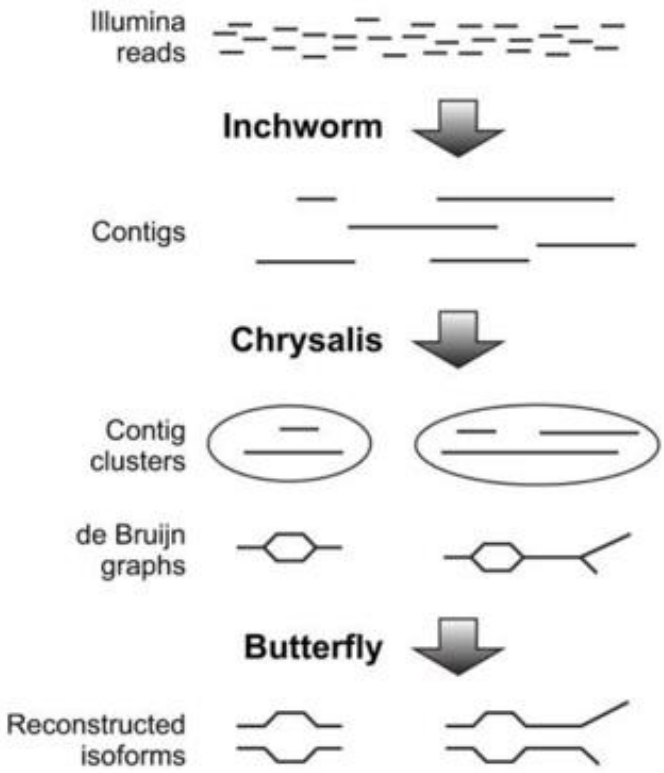

Figure 37. Trinity assembly pipeline, showing the three consecutive modules: Inchworm, Chrysalis and Butterfly. Figure adapted from Haas et al., (2013).

Beginning with the Inchworm module, reads were assembled into unique sequences of transcripts in a six-step process, to produce one representative transcript for a set of alternative variants with shared k-mers. Related contigs were then clustered through the Chrysalis module, with a de Bruijn graph produced for each of the clusters to represent the complexity of overlaps between the variants. Finally, the Butterfly module analysed the read paths along with the de Bruijn graphs to reconstruct all plausible full-length transcripts, forming the *de novo* transcriptome. Distinct isoforms were produced for paralogous genes and splice isoforms. (Grabherr et al., 2011; Haas et al., 2013)

The *de novo* transcriptome was annotated by running a blastx alignment against *Fragaria vesca* (Hawaii_1.0), *Arabidopsis thaliana* (TAIR10) and *Rosa chinensis* (Old Blush-v2). Alignments were performed using Blast+ 2.2.29 (Altschul, 1997) with an e-value cut-off of $1e^{-5}$.

5.2.6 Alignment to the Rosa chinensis *Old Blush reference genome*

The Galaxy web platform and public server at usegalaxy.org was used to process and analyse the raw sequencing data (Afgan et al., 2016) using the pipeline outlined (*Figure 38*). The *Rosa chinensis* Old Blush v2 reference files used for assembly and annotation were obtained through the Genome Database for Rosaceae (GDR), a web-based resource for Rosaceae research (Jung et al., 2014; Raymond et al., 2018).

Adapters were removed and low-quality reads were filtered and trimmed using Trim Galore! v0.4.3.1 (Krueger, 2017). Default advanced settings were used on the paired end reads, with a phred quality score (Q score) cut off of 20 applied and trimming of 1 base pair at the 3' end of every read turned off. The trimmed reads were then aligned to the *Rosa chinensis* Old Blush homozygous genome v2 (Raymond et al., 2018) to create bam files for each sample, using HISAT v2.1.0 (Kim et al., 2015) with default settings. Using the *Rosa chinensis* gene model as a guide, read counts were produced per exon for each bam file using DEXSeq count v1.20.1 (Anders et al., 2012), with a minimum alignment quality threshold of 10.

Homology of the *Rosa chinensis* genome with *Arabidopsis thaliana* (TAIR10) proteins is publicly available through the GDR (Jung et al., 2014) and was completed by pairwise sequence comparison using the Blastp algorithm with an e-value cut off of $1e^{-6}$. Annotation of the genome alignment transcriptome with *Arabidopsis thaliana* identifiers was completed using the VLOOKUP tool in Microsoft Excel, with the GDR best hit homology report as a search file and the *Rosa chinensis* identifiers as a corresponding reference.

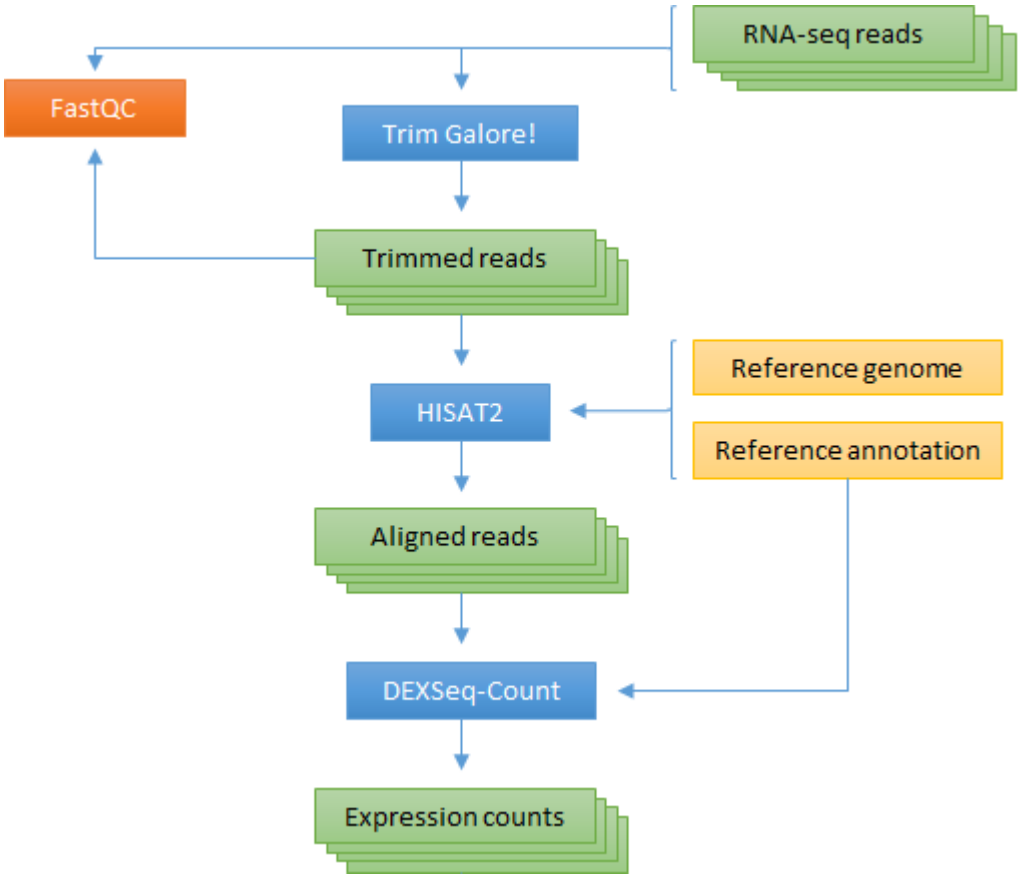

Figure 38. Bioinformatics workflow for the Rosa chinensis *genome guided alignment*

5.3 Results

5.3.1 Raw sequence data

Millions of paired-end reads were produced through the RNA extraction and sequencing of rose peduncle tissue for each of the three stages of necking. Replicate 1 samples were sequenced at a greater read depth, prior to replicates 2 and 3, as seen by the higher read counts for replicate 1 samples (Table *12*). FastQC analysis of raw reads flagged no sequences for poor quality and showed a mean quality score of 35 (*Figure 39*) for all samples. A quality score (Q score) is logarithmically related to the probability of a base being called incorrectly, with a Q score of 30 representing a 99.9 % base call accuracy, or an error rate of 1 in 1000 (0.1 %). A warning is displayed if the mean quality peak has a Q score

below 27 or a 0.2 % error rate, therefore a mean Q score of 35 as found in this study is indicative of high read quality (Babraham Bioinformatics, 2019a).

Table 12. Total number of paired-end reads in millions per sample

Stage	Replicate 1	Replicate 2	Replicate 3
Straight	62.5	23.5	27.0
<90	73.5	27.7	25.0
≥90	51.6	22.6	26.1

Values are shown to 3 significant figures.

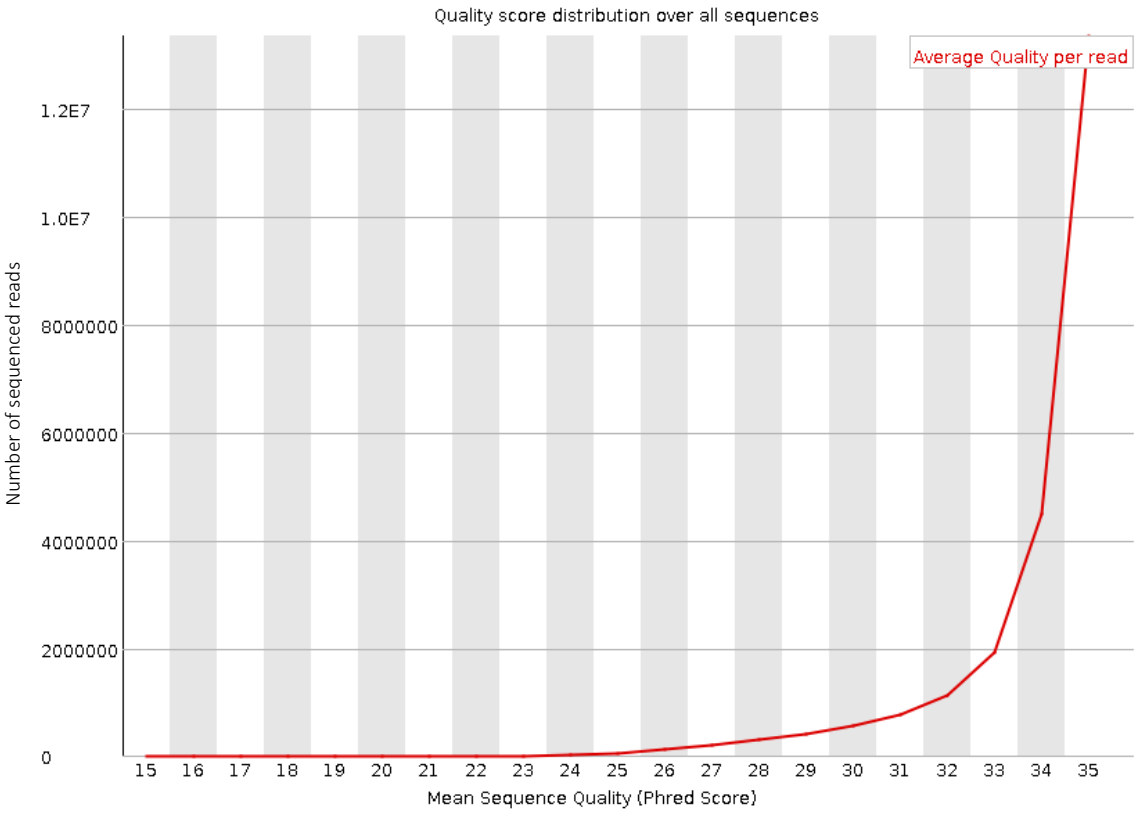

Figure 39. Mean sequence quality score of raw reads. The graph was produced using FastQC (Andrews, 2014) for sample Str_2 read 1 and is representative of the dataset.

5.3.2 De novo *transcriptome assembly*

Trimmomatic trimming removed 0.8% of reads due to being unpaired or below threshold quality or length, leaving a total of 336,692,226 paired-end reads to be passed into the Trinity assembly pipeline. The ARCCA supercomputer enabled

this large amount of sequencing data to be assembled into a Trinity transcriptome of 203,565 contigs with unique identifiers.

Through a Blastx analysis, a total of 67.3 % of the transcriptome contigs were aligned to either rose, Arabidopsis or strawberry (E-value $1e^{-5}$; *Figure 40*). As expected, the rose genome provided the largest number of hits to the *de novo* assembled transcripts, covering 66.5 % of the transcriptome, with 25 % and 11 % more hits than Arabidopsis and strawberry respectively (*Table 13*).

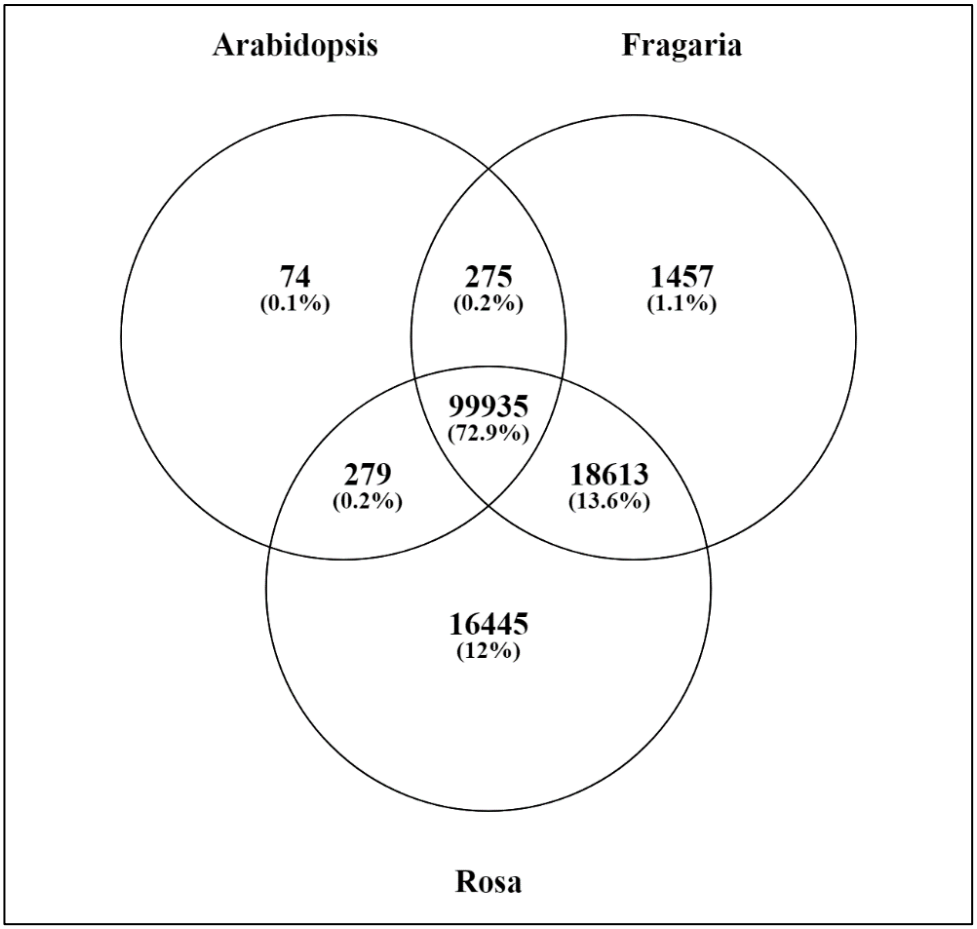

Figure 40. Number of overlapping homologous genes. Comparison of Blastx alignments against Arabidopsis thaliana (TAIR10), Fragaria vesca and Rosa chinensis. (%) percentage of total identified. E value cut off of $1e^{-5}$. The Venn diagram was produced using Venny 2.1.0 (Oliveros, 2015)

Table 13. Number of unique accession codes following Blastx alignment

	Number of Trinity contigs with blastx hits	Number of unique accession codes
Rosa chinensis	135,272	26,704
Fragaria vesca	120,280	20,897
Arabidopsis thaliana	100,563	17,701

E value cut off of $1e^{-5}$.

5.3.3 Reference-based assembly

The Trim Galore! tool trimmed the remaining Illumina adapters from 35 % of the forward and 33 % of the reverse raw reads and removed 1.9 % of reads due to being unpaired or below threshold quality or length. The remaining paired end reads showed an improved base sequence Q score, compared to raw untrimmed reads (*Figure 41*). As can be seen by the shift of the lower 90 % data points from the red, 'poor' quality zones, to the green and orange 'very good' and 'acceptable' quality zones (Babraham Bioinformatics, 2019b). Along with an increase in the tail end mean Q score of the reads, shown by the blue line.

Alignment of the Trim Galore! trimmed reads to the *Rosa chinensis* Old blush genome with HISAT2 achieved an overall average read alignment rate of 87.6%, with an average of 86.5 % for replicate 1 reads sequenced at a deeper read depth and an average 88.1 % for the replicate 2 and 3 reads (*Table 3*). Although Trim Galore! removed a greater number of reads due to low quality than Trimmomatic, the percentage alignment rate represents a higher number of mapped reads than was achieved with Trimmomatic trimmed or raw reads.

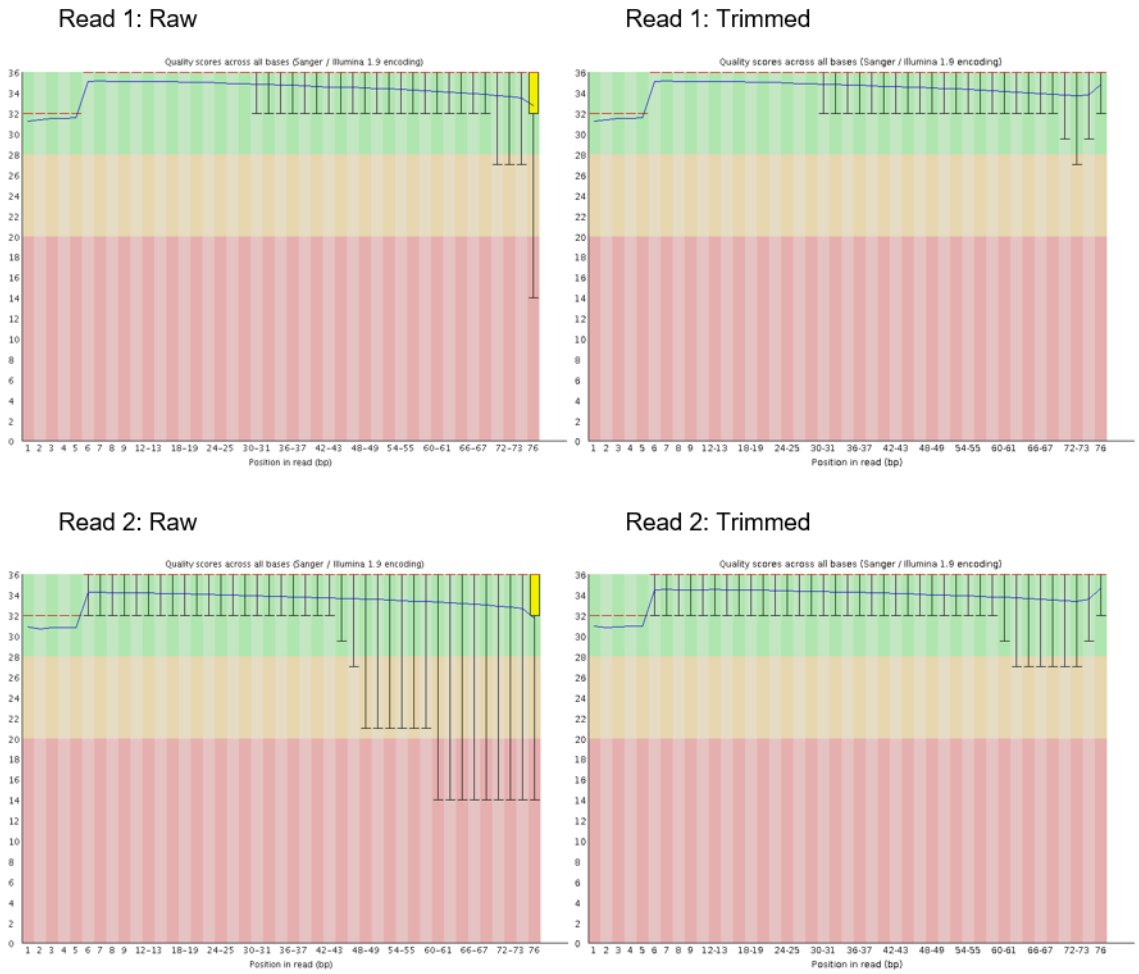

Figure 41. Base sequence quality scores pre and post trimming with TrimGalore!. Graphs were produced using FastQC (Andrews, 2014) and are shown for reads of 'Str_2' as a representative of the dataset. The blue line represents the mean quality of the reads, the yellow box represents the inter-quartile range (25-75 %) and the upper and lower whiskers represent the 10 % and 90 % data points. The background colours divide the y-axis quality scores into very good (green), acceptable (orange) and poor (red) (Babraham Bioinformatics, 2019b).

Table 14. Alignment statistics of reads to the *Rosa chinensis* genome

Sample	Alignment of reads to *Rosa chinensis* genome (%)	Total number of unique *Rosa chinensis* identifiers
Str_1	86.9	34,775
<90_1	86.0	34,987
≥90_1	86.7	34,155
Str_2	87.8	32,601
<90_2	88.4	33,002
≥90_2	87.9	32,546
Str_3	88.2	33,392
<90_3	88.2	33,125
≥90_3	87.9	33,004

A total of 38,956 unique *Rosa chinensis* genes were identified across all samples, with 34,252 (87.9 %) of the genes appearing in all three of the necking stages. Stage ≥90 consistently had the lowest number of identified genes within each of the replicates with an average 33,235 unique genes identified, 354 (1.1 %) and 469 (1.4 %) less genes on average than stage Str and <90 samples. (Table 14)

Following alignment to the *Rosa chinensis* vs. *Arabidopsis thaliana* GDR Blastp file, 76.2 % of the 38,956 total identified genes had homology to *Arabidopsis thaliana* (TAIR10) proteins. This resulted in 14,983 unique TAIR10 identifiers, equal to 95.3 % of the total TAIR10 proteins with homology to the *Rosa chinensis* genome as seen in *Figure 42*.

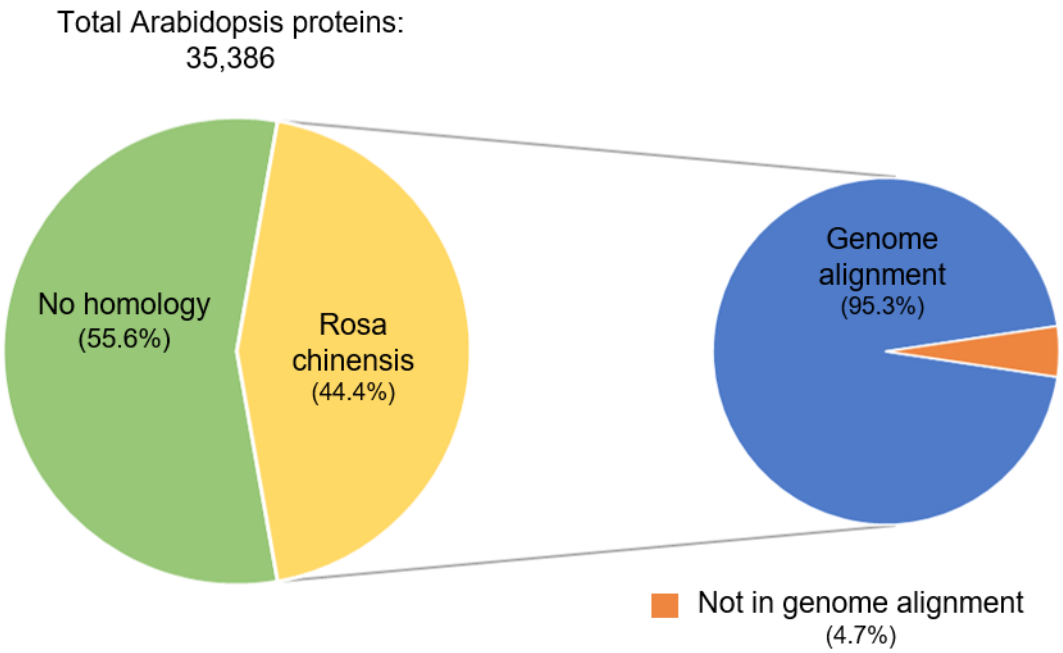

Figure 42. Proportion of Arabidopsis thaliana *TAIR10 proteins with homology to the* Rosa chinensis *genome (left-hand pie chart), and the sub proportion with homology to the genome alignment transcriptome (right-hand pie chart). Homology Blastp alignment to TAIR10 was carried out with an e-value cut off of* $1e^{-6}$ *and is publicly available through the Genome Database for Rosaceae (GDR; Jung et al., 2014).*

5.4 Discussion

De novo assembly methods have been used successfully in many studies and have allowed for the progression of transcriptomic studies on non-model organisms (Garcia-Seco et al., 2015; Zhang et al., 2015; Li et al., 2014). The Trinity pipeline for *de novo* transcriptome assembly has been shown to be superior to other *de novo* transcriptome assemblers such as ABySS and SOAPdenovo in its ability to produce full-length transcripts and is equal to genome alignment methods in some organisms (Grabherr et al., 2011). It was therefore used in this study as a comparative method. A Blastx alignment of the *de novo* reference transcriptome to the *Fragaria vesca* genome provided hits for 59.1% of the contigs (e value cut off $1e^{-5}$; *Figure 40; Table 13*). This is in line with the transcriptome study by Koning-Boucoiran et al. (2015), who found that 60.7% of their rose *de novo* transcripts mapped to strawberry genes. Prior to the release of the *Rosa chinensis* genome in 2018, strawberry was the closest related

species for which a genome sequence was available and therefore provides validation for the success of the Trinity *de novo* assembly produced in this study.

D*e novo* pipelines have high memory workloads and often require specialist supercomputers such as the ARCCA (used in this study) to meet the processing requirements of the programmes. Supercomputers such as the ARCCA also require an understanding of Unix script to control the set up and parameters of jobs. The production of the *Rosa* genome has allowed rose research to move away from *de novo* assemblers, towards faster genome alignment methods with lower memory requirements which can be run through freely available web resources such as usegalaxy.org (Galaxy) as used in this study (Afgan et al., 2016; Hibrand Saint-Oyant at al., 2018; Kim et al., 2015; Raymond et al., 2018). Unlike the ARCCA, Galaxy does not require knowledge of Unix script but instead comes pre-loaded with a set of 'tools' within a user-friendly interface, therefore making workflows highly accessible and reproducible (Afgan et al., 2016).

Mapping of reads to a reference genome is a key stage in the success of transcriptomic data analysis, and alignment success can be attributed to the quality of the genome available. As the *Rosa* genome has been stated to be 'one of the most contiguous plant genomes to date' (Raymond at al., 2018), it can be assumed that a high alignment rate will yield reliable results for downstream analysis. The mapping programme HISAT combines a novel hierarchal indexing strategy with specifically designed alignment algorithms to provide improved speed and reduced memory requirements (Kim et al., 2015). HISAT has been shown to outperform or be on par with other much slower aligners such as TopHat2 (Baruzzo at al., 2017; Kim et al., 2015, Medina et al., 2016), and was found here to effectively align more reads than other aligners tested, including Bowtie2 (data not shown). The 87.6 % average alignment rate in this study falls within the range accomplished within recent Rosacea studies; with 78.2 % achieved for pear (*Pyrus pyrifolia*) RNA seq reads aligned against the *Pyrus bretschneideri* 'Dangshansuli' genome assembly (Li et al., 2019; Xue, et al., 2018) and 95.2 % achieved by Silva et al., (2019) for *Malus x domestica* against the *Malus x domestica* GDDH13 v 1.1 reference genome (Daccord et al., 2017).

Multicellular organisms can have expression patterns that are highly tissue or organ specific, resulting in a low abundance of genes in some RNA datasets (Vaattovaara et al., 2019). However, the total 38,956 unique genes identified in the reference alignment represents a substantial 85.7 % *Rosa chinensis* genome coverage. Just over 18 % greater genome coverage than was found for the *de novo* transcriptome. *Arabidopsis thaliana* is the model species for plant research and therefore has a high-quality genome with the latest and most thoroughly verified gene annotations due to continuous input from the scientific community (Vaattovaara et al., 2018). Homology searches to *A. thaliana* proteins can therefore be beneficial for inferring gene function, for comparative analysis to novel studies and for use in downstream pathway analysis and gene ontology programmes such as AgriGo, DAVID and Mapman which are not yet compatible with new gene identifiers in their default set up (Du et al., 2010; Huang et al., 2009; Thimm et al., 2004). Blast alignment of the two transcriptomes to *A. thaliana* provided differing numbers of TAIR10 identifiers, this time with the de novo transcriptome showing a 7.7 % higher TAIR10 genome coverage than the reference aligned transcriptome (*Table 13; Figure 42*). The TAIR10 identifiers associated with the reference aligned transcriptome, were limited to those identified to have homology to the *Rosa* genome by GDR. Therefore, it is possible that some of the TAIR10 identifiers associated with the *de novo* transcriptome do not share homologous genes in *Rosa chinensis* but do in *Rosa hybrida* cv H30. It is also possible that the increase in homologous genes is due to the mis-alignment of lower quality reads or contamination within the de novo assembly (Sangiovanni et al., 2019). However, consideration should be taken when comparing the two transcriptomes directly as different methods were used to both generate and annotate the genes, making results from each difficult to assess.

Another approach not tested in this study would be to combine both methods, in a reference guided transcriptome assembly. This method can reduce the complexity of a *de novo* assembly with the assistance of a reference genome and has been found to produce a better assembly than a regular *de novo* assembly (Lischer & Shimizu, 2017). Allowing for divergent regions to be included into the transcriptome which may be lost with a standard reference alignment method. However, although memory requirements are lower with this approach compared

to a de novo assembly, run times are much longer therefore access to specialist computing equipment may still be required.

5.5 Conclusions

Rosa hybrida peduncles at three stages of necking were successfully sequenced to produce millions of high-quality reads. Both the de novo transcriptome assembly and the reference genome alignment transcriptome methods proved to be successful and therefore provide a huge new resource for studying peduncle necking. However, as a standard *de novo* approach to assembling *R. hybrida* sequencing data did not appear to be of increased benefit, the reference aligned transcriptome was used in further analysis to explore the potential molecular mechanisms associated with the necking phenomenon.

Chapter 6 Differential gene expression and pathway analysis of Rosa hybrida cv. ‘H30’ at three peduncle necking stages

6.1 Introduction

Necking is thought to be initiated by a blockage of the xylem, causing a reduced uptake of water and a bending of the peduncle. However, it is unknown if this is a purely physical (passive) process or if molecular mechanisms are involved. Differential expression analysis of RNA sequencing data is a widely adopted method for determining differences in expression between treatments and has previously been used to identify transcriptional changes associated with petal development in *Rosa chinensis* and floral transitioning in *Rosa odorata* (Han et al., 2017; Guo et al., 2018). Differential expression analysis can be performed from gene counts using programmes such as RSEM, EdgeR and DESeq2 to produce a list of significantly up and down regulated genes, with the expression level and the magnitude of difference reported for each gene (Li & Dewey, 2011; Robinson et al., 2009; Love et al., 2014). Which can then be analysed by a multitude of tools, packages and databases to uncover biologically meaningful information from the data.

Gene set enrichment analysis is a high-throughput method for gene expression analysis and helps to identify key biological processes, molecular mechanisms and cellular components associated with a dataset. Gene set enrichment analysis includes both singular enrichment analysis (SEA) and parametric analysis of gene set enrichment (PAGE). SEA can be used to identify enriched gene ontology (GO) terms from a list of genes, with enrichment levels calculated against expected (pre-calculated) background levels. Results are reported as p values usually using a Fishers exact or a binomial probability test with multi-test adjustment. PAGE also identifies enriched GO terms but unlike SEA, PAGE takes expression level into account and can deal with whole gene sets, with statistical enrichment determined using the central limit theorem and results reported as two-tailed Z scores (Huang et al., 2008; Kim & Volsky, 2005). Many web analysis platforms such as DAVID which can complete enrichment analysis are tailored towards analysis of data from humans or of human diseases in model species However, the web platform agriGO, was designed specifically for the analysis of data from plant and agricultural species and is therefore more suitable for data

acquired from plants such as *Rosa hybrida*. (Du et al., 2010; Tian et al., 2017; Huang et al., 2009).

The STRING database (‘Search Tool for Retrieval of Interacting Genes/Proteins) combines all publicly available information regarding known and predicted protein-protein interactions, with interaction data stemming from genomic context predictions, high-throughput lab experiments, co-expression, text-mining and from other knowledge databases. The STRING database features around 24.6 million proteins, covering 5090 organisms and has been awarded the status of a European Core Data Resource by ELIXIR, a European initiative for sustainable bioinformatics infrastructure and is therefore freely available under the Creative Commons Attribution license (Szklarczyk et al., 2018). As well as reporting protein interaction networks and information, STRING can also perform enrichment analysis with either a small subset of genes using SEA or on whole gene-sets with PAGE and display results combined from other databases such as KEGG and Gene Ontology for pathway mapping and gene function enrichment (Kanehisa, 2017; Ashburner et al., 2000; The Gene Ontology Consortium, 2018).

Alternatively, differential expression data can be analysed to determine the expression of transcription factors using the plant transcription factor database (Jin et al., 2016). Transcription factors act as molecular switches, regulating gene expression by binding to promotor regions of genes. By activating and repressing gene expression, transcription factors can induce a cascade of molecular responses through signalling pathways and therefore have essential roles in plant stress responses (Joshi et al., 2016). Plant transcription factors are arranged into gene families dependent on their DNA binding domains and into sub-families dependent on auxiliary domains (*Figure 43*; Jin et al., 2013). The *Rosa chinensis* genome currently has 1938 identified transcription factors, classified into 57 families and sub families of which WOX, MYB, bHLH, ERF, NAC, B3, C2H2, WRKY, MYB-related and GRAS represent the top 10 largest transcription factor families for *Rosa chinensis (*PlantTFDB v5.0, 2019*)*. WOX and GRAS family transcription factors have primary roles in plant growth and developmental processes however ERF, NAC and WRKY families also have roles in abiotic and biotic stress responses, hormonal signal transduction and senescence (Graaff et

al., 2009; Bolle, 2004; Koyama, 2014; Nakano et al., 2006; Zhuo et al., 2018; Bakshi & Oelmüller, 2014). Analysing the expression of these transcription factors can therefore help to both identify the initial response and understand the complex web of downstream molecular responses.

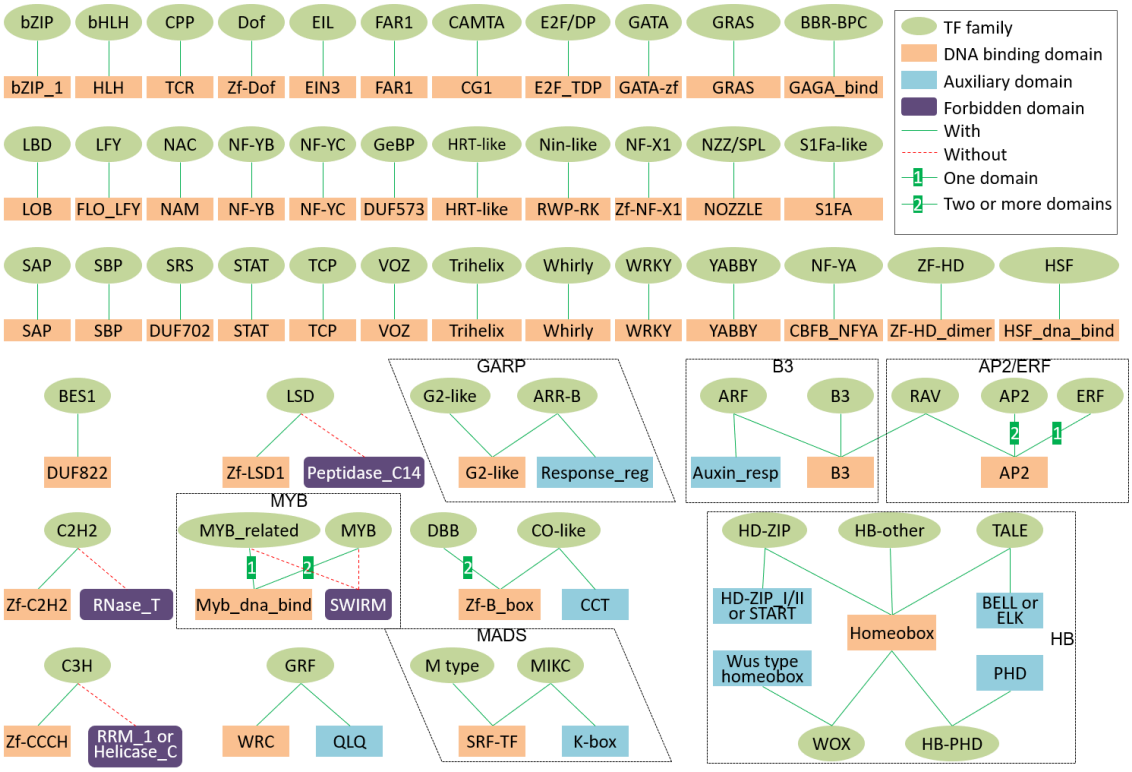

Figure 43. Transcription factor family assignments. DNA binding sites and auxiliary binding sites are shown by orange and blue boxes respectively. Forbidden domains shown in purple infer a lack of transcriptional activity of a transcription factor. Proteins containing a forbidden domain are excluded from family classification (red dashed line). Superfamilies are outlined in grey boxes. Figure from Jin et al. (2013).

Aquaporins are small transmembrane proteins important for the transport of water and small neutral solutes across biological membranes (Maurel et al., 2008). Aquaporins can be divided into sub families including plasma membrane intrinsic proteins (PIPs), tonoplast intrinsic proteins (TIPs), Nodulin-like intrinsic proteins (NIPs) and the less well characterised small basic intrinsic proteins (SIPs) (Šurbanovski et al., 2013). PIPs make up the largest sub family and are known to be highly responsive to environmental stimuli including cold, salt, drought stress and microbial infection to help control and maintain water homeostasis (Šurbanovski et al., 2013; Kayum et al., 2017). It is hypothesised that aquaporins may therefore be differentially expressed in necking peduncles,

along with other water stress responsive genes as necking is thought to be water stress related.

Senescence is an active process whereby nutrients are remobilised, eventually leading to cell degradation with the initiation of programmed cell death (Rogers, 2011). Senescence can be either age-dependent or stress induced and initiated by reproductive development, phytohormonal changes and age, or by pathogen infection, salinity, drought, environmental toxins, extremes of temperature or light and nutrient deficiency respectively (Podzimska-Sroka et al., 2015). As senescence involves many molecular mechanisms and is extremely complex, the potential involvement of senescence in necking may be missed through conventional enrichment analysis methods. Expression of senescence genes was therefore determined in a targeted approach, using senescence as a search term within Uniprot to compile a database of all known senescence associated genes for analysis.

Differential expression analysis was carried out on RNA sequencing data for three stages of necking in *Rosa hybrida* cv. H30. Analysis by both enrichment analysis methods and through targeted searches identified potential transcriptomic changes associated with the necking process and will be discussed.

6.2 Methods

6.2.1 Rosa chinensis *Old Blush genome guided transcriptome assembly*

Rosa hybrida cv. H30 peduncle sections were sampled at three necking stages straight (Str), less than 90° (<90) and at equal to or more than 90° (≥90) of peduncle bending. The RNA was extracted, processed and sequenced as described in 2.4 to provide three replicates for each necking stage. Sequenced reads where then aligned to the *Rosa chinensis* Old Blush genome as previously described Chapter 5.

6.2.2 Differential expression analysis

Differential expression analysis was completed using the Galaxy web platform available at usegalaxy.org (Afgan et al., 2016). Read count files produced by DEXSeq count v1.20.1 (Anders et al., 2012, 5.2.6) were pre-processed using the text manipulation tool 'Remove beginning' v1.0.0 to remove heading text before being input into the differential expression analysis tool DESeq2 v2.11.40.1 (Love et al., 2014). Two factors were considered in the statistical model, necking stage and sequencing year. Necking stage was used as the primary factor for differential gene expression and included the three factor levels Str, <90 and >90. Sequencing year was included as a secondary factor to account for the difference in sequencing depth used between the two sequencing runs, with replicate 1 samples run in 2016 and replicate 2 and 3 run together at a shallower depth in 2017. A linear model was used as a best fit for the sequencing data and default outlier replacement, outlier filtering and DESeq2 independent filtering was turned on. For each of the three comparison groups (<90 vs Str, ≥90 vs Str, ≥90 vs <90) a differential expression table was produced, listing the mean average count, the log2 fold change and the p value for each gene. A false discovery rate (FDR)-adjusted p-value threshold of <0.05 was applied to the differential expression data to account for multiple testing.

6.2.3 Gene ontology analysis

The *Rosa chinensis* genome has been functionally annotated using InterProScan to assign gene ontology (GO) terms to the proteins, with annotation files publicly available through GDR (Jung et al., 2014). Using this resource, the three differential expression tables produced by DESeq2 for each comparison were annotated with their corresponding GO terms through the Join to files tool v1.1.1 in Galaxy. GO terms were then grouped into broader Plant GO slim biological process groups for visual analysis.

6.2.4 Parametric Analysis of Gene Set Enrichment (PAGE) and Singular Enrichment Analysis (SEA)

Singular enrichment analysis (SEA) and parametric analysis of gene set enrichment (PAGE) were used to identify enriched GO terms in the ≥90° vs

Straight gene set. Both AgriGO v2.0 the web-based tool for gene ontology (Tian et al., 2017) and the STRING database for protein-protein interactions (Szklarczyk et al., 2018) were used for enrichment analyses, using *Arabidopsis thaliana* (TAIR10) identifiers. Annotation of the *R. chinensis* genes with *A. thaliana* identifiers was completed as previously described (Chapter 5). Plant GO slim terms were used for AgriGo analysis, with a minimum of 10 mapping entries. An FDR multi-test p adjustment method was applied to all analyses, with a 'medium' p adjust. <0.05 threshold set for STRING functional enrichment. For PAGE enrichment analysis, Log2 FC values were input alongside the TAIR10 identifiers for z-score calculations.

6.2.5 Analysis of differentially expressed transcription factors (TFs)

A list of the known transcription factors for *Rosa chinensis* was downloaded from the Plant transcription factor database (PlantTFDB) v5.0 (Jin et al., 2016). The 1938 transcription factors categorised into the 57 families were matched to *Rosa chinensis* identifiers using the Excel VLOOKUP tool to identify all the differentially expressed transcription factors within the DESeq2 comparison lists (p adjust <0.05).

6.2.6 Expression analysis of senescence associated genes

All genes associated with the term 'senescence' for *Arabidopsis thaliana* were downloaded from uniprot and matched against the >90 vs Straight dataset using the Excel VLOOKUP tool. Identified genes were then analysed using the STRING database for protein-protein interactions to determine gene connections within the dataset (Szklarczyk et al., 2018).

6.3 Results

6.3.1 Differential gene expression and gene ontology overview

Following differential expression analysis with DESeq2, a total of 3,647 genes were found to have significant differential expression across all three comparison groups at a p adjusted threshold of <0.05 (*Figure 44*). As expected, comparison

between >90° and Straight resulted in the largest number of up- and down-regulated genes, with a total of 3,598 differentially expressed genes (Table *15*). Necking stages <90° and Straight were shown to have the least differences in gene expression, with just 56 differentially expressed genes identified. Across both <90° vs Straight and >90° vs <90° contrast groups, more statistically down-regulated than up-regulated genes were discovered with 39.2 % and 12.6 % more down-regulated genes respectively (Table 15). Although >90 vs Straight showed the opposite trend, there was just a 0.8 % increase in the number of up-regulated to down-regulated genes.

Table 15. Differential expression gene counts

	<90 vs Straight	>90 vs Straight	>90 vs <90
Up regulation	17	1813	353
Down regulation	39	1785	454

P.adjust <0.05

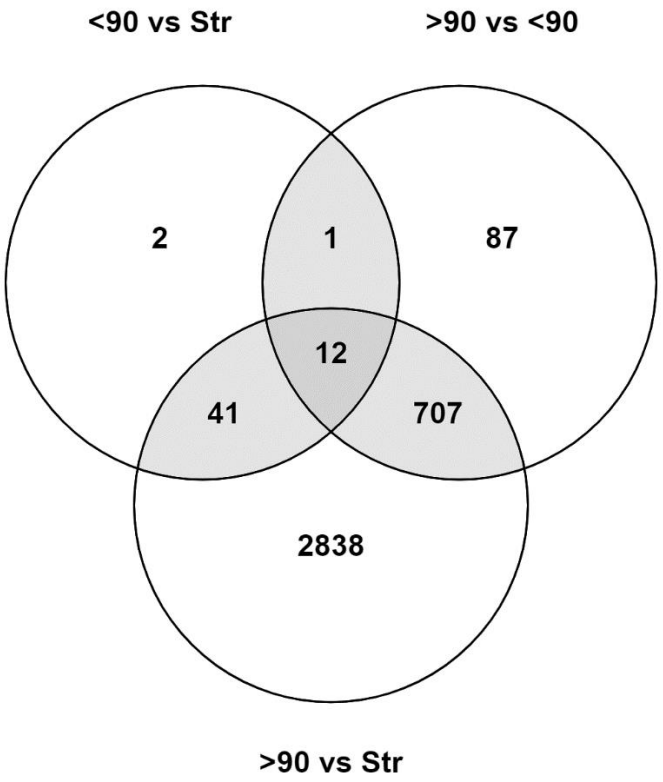

Figure 44. Overlapping differentially expressed genes between the three comparison groups of necking stages (p adjust. <0.05). The Venn diagram was produced using Venny 2.1.0 (Oliveros, 2015).

To compare expression between the three necking comparisons, overlapping genes in more than one comparison group were functionally annotated with gene ontology terms. Of the 761 overlapping genes (shown in grey, *Figure 44*), 234 genes were assigned a biological process GO term and could be arraged into biological process heatmap as shown in *Figure 45*. In general, genes involved with protein phosphorylation, protein ubiqutination and proteolysis were down-reglated and genes involved with protein de-phosphorylation and protein glycosylation were shown to be up-regulated in ≥90° necking peduncles. For metabolic processes (including carbohydrate metabolism and oxidation-reduction), regulation of transcription and transmembrane transport both an up- and down- regulation of genes can be seen across the necking stages. Down-regulation of genes involved with starch biosynthesis, photosynthesis, phosphorelay signal transduction and metal ion transport can be seen for ≥90° stage necking peduncles, when compared to straight (control) and <90°

peduncles. In contrast microtuble-based process, lipid metabolism and response to stimuli related genes showed down-regulation in both <90° and >90° necking stages in comparison to Straight (control) genes, and trehalose biosynthesis genes showed up- reguation. Of the biological processes represented, protein metabolism, metabolism (general) and transport were the three largest gene clusters.

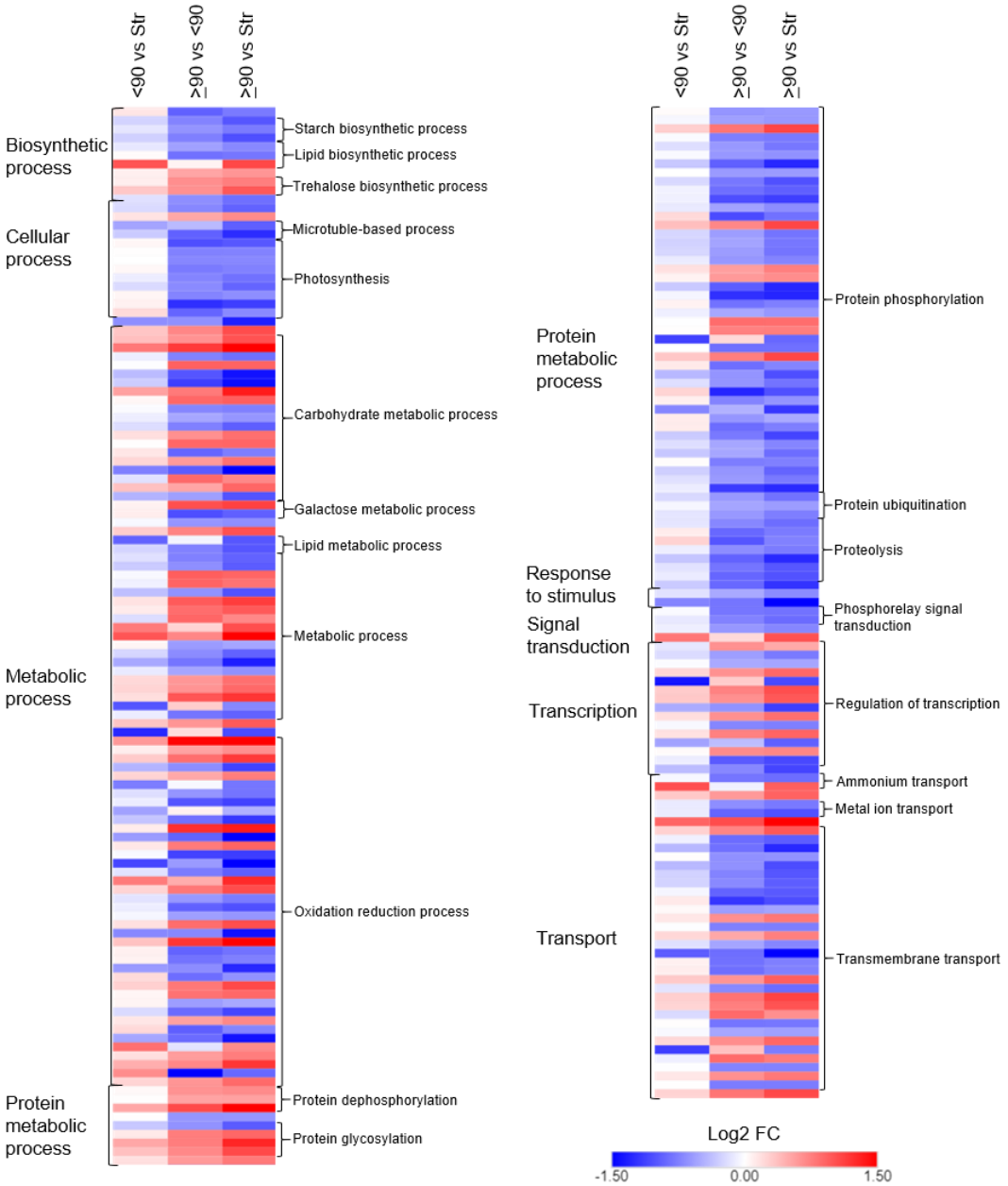

Figure 45. Biological process heatmap of overlapping differentially expressed genes (p adjust <0.05). Up (red) and down (blue) differential expression is shown for each comparison on a log2 fold change scale. Rosa chinensis *identifiers are arranged in biological process clusters for genes with significant expression in at least two comparison groups. The heatmap was created using Morpheus with manual annotations (Morpheus, https://software.broadinstitute.org/morpheus).*

6.3.2 Enrichment analysis of ≥90 vs Str differentially expressed genes

As the ≥90 vs Straight comparison yielded the largest number of differentially expressed genes, this group of genes were further analysed with the enrichment analysis tools AgriGO v2 (Tian et al., 2017) and STRING (Szklarczyk et al., 2018) using *Arabidopsis thaliana* (TAIR10) identifiers (Table *15*). Of the 3,598 *Rosa chinensis* genes in the ≥90 vs Straight gene list, 92 % (3,312 genes) were assigned a TAIR10 identifier, equalling a total of 2,865 unique TAIR10 identifiers.

6.3.2.1 AgriGO enrichment analysis

Parametric analysis of gene set enrichment (PAGE) for biological process with AgriGO v2 identified more significantly down- than up-regulated GO terms (*Figure 46).* Transport (GO:0006810) was found to be a significantly up-regulated, with a z score of 4.21 and a total of 315 transport associated genes (p adjust. <0.05). Under the parent terms of biological regulation and developmental process: growth (GO:0040007), regulation of cell size (GO:0008361) and cell differentiation (GO:0030154) all showed significant down-regulation, with 86, 61 and 107 associated genes respectively (p adjust <0.05). Interestingly, the child terms of response to stimulus: tropism (GO:0009606) and response to abiotic stimulus (GO:0009628) were also found to be significantly down-regulated with 310 and 23 identified genes respectively (*Figure 46*). From the 23 tropism related genes identified, 18 were found to be associated with gravitropism and three with phototropism. All three phototropism genes (NPH3, PHYB and PKS1) were found to be down-regulated. As were all the tropism genes associated with auxin-activated signalling pathways (ACB1, ABCB19, AUX1, PIN1 and RAC3). (Table *16*)

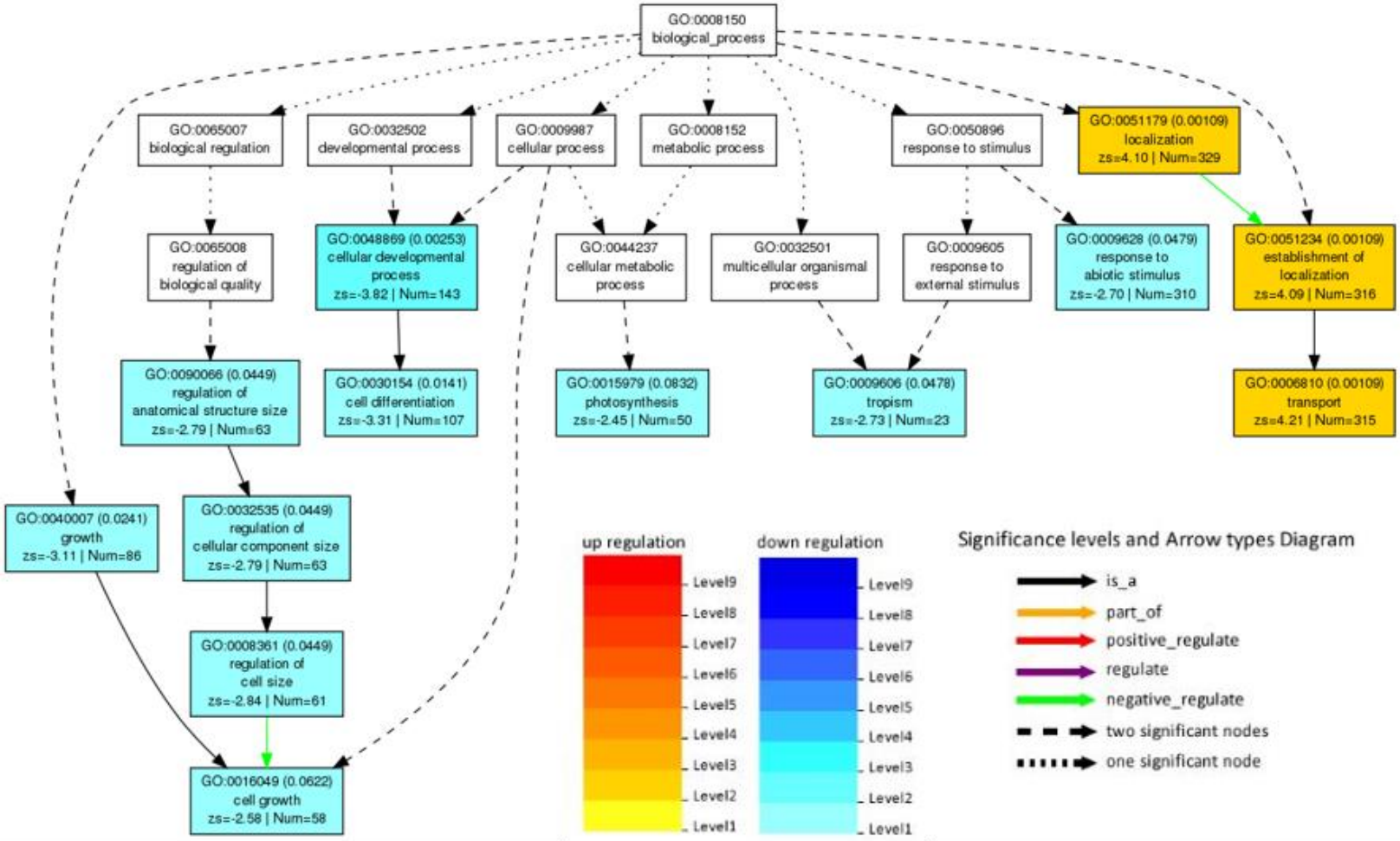

Figure 46. PAGE analysis of significant biological processes for ≥90 vs Straight differentially expressed genes. AgriGO v2 (Tian et al., 2017) was used for analysis, with Arabidopsis TAIR10 identifiers and plant GO slim gene ontology.

Table 16. Tropism related genes with significant differential expression in ≥90 when compared to straight (control) necking peduncles

TAIR10 ID	Name	Description	LFC
AT2G38120	AUX1	Transmembrane amino acid transporter family protein	-1.01
AT1G68370	ARG1	Chaperone DnaJ-domain superfamily protein	0.34
AT4G35020	RAC3	Rac-like GTP-binding protein ARAC3	-0.36
AT5G64330	NPH3	Phototropic-responsive NPH3 family protein	-0.58
AT2G41660	MIZ1	Protein of unknown function, DUF617	-0.82
AT2G18390	TTN5	ADP-ribosylation factor family protein	0.53
AT2G14820	NPY2	Phototropic-responsive NPH3 family protein	-0.68
AT1G31480	SGR2	Shoot gravitropism 2 (SGR2)	0.44
AT2G36910	ABCB1	ABC transporter B family member 1	-0.72
AT5G02750	SGR9	E3 ubiquitin-protein ligase SGR9, amyloplastic	-0.95
AT1G73590	PIN1	Auxin efflux carrier	-0.75
AT1G42540	GLR3.3	Glutamate receptor 3.3	-0.44
AT3G28860	ABCB19	ABC transporter B family member 19	-0.80
AT3G54640	TSA2	Tryptophan synthase alpha chain, chloroplastic	-0.26
AT2G01940	SGR5	C2H2-like zinc finger protein	-0.57
AT2G02950	PKS1	Phytochrome kinase substrate 1	-0.84
AT1G56590	AP3M	Clathrin adaptor complexes medium subunit family protein	0.40
AT3G54220	SCR	GRAS family transcription factor	-0.59
AT2G18790	PHYB	Phytochrome B	-0.28
AT5G50375	CPI1	Cycloeucalenol cycloisomerase	-0.31
AT5G58960	GIL1	Plant protein of unknown function (DUF641)	-0.94
AT3G47690	EB1a	Microtubule-associated protein RP/EB family member 1A	-0.46
AT2G20180	PIL5	Phytochrome interacting factor 3-like 5	-0.53

6.3.2.2 STRING enrichment analysis

Singular enrichment analysis (SEA) was carried out with STRING (Szklarczyk et al., 2018), with statistically up- and down-regulated genes entered separately from the ≥90 vs Straight gene set. Annotation with TAIR10 identifiers resulted in 762 up- and 1261 down-regulated genes, to a Log2 fold change (FC) of ≥0.5 and ≤-0.5 respectively (p adjust. <0.05). Analysis of the up-regulated genes identified Galactose metabolism (GO:ath00052) to be a statistically up-regulated pathway (FDR <0.05; *Table 17*).Whereas analysis of the down-regulated genes identified

photosynthetic pathways (ath00196 and ath00195) and phenylpropanoid biosynthesis (ath00940) to be significantly down-regulated (FDR <0.05; Table *18*). Starch and sucrose metabolism (ath00500) and the more general biosynthesis of secondary metabolites (ath01110) and metabolic pathways (ath01100) featured on both outputs, suggesting both significant up- and down regulation of genes in these pathways (FDR <0.05; Table 17; Table 18).

Table 17. Significantly up-regulated pathways between necking stages ≥90 and Str

KEGG ID	Pathway name	Observed	Total	FDR
ath00052	Galactose metabolism	9	56	0.0023
ath00500	Starch and sucrose metabolism	13	147	0.0065
ath01100	Metabolic pathways	72	1899	0.0076
ath01110	Biosynthesis of secondary metabolites	43	1063	0.033

Table 18. Significantly down-regulated pathways between necking stages ≥90 and Str

KEGG ID	Pathway name	Observed	Total	FDR
ath00196	Photosynthesis - antenna proteins	10	21	1.47E-05
ath01110	Biosynthesis of secondary metabolites	71	1063	0.0027
ath00195	Photosynthesis	11	76	0.0168
ath00940	Phenylpropanoid biosynthesis	17	167	0.0203
ath00500	Starch and sucrose metabolism	15	147	0.0288
ath01100	Metabolic pathways	104	1899	0.0288

Further analysis of the starch and sucrose metabolism pathway (ath00500) was carried out with KEGG (Kanehisa, 2017), using all the up- and down-regulated genes with TAIR10 identifiers from the ≥90 vs Straight gene set as input (p adjust. <0.05; *Figure 47*). Colour scale annotations of the pathway were carried out to hightlight differential expression, with red indicating up-regulated and blue indicating down-regulated genes at each enzyme commission number (EC number). EC numbers are not specific to an enzyme but to an enzyme-catalysed reaction, therefore multiple genes (enzymes) may be associated with the same EC number (Kanehisa, 2017). Where multiple genes were associated with the

same EC number, a count-weighted mean Log2 FC was calculated and the representative colour for the average Log2 FC shown.

The large and small subunits for ADP glucose pyrophosporylase, APL1 and ADG1, were both shown to be down-regulated with an average Log2 FC of -0.99 at EC: 2.7.7.27. The glucose-starch glycosyltransferase, GBSS1 at EC: 2.4.1.242 was also found to be down-regulated with a Log2 FC of -0.75, together indicating a reduction in starch biosynthesis in ≥90° necking peduncles in comparisson to straight peduncles (*Figure 47*). Genes involved with starch catabolism, α-amylase AMY2 (EC: 3.2.1.1) and β-amylase BAM1 (EC: 3.2.1.2) were both found to be up-regulated. Although β-amylase 2 (BAM2) was found to be downregulated at EC: 3.2.1.2, there was a mean up-regulation of 0.93 (Log2 FC) of BAM1 and BAM2. However, the enzymatic activity of BAM2 is also known to be much weaker than BAM1, therefore and an overall increase in starch breakdown is likely (*Figure 47;* Fulton et al., *2008*).

A down-regulation of glycosidase genes including glucan endo-1,3-β-glucosidase genes 1, 2 and 4 at EC: 3.2.1.39 and glycosyl hydrolase 9B1, 9B3 and 9C2 at EC: 3.2.1.4, indicate a reduction in 1,3-β-Glucan and cellulose degradation (*Figure 47*). However, up-regulation of genes involved with the conversion of UDP-glucose to sucrose and D-fructose, sucrose to D-glucose and D-fructose, D-fructose to D-fructose-6P and D-glucose to D-glucose-6P could all be seen. Togther these lead to a potential increase in both D-fructose-6P and D-glucose-6P for use in glycolysis. Trehalose biosynthetic genes were also shown to be up-regulated, including trehalose-phosphatase/synthase 9 and 11 and trehalose-6-phosphate phosphatase G and J. No trehalase genes were found to have significant differential expression in the ≥90 vs Straight comparisson, indicating a potential increase in trehalose accumulation.

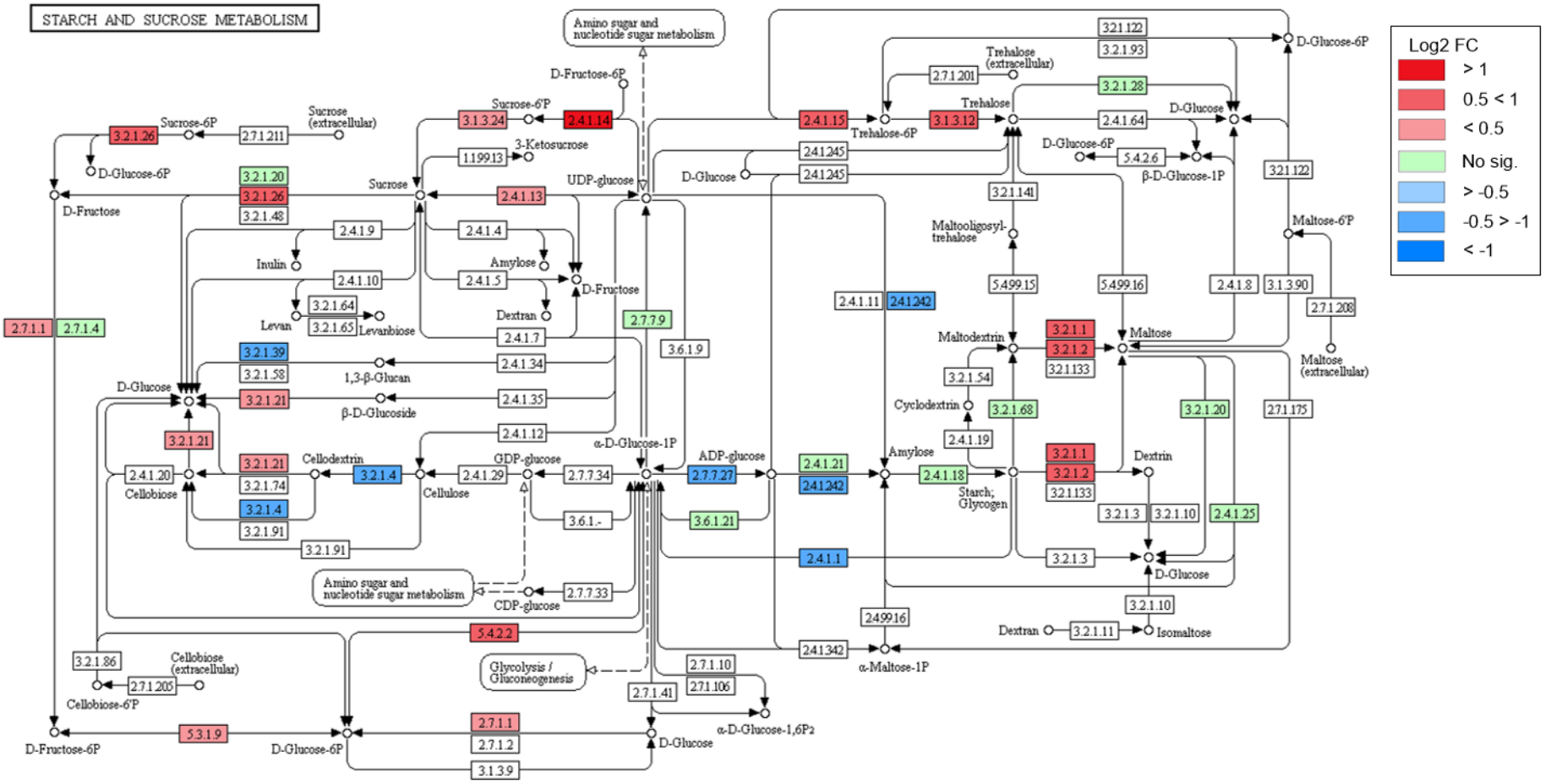

Figure 47. Starch and sucrose metabolism pathway with ≥90 vs Str differentially expressed genes. Pathway adapted from KEGG, annotated using Arabidopsis thaliana *TAIR10 identifiers (ath00500; Kanehisa, 2017). Significantly up and down regulated genes expressed using a red and blue colour scale respectively. Green coloured rectangles represent* Arabidopsis thaliana *genes that are not significantly expressed in the dataset.*

As well as SEA, PAGE analysis was also carried out with STRING, using the entire ≥90 vs Straight dataset and corresponding Log2 FC values (p adjust, <0.05). Enrichment analysis of gene functions revealed water channel activity to be significantly enriched, with an enrichment score of 4.10. Out of the nine aquaporin genes identified, eight showed down-regulation (*Figure 48*). TIP1-2 was the only water channel gene to be up-regulated. However, TIP1-2 also had the lowest mean count of all the aquaporin genes, with an average count of just 34 compared to an average count of over 9,500 for PIP2-7 and almost 1,400 for TIP4-1. Epidermal patterning factor and stomatal complex development genes were shown to be enriched 'network neighbours', with an enrichment score of 5.67. All of the four genes associated to this term, epidermal patterning factor 4, 6 and 8 and a LRR receptor-like protein kinase 'ERECTA' were found to be significantly down-regulated in ≥90° necking peduncles when compared to Straight (control) peduncles (Table 19).

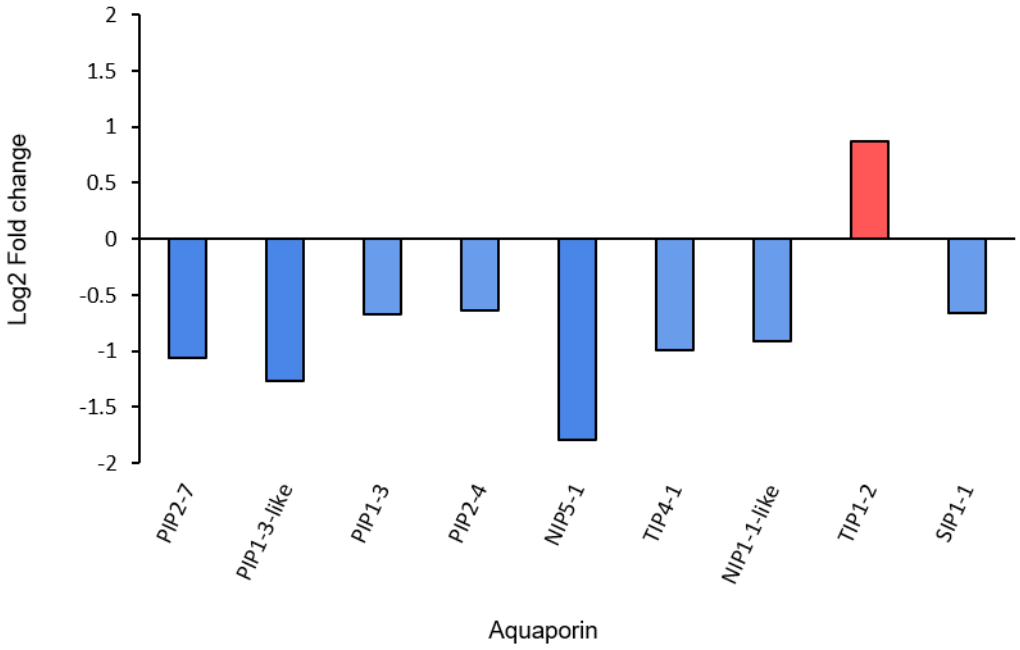

Figure 48. Aquaporin genes with differential expression between necking stages >90 and straight (p adjust. <0.05) Aquaporin genes are labelled with Rosa chinensis *descriptive IDs.*

Table 19. Epidermal patterning factor and stomatal complex development genes

Rosa chinensis RefSeq ID	*Arabidopsis thaliana* TAIR10 ID	Name(s)	Description	Log2 FC
XP_024180022	AT1G80133	EPFL8	Epidermal patterning factor-like 8	-0.90
XP_024163358	AT2G26330	TE1; ERECTA	LRR receptor-like protein kinase	-1.16
XP_024158540	AT2G30370	CHAL; EPFL6	Epidermal patterning factor-like 6	-1.29
XP_024197637	AT4G14723	CLL2; EPFL4	Epidermal patterning factor-like 4	-0.84

6.3.3 Differential expression analysis of transcription factors (TFs)

Annotation of the ≥90 vs Straight and <90 vs Straight against the transcription factor gene list identified 225 genes from 43 transcription factor families to be differentially expressed in at least one of the two contrast groups (p adjust. <0.05; *Figure 50A*). Growth regulating factor (GRF), squamosa promoter binding proteins (SBPs), TCP, YABBY and Zinc-finger homeodomain (ZF-HD) transcription factor families all showed down-regulation for the ≥90 vs Straight differentially expressed genes (*Figure 50B & C*). GRF, SBP and YABBY also showed down-regulation for genes in the <90 vs Straight comparison. All of the differentially expressed genes in the WRKY transcription factor family, and the majority of genes in the MYB-related, NAC and WUS homeobox-containing (WOX) transcription factor families showed significant up-regulation (*Figure 50*). A mixture of significantly up- and down- regulated TFs could be seen for ethylene-responsive factor (ERF) and GRAS transcription factor families in response to necking (*Figure 50B*).

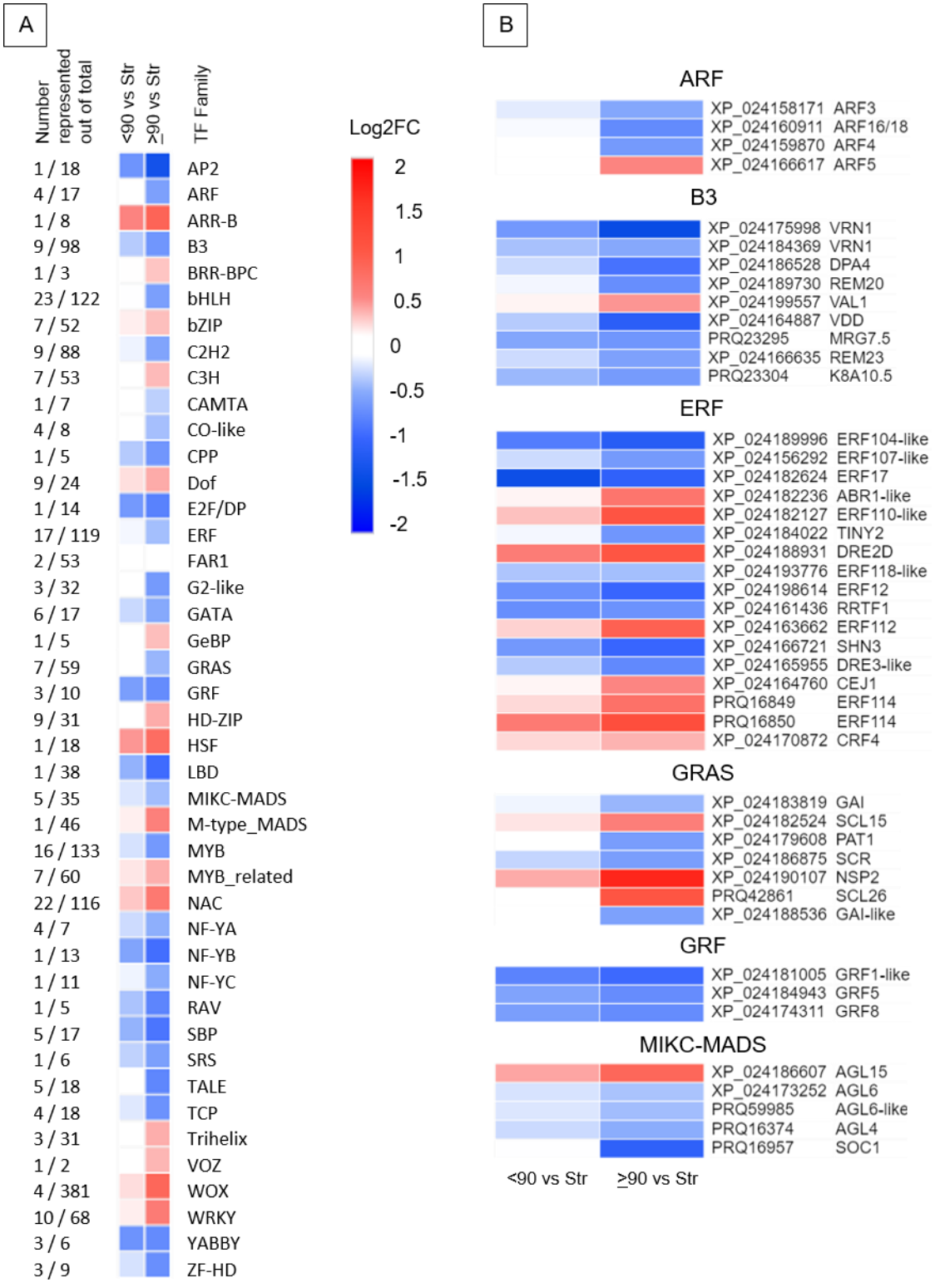

Figure 49. Heatmaps of differentially expressed transcription factors. (A) condensed heatmap of all transcription factor families, showing median Log2 fold changes. (B) and (C) individual heatmaps for transcription factor families showing Log2 fold changes for each Rosa chinensis *identifier. Up (red) and down (blue) log2 fold changes are shown for <90 and >90 in relation to straight (control) peduncles. For each datapoint, there is significant difference in expression for at least one comparison group (i.e. >90 vs Str or <90 vs Str). Heatmaps were generated using Morpheus with default and 'collapse group' settings (Morpheus, https://software.broadinstitute.org/morpheus).*

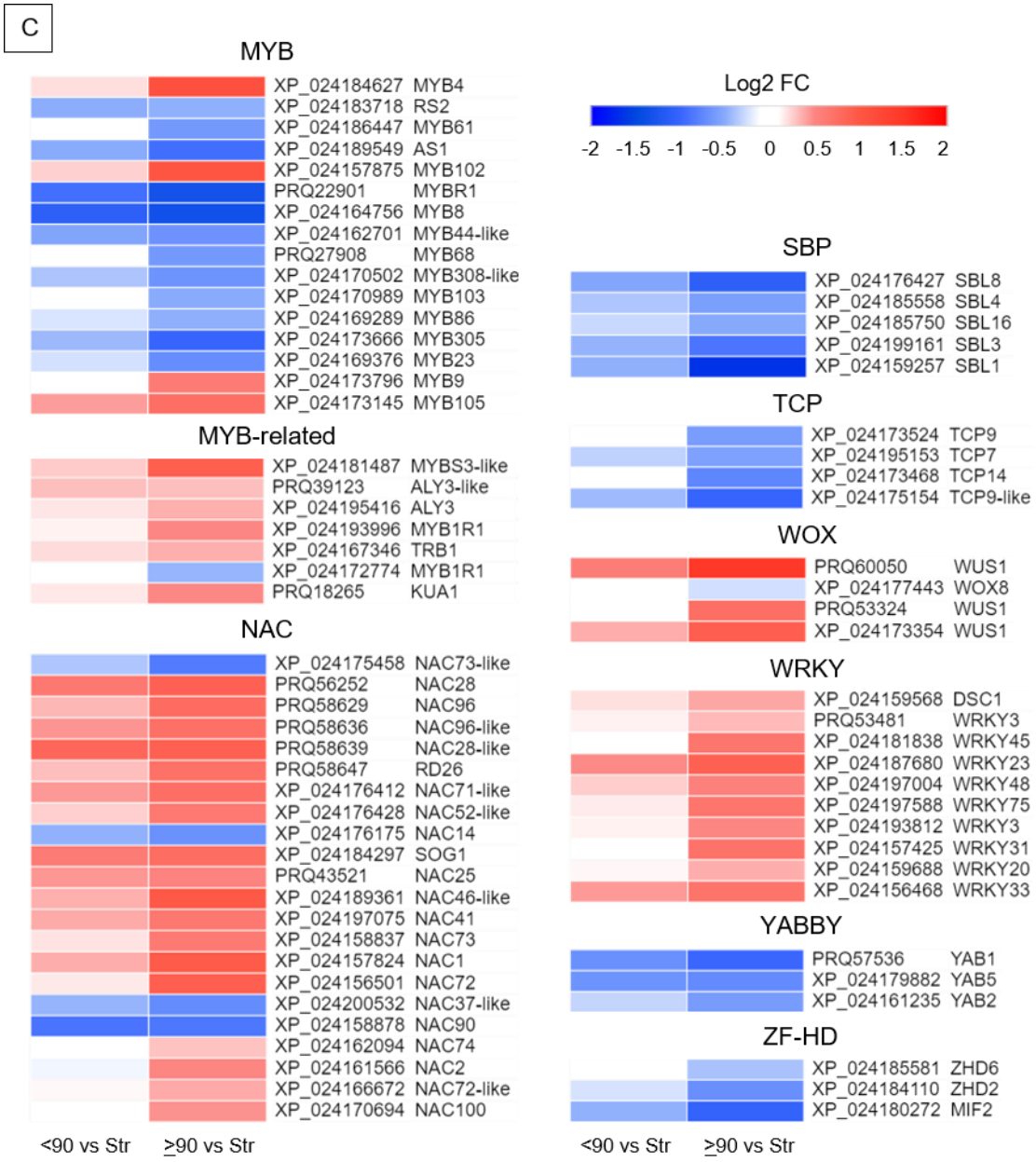

6.3.4 Analysis of senescence associated genes

The ≥90 vs Straight data set was found to have 64 senescence related terms, following annotation to the downloaded uniprot gene list. STRING's multiple protein search identified 44 of these genes to have connected nodes, as shown in *Figure 50*. A cluster of 11 autophagy-related gene (ATG) members were found to be significantly up-regulated and were all shown to have co-expression, with many of the connections having been experimentally determined (*Figure 50*). Histone deacetylase 9 (HDA9) was also shown to be significantly up-regulated, with co-expression to APG9 (ATG9). Linking the ATG cluster to the four histone

proteins H2AXA, HTB9, HTA12 and AT1G09200, all with significant down-regulation (p adjust. <0.05). A cluster of three mitogen-activated protein kinases (MPKs), MPK1, 4 and 13, and a MPK kinase (MKK2) were also shown to be differentially expressed, with MPK13 largest change in expression with a 1.09 Log2 FC for ≥90 vs Straight. Histone 3.1 (AT1G09200/ AT5G65360), the bidirectional sugar transporter (SAG29) and ribulose carboxylase/oxygenase activase (RCA) were the most down-regulated genes with connected nodes, with Log2 FC values of -1.16, - 1.09 and -0.91 respectively (p adjust. <0.05; *Figure 50*). Transcription factor TCP9 and mechanosensitive ion channel protein 10 (MSL10) were amongst the most down-regulated, with Log2 FC values of -1.02 and -0.99 (p adjust. <0.05), however neither were shown to have known connections to the other senescence genes identified and are therefore not shown in *Figure 50*. Nitrate transporter (NRT1.5) was the most up-regulated of the all the senescent related genes identified, with a Log2 FC of 1.71 (p adjust. <0.05, *Figure 50*). NDR1/HIN1-lie protein 10 (YLS9) was the second most up-regulated with a mean count of 13,487 and a Log2 FC of 1.64 (p adjust. <0.05). However, YLS9 also had no known connections to the other senescence associated genes and was therefore also not shown.

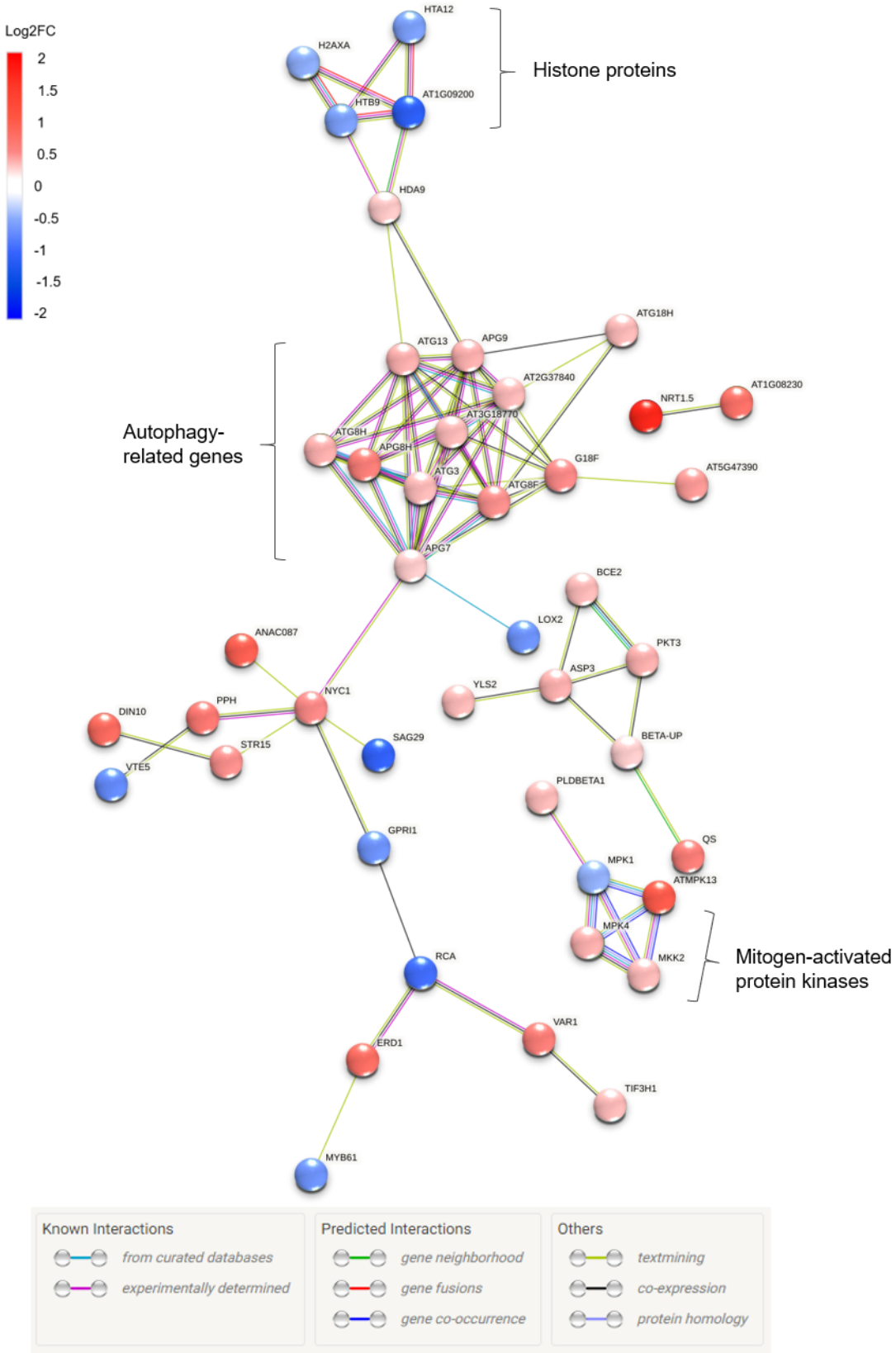

Figure 50. Protein connections of senescent related genes differentially expressed in ≥90 vs Str. Figure produced using STRING (Szklarczyk et al., 2018).

6.4 Discussion

Differential expression analysis following *Rosa chinensis* genome alignment successfully identified significant changes in gene expression between each of the necking stages (Table 15). The <90° necking stage is expected to be the mid-point between straight and >90° peduncles however, very few significant gene expression changes were identified between necking stages <90° and straight in comparison to the amount found between >90° and straight following the present workflow. The <90° necking stage proved difficult to classify as it is unknown if the peduncles harvested would have developed into full >90° necking. Greater variance within this stage may therefore have resulted in less gene expression changes being deemed 'significant' by DESeq2. In order to capture the full array of gene expression changes occurring during the necking process, the >90° vs straight comparison dataset was used for the majority of initial differential expression analyses.

6.4.1 Enrichment analysis (SEA and PAGE)

Photosynthesis was shown to be significantly down-regulated in >90° necking peduncles in the biological process heatmap and through enrichment analysis with AgriGO and STRING (*Figure 45*; Table 18). HAD9 is known to repress photosynthesis related genes and was shown to be up regulated in *Figure 50*. Expression of HAD9 is induced by ABA and salt stress in *Arabidopsis thaliana* and in response to temperature, salt and dehydration but not by ABA in tomato (Luo et al., 2017). As necking in *Rosa hybrida* peduncles is thought to be water stress related, it is likely that HAD9 expression may be up regulated in response to dehydration. Raffinose production has also been shown to increase in response to dehydration along with a down regulation in photosynthesis (Farrant et al., 2015). With a potential increase in raffinose production also seen in this study, as raffinose is synthesised in the galactose metabolism pathway which was found to be significantly up regulated in >90° peduncles compared to straight controls (Table 17).

The starch and sucrose metabolism pathway was also found to be significantly expresses in >90° necking peduncles by SEA in STRING (Table 17; Table 18).

Starch biosynthesis and photosynthesis are known to be strongly interlinked, with starch degradation often increasing in response to a reduction in photosynthesis to meet the energy requirements of cells (Zanella et al., 2016). Analysis of the starch and sucrose metabolism pathway indicated a significant up-regulation of starch breakdown by α-amylase (AMY2) and β-amylase (BAM1) in >90° necking peduncles (*Figure 47*). Under normal conditions BAM1 is not the primary β-amylase responsible for starch degradation, however expression has been shown to increased following osmotic stress (Valerio et al., 2010) and is essential for proline accumulation in *A. thaliana* to provide osmoprotection and protect against oxidative damage (Zanella et al., 2016). Both the gene ontology heat map and the starch metabolism annotated pathway also indicate an increase in trehalose biosynthesis (*Figure 45; Figure 47*). Trehalose is a non-reducing disaccharide which also functions as an osmoprotectant, accumulated in response to dehydration to stabilise proteins and membranes (Figueroa & Lunn, 2016; Iturriaga, Gaff & Zentalla, 2001). These changes in gene expression are therefore all consistent with a possible dehydration response in necking peduncles. However, the breakdown of starch by BAM1 is generally associated with leaf mesophyll cells where starch is primarily stored from photosynthesis (Valerio et al., 2010). As necking is associated with a xylem blockage, the transport of sugars between the leaves and peduncle may be limited, therefore resulting in a potential breakdown of starch by AMY2 and BAM1 within the peduncle, both for osmoprotection and if energy requirements are not met.

Starch containing plastids called amyloplasts are found in the endodermal layer of inflorescence stems and sediment in response to gravity (Sack, 1991; Nakamura et al., 2001). Amyloplasts are hence important for gravity perception, however it is unknown if increased starch degradation in the peduncle would include the degradation of amyloplasts as a source of starch in *R. hybrida* stems under osmotic stress and therefore whether this would alter gravity perception in the peduncle. In *A. thaliana* GRAS transcription factor scarecrow (SCR) mutants result in the absence of a normal endodermal layer and cause a lack of response to gravity (Fukaki et al., 1998). Significant down regulation of *SCR* and auxin associated tropism genes was seen in >90° necking peduncles compared to straight control stems, along with a significant down regulation of phototropic

genes (Table 16; *Figure 49*). Tropic responses to gravity and light are active processes, therefore it is unclear what potential effect the down regulation of these tropism related genes may have on the peduncle. However, downregulation of auxin transporters AUXIN1 (AUX1) and PIN1 may alter auxin transport and result in an imbalance within the peduncle (Yoshihara & Spalding, 2019; Swarup & Bhosale, 2019). SHOOT GRAITROPISM9 (SGR9), also found to be downregulated, modulates amyloplast dynamics and sedimentation and is therefore important for gravity perception (Nakamura et al., 2011). The identified tropism genes may therefore be interesting targets for further study, along with analysis of amyloplast content and distribution, to determine whether the necking phenomenon is associated with a disruption in a tropism response. As gravitropism bending sites in inflorescence stems are thought to be at a constant distance relative to the flower head, at the point where a gravitropism response is most sensitive, this may explain why necking occurs at a relative point in the peduncle and not elsewhere on the stem (Wyatt et al., 1997; Weise et al., 2000).

ERECTA is a transmembrane-type receptor kinase associated with the epidermis, phloem and xylem of inflorescence stems (Uchida et al., 2012). Ligands EPFL4 and EPFL6 together with ERECTA are involved with procambial maintenance and stomatal density (Uchida & Tasaka, 2013). ERECTA, EPFL4 and EPFL6 have also been shown to regulate elongation of inflorescence stems through the modulation of cell size (Uchida et al., 2012). These genes were all found to be significantly down regulated in >90° peduncles when compared to straight peduncles through PAGE analysis with STRING (Table 19) and therefore may also be interesting candidates for future research into necking. In particular, it would be interesting to see if expression of these genes is uniform across the peduncle, or if a reduction in gene expression only occurs on one side of the stem as this could contribute towards stem bending and therefore the necking process.

PAGE analysis with STRING also identified aquaporin genes to be significantly enriched, with the majority showing down regulation in >90° necking peduncles compared to straight (*Figure 48*). Most studies on aquaporin expression in Rosaceae species have focused on the expression of PIP1-1 and PIP2-1, neither of which were found to be differentially expressed in this study (Liu et al., 2019;

Ma et al., 2008; Mut et al., 2008; Šurbanovski et al., 2013). However, Šurbanovski et al. (2013) found aquaporin PIP2-2 (homologous to *R. chinensis* PIP2-4) to decrease in expression in response to drought stress in *Fragaria vesca* (strawberry) root and leaf tissue. PIP2-7 has also been shown to be down-regulated and degraded in response to abiotic stress in *A. thaliana*, with the number of PIP2-7 aquaporins reduced to modulate the osmotic permeability of membranes (Wang et al., 2017; Hachez et al., 2014). In this study both PIP2-4 and PIP2-7 were significantly down-regulated in >90° necking peduncles compared to straight controls. This may indicate a stress response within the peduncle tissue, with PIP2-4 and PIP2-7 down-regulated to help maintain osmotic balance and cell turgor (*Figure 48*).

6.4.2 Analysis of differentially expressed transcription factors

Transcription factors primarily associated with plant growth and development including GRF, MIKC-MADS, MYB, SBP, TCP, YABBY transcription factor families all showed significant down regulation in necking peduncles (*Figure 49*; Díaz-Riquelme et al., 2008; Kim et al., 2003; Li et al., 2013; Zhang et al., 2019; Zhou et al., 2016). WOX and GRAS transcription factor families were the exception to this and showed both up- and down regulation in >90° necking stage peduncles. However, of the significantly up- regulated GRAS transcription factors, SCL15 was found to repress the expression of genes associated with seed maturation in A. thaliana, therefore also resulting in the potential down-regulation of a developmental process (*Figure 49*; Gao et al., 2015).

NAC and WRKY transcription factors are both generally associated with stress responses and senescence, with most found to be up regulated in necking peduncles compared to straight controls (*Figure 49C*; Koyama, 2014). Specifically, NAC transcription factors NAC72, NAC2, NAC100 and responsive to desiccation 26 (RD26) were all shown to be significantly up regulated in >90° necking peduncles and are associated with drought stress responses (*Figure 49C*). NAC72, NAC2 and NAC100 were found to be significantly up regulated in *Pyrus bretschneideri* (white pear) following drought treatment (Gong et al., 2019) and RD26 shown to increase expression of drought responsive genes and negatively regulates plant growth in *A. thaliana* (Ye et al., 2017). RD26 and NAC2 (ATAF1)

are positive regulators of senescence, with NAC2 found to regulate autophagy related genes and RD26 found to induce protein degradation (including chloroplast degradation) and increase expression of AMY and SUS starch and sucrose catabolism genes (Kamranfar et al., 2018). This is consistent with both autophagy as well as starch and sucrose catabolism genes shown to be up regulated and photosynthesis down regulated in >90° necking peduncles (*Figure 50*; Table 17; Table 18). Unlike the majority of NAC transcription factors, NAC73-like (homologous to *A. thaliana* NAC73/SND2) and MYB transcription factor MYB103 were both significantly down-regulated in >90° necking peduncles and have been found to induce the expression of secondary cell wall biosynthesis genes, including cellulose, hemicellulose and lignin biosynthetic genes in *A. thaliana* (*Figure 49C*; Zhong et al., 2008). This is consistent with the STRING SEA analysis as lignin is synthesised in the phenylpropanoid biosynthesis pathway which was also found to be significantly down regulated in >90° necking peduncles (Table 18).

ERF (Ethylene-responsive transcription factor) family transcription factors are involved with stress responses and senescence, but also have major roles in other plant developmental processes and showed significant up and down regulation in necking peduncles (*Figure 49B*; Nakano et al., 2006). Both ABR1-like and ERF110-like ERF transcription factors were significantly up regulated in >90° necking peduncles compared to controls (*Figure 49B*) and are homologous to *A. thaliana* abscisic acid (ABA) repressor 1 (ABR1). ABR1, also known as ERF111 is expressed in *A. thaliana* in response to abiotic stress including wounding (mechanical stress) or reduced levels of oxygen (hypoxia). However, contrary to its name, ABR1 is no longer thought to be a negative regulator of ABA or thought to be induced by drought stress (Pandey et al., 2005; Bäumler et al., 2019). As both the control stems and the necking stems are both cut flowers, it is unlikely that ABR1 expression is induced due to wounding at the cut stem end. However, stems showing necking symptoms may have incurred more damage during transport, or it is possible that ABR1 expression may be up regulated in necking peduncles due to the mechanical stress of the necking process itself.

6.4.3 Analysis of senescence associated genes

Nitrate transporter NRT1.5 was the most up regulated of all the identified genes associated with the term senescence in >90° peduncles compared to straight controls and has been found to be up regulated during senescence in *A. thaliana* leaves to remobilise nitrates and ammonium and modulate phosphate levels (*Figure 50*; Havé et al., 2016). NRT1.5 was identified by STRING to be co-expressed with AT1G08230 (GAT1), a gamma-aminobutyric acid (GABA) transporter also significantly up regulated in >90° necking peduncles (*Figure 50*). GAT1 is expressed in response to elevated levels of GABA due to wounding and both stress-induced and developmental senescence (Meyer et al., 2006). Transcription factor ANAC087 (R. chinensis NAC46-like) positively regulates senescence in *A. thaliana* leaves by promoting the expression of genes associated with chlorophyll catabolism including non-yellow colouring 1 (NYC1) and pheophytinase (PPH) (Oda-Yamamizo et al., 2016). ANAC087, NYC1 and PPH all showed significant increases in expression in >90° necking peduncles, correlating with the significant down regulation of photosynthesis related genes seen in >90° necking peduncles and also indicating the likelihood of a senescence response in >90° necking peduncles (*Figure 50*; Table 18).

NYC1 was also connected by STRING to senescence associated gene (SAG) 15, also known as SWEET15, a sugar transporter whose expression has been shown to play a positive role in senescence (*Figure 50*). SAG29 expression is induced in *A. thaliana* by osmotic stress in an abscisic acid-dependent manner (Gao et al., 2016; Seo et al., 2010). However, SAG29 was interestingly one of the most down regulated senescence identified genes in >90° necking peduncles (*Figure 50*). SAG29 is thought to be involved with later stage senescence, rather than early stage senescence and may regulate cell death, therefore reduced expression of SAG29 in necking peduncles could indicate that cells at this stage are still viable and not experiencing late stage senescence responses (Seo et al., 2010). Alternatively, reduced expression of SAG29 may indicate a lack of ABA involvement in >90° necking stage processes compared to straight controls, however this would need to be experimentally determined.

Autophagy is essential for degrading unnecessary or dysfunctional cellular components, allowing for nutrient recycling and ensuring cellular and organismal homeostasis during stress responses (Batoko et al., 2017). Trehalose has been shown to initiate controlled autophagy to protect cells in abiotic stress conditions and genes for trehalose synthesis were significantly up regulated in >90° necking peduncles (*Figure 47*; Williams at al, 2015). A potential increase in trehalose may therefore in part contribute to the significant up regulation of the 11 autophagy-related gene (ATG) members seen in >90° necking peduncles (compared to controls, *Figure 50*). These include ATG8 isoforms (ATG8F and ATG8H) which are central proteins involved in autophagy and abiotic stress responses, including osmotic stress, as well as ATG13a, ATG13b and ATG11 autophagy genes which are involved in responses to carbon and nitrogen starvation (*Figure 50*; Wang at al., 2017).

6.5 Conclusions

This is the first study to explore differential expression changes associated with the necking phenomenon in *Rosa hybrida* following alignment to the *Rosa chinensis* genome and has successfully identified many significant changes in gene expression. Several methods were used to analyse the expression data, with many of the changes in gene expression relating to dehydration or osmotic stress and also wounding. Differential expression analysis of the transcription factors and senescence associated genes suggests that developmental processes are becoming down regulated in >90° necking peduncles due to entering a senescent state. As stems were of the same age and many stress associated genes were up regulated, senescence in >90° necking peduncles is hypothesised to be stress -induced rather than developmental.

Due to a lower than expected proportion of significant differentially expressed genes in the <90° vs Straight dataset, the >90° vs Straight comparison stage was used for the majority of analyses. Expression changes at this comparative stage including senescence associated genes are likely to represent genes being expressed as a result of necking, rather than potentially being causative to the necking process. As the galactose metabolism and phenylpropanoid biosynthesis

pathways were both found to be differentially expressed, these have been further analysed in (Chapter 7) with qPCR to verify gene expression in >90° and <90° stage necking peduncles. The potential involvement of tropism related genes and epidermal patterning factor genes in the necking process may also be worth investigating in future studies.

Chapter 7 Quantitative PCR of galactose metabolism and phenylpropanoid biosynthesis genes in *Rosa hybrida* cv. H30 necking peduncles

7.1 Introduction

Necking often results in roses terminating prematurely and causes postharvest losses within the cut flower industry. This is a physiological process likely to affect the biochemistry and hence the gene expression of the peduncle tissue. An understanding of the gene expression during this process may help to devise preventative measures and reduce occurrence and postharvest waste. An RNA-sequencing study of the transcriptional changes occurring through-out three stages of necking (Straight, <90° and >90°) identified the galactose metabolism and phenylpropanoid biosynthesis pathways to be significantly up- and down-regulated respectively (Chapter 6). The galactose metabolism pathway leads to the synthesis of galactinol and raffinose family oligosaccharides (ROFs), including the trisaccharide raffinose and the tetrasaccharide stachyose (Nishizawa et al., 2008). ROFs are water soluble carbohydrates, made up of sucrose with a number of additional galactosyl units (Gangl & Tenhaken, 2016). ROFs are known to accumulate in maturing seeds as sources of carbohydrate for germination, however ROFs also show important roles in plant stress responses due to their osmoprotectant and antioxidant activity (Gangl & Tenhaken, 2016; ElSayed et al., 2013; Nishizawa et al., 2008).

Phenylpropanoids on the other hand are secondary metabolites derived from phenylalanine, a product of the shikimate pathway and can be divided into five main sub-groups including stilbenes, monolignols, coumarins, flavonoids and phenolic acids. Phenolic acids can be further divided into the seven carbon (C6-C1) hydroxybenzoic acids and nine carbon (C6-C3) hydroxycinnamic acids (*Figure 51; Deng & Lu, 2017*). Although phenylpropanoids are referred to as secondary metabolites, products of the phenylpropanoid pathway have diverse and important functions within plants, providing scent, colour, structural support and also play vital roles in stress responses and plant defence (Biała & Jasiński, 2018). Monolignols or hyrdoxycinnamyl alcohol monomers for example, including p-coumaryl alcohol, coniferyl alcohol and sinapyl alcohol are the building blocks for lignin and lignan biosynthesis (Deng & Lu, 2017). Whereas hydroxycinnamic acids such as p-coumaric, caffeic, ferulic and sinapic acids which occur widely

among higher plants and are also known for their antioxidant activity (Teixeira et al., 2013)

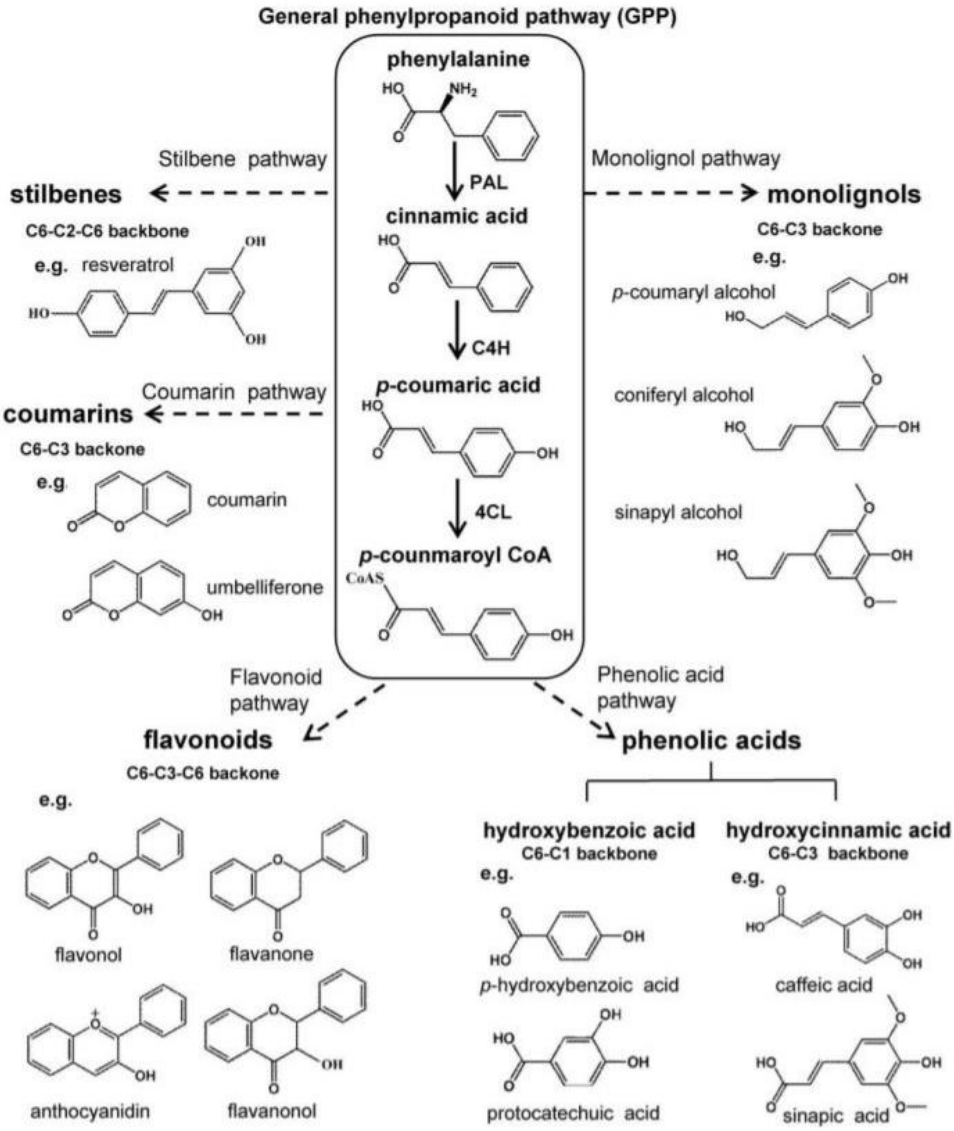

Figure 51. Phenylpropanoid biosynthesis and chemical structures. The conversion of phenylalanine to p-coumaryl CoA includes the first three steps of phenylpropanoid biosynthesis, known as the general phenylpropanoid pathway (GPP). These three steps produce the precursors for the five main phenylpropanoid groups: stilbenes, monolignols, coumarins, flavonoids and phenolic acids. Solid arrows represent single biosynthetic steps and dashed arrows indicate multiple biosynthetic steps. PAL, phenylalanine ammonia lyase; C4H, cinnamate 4-hydroxylase; 4CL, 4-coumaroyl CoA ligase. Figure from Deng & Lu, (2017).

RNA sequencing (RNA seq.) allows for whole transcriptome analysis and provides a non-biased approach to gene expression studies as no prior knowledge of the transcriptome is needed. However, there is currently no

standard workflow or set protocol for completing the data analysis, with all methods differing in performance and how they normalise datasets and quantify gene expression levels (Everaert et al., 2017). Validation of gene expression data from RNA seq. experiments by quantitative PCR (qPCR) is therefore still common practice. qPCR data however is relative, with expression normalised to a reference gene. Choosing an appropriate reference gene with stable expression is therefore important for producing reliable qPCR results (Bustin et al., 2009).

Elongation factor 1α is a traditionally used gene for qPCR normalisation and was found to be one of the most stable reference genes out of four novel and 12 traditional candidates analysed in the Rosaceae family member, *Prunus persica* L. Batsch (peach; Kou et al., 2017). However, Klie and Debener (2011) found protein phosphatase 2A (PP2A) to be one of the best general reference genes for *Rosa hybrida*, outperforming EF1-α and other classically used reference genes including glyceraldehyde-3-phosphate dehydrogenase (GAPDH) and tubulin. Although these were overall the most stable reference genes for both studies, expression and suitability varied between tissue type and whether a stress treatment was applied. Reference genes suitable for studying necking in *Rosa hybrida* must be stable in peduncle tissue and under water stress conditions. Most studies focused on peduncle or pedicel tissue are related to flower or fruit abscission, rather than water stress and use a variety of reference genes including SAND family proteins in tomato (*Solanum lycopersicum*), and actin in yellow lupine (*Lupinus luteus*) and apple (*Malus × domestica*) respectively (Nakano et al., 2014; Glazinska et al., 2017; Heo & Chung, 2019). However, GAPDH is often found to be the most stable reference gene in drought and water stress conditions and has been used in the study of postharvest dehydration of citrus fruit (*Citrus sinensis*) rind, in drought stressed potato (*Solanum tuberosum*) leaves and also to successfully analyse drought stress in rice (*Oryza sativa*) peduncles (Tian et al., 2015; Romero et al., 2013; Yang et al., 2019; Muthurajan et al., 2010).

A qPCR study of genes within the galactose metabolism and phenylpropanoid biosynthesis pathways was carried out and compared to the differential

expression RNA sequencing results, with EF1α, PP2A and GAPDH selected as potential reference genes for qPCR normalisation.

7.2 Methods

7.2.1 Plant material for qPCR

Rosa hybrida cv. H30 stems were grown, transported and processed as described in section (2.1). Stems were held in standard experimental conditions for the duration of the experiment, arranged in bunches of 10 and placed in vases containing 1 L of 2 % sucrose solution (w/v). Vases were supplemented with a *Pseudomonas fluorescens* suspension to induce necking in the H30 stems and was prepared as described in (4.2.5) to an initial vase concentration of 2.5 x 10^5 cfu per mL.

Peduncle samples for each stage (Str, <90° and >90°) were taken as previously described (5.2.1). Samples were collected on day 4 and 5 of vase life, as necking occurred. All of the stages (Str, <90° and >90°) making up one biological replicate were harvested at the same time.

7.2.2 RNA extraction and cDNA synthesis

RNA was extracted from the rose peduncles and the quality measured as previously described (2.4). Genomic DNA (gDNA) removal and cDNA synthesis were then performed using the Quantitect Reverse Transcription Kit (Qiagen), following the manufacturers guidelines. For every 1 µg of RNA, 2 µL of gDNA wipeout buffer (7x) was added, in a 14 µL final volume with RNase free water and incubated at 42 °C for 2 min to ensure gDNA elimination. The reactions were placed immediately on ice and 1 µL of Quantiscript Reverse Transcriptase, 4 µL of Quantiscript RT buffer (5x) and 1 µL of RT primer mix were added for a total 20 µL reaction volume. cDNA synthesis was performed at 42 °C for 15 min, followed by a 95 °C incubation for 3 min to inactivate the reverse transcriptase. The cDNA was 1/10 diluted with RNase free water, for a working concentration of 5 ng/µL (assuming equal efficiency of reverse transcription) and stored at -20 °C for direct use in qPCR.

7.2.3 Primer design

Genes of interest were chosen from the galactose metabolism and phenylpropanoid biosynthesis pathways due to their significant differential expression in the RNA sequencing dataset. Reference genes GAPDH, EF1-α and PP2A were selected based on their use in previous studies and their expression stability in the RNA sequencing dataset.

Table 20. qPCR target genes

	Gene name	Gene description	Gene ID (Locus)
GM	UGE5	UDP-glucose 4-epimerase	112179506
	SIP2	Probable galactinol—sucrose galactosyltransferase 2	112191944
	DIN10	Probable galactinol—sucrose galactosyltransferase 6	112186834
	ATBF1	Beta-fructofuranosidase	112187488
	PGM2	Phosphoglucomutase, cytoplasmic	112197974
	AGAL3	Alpha-galactosidase 3	112185187
	GolS2	Galactinol synthase 2	112197839
PB	OMT1	Caffeic acid 3-O-methyltransferase	112184684
	PRXPX	Peroxidase 42	112167574
	CAD9	Probable cinnamyl-alcohol dehydrogenase 9	112184982
	HCT	Shikimate o-hydroxy-cinnamoyltransferase	112201402
R	GAPC2	Glyceraldehyde-3-phosphate de-hydrogenase, cytosolic	112179622
	EF1-α	Elongation factor 1-alpha	112198567
	PP2A	Serine/threonine-protein phosphatase PP2A catalytic subunit	112180536

GM= galactose metabolism genes, PB= phenylpropanoid biosynthesis genes and R= reference genes

The qPCR primers were designed using NCBI's Primer-BLAST with the following parameters: Tm between 57 and 63 °C (optimum Tm of 60 °C), with a maximum Tm difference of 2 °C; primer length of 18–25 base pairs (bp), with an optimum length of 20 bp; GC content of 35–75 % and a PCR product size of between 90 and 170 bp (Table 21). Template gene of interest (GOI) and reference gene

mRNA sequences were obtained from the Genome Database for Rosaceae (GDR), using the 'Search Genes and Transcripts' function for the *Rosa chinensis* Old Blush genome. Primer-BLAST searches were limited to 'Rosa (taxid: 3764)' within the Refseq mRNA database to ensure specificity to intended target sequences.

Primer specificity was determined by conventional PCR for each of the primer pairs. A 20 µL PCR reaction was performed with 0.5 µM forward primer, 0.5 µM reverse primer, 10 µl of PCRBIO Taq Mix Red (PCR Biosystems) and 10 ng of straight (control) cDNA (2 µL of 1/10 diluted cDNA). PCR cycle conditions included an initial 1 min denaturation and enzyme activation step at 95 °C, followed by 37 cycles of 15 sec denaturation at 95 °C, 15 sec annealing at 55 °C and a 10 sec extension at 72 °C, with a final extension of 4 mins at 72 °C. PCR product was analysed by electrophoresis on a 1 % agarose gel stained with SYBR safe DNA gel stain (Invitrogen) and purified using the Wizard SV Gel and PCR Clean-up System (Promega), following the manufacturer's purification by centrifugation protocol. Purified amplicons were measured using a Nanodrop spectro-photometer and sent for sequencing using MixSeq tubes (Eurofins genomics). Retrieved sequences were then submitted to an NCBI's BLASTn search to ensure the intended product was amplified.

Table 21. Primer sequences and product sizes

Gene name	Primer sequences	Position	Product size (bp)
UGE5	F: GGAACTGAACTGGAAGGCGA R: TGTCTTGAGGTCCATAGCCA	1138-1235	98
SIP2	F: TGTTCAACTCCAGTGGTGCT R: GGTTTTGATGGTGACTGTGGC	2199-2326	128
DIN10	F: GGTTAGAGGGTGTGGCAAGT R: AAGTCACCAACCCAGATGCC	2222-2334	113
ATBF1	F: TGGGGCATTTGTAACTGTGGA R: AATTGAAAGCATATAAGTGGGCATC	1618-1784	167
PGM2	F: CGCAACCATTCGTCTCTACA R: GCAGATCGGCCAGTGAATTC	1745-1882	138
AGAL3	F: GGAATCGGGGTTCAACAGCA R: ACCAGAGCACCAAATGAGGA	1163-1304	142
GolS2	F: TGGTGAAGAAATGGTGGGACA R: GTACGCTCATTCTCGGCCTT	917-1007	91
OMT1	F: TATGCAGCGCTTCCAGACAAT R: GAGCCAACATGATCACGTCG	937-1054	118
PRXPX	F: ACGTGAGAAATGACCGTGGT R: GGTCCTCTTGTCTGTGGCAA	745-860	116
CAD9	F: GGGAAACTGGTTACTGTGGGT R: TTATCCCTCCAACGTCGCTT	894-999	106
HCT	F: GGTTTACGCTGCCCCTCTAT R: CGTGTTCATATGCCGAGAATGC	1259-1419	161
GAPC2	F: GCTTGAGAAGAAGGCCACAT R: TGCTTGATCTGTTGTCACCGA	877-1013	137
EF1-α	F: CCTTCTCTGAGTACCCACCCT R: ACTTCTTCTTGGCAGCAGACTT	1376-1513	138
PP2A	F: GTGCCAGGAAAAGAACGTTGT R: GGTGCTGGGTCAAATTGAAGG	942-1070	129

7.2.4 qPCR conditions

The qPCR's were performed using a Rotor-Gene Q thermo cycler (Qiagen, Model: 5-Plex) in 20 µL reactions with 1x Rotor-gene SYBR Green PCR master mix (Qiagen), 0.5 µM forward primer, 0.5 µM reverse primer, RNase-free water and 10 ng cDNA (2 µl of 1/10 diluted template cDNA). A two-step cycling program was used as recommended by the manufacturer: initial DNA polymerase activation at 95 °C for 5 min, followed by 40 cycles of denaturation at 95 °C for 5 sec and a combined annealing and extension at 60 °C for 10 sec. An additional melt curve analysis step was then performed by ramping the temperature from 50-95 °C to determine primer specificity. All qPCRs were run with two technical replicates and for four biological replicates of each stage. Ct values were recorded at a 0.2 threshold and only technical replicates with a Ct value within 0.5 of each other were used in analysis (any outside of this were re-run).

7.2.5 Primer efficiency and expression analysis

A standard curve was generated for each primer set to calculate the percentage primer efficiencies, using a 1:10 dilution series of straight (control) cDNA and standard qPCR conditions (7.2.4). Efficiencies were calculated manually with Equation 5. 'Slope' was calculated for each primer set using the Excel 'SLOPE' function, where y equals the average Ct values of the technical replicates and x equals the Log of the dilution factors. Percentage efficiencies should be between 90-110 %.

Equation 5.

$$Efficiency\ (\%) = \left(10^{\frac{-1}{Slope}} - 1\right) \text{x} 100$$

Relative expression levels were calculated according to the Pfaffl equation (*Equation 6*; Pfaffl, 2001), which takes into account differences in primer efficiencies for increased reproducibility. 'E' in *Equation 6.* refers to the percentage

primer efficiency (*Equation 5*) for the gene of interest (GOI) and reference gene (Ref), converted using Equation 7.

Equation 6.

$$Gene\ expression\ ratio = \frac{(E_{GOI})^{\Delta Ct\ GOI}}{(E_{Ref})^{\Delta Ct\ Ref}}$$

Equation 7.

$$E = \left(\frac{Efficiency\ (\%)}{100}\right) + 1$$

7.2.5.1 Statistical analysis of relative expression

Relative expression data for each gene were analysed with one-way ANOVA tests to determine the effect of necking stage on relative gene expression. Tukey post hoc tests were then used for multiple comparisons of means to determine significant differences between necking stages. Pfaffl gene expression ratios were transformed using the Log2 scale prior to analysis.

7.2.6 RNA sequencing differential expression data

Differential expression Log2 FC values for galactose metabolism and phenylpropanoid biosynthesis genes were taken from the DESeq2 output files generated in Chapter 6 for the three comparative necking stages using the VLOOKUP excel function and the *Arabidopsis thaliana* gene identifiers for each pathway identified by STRING. *Rosa hybrida* cv. H30 flower material for this expression data was harvested, sequenced and aligned to the *Rosa chinensis* genome as described in Chapter 5 and processed as described in Chapter 6.

7.3 Results

Good quality RNA was extracted for each of the biological replicates, in which necking had been induced by *Pseudomonas fluorescens,* and was successfully synthesised into cDNA following gDNA removal (*Appendix 1.1*). The seven galactose metabolism primers, four phenylpropanoid biosynthesis primers and three reference gene primers were all initially run using conventional PCR with straight peduncle cDNA (pilot sample, Str_0). PCR products were achieved for all of the primer pairs and were of the predicted size, with the exception of the galactinol synthase 2 (GolS2) primers (*Figure 52*). Each of these reference genes and the genes of interest successfully produced a single peak in a qPCR melting curve analysis, indicating amplification of a single gene product. The primer pairs were all verified to amplify their intended target sequences, with an example melt curve analysis and the Blast results of the PCR products shown in Appendix 1.1.

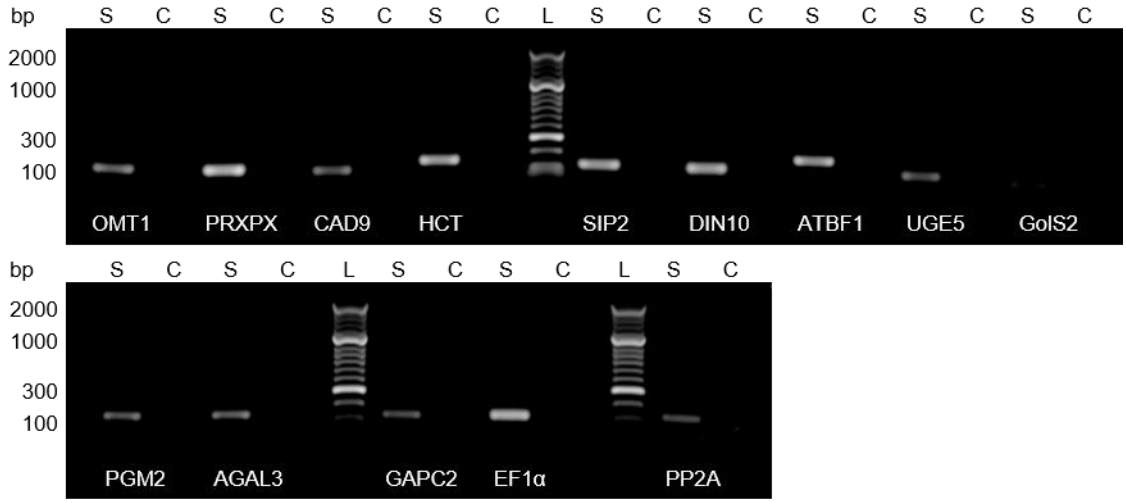

Figure 52. Gel electrophoresis image showing amplified PCR product for each of the target genes. 'S' indicates lanes containing PCR product run from the initial 'pilot' Straight sample cDNA (Str_0) and 'C' indicates lanes containing negative PCR controls, run with RNase free H20. Bands are shown in reference to hyperladder 50bp (Bioline) shown as lanes labelled 'L', with the corresponding number of base pairs (bp) for each main band detailed on the left-hand side of the gel image.

7.3.1 Identification of a reference gene

The candidate reference genes glyceraldehyde-3-phosphate de-hydrogenase (GAPC2), elongation factor 1-alpha (EF1-α) and serine/threonine-protein phosphatase PP2A catalytic subunit (PP2A) all showed relatively uniform

expression in each of the replicate one necking stages (Str_1, <90_1 and ≥90_1) and between the two straight biological replicates (pilot sample Str_0 and replicate one Str_1) in conventional PCR (*Figure 53*). Following primer efficiency analysis with qPCR, GAPC2 was found to have the closest percentage efficiency to the genes of interest (GOI), with an efficiency of 97.3 % compared to a mean GOI efficiency of 98.68 % (Table *22*). GAPC2 and PP2A were also shown to have the closest mean CT values to the GOI, which had an overall mean CT value of 22.6 (Table *22*). As it is preferable to have a reference gene with a similar expression to the GOI and therefore a similar CT value (Delporte et al., 2015), GAPC2 was found to be the most suitable reference gene for the dataset and was used in further analysis to calculate the relative log2 FC of the genes. The primer efficiencies of UGE5 and PGM2 fell slightly outside of the preferred range (90-110 %; Table *22*), therefore the Pfaffl method was adopted to calculate relative gene expression as it accounts for variance in primer efficiencies unlike the delta-delta CT method which assumes similar GOI primer efficiencies.

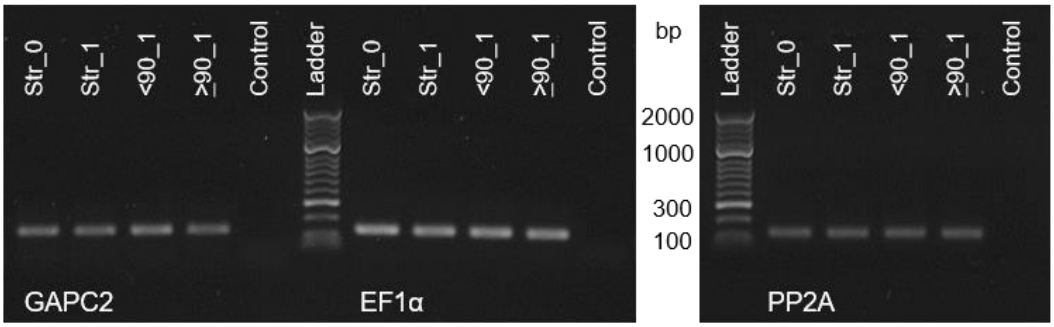

Figure 53. PCR product for the candidate reference genes at each of necking the stages. Lanes labelled Str_1, <90_1 and >90_1 refer to PCR product from each of the necking stages in biological replicate one, with Str_0 referring to a Straight necking stage sample used as an initial pilot. Bands are shown in reference to hyperladder 50bp (Bioline), with the corresponding number of base pairs (bp) for each main band detailed in between the two gel images.

Table 22. qPCR primer efficiencies and mean CT values

Primer	Efficiency (%)	Mean CT value
UGE5	110.9	24.4
SIP2	96.7	20.8
DIN10	96.5	22.4
ATBF1	100.5	23.0
PGM2	89.3	20.7
AGAL3	101.8	25.2
OMT1	104.4	20.1
PRXPX	97.2	20.0
CAD9	93.3	25.3
HCT	96.2	24.2
GAPC2	97.3	24.2
EF1-α	95.0	19.2
PP2A	95.2	23.9

Primer efficiencies and mean CT values shown to 1 decimal place. Mean CT values were calculated for each of the primers using all of the necking stage CT values for all four biological replicates.

7.3.2 Galactose metabolism

Previous differential expression analysis of the RNA sequencing data identified nine galactose metabolism genes to be up-regulated during >90° necking, compared to Straight peduncles as shown in *Figure 54* (>0.5 Log2 FC, p adjust <0.05; Chapter 6). The seven galactose metabolism pathway genes selected for qPCR analysis included all these differentially expressed genes, excluding the two ATP-dependent 6-phosphofrucyokinase genes PFK2 and PFK4 at EC 2.7.1.11. Genes from EC 2.7.1.11 were not included as this EC point appears to fall outside of the central galactose metabolism pathway (*Figure 54*).

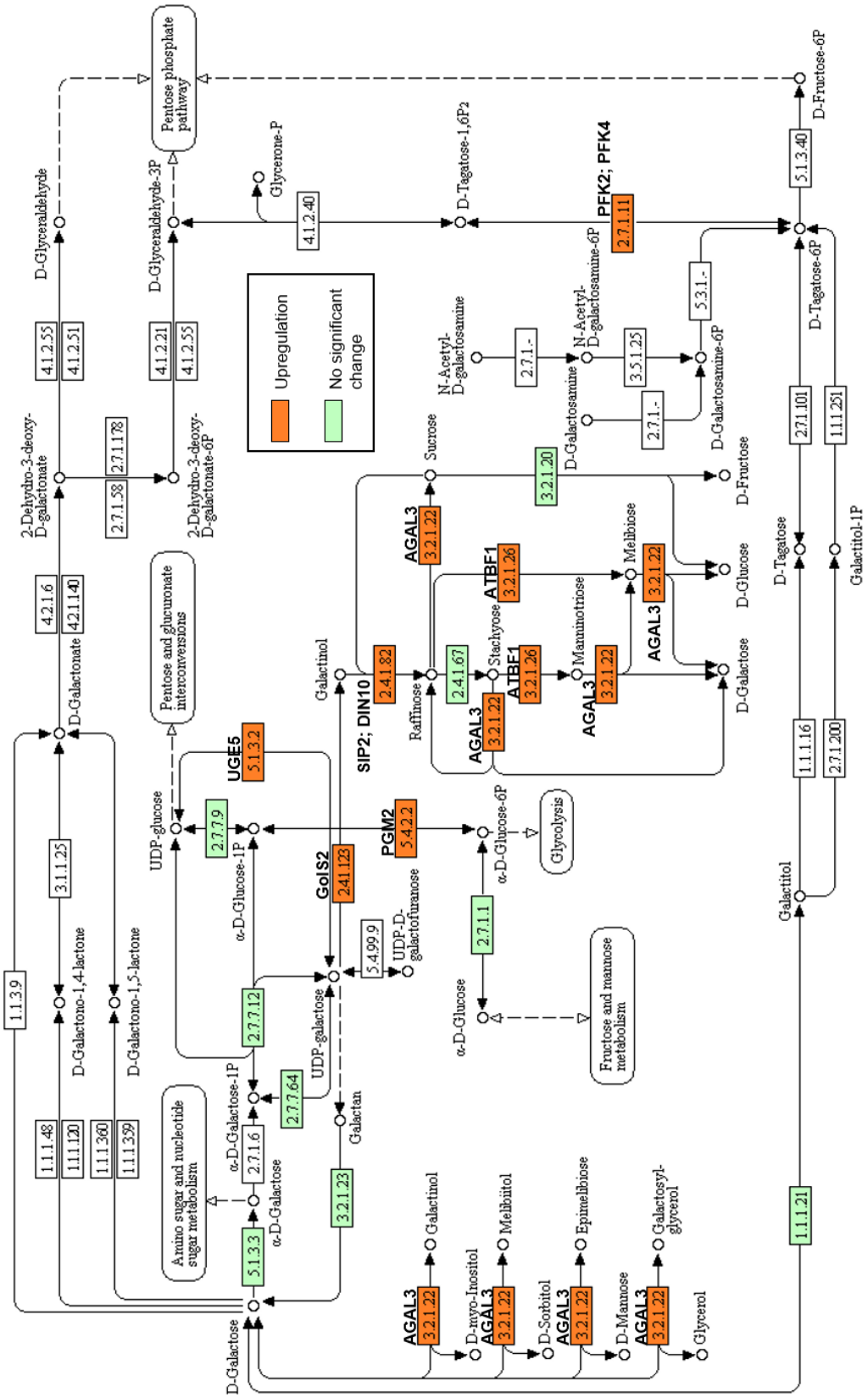

Figure 54. RNA seq. differentially expressed galactose metabolism genes. The green colour represents genes present within the Rosa chinensis *genome, and the orange colour EC numbers represent significantly up-regulated genes in the >90 vs Str dataset, with a Log2 FC >0.5 and a p adjust value <0.05. Pathway adapted and annotated from KEGG (pathway: rcn00052; Kanehisa, 2017).*

In the RNA seq. analysis, although significant expression was seen for all of the >90 necking stage peduncles in comparison to straight, no significant difference was seen between the <90 and straight necking stages for any of the analysed galactose metabolism genes (*Figure 55*). However, in the qPCR analysis SIP2 (EC 2.4.1.82) showed significant difference between the <90 and straight necking stages, as well as between the >90 and straight and >90 and <90 necking stages (*Figure 56*). Significant up-regulation was also seen for UGE5 (EC 5.1.3.2) and DIN10 (EC 2.4.1.82) in fully necked (>90) peduncles for both RNA seq. and qPCR analysis (*Figure 56; Figure 56*). However, no significant differential expression was seen for the other three galactose metabolism genes (ATBF1, PGM2 or AGAL3) relative to GAPC2 expression in the necking peduncle tissue analysed with qPCR (*Figure 56*).

ANOVA results for all galactose metabolism pathway genes analysed through qPCR are presented in Appendix 1.2.3.1.

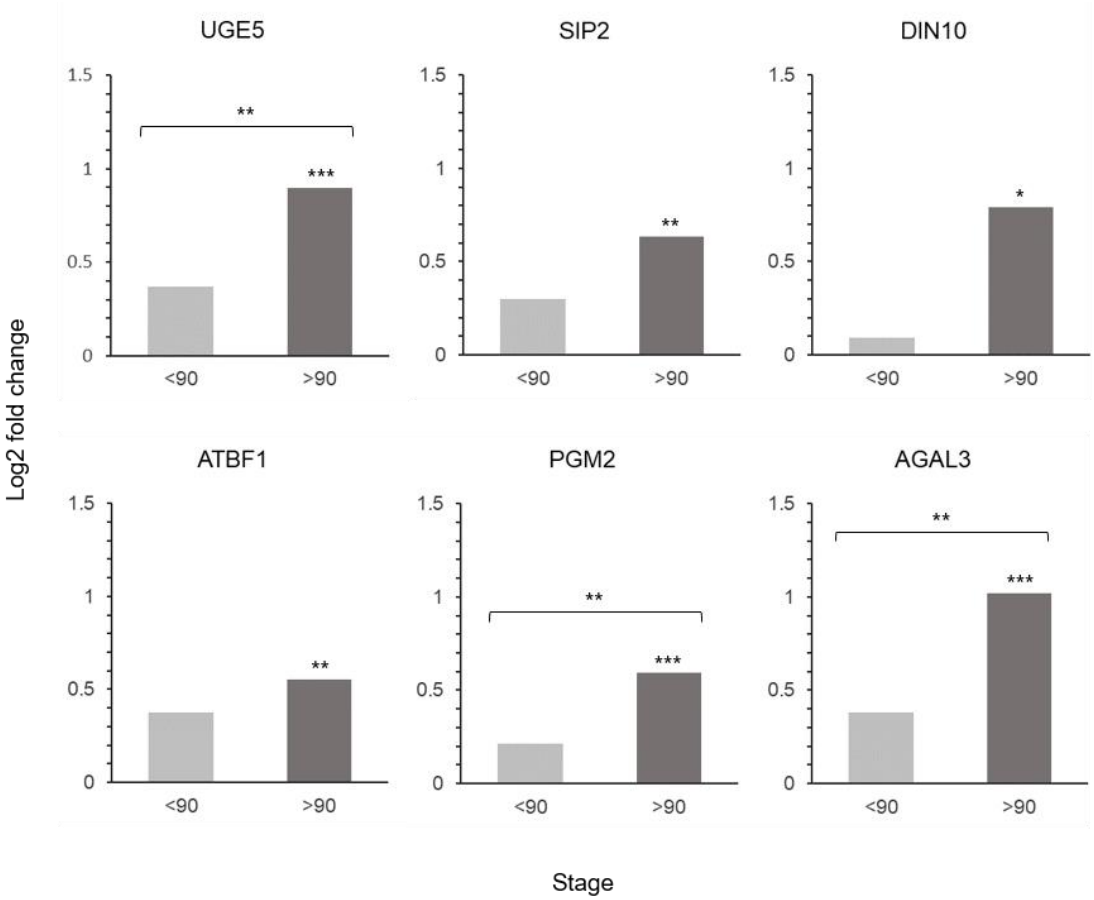

*Figure 55. RNA seq. differential expression bar charts for galactose metabolism genes. Rose peduncles at Straight, <90 and >90 necking stages were harvested during vase life of roses held in commercial flower food. Log2 FC values are shown relative to straight control peduncles, with significance calculated using DESeq2. Significant difference between <90 and straight, and >90 and straight is indicated above the relative bar. Significant difference between <90 and >90 is indicated between the two bars, where *** indicates significance to a p adjusted value of <0.001, ** to <0.01 and * to <0.05.*

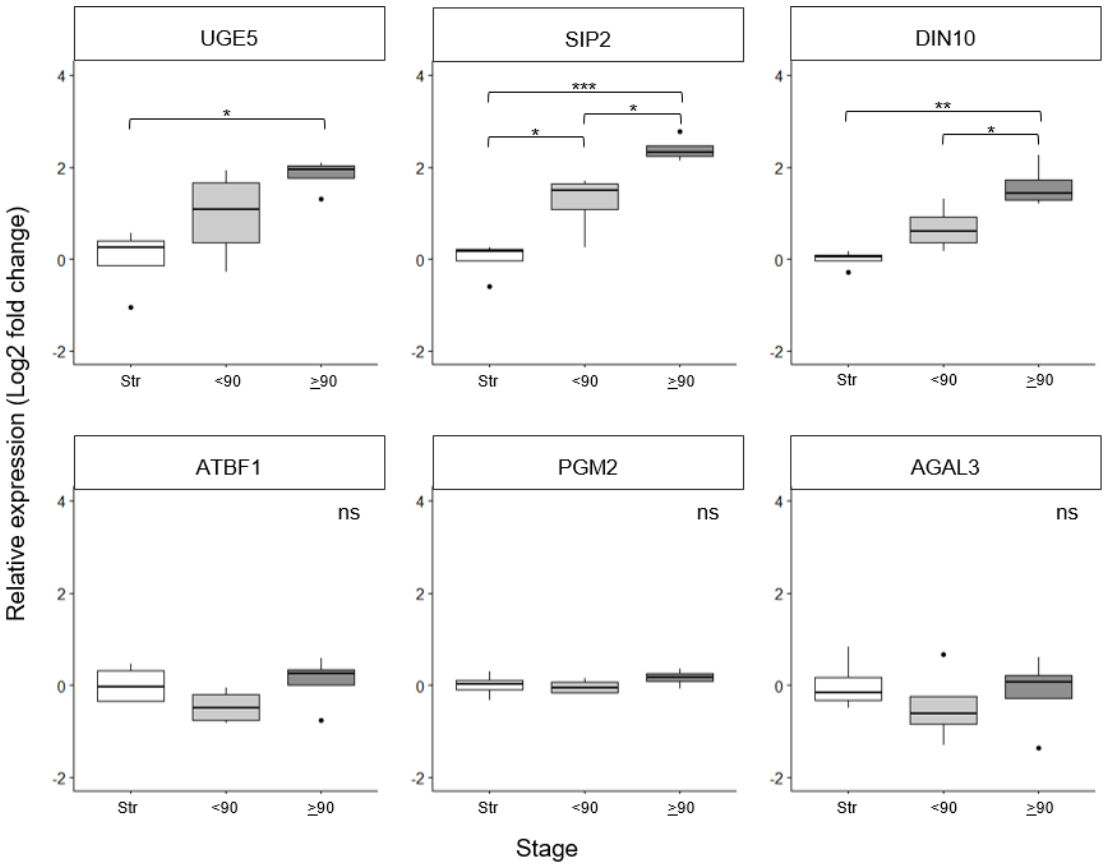

Figure 56. qPCR relative expression boxplots for galactose metabolism genes. Rose peduncles at Straight, <90 and >90 necking stages were harvested during vase life of roses induced by treatment with Pseudomonas fluorescens. *Pfaffle analysis is relative to GACPC2 expression using necking stage Straight as the control. Statistical analysis was calculated using a one-way ANOVA of Log2 FC vs Stage with a Tukey post hoc test, where *** indicates significance difference in expression to a p value of <0.001, ** to <0.01, * to <0.05 and 'ns' indicates no significant difference.*

7.3.3 Phenylpropanoid biosynthesis

As with the galactose metabolism, a previous differential expression analysis of the RNA sequencing data identified 17 phenylpropanoid biosynthesis genes to be down-regulated during >90° necking, compared to Straight peduncles as shown in *Figure 57* (>0.5 Log2 FC, p adjust <0.05; Chapter 6). Of the 17 down-regulated phenylpropanoid biosynthesis genes identified, nine peroxidase genes were associated with EC 1.11.1.7. As peroxidase 42 (PRXPX) had a mean count of 18,556 compared to 451 and 288 of peroxidase 64 (PER64) and peroxidase 73 (RHS19) respectively with the second and third highest mean counts, PRXPX was chosen as a representative gene at this EC point. Similarly, elicitor-activated gene 3-1 (EL13-1) and (CAD9) were found to be significantly down-regulated at

EC 1.1.1.195. However, EL13-1 was shown to have a mean count of just 24, compared to a mean count of 11,491 for CAD9 therefore CAD9 was chosen to represent this EC point. Shikimate O-hydroxycinnamoyltransferase (HCT) and caffeic acid 3-O-methyltransferase (OMT1) are the only genes associated with EC numbers 2.3.1.133 and 2.1.1.68 respectively and therefore were both selected for qPCR analysis. Although beta-glucosidase 17, 41, 44 and beta-glucosidase BGLC1 associated with EC 3.2.1.21 were all significantly down-regulated, none of these genes were analysed in this study due to the EC point appearing separate from the main pathway (*Figure 57*). Genes found to be significantly up-regulated in the phenylpropanoid biosynthesis pathway, 4-coumarate-CoA ligase 7 (4CLL7) at EC 6.2.1.12 and caffeoyl coenzyme A ester o-methyltransferase 7 (CCOAOMT7) at EC 2.1.1.104 were also not analysed by qPCR, due to the down-regulated genes being the main focus of study (*Figure 57*).

Significant down-regulation between >90 and straight peduncles for PRXPX, CAD9 and HCT genes was seen in both the RNA seq. and qPCR datasets. Significant down-regulation was also seen for PRXPX, CAD9 and HCT for <90 necking peduncles compared to straight control peduncles through qPCR. Although there was a comparable mean log2 FC of -0.67 between >90 and straight, this difference was not significant for OMT1 with qPCR while it is significant in the RNA sequencing dataset (*Figure 58, Figure 59*). Down regulation was also seen for OMT1 between <90 and straight with qPCR, however this change was only significant to a p value of <0.1 (*Figure 59*). The phenylpropanoid biosynthesis genes analysed with qPCR therefore all showed down-regulation in <90° and >90° necking tissue compared to straight control tissue, with this change in gene expression found to be significant in three of the four genes analysed (*Figure 59*).

ANOVA results for all phenylpropanoid pathway genes analysed through qPCR are presented in Appendix 1.2.3.2.

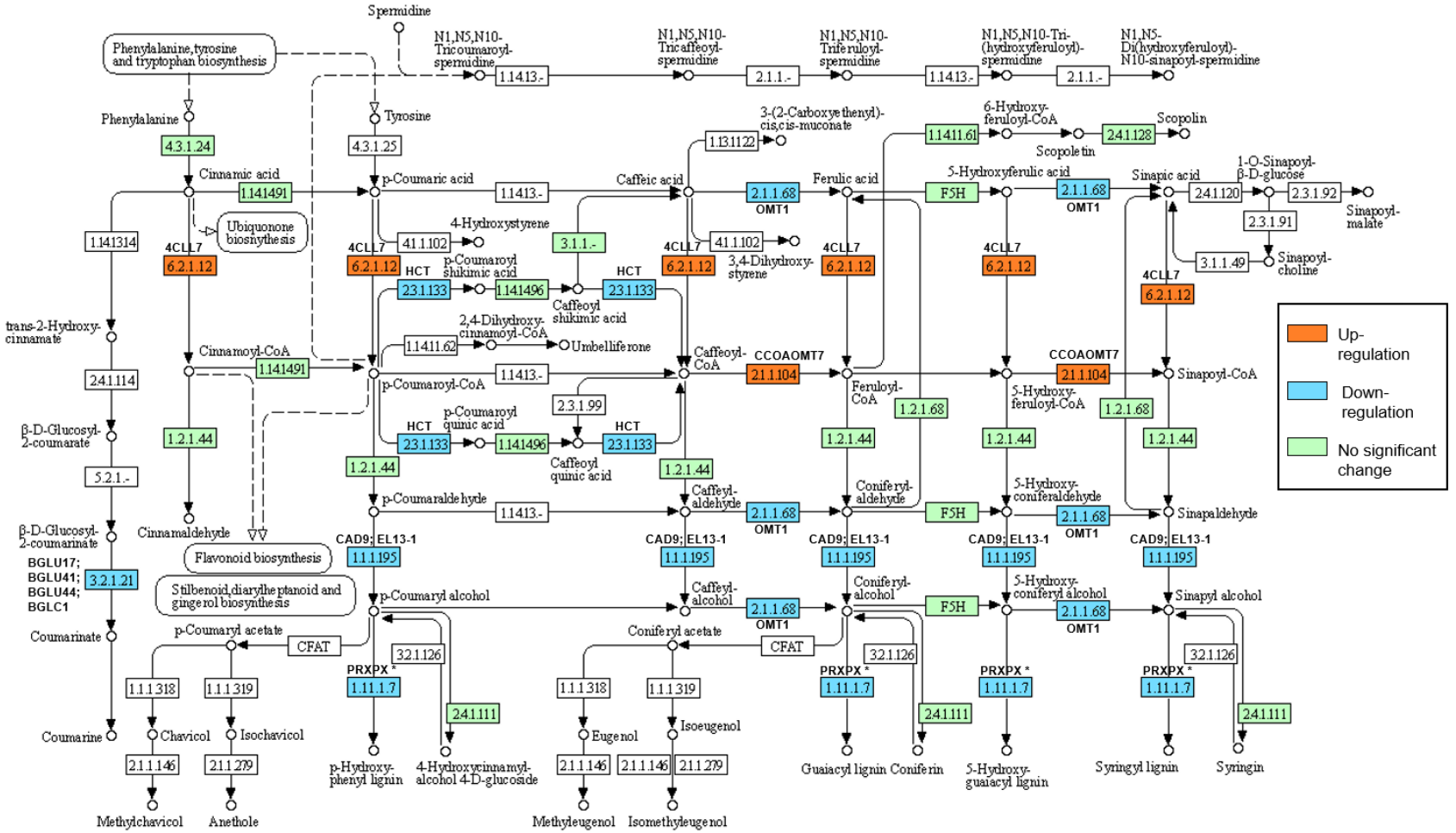

Figure 57. RNA seq. differentially expressed phenylpropanoid biosynthesis genes in the >90 vs Str dataset. The green colour represents genes present within the Rosa chinensis *genome, the blue coloured EC numbers represents down-regulated genes with a <-0.5 Log2 FC and the orange EC numbers represent up-regulated genes with a >0.5 Log2 FC (p adjust. <0.05). *EC number 1.11.1.7 has nine associated down-regulated peroxidase genes, of which PRXPX has the highest mean count (other genes not shown). Pathway adapted and annotated from KEGG (pathway: rcn00940 ; Kanehisa, 2017).*

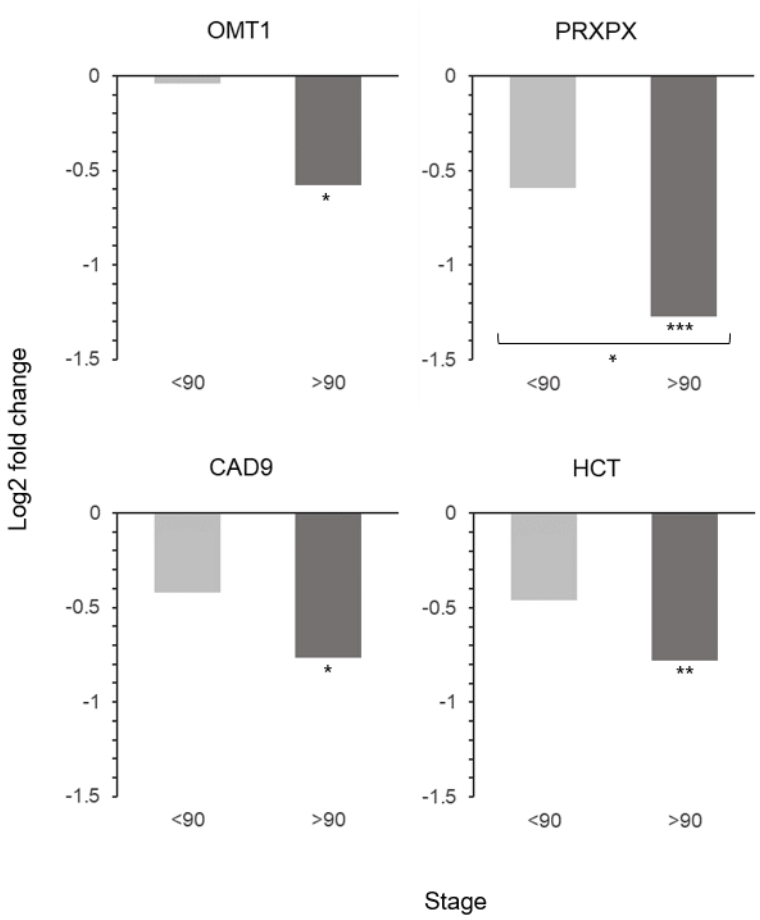

*Figure 58. RNA seq. differential expression bar charts for phenylpropanoid biosynthesis genes. Log2 FC values are shown relative to straight control peduncles, with significance calculated using DESeq2. Significant difference between <90 and straight, and >90 and straight is indicated above the relative bar. Significant difference between <90 and >90 is indicated between the two bars, where *** indicates significance to a p adjusted value of <0.001, ** to <0.01 and * to <0.05.*

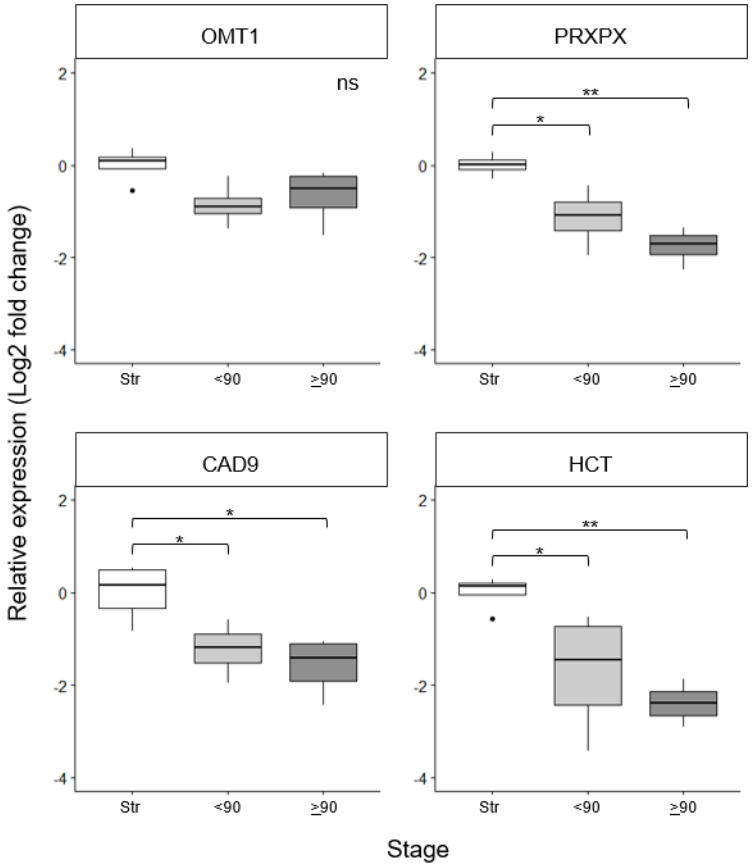

*Figure 59. qPCR relative expression box plots for phenylpropanoid biosynthesis genes. Pfaffle analysis is relative to GACPC2 expression using necking stage Straight as the control. Statistical analysis was calculated using an one way ANOVA of Log2 FC vs Stage with a Tukey post hoc test, where *** indicates significance difference in expression to a p value of <0.001, ** to <0.01, * to <0.05 and 'ns' indicates no significant difference.*

7.4 Discussion

The galactose metabolism and phenylpropanoid biosynthesis pathways have not previously been analysed in relation to the necking phenomenon in *Rosa hybrida*, therefore new primers were designed for qPCR analysis. Access to the *Rosa hybrida* genome resources along with the *Rosa hybrida* transcriptome greatly aided primer design, with all of the primers designed bar the GolS2 primer pair successfully amplifying the target genes. Failure of the GolS2 primers to produce a product is thought to be due to the low abundance of GolS2 mRNA in the samples, as GolS2 had a mean count of just 109 in the RNA sequencing dataset. Successful amplification may be achieved with further manipulation of the PCR cycle conditions or through re-designing the primers, however such low-level

differences in expression between the necking stages may still be difficult to quantify.

Cut rose vase life has been shown to be seasonal, due to changes in humidity and stomatal function (In & Lim, 2018). Vase life studies conducted in preparation for qPCR analysis in spring 2019 (April and May) showed reduced rates of necking (data not shown). Therefore in order to harvest enough material for each stage, a *Pseudomonas fluorescens* solution was added to induce necking, at a final vase water concentration of 2.5 x 10^5 cfu per mL in a 2 % sucrose solution rather than commercial flower food (*7.2.1*). Peduncles were then harvested 1-3 days earlier than the RNA sequencing flower material as necking occurred. Differences in gene expression between the qPCR data set and the RNA sequencing data set may therefore be attributed to factors associated with the differing experimental conditions. Conversely, significant differences seen within both datasets can be considered more robust and validate potential gene expression changes associated with the necking phenomenon.

7.4.1 Galactose metabolism

In the galactose metabolism pathway, significant up-regulation was seen in necking peduncles for both UDP-glucose 4-epimerase (UGE5) and galactinol-sucrose galactosyltransferase genes 2 (SIP2) and 6 (DIN10) in the RNA seq. and qPCR datasets (Figure 55*; Figure 56*). Although qPCR was unsuccessful for galactinol synthase 2 (GolS2), GolS2 also showed significant up-regulation in the RNA-seq. dataset in (≥90°) necking peduncles compared to straight controls. These enzymes catalyse the first steps in the synthesis of raffinose family oligosaccharides, with UGE5 catalysing the synthesis of UDP-galactose from UDP-glucose, GolS2 catalysing the conversion of UDP-galactose and myo-inositol to galactinol and both SIP2 and DIN10 catalysing the synthesis of raffinose from galactinol and sucrose (Suarez et al., 1999; Nishizawa et al., 2008; *Figure 60*). Up-regulation of UGE5, GolS2 and SIP2/DIN10 therefore indicates a potential up-regulation of raffinose synthesis in fully necked (>90°) peduncles. Raffinose has an important role in osmoprotection and reactive oxygen species (ROS) scavenging (ElSayed et al., 2014). Up-regulation of raffinose synthase genes such as SIP2 are commonly seen in response to water deficit, salt or

drought stress to protect plants from osmotic and oxidative damage (ElSayed et al., 2014; Hu et al., 2018; Fàbregas & Fernie, 2019; Nishizawa et al., 2008). As necking is induced by a vascular blockage and reduced water uptake, an up-regulation of raffinose synthesis is consistent with rose peduncles experiencing and responding to a water deficit.

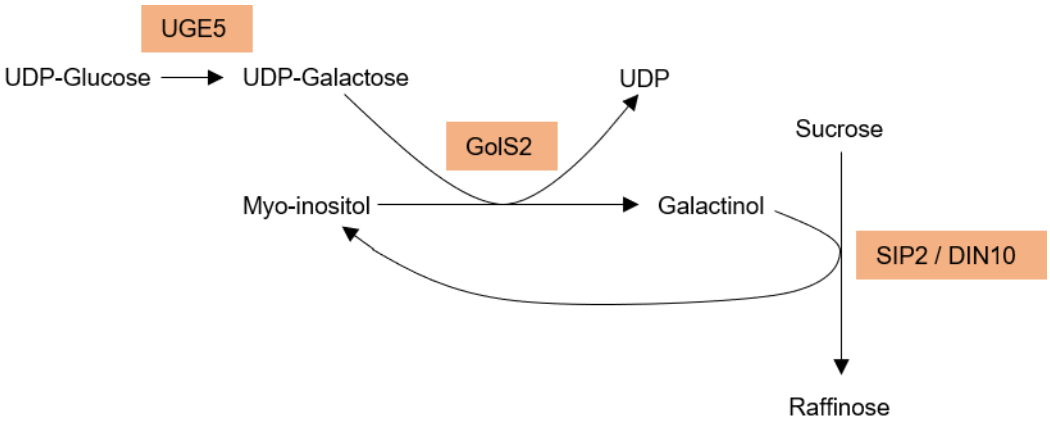

Figure 60. Raffinose synthesis pathway. Orange boxes show the enzymes catalysing each reaction in the pathway. Figure adapted from Suarez et al., (1999)

Galactinol synthase is seen as a key regulatory enzyme in the synthesis of raffinose family oligosaccharides (ElSayed et al., 2014). Transgenic *Arabidopsis thaliana* lines expressing *Malus x domestica* (apple) GolS2 were found to accumulate higher amounts of galactinol and raffinose and were more capable of surviving water deficit conditions than wildtype plants (Falavigna et al., 2018). Although galactinol synthases are known to be highly expressed in dormant flower buds and seeds as well as in leaves, expression levels in other plant organs and at other developmental stages are thought to be low (Falavigna et al., 2018). This may explain the low expression levels seen in peduncle tissue in this study compared to UGE5, SIP2 and DIN10. However, as the rose cultivar H30 used in this study is a necking susceptible cultivar, it is possible that the reduced level GolS2 seen may limit raffinose synthesis in the peduncle and therefore its ability to tolerate water stress. The osmolyte properties of raffinose can help to maintain cell turgor and stabilise cell proteins and membranes (Elsayed et al., 2014), all of which are important factors for maintaining structural support of a stem and therefore the susceptibility of a stem to bend following a xylem

blockage. A Comparative study of relative GolS2 and raffinose levels in other *Rosa hybrida* cultivars would therefore be interesting for future work.

7.4.2 Phenylpropanoid biosynthesis

The biosynthesis of phenylpropanoids is highly regulated, with gene expression differentially induced by developmental processes and by biotic and abiotic stresses (Sharma et al., 2019). Previous studies in *Arabidopsis thaliana*, flax (*Linum usitatissimum*) and pea (*Pisum sativum*) have all shown up-regulation of phenylpropanoid biosynthesis genes involved with lignin biosynthesis including shikimate o-hydroxy-cinnamoyltransferase (HCT) in response to bacterial and fungal plant pathogens (Chezem et al., 2017; Boba et al., 2017; Patel et al., 2017). However, in this study significant down-regulation of HCT was seen in necking peduncles (<90° and ≥90°) when compared to straight controls, as well as significant down-regulation of a cinnamyl alcohol dehydrogenase gene (CAD9) and peroxidases including peroxidase 42 (PRXPX) involved with the reduction and oxidation of lignin monomers respectively (*Figure 57; Figure 59*). Together these indicate a potential reduction rather than increase in monolignol and lignin biosynthesis in necking peduncles and suggests that the gene expression changes seen are not an active response to vase water microorganisms or external pathogens.

HCT is known to catalyse two steps in the phenylpropanoid pathway, including the transfer of p-coumaroyl CoA to p-coumaroyl shikimate and the transfer of caffeoyl shikimate to caffeoyl CoA following 3'hydroxylation for use in lignin biosynthesis (Fraser & Chapple, 2011). As flavonoid biosynthesis requires p-coumaroyl CoA as a precursor, silencing of HCT in *Arabidopsis thaliana* resulted in an over-accumulation of flavonoids and a reduced lignin content (Li et al., 2010). In the RNA-sequencing dataset of this study, 4-coumarate-CoA ligase-like 7 (4CLL7) a gene associated with the third step and the biosynthesis of p-coumaroyl CoA was found to be significantly up-regulated in >90° necking peduncles compared to straight (*Figure 51; Figure 57*; Deng & Lu, 2017). This combined with the significant down-regulation of HCT in necking peduncles may mean a potential increase in available p-coumaroyl CoA for use in other

phenylpropanoid biosynthesis pathways including flavonoid biosynthesis. Flavonoids are drought stress responsive metabolites and have been found to accumulate in *Arabidopsis thaliana* and more recently in *Achillea pachycephala* and *Fragaria x ananassa* (strawberry) to prevent oxidative damage from ROS accumulated during water deficit (Nakabayashi et al., 2014; Gharibi et al., 2019; Perin et al., 2019). As necking is known to be water stress related, a potential shift towards flavonoid biosynthesis in necking peduncles would therefore help to prevent oxidative damage in the peduncle. However, as gene expression changes in relation to flavonoid biosynthesis were not analysed in this study, the potential role of flavonoids in necking is speculative and would need to be further investigated.

Phenylpropanoid biosynthesis genes associated with lignification are known to be induced by myb transcription factors (Chezem at al., 2017). Therefore the significant down-regulation seen for HCT, CAD9 and PRXPX in <90° and ≥90° necking peduncles when compared to straight controls is consistent with the down-regulation of myb-transcription factors previously shown (*Figure 59;* Chapter 6). This down-regulation of myb transcription factors in necking peduncles was attributed to stress induced senescence. As the majority of phenylpropanoid biosynthesis genes were found to be down-regulated in necking peduncles, these changes in gene expression may also be a factor of senescence, with secondary metabolism and biosynthesis in general becoming down-regulated during senescence as cellular functions shut-down and nutrients are relocated (Rogers, 2011).

Although this study provides an overview of the expression of galactose metabolism and phenylpropanoid biosynthesis genes during the necking process, it should be noted that both the RNA sequencing and qPCR were conducted on rose peduncles as a whole, yet phenylpropanoid biosynthesis often differs between tissue types (Biała & Jasiński, 2018). It would therefore be interesting to determine if the changes in gene expression seen for galactose metabolism and phenylpropanoid biosynthesis vary between different cell types and areas of the peduncle.

7.5 Conclusions

Expression changes in galactose metabolism and phenylpropanoid biosynthesis pathway genes were successfully analysed in relation to necking by qPCR, validating the RNA sequencing differential expression analysis. Overall, the significant gene expression changes seen in necking peduncles indicate a response to water stress, with genes differentially regulated to help maintain osmotic balance as well as protect plant proteins from ROS and osmotic damage. Down-regulation of phenylpropanoid biosynthesis genes in necking peduncles however may be part of a general down-regulation of secondary metabolism due to stress-induced senescence. As gene expression changes do not always result in changes at a protein or metabolite level, further analysis with enzyme and metabolite assays would be recommended to verify the results found in this study.

Chapter 8 Final discussion

8.1 Overview of objectives and main findings

Table 23. Summary of the main objectives and findings of each experimental chapter

Chapter 3. Physiological factors contributing to necking in cut *Rosa hybrida*
Objectives: • Study termination factors and occurrence of necking in Kenyan grown *Rosa hybrida* cultivars and select suitable necking susceptible and necking resistant cultivars for further study. • Measure stem strength in a necking susceptible and necking resistant cultivar and explore the association between water content and necking • Analyse the anatomy of *R. hybrida* peduncles during different stages of necking *Summary of main findings:* H30 and Fuchsiana were selected as the necking susceptible and non-susceptible Kenyan grown cultivars for further study based on termination factors seen in preliminary studies. Differences in stem flex between the two cultivars were found to be inconclusive due to differences in water content at the time of testing. However, relative fresh weight was found to significantly differ at distinct stages of necking for both H30 and Fuchsiana. During necking, bending was found to occur within discrete regions of the peduncle in H30. Undulation of the epidermis and shrinkage of the pith were identified by electron and light microscopy suggesting a loss of osmotic balance and turgor pressure in necking peduncles.
Chapter 4. Microbial audit of the *Rosa hybrida* supply chain and identification of stem end micro-organisms
Objectives: • Conduct a microbial audit of the Kenyan supply chain and identify the prevalence of fungi on cut *Rosa hybrida* stems • Identify bacterial and fungal species associated with Kenyan grown roses by colony PCR and sequencing • Determine the effect of microbial additions to the vase water of cut *R. hybrida* cultivars in relation to the incidence of necking *Summary of main findings:* Fungal colonies were present on *R. hybrida* stems at all stages of the Kenyan supply chain, with colony counts highest at the final processing stage prior to dry transport. No significant difference was found between the fungal colony counts on the necking susceptible cultivar H30 and the non-susceptible cultivar Fuchsiana at any of the stages tested. Bacterial and fungal counts on H30 stem ends were found to differ following rehydration, yet not upon arrival in the UK. A total of 24 bacterial species and 30 fungal species were successfully cultured from *R. hybrida* stems and identified by sequencing, with many species novel to this study. *R. hybrida* cv.'s H30 and Fuchsiana were differentially affected by microbial additions to the vase water, with necking in H30 induced by yeast, filamentous fungi and bacterial additions.

Table 23 continued…

Chapter 5. A transcriptome analysis of peduncle necking in cut *Rosa hybrida* cultivar 'H30'
Objectives: • Extract RNA from peduncle tissue undergoing stages of necking and sequence transcripts • Produce a *de novo* transcriptome assembly and a *Rosa chinensis* reference genome alignment and determine the preferential method for further study *Summary of main findings:* Over 300 million high quality reads were successfully sequenced from *R. hybrida* peduncles from three stages of necking (Straight, <90 and >90). A *de novo* transcriptome assembly and a reference genome alignment were both successfully produced for *R. hybrida* cv. H30, with the reference aligned transcriptome determined to be preferential and chosen for further analysis of the necking phenomenon.
Chapter 6. Differential gene expression and pathway analysis of *Rosa hybrida* cv 'H30' at three peduncle necking stages
Objectives: • Carry out differential expression analysis on the RNA sequencing data for three stages of peduncle necking in *Rosa hybrida* cv. H30 • Determine biologically meaningful information from the data and potential transcriptomic changes associated with the necking process *Summary of main findings:* A total of 3,647 genes were found to be differentially expressed across the three necking stage comparisons. Many changes in gene expression were identified to be related to dehydration, osmotic stress and wounding associated with the necking phenomenon. Genes related to developmental processes were found to be down-regulated in >90 necking stage peduncles, with peduncles hypothesised to be entering a stress-induced senescent state.
Chapter 7. Quantitative PCR of galactose metabolism and phenylpropanoid biosynthesis genes in *Rosa hybrida* cv. H30 necking peduncles
Objectives: • Identify an appropriate reference gene for qPCR analysis of necking peduncles • Analyse the expression of genes in the galactose metabolism and phenylpropanoid biosynthesis pathways using qPCR and compare to RNA sequencing findings *Summary of main findings:* GAPC2 was found to be the most suitable reference gene for qPCR normalisation. Analysis of galactose metabolism and phenylpropanoid biosynthesis genes by qPCR indicated a response to water stress and the protection of plant proteins from ROS and osmotic damage. Gene expression changes also showed a potential down regulation of secondary metabolism which may be due to the onset of stress induced senescence in necking peduncles. Overall the qPCR results validated the RNA sequencing findings.

8.2 Physiological factors of necking

Kenyan grown roses account for around 70% of roses in the UK cut flower market (Wilson, 2015). However, despite their large market share, little is currently known about Kenyan grown roses in relation to necking. One aim of this project was therefore to identify potential variation in susceptibility to necking in commercially available Kenyan grown rose cultivars. Following vase life analysis of six *Rosa hybrida* cultivars, cv. H30 and Fuchsiana were identified as cultivars most and least susceptible (tolerant) to necking respectively and were chosen as suitable cultivars for further study due to their wide use in straight line bunches and bouquets for the UK market. These cultivars were therefore used in further analysis throughout this study.

8.2.1 Peduncle strength

Previous studies have found that peduncle strength is increased in cultivars less susceptible to necking (Zamski et al., 1991; Chabbert et al., 1993; Graf et al., 2006). Stem strength is a combination of mechanical strength and turgor pressure, therefore increased water loss often results in a reliance on mechanical strength provided by stem structures such as the vascular bundles and the epidermal layer (Zamski et al., 1991; Matsushima et al., 2010). In this study the necking susceptible cultivar H30 was found to flex less with the addition of a weight than the necking tolerant cultivar Fuchsiana. However, due to the experimental set up, stem strength as a whole was analysed, rather than purely mechanical strength. As H30 also had an increased flower head water content than Fuchsiana, it was therefore hypothesised that any increase in stem strength seen may have been due to increased turgor pressure rather than due to a difference in mechanical strength.

Stem strength between the two cultivars was measured following re-hydration, prior to when the stems would have entered the vase. Analysis of water balance during vase life showed Fuchsiana and H30 to both have a positive water balance on day one. However, the water balance of H30 became negative and was significantly reduced compared to Fuchsiana on day two and three. A negative water balance indicates that water uptake is lower than water lost through

transpiration, therefore leading to a net loss of water from the flower stem and a potential reduction in turgor pressure. Although stem strength was found to be increased in H30 stems compared to Fuchsiana prior to vase life, analysis of stem strength on day two or three of vase life may have shown H30 stems to be weaker than Fuchsiana due to a higher rate of water loss from the stem and a potentially reduced turgor pressure.

Factors associated with increased mechanical stem strength can naturally vary between cultivars but are also dependent on developmental stage. Peduncle development is tightly associated with flower development and can also vary at the point of harvest between cultivars (Matsushima et al., 2010). Zieslin et al. (1989) found reduced extent of necking in cultivars Mercedes and Nubia following 30 mins water stress (stems held dry) when harvested at later stages of flower development. Therefore, it would be interesting to determine in further work if stems of H30 harvested at later stages of flower development would see increased peduncle development and a reduced incidence of necking. Indeed this could therefore be a simple measure to help reduce post-harvest waste. However, although occurrence of necking may be reduced it must be considered that unless water relations are also improved, other symptoms of water stress such as petal wilting may still occur.

The necking tolerant cultivar Fuchsiana analysed during this project is known to be a fast opening rose cultivar and often opens to a stage seven of flower development within the vase as seen in *Figure 17*. H30 however is not known as a fast opening cultivar and often will achieve a stage four or five flower development during vase life *Figure 17*. As peduncle development and strength is associated with flower development, it may also be interesting to determine if Fuchsiana peduncles develop during the course of vase life and if resistance to necking therefore increases over time. Differences in peduncle development may explain why some stems in a bunch neck and others don’t when exposed to the same transport and environmental conditions I.e. stems may have been harvested at a slightly different stage and may have a differing level of stem development.

8.3 Microbial analysis

8.3.1 Prevalence of fungi in the supply chain

Reduced water uptake of cut rose stems during vase life is often attributed to microbial growth at the stem end or in the vase water, blocking the xylem. However, these microbial occlusions are often associated with bacteria rather than fungi (de Witte & van Doorn, 1988; van Doorn & Perik, 1990; Put & Jansen, 1989). The prevalence of fungi in the supply chain and their potential impact on the occurrence of necking is both largely unknown and overlooked.

In this study fungal counts were analysed at three points in the Kenyan supply chain for both the necking susceptible and necking tolerant rose cultivars H30 and Fuchsiana as well as upon arrival in the UK following air freight. Fungi were found at all stages of the supply chain, however both stem end and mid stem fungal counts were found to increase at the processing (bunching) stage, with stem end sections found to have a higher fungal load than mid stem sections. Higher microbial loads at the stem end compared to at the mid stem have also been found in previous studies, due to rapid growth on the cut surface of the stem end (Put & Clerkx, 1988; van Doorn et al., 1991). As damaged or wounded tissue is a better medium for the growth of microorganisms than intact or healthy tissue (Zagory, 1999). Increased wounding and microbial growth along the length of the stem can be caused by practices such as leaf and thorn removal and are the likely cause of the increased microbial growth seen at the mid stem section during the processing stage of the supply chain in this study (Woltering, 1987). As well as causing increased microbial loads and potential air embolisms, which may increase the incidence of necking, wounding can also cause the release of plant hormones such as ethylene which may cause a general decrease in vase life of cut roses (Woltering, 1987). Although wounding at the stem end cannot be avoided in cut flowers, the extent of damage can be reduced with the use of sharp blades (Zagory, 1999). A re-evaluation of current practices within the supply chain that lead to stem wounding (i.e. leaf removal, potential use of blunt blades) and increased microbial load would likely lead to a reduced occurrence of necking and post-harvest loss of cut roses.

Fungal colony counts were not found to differ from bacterial counts on arrival in the UK, however, were they were found to become significantly lower than bacterial counts following rehydration. Falling from a mean count of 3.2 x 10^4 down to 3 x 10^2 cfu per mL. This disparity between fungal and bacterial counts at the start of vase life has previously been found by Li et al. (2015) and Put & Clerkx (1988) and therefore is in line with current findings. However, these studies used cut flower material harvested and taken directly to the lab for vase life and are unlikely to be representative of bacterial or fungal levels found at the consumer stage following a full supply chain. In the present study the addition of fungi at 1.1 x 10^5 cfu per mL (*Neocosmospora rubicola*) and 3.4 x 10^5 cfu per mL (*Papilotrema flavescens*) significantly induced necking in the necking susceptible cultivar H30 compared to control stems at day three of vase life. This indicates that fungi do impact the occurrence of necking and even if occur at potentially lower levels, are still likely contribute to the effect of overall microbial load and the incidence of necking.

8.3.2 Bacterial and fungal species associated with Kenyan grown rose stems

Bacterial and fungal species associated with the vase water and stem ends of cut roses have previously been identified. However, these studies have focused on cut roses either grown in the Netherlands (Put, 1990; de Witte & van Doorn, 1988; van Doorn et al., 1991) or Columbia (Muñoz et al., 2019). In the present study, 24 species of bacteria and 30 species of fungi were identified from the stem ends and vase water of cut roses cv. H30 and Fuchsiana grown in Kenya. Although bacterial and fungal generas *Pseudomonas, Bacillus, Acinteobacter, Citrobacter, Pantoea, Candida, Cladosporium, Penicilium* and *Rhodotorula,* were identified in this study and in previous studies, little overlap at a species levels was found. A total of 24 novel genera were also found to be associated with cut roses including species in the bacterial genera *Burkholderia, Kluyvera, Rahnella, Raoultella* and fungal genera *Vishniacozyma, Papilotrema, Wickeramomyces* and *Gibellulopsis*. This study therefore provides a greater insight into the bacterial and fungal cultures which may be associated with Kenyan grown roses.

The use of biocides throughout the supply chain and within the vase water are likely to disrupt the microbial populations naturally associated with the stem end, which can lead to an increased relative abundance of opportunistic, fast growing microorganisms (Zagory, 1999). The ascomycetous yeast *Wickeraramomyces anomalus* (formerly *Saccharomyces anomalus*) and the bacterium *Pantoea agglomerans* (formerly *Erwinia herbicola*) isolated in this study are known biocontrol agents used to prevent spoilage of grains and fruit and control plant pathogenic species responsible for fire blight (*Erwinia amylovora*), root rot (*Fusarium culmorum*) and leaf rust (*Puccinia recondite*) respectively (Passoth et al., 2006; Fredlund et al., 2002; Özaktan & Bora, 2004; Vanneste et al., 1992; Kempf & Wolf, 1989). Other species identified in this study that are known to have antibacterial or antifungal activity include *Burkholderia vietnamiensis*, *Bacilius licheniformis* and *Candida saitoana (*Compant et al., 2008; Govender et al., 2005; Arras et al., 2006*)*. Antagonistic growth of these fungi and bacteria as biocontrol agents for controlled (limited) growth of stem end microorganisms may therefore be a potential area of further research. As these may offer sustained management of microbial load (Zagory, 1999) and therefore potentially reduce the occurrence of microbial occlusions.

Although this study used colony PCR and sequencing to identify species, analysis of stem end microflora has so far been limited to species which may be cultured in vivo and may account for as little as 0.5 - 0.1 % of bacteria present (Torsvik et al., 1990; Turner et al., 2013). A metagenomic study of stem end microorganisms would therefore be an interesting avenue for further work and may be used to determine potential differences in the microbiome of *R. hybrida* stem exhibiting necking compared to straight (control stems) and between necking susceptible and necking tolerant cultivars.

As stem end counts of bacteria and fungi in this study and by others have also relied upon culturing methods, stem end colony counts have therefore only likely been indicative of the microbial load. Colony counts also do not include non-viable cells which can contribute towards stem end blockages (Put & Jansen, 1989). A move towards real time methods such as flow cytometry or the use of an automated cell counter may therefore provide a clearer understanding of the

relationship between microbial load and the occurrence of necking (Vembadi et al., 2019; Ou et al., 2017). The use of real time methods over culturing methods would also be preferential for use in industry and may help to tackle the occurrence of necking. As batches of roses identified to have a higher microbial load could then be subjected to additional treatments in a targeted manner.

8.4 Molecular analysis of necking

Although it has been established that necking occurs due to a reduced water uptake, no previous studies have analysed the potential molecular mechanisms associated with the phenomenon. RNA sequencing analysis of *Rosa hybrida* cv. H30 peduncles at three stages of necking (Str, <90° bending, >90° bending) was therefore carried out in this study.

8.4.1 Water stress

As expected, RNA sequencing analysis revealed many gene expression responses related to water stress in necking peduncles, including upregulation of genes involved in the synthesis and metabolism of osmoprotectants such as raffinose and trehalose and down-regulation of aquaporin genes *PIP2-7* and *PIP2-4*. Loss of turgor was shown to occur during necking in the light microscopy and scanning electron microscopy images of H30 peduncles, with shrinkage of the pith and undulation of the epidermis seen by necking stage >90°. Osmoprotectants such as raffinose and aquaporin genes are up and down regulated respectively in response to water stress in order protect plants from osmotic damage and maintain cell turgor (Elsayed et al., 2014; Wang et al., 2016; Hachez et al., 2014). However, it is unclear if upregulation of these gene products would help to delay the loss of turgor pressure in the peduncle and the occurrence of the necking. Genes of the galactose metabolism pathway have been validated with qPCR and indicate a potential increase in raffinose synthesis in necking peduncles. However, a comparative analysis of raffinose content and expression of aquaporins in other *R. hybrida* cultivars would be interesting for future work.

8.4.2 Wounding

Ethylene responsive transcription factors *ABR1-like* and *ERF110-like* were significantly up-regulated in necking peduncles. *ABR1-like* and *ERF110-like* are homologous to *Arabidopsis thaliana abscisic acid repressor 1* (*ABR1*). *ABR1* expression is upregulated in response to wounding and indicates a wounding response in necking peduncles. However, it remains unclear if this response may be caused by the necking process itself, or due to handling practices along the supply chain such as de-leafing and de-thorning previously mentioned or mechanical stress on the peduncle such as excessive vibrations during transport (Woltering, 1987; Pouri et al., 2017). Wounding responses caused by mechanical stress have been shown to lead to an increase in reactive oxygen species (ROS) production, a decreased aquaporin expression and alter turgor pressure (Hernández-Hernández et al., 2019). As turgor pressure is relative to stem strength as previously mentioned, wounding may therefore also have a direct effect on the incidence of necking.

8.4.3 Tropism and epidermal patterning factor genes

In this study differential expression analysis identified 23 tropism related genes to be differentially expressed in necking peduncles, including the down-regulation of five auxin-activated tropism genes. GRAS transcription factor scarecrow (SCR) was also found to be down-regulated in necking peduncles and is associated with a lack of response to gravity in *Arabidopsis thaliana* mutants (Fukaki et al., 1998). As tropism is an active response, it is unclear what affect down-regulation of these genes may have. However, it is possible that auxin transport in cut roses may be altered due to a downregulation of auxin transporters, causing an unbalance within the peduncle.

ERECTA, *EPFL4* and *EPFL6* genes were also found to be significantly down regulated in necking peduncles and have been shown to regulate the elongation of inflorescence stems (Uchida et al., 2012). Further work is therefore needed to determine the potential role of tropism and ERECTA genes in the necking process. In particular, it would be interesting to see if the expression of these genes identified through differential analysis are uniform across the peduncle, or

if a reduction in gene expression only occurs on one side of the stem, as this could contribute towards stem bending and therefore the necking process. Amyloplast content and distribution could also be determined though microscopy analysis of fresh cut sections of peduncle as amyloplasts are involved with gravity perception in the stem.

8.4.4 Senescence

Senescence is a complex active process whereby nutrients are remobilised and can be age-dependent or stress induced (Rogers, 2011; Podzimska-Sroka et al., 2015). Targeted analysis of senescence associated genes identified many genes to be differentially expressed in necking compared to straight peduncles and indicates an onset of senescence in necking peduncles. As many genes were also found to be related to water stress responses and rose stems were of the same age it was hypothesised that senescence was stress induced rather than age-dependent or developmental.

8.4.5 Abscission

The abscission zone present at the junction between the stem and the peduncle is known as a point of reduced hydraulic conductance and is the likely cause of increased turgor loss within the peduncle (Darlington & Dixon, 1990). Although no abscission related genes were found in the region of peduncle analysed in this study, it is unknown if abscission is ‘activated’ during necking. Zieslin et al. (1989) found abscission of the peduncle to occur in a necking susceptible *R. hybrida* cultivar Nubia following removal of the flower head, however this response was not seen in the necking tolerant cultivar Mercedes. Gene expression analysis of abscission related genes at the abscission zone is therefore recommended as future work through qPCR.

8.5 Evaluation of methods

Flower material used in this project was collected directly from the wholesaler upon arrival in the UK. This limited the number of unknown variables that can be introduced at the 'in store' phase i.e. from supermarkets and ensured experiments and results were more reproducible and consistent. However, as with most other studies, the quality of the flower material and therefore the microbial levels on the stem are unlikely to be representative of what is experienced by the consumer and must be taken into consideration.

Dry medium culture plate methods were adopted in this study for the enumeration of bacteria and fungi due to their simplicity, convenience and suitability for use during field work in Kenya. However, due to their simple form and the use of indicator dyes for improved counting (as was the case for Petrifilms used in this study), species variation could not be determined by studying the plates alone. Any indication of species abundance was therefore missed and could not be reported on and was an unforeseen limitation of this method.

Identification of microbial species by colony PCR gave an indication of species present on rose stems grown in Kenya and did not require a multitude of biochemical tests or skilled microscopical analysis as with more traditional techniques. However, as previously mentioned in *8.3.2*, colony PCR was still limited to the microbial species that could be cultured prior to sequencing. Quantitative analysis of species proportion and prevalence was also not possible due to the experimental design. A microbiome analysis of rose stem ends would therefore be a recommended next step and can be used to both identify microorganisms which cannot be cultured in vitro and enable quantitative analysis of species.

RNA sequencing of *Rosa hybrida* peduncles during necking has not previously been completed and provides a rich new resource for future research in the area. However, due to the sampling technique of taking the peduncle as a whole; tissue specific information may have been lost due to 'noise'. Further investigation into specific tissues within the peduncle, i.e. through in situ hybridisation may be a promising approach for future research into necking. As previously mentioned in

8.4.5, it may also be interesting to analyse gene expression lower down the peduncle, at the abscission zone or at the beginning of the bend rather than at the mid-point in necking as studied here.

As gene expression changes do not always result in actual changes in gene products or responses, analysis of these gene expression changes should be further validated by other means i.e. with metabolomics, enzyme assays and microscopy. Validation of gene expression changes is also needed within other *Rosa hybrida* cultivars as only *R. hybrida* cv. H30 was sequenced and used in qPCR analyses. Further analysis is therefore needed to determine if similar transcriptomic changes are seen in response to necking in other cultivars. Although Fuchsiana was used as the main comparative cultivar in this study, it may also be interesting to select cultivars which show symptoms of water stress but do not neck. In addition, as roses used in the RNA sequencing were likely to be pre-stressed due to dry transport, gene expression changes may be showing secondary responses. Therefore, gene expression analysis of cut roses which have not been transported and with necking induced by a known source (i.e. *Pseudomonas florescens* cultures) may be an interesting comparison and could produce more distinct results in relation to necking.

8.6 Conclusions

In conclusion, the occurrence of necking in cut roses is complex and involves numerous factors, including both cultivar specific and environmental variables many of which are interconnected (*Figure 61*). This study has provided an insight into the factors associated with Kenyan grown roses, including the prevalence and impact of fungi. Although no conclusive difference in stem strength was found between the two cultivars in this study, harvesting of necking susceptible cultivars such as cv. H30 at a later stage may increase mechanical strength and provide some resistance to turgor loss and necking.

This is also the first study have carried out a transcriptomic study on peduncle tissue during necking and has identified potential molecular mechanisms which may be involved with the necking process. The association between these

molecular processes and their potential involvement in the occurrence of necking have been hypothesised in *Figure 61*. These provide new avenues for further research and contribute to the current understand of necking in cut *Rosa hybrida*.

For rose growers, wholesalers, supermarkets and florists, this study reinforces the importance of appropriate handling of flowers as a fresh produce, with increased microbial levels found to induce necking in both necking susceptible and necking tolerant cultivars. Practices that may increase microbial load such as poor temperature control and wounding should therefore be controlled and re-evaluated for the occurrence of necking to be reduced. Greater awareness and communication of cut flower hygiene and handling practices would also greatly benefit the consumer and may reduce the occurrence of necking and premature termination of stems. This would in turn help to both reduce post-harvest waste and increase consumer satisfaction.

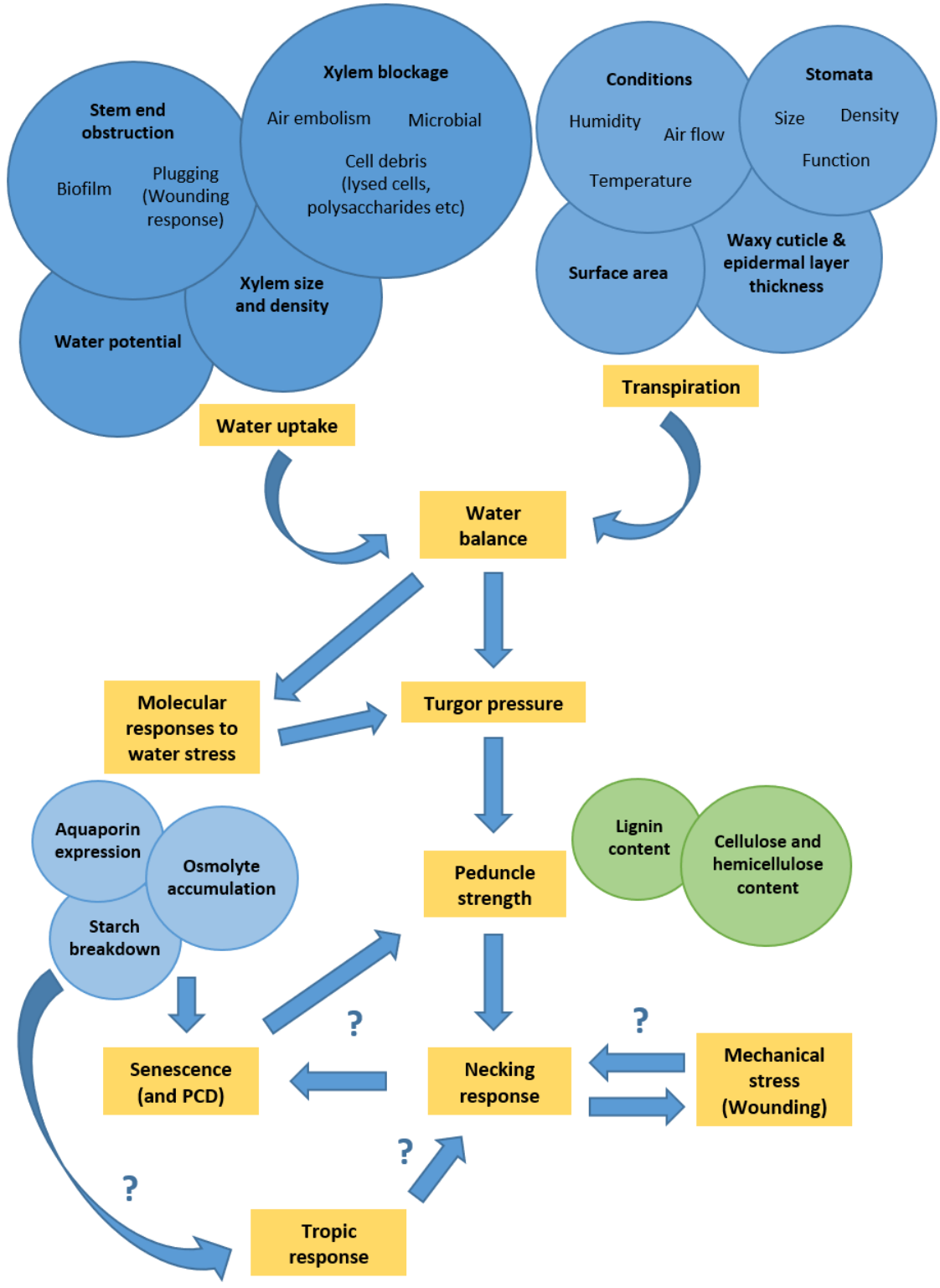

Figure 61. Summary of factors associated with the occurrence of necking in cut R. hybrida *flowers. Question marks indicate hypothesised connections which need to be experimentally determined.*

Bibliography

Afgan, E., Baker, D., van den Beek, M., Blankenberg, D., Bouvier, D., et al. (2016). The Galaxy platform for accessible, reproducible and collaborative biomedical analyses: 2016 update. *Nucleic Acids Research. 44*, 3–10. doi:10.1093/nar/gkw343

Ahmad, I., Dole, J. M., Amjad, A., & Ahmad, S. (2012). Dry Storage Effects on Postharvest Performance of Selected Cut Flowers. *Hort Technology*, 22(4), 463–469. doi:10.21273/horttech.22.4.463

Altschul, S. (1997). Gapped BLAST and PSI-BLAST: a new generation of protein database search programs. *Nucleic Acids Research*. *25* (17), 3389–3402. doi:10.1093/nar/25.17.3389

Anders, S., Reyes, A., & Huber, W. (2012). Detecting differential usage of exons from RNA-seq data. *Genome Research.* 22 (10), 2008–2017. doi:10.1101/gr.133744.111

Andre, J.P. (2003). Shoots and stems. In A.V. Roberts, T. Debener & S. Gudin. *Encyclopedia of Rose Science* (Vol. 2, 504-512). Oxford, UK: Elsevier Ltd.

Andrews, S. (2014). FastQC: A quality control tool for high throughput sequence data. [online] Available at: http://www.bioinformatics.babraham.ac.uk/projects/fastqc/

Arnold, Z. (1930). Einige orientierende Veruche zur frage der kunstlichen frischerhaltung der schnittblumen (Some orientative experiments on the question of the artificial freshness of cut flowers). *Gardenbauwissenschaff, 3*, 47-58.

Arras, G., Molinu, M.G., Dore, A., Venditti, T., Fois, M., Petretto, A., & D'hallewin, G. (2006). Inhibitory activity of 2-deoxy-D-glucose and Candida saitoana against Penicillium digitatum. *Communications in agricultural and applied biological sciences, 71* (3), 929-936.

Ashburner, M., Ball, C. A., Blake, J. A., Botstein, D., Butler, H., Cherry, J. M., … Sherlock, G. (2000). Gene Ontology: tool for the unification of biology. *Nature Genetics, 25*(1), 25–29. doi:10.1038/75556

Babraham Bioinformatics. (2019a). FastQC Per sequence quality scores. [online] Available at: https://www.bioinformatics.babraham.ac.uk/projects/fastqc/Help/3%20Analysis%20Modules/3%20Per%20Sequence%20Quality%20Scores.html [Accessed 13 November 2019].

Babraham Bioinformatics. (2019b). FastQC Per base sequence quality. [online] Available at: https://www.bioinformatics.babraham.ac.uk/projects/fastqc/Help/3%20Analysis%20Modules/2%20Per%20Base%20Sequence%20Quality.html [Accessed 13 November 2019].

Bakshi, M., & Oelmüller, R. (2014). WRKY transcription factors. Plant *Signaling and Behavior, 9*(2), e27700. doi:10.4161/psb.27700

Baruzzo, G., Hayer, K. E., Kim, E. J., Di Camillo, B., FitzGerald, G. A., & Grant, G. R. (2017). Simulation-based comprehensive benchmarking of RNA-seq aligners. *Nature methods*, *14*(2), 135–139. doi:10.1038/nmeth.4106

Bates, D., Mächler, M., Bolker, B., & Walker, S. (2015). Fitting linear mixed-effects models using lme4. *Journal of Statistical Software.* 67(1). doi:10.18637/jss.v067.i01

Batoko, H., Dagdas, Y., Baluska, F., & Sirko, A. (2017). Understanding and exploiting autophagy signaling in plants. *Essays in Biochemistry, 61*(6), 675–685. doi:10.1042/ebc20170034

Bäumler, J., Riber, W., Klecker, M., Müller, L., Dissmeyer, N., Weig, A. R., & Mustroph, A. (2019). AtERF#111/ABR1 is a transcriptional activator involved in the wounding response. *The Plant Journal, 100*(5), 969–990. doi:10.1111/tpj.14490

Beauzamy, L., Nakayama, N., & Boudaoud, A. (2014). Flowers under pressure: ins and outs of turgor regulation in development. Annals of Botany, 114(7), 1517–1533. doi:10.1093/aob/mcu187

Bendahmane, M., Dubois, A., Raymond, O., & Bris, M. L. (2013). Genetics and genomics of flower initiation and development in roses. *Journal of Experimental Botany, 64*(4), 847–857. doi:10.1093/jxb/ers387

Berkholst, C.E.M. (1980). De waterhuishouding van afgesneden rozen (Water relations of cut roses). *Bedrijfsontwikkeling, 11*, 332-336.

Biała, W., & Jasiński, M. (2018). The Phenylpropanoid Case – It Is Transport That Matters. *Frontiers in Plant Science, 9*. doi:10.3389/fpls.2018.01610

Blaalid, R., Kumar, S., Nilsson, R. H., Abarenkov, K., Kirk, P. M., & Kauserud, H. (2013). ITS1 versus ITS2 as DNA metabarcodes for fungi. *Molecular Ecology Resources, 13*(2), 218–224. doi:10.1111/1755-0998.12065

Bleeksma, H. C., & van Doorn, W. G. (2003). Embolism in rose stems as a result of vascular occlusion by bacteria. *Postharvest Biology and Technology, 29*(3), 335–341. doi:10.1016/s0925-5214(03)00049-8

Boba, A., Kostyn, K., Kostyn, A., Wojtasik, W., Dziadas, M., Preisner, M., … Kulma, A. (2017). Methyl Salicylate Level Increase in Flax after Fusarium oxysporum Infection Is Associated with Phenylpropanoid Pathway Activation. *Frontiers in Plant Science, 7*. doi:10.3389/fpls.2016.01951

Bolger, A.M., Lohse, M., & Usadel, B. (2014). Trimmomatic: a flexible trimmer for Illumina sequence data. *Bioinformatics. 30* (15), 2114–2120. doi:10.1093/bioinformatics/btu170

Bolle, C. (2004). The role of GRAS proteins in plant signal transduction and development. *Planta, 218*(5), 683–692. doi:10.1007/s00425-004-1203-z

Britannica Acadamic (2015a) Rosaceae. Available from: http://academic.eb.com/EBchecked/topic/509628/Rosaceae [Accessed December 2015]

Britannica Acadamic (2015b) Rose. Available from: http://academic.eb.com/EBchecked/topic/509710/rose [Accessed December 2015]

Bustin, S. A., Benes, V., Garson, J. A., Hellemans, J., Huggett, J., Kubista, M., … Wittwer, C. T. (2009). The MIQE Guidelines: Minimum Information for Publication of Quantitative Real-Time PCR Experiments. *Clinical Chemistry, 55*(4), 611–622. doi:10.1373/clinchem.2008.112797

Cevallos, J.C., & Reid, M. S. (2001). Effect of Dry and Wet Storage at Different Temperatures on the Vase Life of Cut Flowers. *HortTechnology, 11*(2), 199–202. doi:10.21273/horttech.11.2.199

Chabbert, B., Monties, B., Zieslin, N., & Ben-Zaken, R. (1993). The relationship between changes in lignification and the mechanical strength of rose flower peduncles. *Acta Botanica Neerlandica, 42*(2), 205–211. doi:10.1111/j.1438-8677.1993.tb00697.x

Chang, S., Puryear, J., & Cairney, J. (1993). A simple and efficient method for isolating RNA from pine trees. *Plant Molecular Biology Reporter, 11*(2), 113–116. doi:10.1007/bf02670468

Chen, F., Song, Y., Li, X., Chen, J., Mo, L., Zhang, X., … Zhang, L. (2019). Genome sequences of horticultural plants: past, present, and future. *Horticulture Research, 6*(1). doi:10.1038/s41438-019-0195-6

Chezem, W. R., Memon, A., Li, F.-S., Weng, J.-K., & Clay, N. K. (2017). SG2-Type R2R3-MYB Transcription Factor MYB15 Controls Defense-Induced Lignification and Basal Immunity in Arabidopsis. *The Plant Cell, 29*(8), 1907–1926. doi:10.1105/tpc.16.00954

Chimonidou D. (2003). Flower development and the abscission zone. In A.V. Roberts, T. Debener and S. Gudin. *Encyclopedia of Rose Science* (Vol. 2, 504-512). Oxford, UK: Elsevier Ltd.

Christensen, R.H.B. (2019) Ordinal – Regression Models for Ordinal Data. R package version 2019.12-10. https://CRAN.R-project.org/package=ordinal

Clerkx, A. C. M., Boekestein, A., & Put, H. M. C. (1989). Scanning electron microscopy of the stem of cut flowers of rosa cv. Sonia and gerbera cv. Fleur. *Acta Horticulturae*, (261), 97–106. doi:10.17660/actahortic.1989.261.12

Climate-Data.org (2020). Naivasha climate. *Climate-Data.* Available at: https://en.climate-data.org/africa/kenya/nakuru/naivasha-11126/ [Accessed March 2020]

Compant, S., Nowak, J., Coenye, T., Clément, C., & Ait Barka, E. (2008). Diversity and occurrence of Burkholderiaspp. in the natural environment. *FEMS Microbiology Reviews, 32(*4), 607–626. doi:10.1111/j.1574-6976.2008.00113.x

Daccord, N., Celton, J.-M., Linsmith, G., Becker, C., Choisne, N., Schijlen, E., … Bucher, E. (2017). High-quality de novo assembly of the apple genome and methylome dynamics of early fruit development. *Nature Genetics, 49*(7), 1099–1106. doi:10.1038/ng.3886

Damunupola, J. W., & Joyce, D. C. (2008). When is a Vase Solution Biocide not, or not only, Antimicrobial? *Journal of the Japanese Society for Horticultural Science, 77*(3), 211–228. doi:10.2503/jjshs1.77.211

Darlington, A. B., & Dixon, M. A. (1991). The hydraulic architecture of roses (Rosa hybrida). *Canadian Journal of Botany, 69*(4), 702–710. doi:10.1139/b91-095

Dash, P. K. (2013). High quality RNA isolation from ploy phenol-, polysaccharide- and protein-rich tissues of lentil (Lens culinaris). *Biotech, 3*(2), 109–114. doi:10.1007/s13205-012-0075-3

de Witte, Y., & Van Doorn, W. G. (1988). Identification of bacteria in the vase water of roses, and the effect of the isolated strains on water uptake. *Scientia Horticulturae, 35*(3-4), 285–291. doi:10.1016/0304-4238(88)90122-7

Delporte, M., Legrand, G., Hilbert, J.-L., & Gagneul, D. (2015). Selection and validation of reference genes for quantitative real-time PCR analysis of gene expression in Cichorium intybus. *Frontiers in Plant Science, 6*. doi:10.3389/fpls.2015.00651

Deng, Y., & Lu, S. (2017) Biosynthesis and Regulation of Phenylpropanoids in Plants. *Critical Reviews in Plant Sciences, 36*(4), 257-290. doi:10.1080/07352689.2017.1402852

Díaz-Riquelme, J., Lijavetzky, D., Martínez-Zapater, J. M., & Carmona, M. J. (2008). Genome-Wide Analysis of MIKCC-Type MADS Box Genes in Grapevine. *Plant Physiology, 149*(1), 354–369. doi:10.1104/pp.108.131052

Du, Z., Zhou, X., Ling, Y., Zhang, Z., & Su, Z. (2010). agriGo: a GO analysis toolkit for the agricultural community. *Nucleic Acids Research. 38* (2), 64-70. doi:10.1093/nar/gkq310

Dubois, A., Carrere, S., Raymond, O., Pouvreau, B., Cottret, L., Roccia, A., Onesto, J., Sakr, S., Atanassova, R., Baudino, S., et al. (2012). Transcriptome database resource and gene expression atlas for the rose. *BMC Genomics. 13*, 638. doi:10.1186/1471-2164-13-638

Dubois, A., Raymond, O., Maene, M., Baudino, S., Langlade, N. B., Boltz, V., … Bendahmane, M. (2010). Tinkering with the C-Function: A Molecular Frame for the Selection of Double Flowers in Cultivated Roses. *PLoS ONE, 5*(2), e9288. doi:10.1371/journal.pone.0009288

ElSayed, A. I., Rafudeen, M. S., & Golldack, D. (2013). Physiological aspects of raffinose family oligosaccharides in plants: protection against abiotic stress. *Plant Biology, 16*(1), 1–8. doi:10.1111/plb.12053

Everaert, C., Luypaert, M., Maag, J. L. V., Cheng, Q. X., Dinger, M. E., Hellemans, J., & Mestdagh, P. (2017). Benchmarking of RNA-sequencing analysis workflows using whole-transcriptome RT-qPCR expression data. *Scientific Reports, 7*(1). doi:10.1038/s41598-017-01617-3

Fàbregas, N., & Fernie, A. R. (2019). The metabolic response to drought. *Journal of Experimental Botany, 70*(4), 1077–1085. doi:10.1093/jxb/ery437

Falavigna, V. da S., Porto, D. D., Miotto, Y. E., Santos, H. P. dos, Oliveira, P. R. D. de, Margis-Pinheiro, M., … Revers, L. F. (2018). Evolutionary

diversification of galactinol synthases in Rosaceae: adaptive roles of galactinol and raffinose during apple bud dormancy. *Journal of Experimental Botany, 69*(5), 1247–1259. doi:10.1093/jxb/erx451

Fanourakis, D., Carvalho, S. M. P., Almeida, D. P. F., van Kooten, O., van Doorn, W. G., & Heuvelink, E. (2012). Postharvest water relations in cut rose cultivars with contrasting sensitivity to high relative air humidity during growth. *Postharvest Biology and Technology, 64*(1), 64–73. doi:10.1016/j.postharvbio.2011.09.016

Fanourakis, D., Pieruschka, R., Savvides, A., Macnish, A. J., Sarlikioti, V., & Woltering, E. J. (2013). Sources of vase life variation in cut roses: A review. *Postharvest Biology and Technology, 78*, 1–15. doi:10.1016/j.postharvbio.2012.12.001

Fanourakis, D., Velez-Ramirez, A. I., In, B.-C., Barendse, H., van Meeteren, U., & Woltering, E. J. (2015). A survey of preharvest conditions affecting the regulation of water loss during vase life. *Acta Horticulturae,* (1064), 195–204. doi:10.17660/actahortic.2015.1064.22

Farrant, J. M., Cooper, K., Hilgart, A., Abdalla, K. O., Bentley, J., Thomson, J. A., … Rafudeen, M. S. (2015). A molecular physiological review of vegetative desiccation tolerance in the resurrection plant Xerophyta viscosa (Baker). *Planta, 242*(2), 407–426. doi:10.1007/s00425-015-2320-6

Figueroa, C. M., & Lunn, J. E. (2016). A Tale of Two Sugars: Trehalose 6-Phosphate and Sucrose. *Plant Physiology, 172*(1), 7–27. doi:10.1104/pp.16.00417

Florack, D. E. A., Stiekema, W. J., & Bosch, D. (1996). Toxicity of peptides to bacteria present in the vase water of cut roses. *Postharvest Biology and Technology, 8*(4), 285–291. doi:10.1016/0925-5214(96)00009-9

Flowers and Plants Association (2015) *The Uk Market.* Available from: http://www.flowersandplantsassociation.org.uk/industry/uk-market.htm [Accessed November 2015]

Fox, J., & Weisberg, S. (2019). An R Companion to Applied Regression, Third Edition. Thousand Oaks CA: Sage. https://socialsciences.mcmaster.ca/jfox/Books/Companion/

Fraser, C. M., & Chapple, C. (2011). The Phenylpropanoid Pathway in Arabidopsis. *The Arabidopsis Book, 9*, e0152. doi:10.1199/tab.0152

Fredlund, E., Druvefors, U., Boysen, M., Lingsten, K., & Schnurer, J. (2002). Physiological characteristics of the biocontrol yeast J121. *FEMS Yeast Research, 2*(3), 395–402. doi:10.1016/s1567-1356(02)00098-3

Fukaki, H., Wysocka-Diller, J., Kato, T., Fujisawa, H., Benfey, P. N., & Tasaka, M. (1998). Genetic evidence that the endodermis is essential for shoot gravitropism inArabidopsis thaliana. *The Plant Journal, 14*(4), 425–430. doi:10.1046/j.1365-313x.1998.00137.x

Fulton, D. C., Stettler, M., Mettler, T., Vaughan, C. K., Li, J., Francisco, P., … Zeeman, S. C. (2008). β-AMYLASE4, a Noncatalytic Protein Required for

Starch Breakdown, Acts Upstream of Three Active β-Amylases in Arabidopsis Chloroplasts. *The Plant Cell, 20*(4), 1040–1058. doi:10.1105/tpc.107.056507

Gacheri, C., Kigen, T., & Sigsgaard, L. (2015). Hot-spot application of biocontrol agents to replace pesticides in large scale commercial rose farms in Kenya. *BioControl, 60*(6), 795–803. doi:10.1007/s10526-015-9685-0

Gangl, R., & Tenhaken, R. (2016). Raffinose Family Oligosaccharides Act As Galactose Stores in Seeds and Are Required for Rapid Germination of Arabidopsis in the Dark. *Frontiers in Plant Science, 7*. doi:10.3389/fpls.2016.01115

Gao, S., Gao, J., Zhu, X., Song, Y., Li, Z., Ren, G., … Kuai, B. (2016). ABF2, ABF3, and ABF4 Promote ABA-Mediated Chlorophyll Degradation and Leaf Senescence by Transcriptional Activation of Chlorophyll Catabolic Genes and Senescence-Associated Genes in *Arabidopsis. Molecular Plant, 9*(9), 1272–1285. doi:10.1016/j.molp.2016.06.006

Gao, M. J., Li, X., Huang, J., Gropp, G. M., Gjetvaj, B., Lindsay, D. L., … Hegedus, D. D. (2015). SCARECROW-LIKE15 interacts with HISTONE DEACETYLASE19 and is essential for repressing the seed maturation programme. *Nature Communications, 6*(1). doi:10.1038/ncomms8243

Gao, Y., Reitz, S. R., Wang, J., Xu, X., & Lei, Z. (2012). Potential of a strain of the entomopathogenic fungus Beauveria bassiana (Hypocreales: Cordycipitaceae) as a biological control agent against western flower thrips, Frankliniella occidentalis(Thysanoptera: Thripidae). *Biocontrol Science and Technology, 22*(4), 491–495. doi:10.1080/09583157.2012.662478

Garcia-Seco, D., Zhang, Y., Gutierrez-Mañero, F. J., Martin, C., & Ramos-Solano, B. (2015). RNA-Seq analysis and transcriptome assembly for blackberry (*Rubus sp. Var. Lochness*) fruit. *BMC Genomics, 16*(1). doi:10.1186/s12864-014-1198-1

Gardes, M., & Bruns, T. D. (1993). ITS primers with enhanced specificity for basidiomycetes - application to the identification of mycorrhizae and rusts. Molecular Ecology, 2(2), 113–118. doi:10.1111/j.1365-294x.1993.tb00005.x

Gardinia.net (2020). *Rosa virginiana* (Virginia Rose). *Gardinia*. Available at: https://www.gardenia.net/plant/rosa-virginiana [Accessed March 2020]

Gharibi, S., Sayed Tabatabaei, B. E., Saeidi, G., Talebi, M., & Matkowski, A. (2019). The effect of drought stress on polyphenolic compounds and expression of flavonoid biosynthesis related genes in Achillea pachycephala Rech.f. *Phytochemistry, 162*, 90–98. doi:10.1016/j.phytochem.2019.03.004

Gianfagna, T., Peters, J., & Yam, K. (2015). *Herbal essential oil for biomaterial preservation,* WO2016049015A1 [online] Available at: https://patents.google.com/patent/WO2016049015A1/en [Accessed March 2020]

Glazinska, P., Wojciechowski, W., Kulasek, M., Glinkowski, W., Marciniak, K., Klajn, N., … Kopcewicz, J. (2017). De novo Transcriptome Profiling of Flowers, Flower Pedicels and Pods of Lupinus luteus (Yellow Lupine) Reveals Complex Expression Changes during Organ Abscission. *Frontiers in Plant Science, 8*. doi:10.3389/fpls.2017.00641

Gong, X., Zhao, L., Song, X., Lin, Z., Gu, B., Yan, J., … Huang, X. (2019). Genome-wide analyses and expression patterns under abiotic stress of NAC transcription factors in white pear (Pyrus bretschneideri). *BMC Plant Biology, 19*(1). doi:10.1186/s12870-019-1760-8

Govender, V., Korsten, L., & Sivakumar, D. (2005). Semi-commercial evaluation of Bacillus licheniformis to control mango postharvest diseases in South Africa. *Postharvest Biology and Technology, 38*(1), 57–65. doi:10.1016/j.postharvbio.2005.04.005

Grabherr, M.G., Haas, B.J., Yassour, M., Levin, J.Z., Thompson, D.A., Amit, I., Adiconis, X., Fan, L., Raychowdhury, R., Zeng, Q., et al. (2011). Full-length transcriptome assembly from RNA-Seq data without a reference genome. *Nature Biotechnology. 29*(7), 644–652. doi:10.1038/nbt.1883

Graf, W., Herppich, W. B., Huyskens-Keil, S., & Grüneberg, H. (2009). Gas exchange of flower buds and water transport capacity of the peduncle of two cut roses during vase life. *Acta Horticulturae,* (847), 301–308. doi:10.17660/actahortic.2009.847.40

Graf, W., Huyskens-Keil, S., Herppich, W.B., & Grüneberg, H. (2006). Impact of water status, biochemical and mechanical product properties on bent neck occurrence in cut roses. *Proceedings of the 5th International Plant Biomechanics Conference, Stockholm, Sweden (2006),* pp. 365-370

Guo, X., Yu, C., Luo, L., Wan, H., Zhen, N., Li, Y., … Zhang, Q. (2018). Developmental transcriptome analysis of floral transition in *Rosa odorata* var. gigantea. *Plant Molecular Biology, 97*(1-2), 113–130. doi:10.1007/s11103-018-0727-8

Haas, B. J., Papanicolaou, A., Yassour, M., Grabherr, M., Blood, P. D., Bowden, J., … Regev, A. (2013). De novo transcript sequence reconstruction from RNA-seq using the Trinity platform for reference generation and analysis. *Nature Protocols*. 8(8), 1494–1512. doi:10.1038/nprot.2013.084

Hachez, C., Veljanovski, V., Reinhardt, H., Guillaumot, D., Vanhee, C., Chaumont, F., & Batoko, H. (2014). The Arabidopsis Abiotic Stress-Induced TSPO-Related Protein Reduces Cell-Surface Expression of the Aquaporin PIP2;7 through Protein-Protein Interactions and Autophagic Degradation. *The Plant Cell, 26*(12), 4974–4990. doi:10.1105/tpc.114.134080

Han, Y., Wan, H., Cheng, T., Wang, J., Yang, W., Pan, H., & Zhang, Q. (2017). Comparative RNA-seq analysis of transcriptome dynamics during petal development in *Rosa chinensis. Scientific Reports, 7*(1). doi:10.1038/srep43382

Hanks, G. (2015) *A review of production statistics for the cut-flower and foliage sector 2015.*

Hashemabadi, D., Torkashvand, A.M., Behzad, K., Bagherzadeh, M., Rezaalipour, M., & Mohammad, Z. (2014) Effect of Mentha pulegium extract and 8-hydroxy quinoline sulphate to extend the quality and vase life of rose (Rosa hybrid) cut flower. *Journal of Environmental Biology, 36* (1), 215–220.

Havé, M., Marmagne, A., Chardon, F., & Masclaux-Daubresse, C. (2016). Nitrogen remobilisation during leaf senescence: lessons from Arabidopsis to

crops. *Journal of Experimental Botany, 68*(10), 2513-2529. doi:10.1093/jxb/erw365

Hayer, K. E., Pizarro, A., Lahens, N. F., Hogenesch, J. B., & Grant, G. R. (2015). Benchmark analysis of algorithms for determining and quantifying full-length mRNA splice forms from RNA-seq data. *Bioinformatics, 31*(24), 3938-3945. doi:10.1093/bioinformatics/btv488

He, S., Joyce, D. C., Irving, D. E., & Faragher, J. D. (2006). Stem end blockage in cut Grevillea “Crimson Yul-lo” inflorescences. *Postharvest Biology and Technology, 41*(1), 78–84. doi:10.1016/j.postharvbio.2006.03.002

Heo, S., & Chung, Y. S. (2019). Validation of MADS-box genes from apple fruit pedicels during early fruit abscission by transcriptome analysis and real-time PCR. *Genes and Genomics, 41*(11), 1241–1251. doi:10.1007/s13258-019-00852-4

Hernández-Hernández, V., Benítez, M., & Boudaoud, A. (2019). Interplay between turgor pressure and plasmodesmata during plant development. *Journal of Experimental Botany. 71*(3), 768-777. doi:10.1093/jxb/erz434

Herppich, W. B., Matsushima, U., Graf, W., Zabler, S., Dawson, M., Choinka, G., & Manke, I. (2015). Synchrotron X-ray CT of rose peduncles – evaluation of tissue damage by radiation. *Materials Testing, 57*(1), 59–63. doi:10.3139/120.110675

Hibrand Saint-Oyant, L., Ruttink, T., Hamama, L., Kirov, I., Lakhwani, D., Zhou, N. N., … Foucher, F. (2018). A high-quality genome sequence of Rosa chinensis to elucidate ornamental traits. *Nature Plants, 4*(7), 473–484. doi:10.1038/s41477-018-0166-1

Ho, D. (2017). Notepad++: source code editor. Available online at: https://notepad-plus-plus.org/

Hu, L., Zhou, K., Li, Y., Chen, X., Liu, B., Li, C., … Ma, F. (2018). Exogenous myo-inositol alleviates salinity-induced stress in Malus hupehensis Rehd. *Plant Physiology and Biochemistry, 133*, 116–126. doi:10.1016/j.plaphy.2018.10.037

Huang, D. W., Sherman, B. T., & Lempicki, R. A. (2008). Bioinformatics enrichment tools: paths toward the comprehensive functional analysis of large gene lists. *Nucleic Acids Research, 37*(1), 1–13. doi:10.1093/nar/gkn923

Huang, D.W., Sherman, B.T., & Lempicki, R.A. (2009). Systematic and integrative analysis of large gene lists using DAVID bioinformatics resources. *Nature Protocols. 4*, 44-57. doi:10.1038/nprot.2008.211

In, B.-C., & Lim, J. H. (2018). Potential vase life of cut roses: Seasonal variation and relationships with growth conditions, phenotypes, and gene expressions. *Postharvest Biology and Technology, 135*, 93–103. doi:10.1016/j.postharvbio.2017.09.006

Innovative fresh (2017). Flower quality in supermarkets. [online] Available at: https://innovativefresh.com/en/Article/Flower-Quality-in-Supermarkets

Iturriaga, G., Gaff, D. F., & Zentella, R. (2000). New desiccation-tolerant plants, including a grass, in the central highlands of Mexico, accumulate trehalose. *Australian Journal of Botany, 48*(2), 153. doi:10.1071/bt98062

Janda, J. M., & Abbott, S. L. (2007). 16S rRNA Gene Sequencing for Bacterial Identification in the Diagnostic Laboratory: Pluses, Perils, and Pitfalls. *Journal of Clinical Microbiology,* 45(9), 2761–2764. doi:10.1128/jcm.01228-07

Jin, J., Tian, F., Yang, D.-C., Meng, Y.-Q., Kong, L., Luo, J., & Gao, G. (2016). PlantTFDB 4.0: toward a central hub for transcription factors and regulatory interactions in plants. *Nucleic Acids Research, 45*(1), 1040–1045. doi:10.1093/nar/gkw982

Jin, J., Zhang, H., Kong, L., Gao, G., & Luo, J. (2013). PlantTFDB 3.0: a portal for the functional and evolutionary study of plant transcription factors. *Nucleic Acids Research, 42*(1), 1182–1187. doi:10.1093/nar/gkt1016

Joshi, R., Wani, S. H., Singh, B., Bohra, A., Dar, Z. A., Lone, A. A., Pareek, A., & Singla-Pareek, S. L. (2016). Transcription Factors and Plants Response to Drought Stress: Current Understanding and Future Directions. *Frontiers in Plant Science, 7*, 1029. doi:10.3389/fpls.2016.01029

Jowkar, M. M. (2015). Effects of chlorination and acidification on postharvest physiological properties of alstroemeria, cv. “Vanilla” and on microbial contamination of vase solution. *Horticulture, Environment, and Biotechnology, 56*(4), 478–486. doi:10.1007/s13580-015-0022-4

Jung, S., Ficklin, S.P., Lee, T., Cheng, C.H., Blenda, A., Zheng, P., Yu, J., Bombarely, A., Cho, I., Ru., S., et al. (2014). The Genome Database for Rosaceae (GDR): year 10 update. *Nucleic Acids Research. 42*, 1237-1244. doi:10.1093/nar/gkt1012

Jung, S., Jesundurai, C., Staton, M., Du, Z., Ficklin, S., Cho, I., Abbott, A., Tomkins, J., & Main, D. (2004). GDR (Genome Database for Rosaceae): integrated web-database for Rosaceae genomics and genetics data. *BMC Bioinformatics. 5*, 130. doi:10.1186/1471-2105-5-130

Kamranfar, I., Xue, G.-P., Tohge, T., Sedaghatmehr, M., Fernie, A. R., Balazadeh, S., & Mueller-Roeber, B. (2018). Transcription factor RD26 is a key regulator of metabolic reprogramming during dark-induced senescence. *New Phytologist, 218*(4), 1543–1557. doi:10.1111/nph.15127

Kanehisa, M. (2017). Enzyme Annotation and Metabolic Reconstruction Using KEGG. *Methods in Molecular Biology*, 135–145. doi:10.1007/978-1-4939-7015-5_11

Kassambara, A. (2019). ggpubr: 'ggplot2' Based Publication Ready Plots. R package version 0.2.3. https://CRAN.R-project.org/package=ggpubr

Kayum, M. A., Park, J.-I., Nath, U. K., Biswas, M. K., Kim, H.-T., & Nou, I.-S. (2017). Genome-wide expression profiling of aquaporin genes confer responses to abiotic and biotic stresses in Brassica rapa. *BMC Plant Biology, 17*(1). doi:10.1186/s12870-017-0979-5

Kempf, H. J., & Wolf, G. (1989). *Erwinia herbicola* as a biocontrol agent of *Fusarium culmorum* and *Puccinia recondite* f. sp*. tritici* on wheat. The American Phytopathological Society. 79(9), 990-994.

Kim, J. H., Choi, D., & Kende, H. (2003). The AtGRF family of putative transcription factors is involved in leaf and cotyledon growth in Arabidopsis. *The Plant Journal, 36*(1), 94–104. doi:10.1046/j.1365-313x.2003.01862.x

Kim, D., Langmead, B., & Salzberg, S.L. (2015). HISAT: a fast spliced aligner with low memory requirements. *Nature Methods. 12* (4), 357–360. doi:10.1038/nmeth.3317

Kim, S.Y., & Volsky, D. J. (2005). *BMC Bioinformatics, 6*(1), 144. doi:10.1186/1471-2105-6-144

Klie, M., & Debener, T. (2011). Identification of superior reference genes for data normalisation of expression studies via quantitative PCR in hybrid roses (*Rosa hybrida*). *BMC Research Notes, 4*(1), 518. doi:10.1186/1756-0500-4-518

Koning-Boucoiran, C.F.S., Esselink, G.D., Vukosavljev, M., van 't Westende, W.P.C., Gitonga, V.W., Krens, F.A., Voorips, R.E., van de Weg, W.E., Schulz, D., Debener, T., et al. (2015). Using RNA-Seq to assemble a rose transcriptome with more than 13,000 full-length expressed genes and to develop the WagRhSNP 68k Axiom SNP array for rose (*Rosa* L.). *Frontiers in Plant Science*. 6, 249. doi:10.3389/fpls.2015.00249

Kosse, T. (2018). FileZilla: the free FTP solution. Available online at: https://filezilla-project.org/

Kou, X., Zhang, L., Yang, S., Li, G., & Ye, J. (2017). Selection and validation of reference genes for quantitative RT-PCR analysis in peach fruit under different experimental conditions. *Scientia Horticulturae, 225*, 195–203. doi:10.1016/j.scienta.2017.07.004

Koyama, T. (2014). The roles of ethylene and transcription factors in the regulation of onset of leaf senescence. *Frontiers in Plant Science, 5*. doi:10.3389/fpls.2014.00650

Krueger, F. (2017). Trim Galore!: wrapper script around Catadapt and FastQC to consistently apply adapter and quality trimming to FastQ files. Available online at: https://www.bioinformatics.babraham.ac.uk/projects/trim_galore/

Kudaka, J., Horii, T., Tamanaha, K., Itokazu, K., Nakamura, M., Taira, K., … Kitahara, A. (2010). Evaluation of the Petrifilm Aerobic Count Plate for Enumeration of Aerobic Marine Bacteria from Seawater and Caulerpa lentillifera. *Journal of Food Protection, 73*(8), 1529–1532. doi:10.4315/0362-028x-73.8.1529

Kuznetsova A., Brockhoff P.B. and Christensen R.H.B. (2017). lmerTest Package: Tests in Linear Mixed Effects Models. *Journal of Statistical Software*, 82(13), 1–26. doi: 10.18637/jss.v082.i13.

Laird, G., John, P., & Pearson, S. (2005). Rose vase life: cultivar and contamination source as critical factors. *Acta Horticulturae,* (687), 85–90. doi:10.17660/actahortic.2005.687.9

Li, X., Bonawitz, N. D., Weng, J.-K., & Chapple, C. (2010). The Growth Reduction Associated with Repressed Lignin Biosynthesis in Arabidopsis thaliana Is Independent of Flavonoids. *The Plant Cell, 22*(5), 1620–1632. doi:10.1105/tpc.110.074161

Li, B., & Dewey, C. N. (2011). RSEM: accurate transcript quantification from RNA-Seq data with or without a reference genome. *BMC Bioinformatics, 12*(1). doi:10.1186/1471-2105-12-323

Li, J., Hou, H., Li, X., Xiang, J., Yin, X., Gao, H., … Wang, X. (2013). Genome-wide identification and analysis of the SBP-box family genes in apple (Malus × domestica Borkh.). *Plant Physiology and Biochemistry, 70*, 100–114. doi:10.1016/j.plaphy.2013.05.021

Li, X., Liu, L., Ming, M., Hu, H., Zhang, M., Fan, J., … Wu, J. (2019). Comparative Transcriptomic Analysis Provides Insight into the Domestication and Improvement of Pear (P. pyrifolia) Fruit. *Plant Physiology, 180*(1), 435–452. doi:10.1104/pp.18.01322

Li, L., Qiao, Y., Lv, T., & Wang, L. (2015). Benzalkonium chloride treatments improve water relations of cut roses. *Acta Ecologica Sinica, 35*(4), 95–102. doi:10.1016/j.chnaes.2015.06.001

Li, Y., Zhou, G., Ma, J., Jiang, W., Jin, L., Zhang, Z., … Qiu, L. (2014). De novo assembly of soybean wild relatives for pan-genome analysis of diversity and agronomic traits. *Nature Biotechnology, 32*(10), 1045–1052. doi:10.1038/nbt.2979

Lischer, H. E. L., & Shimizu, K. K. (2017). Reference-guided de novo assembly approach improves genome reconstruction for related species. *BMC Bioinformatics, 18*(1). doi:10.1186/s12859-017-1911-6

Liu, H., Yang, L., Xin, M., Ma, F., & Liu, J. (2019). Gene-Wide Analysis of Aquaporin Gene Family in Malus domestica and Heterologous Expression of the Gene MpPIP2;1 Confers Drought and Salinity Tolerance in Arabidposis thaliana. *International Journal of Molecular Sciences, 20*(15), 3710. doi:10.3390/ijms20153710

Love, M. I., Huber, W., & Anders, S. (2014). Moderated estimation of fold change and dispersion for RNA-seq data with DESeq2. *Genome Biology, 15*(12). doi:10.1186/s13059-014-0550-8

Lü, P., Cao, J., He, S., Liu, J., Li, H., Cheng, G., … Joyce, D. C. (2010). Nano-silver pulse treatments improve water relations of cut rose cv. Movie Star flowers. *Postharvest Biology and Technology, 57*(3), 196–202. doi:10.1016/j.postharvbio.2010.04.003

Luo, M., Cheng, K., Xu, Y., Yang, S., & Wu, K. (2017). Plant Responses to Abiotic Stress Regulated by Histone Deacetylases. *Frontiers in Plant Science, 8.* doi:10.3389/fpls.2017.02147

Ma, N., Xue, J., Li, Y., Liu, X., Dai, F., Jia, W., … Gao, J. (2008). Rh-PIP2;1, a Rose Aquaporin Gene, Is Involved in Ethylene-Regulated Petal Expansion. *Plant Physiology, 148*(2), 894–907. doi:10.1104/pp.108.120154

Macnish, A. J., Morris, K. L., de Theije, A., Mensink, M. G. J., Boerrigter, H. A. M., Reid, M. S., … Woltering, E. J. (2010). Sodium hypochlorite: A promising

agent for reducing Botrytis cinerea infection on rose flowers. *Postharvest Biology and Technology, 58*(3), 262–267. doi:10.1016/j.postharvbio.2010.07.014

Martin, M., Piola, F., Chessel, D., Jay, M., & Heizmann, P. (2001). The domestication process of the Modern Rose: genetic structure and allelic composition of the rose complex. *Theoretical and Applied Genetics, 102*(2-3), 398–404. doi:10.1007/s001220051660

Matsushima, U., Graf, W., Kardjilov, N., & Herppich, W. B. (2010). Non-destructive measurement of water flow in small plants using cold neutron radiography - an application to investigate bent-neck symptom of cut roses. *Acta Horticulturae*, (858), 387–392. doi:10.17660/actahortic.2010.858.59

Matsushima, U., Hilger, A., Graf, W., Zabler, S., Manke, I., Dawson, M., … Herppich, W. B. (2012). Calcium oxalate crystal distribution in rose peduncles: Non-invasive analysis by synchrotron X-ray micro-tomography. *Postharvest Biology and Technology, 72*, 27–34. doi:10.1016/j.postharvbio.2012.04.013

Maurel, C., Verdoucq, L., Luu, D.-T., & Santoni, V. (2008). Plant Aquaporins: Membrane Channels with Multiple Integrated Functions. *Annual Review of Plant Biology, 59*(1), 595–624. doi:10.1146/annurev.arplant.59.032607.092734

Medina, I., Tárraga, J., Martínez, H., Barrachina, S., Castillo, M. I., Paschall, J., … Dopazo, J. (2016). Highly sensitive and ultrafast read mapping for RNA-seq analysis. *DNA Research, 23*(2), 93–100. doi:10.1093/dnares/dsv039

Meyer, A., Eskandari, S., Grallath, S., & Rentsch, D. (2006). AtGAT1, a High Affinity Transporter for γ-Aminobutyric Acid inArabidopsis thaliana. *Journal of Biological Chemistry, 281*(11), 7197–7204. doi:10.1074/jbc.m510766200

Moazzam Jazi, M., Rajaei, S., & Seyedi, S. M. (2015). Isolation of high quality RNA from pistachio (Pistacia vera L.) and other woody plants high in secondary metabolites. *Physiology and Molecular Biology of Plants, 21(*4), 597–603. doi:10.1007/s12298-015-0319-x

Mobatek. (2008). MobaXterm: X server and SSH client. Available online at: https://mobaxterm.mobatek.net/

Morpheus. [online] Available at: https://software.broadinstitute.org/morpheus

Mortensen, L. M., & Gislerød, H. R. (1999). Influence of air humidity and lighting period on growth, vase life and water relations of 14 rose cultivars. *Scientia Horticulturae, 82*(3-4), 289–298. doi:10.1016/s0304-4238(99)00062-x

Mumia, K.N. (2016) Floriculture in Kenya. Available from: http://kenyaflowercouncil.org/?page_id=92 [Accessed January 2016]

Muñoz, M., Faust, J. E., & Schnabel, G. (2019). Characterization of Botrytis cinerea From Commercial Cut Flower Roses. *Plant Disease, 103(*7), 1577–1583. doi:10.1094/pdis-09-18-1623-re

Mut, P., Bustamante, C., Martínez, G., Alleva, K., Sutka, M., Civello, M., & Amodeo, G. (2008). A fruit-specific plasma membrane aquaporin subtype PIP1;1 is regulated during strawberry (Fragaria × ananassa) fruit ripening.

Physiologia Plantarum, 132(4), 538–551. doi:10.1111/j.1399-3054.2007.01046.x

Muthurajan, R., Shobbar, Z.-S., Jagadish, S. V. K., Bruskiewich, R., Ismail, A., Leung, H., & Bennett, J. (2010). Physiological and Proteomic Responses of Rice Peduncles to Drought Stress. *Molecular Biotechnology, 48*(2), 173–182. doi:10.1007/s12033-010-9358-2

Nakabayashi, R., Mori, T., & Saito, K. (2014). Alternation of flavonoid accumulation under drought stress in Arabidopsis thaliana. *Plant Signaling and Behavior, 9*(8), e29518. doi:10.4161/psb.29518

Nakamura, T., Negishi, Y., Funada, R., & Yamada, M. (2001). Sedimentable amyloplasts in starch sheath cells of woody stems of Japanese cherry. *Advances in Space Research, 27*(5), 957–960. doi:10.1016/s0273-1177(01)00171-5

Nakamura, M., Toyota, M., Tasaka, M., & Morita, M. T. (2011). An Arabidopsis E3 Ligase, SHOOT GRAVITROPISM9, Modulates the Interaction between Statoliths and F-Actin in Gravity Sensing. *The Plant Cell, 23*(5), 1830–1848. doi:10.1105/tpc.110.079442

Nakano, T., Fujisawa, M., Shima, Y., & Ito, Y. (2014). The AP2/ERF transcription factor SlERF52 functions in flower pedicel abscission in tomato. *Journal of Experimental Botany, 65*(12), 3111–3119. doi:10.1093/jxb/eru154

Nakano, T., Suzuki, K., Fujimura, T., & Shinshi, H. (2006). Genome-Wide Analysis of the ERF Gene Family in Arabidopsis and Rice. *Plant Physiology, 140*(2), 411–432. doi:10.1104/pp.105.073783

Nell, T.A., Leonard, R.T., & Macnish, A.J. (2006) *Taking the mystery out of flower care solutions.* Available from: https://www.floristsreview.com/main/june2006/featurestory.html [Accessed 10 December 2015]

Nero, L. A., Beloti, V., De Aguiar Ferreira Barros, M., Ortolani, M. B. T., Tamanini, R., & De Melo Franco, B. D. G. (2006). Comparison of petrifilm aerobic count plates and de man rogosa sharpe agar for enumeration of lactic acid bacteria. *Journal of Rapid Methods and Automation in Microbiology, 14*(3), 249–257. doi:10.1111/j.1745-4581.2006.00050.x

Nishizawa, A., Yabuta, Y., & Shigeoka, S. (2008). Galactinol and Raffinose Constitute a Novel Function to Protect Plants from Oxidative Damage. *Plant Physiology, 147*(3), 1251–1263. doi:10.1104/pp.108.122465

Oda-Yamamizo, C., Mitsuda, N., Sakamoto, S., Ogawa, D., Ohme-Takagi, M., & Ohmiya, A. (2016). The NAC transcription factor ANAC046 is a positive regulator of chlorophyll degradation and senescence in Arabidopsis leaves. *Scientific Reports, 6*(1). doi:10.1038/srep23609

Oliveros, J.C. (2015). Venny: An interactive tool for comparing lists with Venn’d diagrams. Available online at: https://bioinfogp.cnb.csic.es/tools/venny/index.html

Ou, F., McGoverin, C., Swift, S., & Vanholsbeeck, F. (2017). Absolute bacterial cell enumeration using flow cytometry. *Journal of Applied Microbiology, 123*(2), 464–477. doi:10.1111/jam.13508

Özaktan, H., & Bora, T. (2004). Biological control of fire blight in pear orchards with a formulation of Pantoea agglomerans strain Eh 24. *Brazilian Journal of Microbiology, 35*(3), 224–229. doi:10.1590/s1517-83822004000200010

Pandey, G. K., Grant, J. J., Cheong, Y. H., Kim, B. G., Li, L., & Luan, S. (2005). ABR1, an APETALA2-Domain Transcription Factor That Functions as a Repressor of ABA Response in Arabidopsis. *Plant Physiology, 139*(3), 1185–1193. doi:10.1104/pp.105.066324

Parups, E. V., & Voisey, P. W. (1976). Lignin Content and Resistance to Bending of the Pedicel in Greenhouse-Grown Roses. *Journal of Horticultural Science, 51*(2), 253–259. doi:10.1080/00221589.1976.11514688

Passoth, V., Fredlund, E., Druvefors, U. Ãdel., & Schnurer, J. (2006). Biotechnology, physiology and genetics of the yeast Pichia anomala. *FEMS Yeast Research, 6*(1), 3–13. doi:10.1111/j.1567-1364.2005.00004.x

Patel, J. S., Kharwar, R. N., Singh, H. B., Upadhyay, R. S., & Sarma, B. K. (2017). Trichoderma asperellum (T42) and Pseudomonas fluorescens (OKC)-Enhances Resistance of Pea against Erysiphe pisi through Enhanced ROS Generation and Lignifications. *Frontiers in Microbiology, 8*. doi:10.3389/fmicb.2017.00306

Perin, E. C., da Silva Messias, R., Borowski, J. M., Crizel, R. L., Schott, I. B., Carvalho, I. R., … Galli, V. (2019). ABA-dependent salt and drought stress improve strawberry fruit quality. *Food Chemistry, 271*, 516–526. doi:10.1016/j.foodchem.2018.07.213

Pfaffl, M. W. (2001). A new mathematical model for relative quantification in real-time RT-PCR. *Nucleic Acids Research, 29*(9), 45e–45. doi:10.1093/nar/29.9.e45

PlantTFDB v5.0 (2019). *Rosa chinensis* Transcription Factors. [online] Available at: http://planttfdb.gao-lab.org/index_ext.php?sp=Rch [Accessed 25 February 2020]

Podzimska-Sroka, D., O'Shea, C., Gregersen, P., & Skriver, K. (2015). NAC Transcription Factors in Senescence: From Molecular Structure to Function in Crops. *Plants, 4*(3), 412–448. doi:10.3390/plants4030412

Pompodakis, N., Terry, L., Joyce, D., Papadimitriou, M., Lydakis, D., & Darras, A. (2010). Effects of storage temperature and abscisic acid treatment on the vase-life of cut "First Red" and "Akito" roses. *The Journal of Horticultural Science and Biotechnology, 85*(3), 253–259. doi:10.1080/14620316.2010.11512664

Pouri, H. A., Nejad, A. R., & Shahbazi, F. (2017). Effects of simulated in-transit vibration on the vase life and post-harvest characteristics of cut rose flowers. *Horticulture, Environment, and Biotechnology, 58*(1), 38–47. doi:10.1007/s13580-017-0069-5

Put, H. M. C. (1990). Micro-organisms from freshly harvested cut flower stems and developing during the vase life of chrysanthemum, gerbera and rose cultivars. *Scientia Horticulturae, 43*(1-2), 129–144. doi:10.1016/0304-4238(90)90044-f

Put, H. M. C., & Clerkx, A. C. M. (1988). The infiltration ability of micro-organisms Bacillus, Fusarium, Kluyveromyces and Pseudomonasspp. into xylem vessels of Gerberacv. “Fleur”andRosacv. “Sonia”cut flowers: a scanning electron microscope study. *Journal of Applied Bacteriology*, *64*(6), 515–530. doi:10.1111/j.1365-2672.1988.tb02443.x

Put, H. M. C., Clerkx, A. C. M., & Durkin, D. J. (2001). Anatomy of cut rosa xylem observed by scanning electron microscope. *Acta Horticulturae,* (547), 331–339. doi:10.17660/actahortic.2001.547.39

Put, H. M. C., & Conway, C. (1986). Investigations into the influence of the microflora from stems of cut flowers on the vase-life of rose “sonia”; gerbera “fleur” and chrysanthemum “spider.” *Acta Horticulturae,* (181), 415–418. doi:10.17660/actahortic.1986.181.56

Put, H. M. C., & Jansen, L. (1989). The effects on the vase life of cut Rosa cultivar “Sonia” of bacteria added to the vase water. *Scientia Horticulturae, 39(*2), 167–179. doi:10.1016/0304-4238(89)90089-7

Put, H. M. C., & Rombouts, F. M. (1989). The influence of purified microbial pectic enzymes on the xylem anatomy, water uptake and vase life of Rosa cultivar “Sonia.” *Scientia Horticulturae, 38*(1-2), 147–160. doi:10.1016/0304-4238(89)90027-7

Put, H. M. C., & van der Meyden, T. (1988). Infiltration of Pseudomonas putidacells, strain 48, into xylem vessels of cut Rosa cv. “Sonia.” *Journal of Applied Bacteriology, 64*(3), 197–208. doi:10.1111/j.1365-2672.1988.tb03376.x

R Core Team (2019). R: A language and environment for statistical computing. R Foundation for Statistical Computing, Vienna, Austria. https://www.R-project.org/.

Rahman, M. M., Ahmad, S. H., Mohamed, M. T. M., & Ab Rahman, M. Z. (2014). Antimicrobial Compounds from Leaf Extracts of Jatropha curcas, Psidium guajava, and Andrographis paniculata. *The Scientific World Journal,* 2014, 1–8. doi:10.1155/2014/635240

Raymond, O., Gouzy, J., Just, J., Badouin, H., Verdenaud, M., Lemainque, A., Vergne, P., Moja, S., Choisne, N., Pont, C., et al. (2018). The Rosa genome provides new insights into the domestication of modern roses. *Nature Genetics. 50*(6), 772-777. doi:10.1038/s41588-018-0110-3

Reid, M. (2001). Advances in shipping and handling of ornamentals. *Acta Horticulturae,* (543), 277–284. doi:10.17660/actahortic.2001.543.33

Robinson, S., Dixon, M. A., & Zheng, Y. (2007). Vascular blockage in cut roses in a suspension of Pseudomonas fluorescens. *The Journal of Horticultural Science and Biotechnology, 82*(5), 808–814. doi:10.1080/14620316.2007.11512310

Robinson, M. D., McCarthy, D. J., & Smyth, G. K. (2009). edgeR: a Bioconductor package for differential expression analysis of digital gene expression data. *Bioinformatics, 26*(1), 139–140. doi:10.1093/bioinformatics/btp616

Rogers, H. J. (2011). Is there an important role for reactive oxygen species and redox regulation during floral senescence? *Plant, Cell and Environment, 35*(2), 217–233. doi:10.1111/j.1365-3040.2011.02373.x

Romero, P., Gandía, M., & Alférez, F. (2013). Interplay between ABA and phospholipases A2 and D in the response of citrus fruit to postharvest dehydration. *Plant Physiology and Biochemistry, 70*, 287–294. doi:10.1016/j.plaphy.2013.06.002

RStudio Team (2019). RStudio: Integrated Development for R. RStudio, Inc., Boston, MA. http://www.rstudio.com/

Ruzin, S.E. (1999). Chemical fixation. *Plant microtechnique and microscopy.* (pp. 33-56) Oxford, UK: Oxford University Press doi:10.1046/j.1469-8137.2000.00735.x

Sack, F. D. (1991). Plant Gravity Sensing. *International Review of Cytology*, 193–252. doi:10.1016/s0074-7696(08)60695-6

Sangiovanni, M., Granata, I., Thind, A. S., & Guarracino, M. R. (2019). From trash to treasure: detecting unexpected contamination in unmapped NGS data. *BMC Bioinformatics, 20*(S4). doi:10.1186/s12859-019-2684-x

Sayed, S. M., Ali, E. F., & Al-Otaibi, S. S. (2019). Efficacy of indigenous entomopathogenic fungus, Beauveria bassiana (Balsamo) Vuillemin, isolates against the rose aphid, Macrosiphum rosae L. (Hemiptera: Aphididae) in rose production. *Egyptian Journal of Biological Pest Control, 29*(1). doi:10.1186/s41938-019-0123-y

Schneider, C. A., Rasband, W. S., & Eliceiri, K. W. (2012). NIH Image to ImageJ: 25 years of image analysis. *Nature Methods, 9*(7), 671–675. doi:10.1038/nmeth.2089

Seo, P. J., Park, J.-M., Kang, S. K., Kim, S.-G., & Park, C.-M. (2010). An Arabidopsis senescence-associated protein SAG29 regulates cell viability under high salinity. *Planta, 233*(1), 189–200. doi:10.1007/s00425-010-1293-8

Shah, D. U., Reynolds, T. P., & Ramage, M. H. (2017). The strength of plants: theory and experimental methods to measure the mechanical properties of stems. *Journal of Experimental Botany, 68*(16), 4497–4516. doi:10.1093/jxb/erx245

Sharma, A., Shahzad, B., Rehman, A., Bhardwaj, R., Landi, M., & Zheng, B. (2019). Response of Phenylpropanoid Pathway and the Role of Polyphenols in Plants under Abiotic Stress. *Molecules, 24*(13), 2452. doi:10.3390/molecules24132452

Shulaev, V., Sargent, D. J., Crowhurst, R.N., Mockler, T.C., Folkerts, O., Delcher, A.L., Jaiswal, P., Mockatis, K., Liston, A., Mane, S.P., et al. (2011). The genome of woodland strawberry (Fragaria vesca). *Nature Genetics. 43*(2), 109–116. doi:10.1038/ng.740

Silva, K. J. P., Singh, J., Bednarek, R., Fei, Z., & Khan, A. (2019). Differential gene regulatory pathways and co-expression networks associated with fire blight infection in apple (Malus × domestica). *Horticulture Research, 6*(1). doi:10.1038/s41438-019-0120-z

Slootweg, G., & van Meeteren, U. (1991). Transpiration and stomatal conductance of roses cv. Sonia grown with supplementary lighting. *Acta Hortic. (298)*, 119-126. doi:10.17660/actahortic.1991.298.12

Song, C.Y., Bang, C.S., Park, Y.S., & Chung, S.K. (1995) Effect of pretreatment and cold storage on vase life and quality of cut hybrid delphinium (Delphinium x elatum). *Journal of the Korean Society for Horticultural Science, 36* (3), 426–431.

Spinarova, S., & Hendriks, L. (2007). Post-harvest water stress tolerance of various rose cultivars: screening and characterisation. *Acta Horticulturae,* (751), 423–430. doi:10.17660/actahortic.2007.751.54

Staby, G. (2015) Some cut flower and potted plant postharvest care and handling facts and recommendations. *Postharvest care, handling and physiology of floral crops.*

Suarez, F. L., Springfield, J., Furne, J. K., Lohrmann, T. T., Kerr, P. S., & Levitt, M. D. (1999). Gas production in humans ingesting a soybean flour derived from beans naturally low in oligosaccharides. *The American Journal of Clinical Nutrition, 69*(1), 135–139. doi:10.1093/ajcn/69.1.135

Šurbanovski, N., Sargent, D. J., Else, M. A., Simpson, D. W., Zhang, H., & Grant, O. M. (2013). Expression of Fragaria vesca PIP Aquaporins in Response to Drought Stress: PIP Down-Regulation Correlates with the Decline in Substrate Moisture Content. *PLoS ONE, 8*(9), e74945. doi:10.1371/journal.pone.0074945

Swarup, R., & Bhosale, R. (2019). Developmental Roles of AUX1/LAX Auxin Influx Carriers in Plants. Frontiers in Plant Science, 10. doi:10.3389/fpls.2019.01306

Szklarczyk, D., Gable, A. L., Lyon, D., Junge, A., Wyder, S., Huerta-Cepas, J., … Mering, C. von. (2018). STRING v11: protein–protein association networks with increased coverage, supporting functional discovery in genome-wide experimental datasets. *Nucleic Acids Research, 47*(1), 607–613. doi:10.1093/nar/gky1131

Teixeira, J., Gaspar, A., Garrido, E. M., Garrido, J., & Borges, F. (2013). Hydroxycinnamic Acid Antioxidants: An Electrochemical Overview. *BioMed Research International, 2013*, 1–11. doi:10.1155/2013/251754

The Gene Ontology Consortium. (2018). The Gene Ontology Resource: 20 years and still GOing strong. *Nucleic Acids Research, 47*(D1), D330–D338. doi:10.1093/nar/gky1055

Thimm, O., Bläsing, O., Gibon, Y., Nagel, A., Meyer, S., Krüger, P., Selbig, J., Müller, L.A., Rhee, S.Y., & Stitt, M. (2004). MAPMAN: a user-driven tool to display genomics data sets onto diagrams of metabolic pathways and other biological processes. *The Plant Journal. 37* (6), 914-939. doi:10.1111/j.1365-313X.2004.02016.x

Thwala, M., Wahome, P. K., Oseni, T. O., & Masarirambi, M. T. (2013). Effects of floral preservatives on the vase life of orchid (*Epidendrum radicans* L.) cut flowers. *Journal or Horticultural Science & Ornamental Plants. 5*, 22–29. doi:10.5829/idosi.jhsop.2013.5.1.268

Tian, C., Jiang, Q., Wang, F., Wang, G.-L., Xu, Z.-S., & Xiong, A.-S. (2015). Selection of Suitable Reference Genes for qPCR Normalization under Abiotic Stresses and Hormone Stimuli in Carrot Leaves. *PLOS ONE, 10(*2), e0117569. doi:/10.1371/journal.pone.0117569

Tian, T., Liu, Y., Yan, H., You, Q., Yi, X., Du, Z., … Su, Z. (2017). agriGO v2.0: a GO analysis toolkit for the agricultural community, 2017 update. *Nucleic Acids Research. 45*(1), 122–129. doi:10.1093/nar/gkx382

Torsvik, V., Goksøyr, J., & Daae, F. L. (1990). High diversity in DNA of soil bacteria. *Applied and Environmental Microbiology, 56*(3), 782–787. doi:10.1128/aem.56.3.782-787.1990

Turner, T. R., James, E. K., & Poole, P. S. (2013). The plant microbiome. *Genome Biology, 14*(6). doi:10.1186/gb-2013-14-6-209

Uchida, N., Lee, J. S., Horst, R. J., Lai, H.-H., Kajita, R., Kakimoto, T., … Torii, K. U. (2012). Regulation of inflorescence architecture by intertissue layer ligand-receptor communication between endodermis and phloem. *Proceedings of the National Academy of Sciences, 109*(16), 6337–6342. doi:10.1073/pnas.1117537109

Uchida, N., & Tasaka, M. (2013). Regulation of plant vascular stem cells by endodermis-derived EPFL-family peptide hormones and phloem-expressed ERECTA-family receptor kinases. *Journal of Experimental Botany, 64*(17), 5335–5343. doi:10.1093/jxb/ert196

Vaattovaara, A., Leppälä, J., Salojärvi, J., & Wrzaczek, M. (2018). High-throughput sequencing data and the impact of plant gene annotation quality. *Journal of Experimental Botany, 70*(4), 1069–1076. doi:10.1093/jxb/ery434

Valerio, C., Costa, A., Marri, L., Issakidis-Bourguet, E., Pupillo, P., Trost, P., & Sparla, F. (2010). Thioredoxin-regulated β-amylase (BAM1) triggers diurnal starch degradation in guard cells, and in mesophyll cells under osmotic stress. *Journal of Experimental Botany, 62*(2), 545–555. doi:10.1093/jxb/erq288

van der Graaff, E., Laux, T., & Rensing, S. A. (2009). The WUS homeobox-containing (WOX) protein family. *Genome Biology, 10*(12), 248. doi:10.1186/gb-2009-10-12-248

van Doorn, W. G. (1989). Role of physiological processes, microorganisms, and air embolism in vascular blockage of cut rose flowers. *Acta Horticulturae*, (261), 27–34. doi:10.17660/actahortic.1989.261.3

van Doorn, W. G. (1995). Vascular occlusion in cut rose flowers: a survey. *Acta Horticulturae,* (405), 58–66. doi:10.17660/actahortic.1995.405.6

van Doorn, W. G. (1997). Water relations of cut flowers. *Horticultural Reviews, 18*, 1-68.

van Doorn, W. G., Buis, H. C. E. M., & de Witte, Y. (1986). Effect of exogenous bacterial concentrations on water relations of cut rose flowers ii. Bacteria in the vase solution. *Acta Horticulturae,* (181), 463–466. doi:10.17660/actahortic.1986.181.66

van Doorn, W. G., de Stigter, H. C. M., de Witte, Y., & Boekestein, A. (1991). Micro-organisms at the cut surface and in xylem vessels of rose stems. *Journal of Applied Bacteriology, 70*(1), 34–39. doi:10.1111/j.1365-2672.1991.tb03783.x

van Doorn, W. G., & de Witte, Y. (1991a). Effect of bacterial suspensions on vascular occlusion in stems of cut rose flowers. *Journal of Applied Bacteriology, 71*(2), 119–123. doi:10.1111/j.1365-2672.1991.tb02965.x

van Doorn, W. G., & de Witte, Y. (1991b). Effect of Dry Storage on Bacterial Counts in Stems of Cut Rose Flowers. *HortScience, 26*(12), 1521–1522. doi:10.21273/hortsci.26.12.1521

van Doorn, W. G., & de Witte, Y. (1997). Sources of the Bacteria Involved in Vascular Occlusion of Cut Rose Flowers. Journal of the American *Society for Horticultural Science,* 122(2), 263–266. doi:10.21273/jashs.122.2.263

van Doorn, W. G., de Witte, Y., & Harkema, H. (1995). Effect of high numbers of exogenous bacteria on the water relations and longevity of cut carnation flowers. *Postharvest Biology and Technology, 6*(1-2), 111–119. doi:10.1016/0925-5214(94)00043-r

van Doorn, W. G., de Witte, Y., & Perik, R. R. J. (1990a). Effect of antimicrobial compounds on the number of bacteria in stems of cut rose flowers. *Journal of Applied Bacteriology, 68(*2), 117–122. doi:10.1111/j.1365-2672.1990.tb02555.x

van Doorn, W. G., & Perik, R. R. J. (1990). Hydroxyquinoline Citrate and Low pH Prevent Vascular Blockage in Stems of Cut Rose Flowers by Reducing the Number of Bacteria. *Journal of the American Society for Horticultural Science, 115*(6), 979–981. doi:10.21273/jashs.115.6.979

van Doorn, W. G., Schurer, K., & de Witte, Y. (1989). Role of Endogenous Bacteria in Vascular Blockage of Cut Rose Flowers. *Journal of Plant Physiology, 134*(3), 375–381. doi:10.1016/s0176-1617(89)80259-7

van Doorn, W. G., Thiel, F., & Boekestein, A. (1990b). Cryoscanning electron microscopy of a layer of extracellular polysaccharides produced by bacterial colonies. *Scanning, 12*(6), 297–299. doi:10.1002/sca.4950120603

van Doorn, W. G., Thiel, F., & Boekestein, A. (1991). Examination of occlusions in xylem vessels of cut rose flowers, using cryoscanning electron microscopy and cryoultramilling cross-sectioning. *Scanning, 13*(1), 37–40. doi:10.1002/sca.4950130108

van Meeteren, U., Schouten, R. E., & Woltering, E. (2015). Predicting rose vase life in a supply chain. *Acta Horticulturae,* (1099), 283–289. doi:10.17660/actahortic.2015.1099.32

Vanneste, J. L., Yu, J., & Beer, S. V. (1992). Role of antibiotic production by Erwinia herbicola Eh252 in biological control of Erwinia amylovora. *Journal of Bacteriology, 174*(9), 2785–2796. doi:10.1128/jb.174.9.2785-2796.1992

Vembadi, A., Menachery, A., & Qasaimeh, M. A. (2019). Cell Cytometry: Review and Perspective on Biotechnological Advances. *Frontiers in Bioengineering and Biotechnology, 7.* doi:10.3389/fbioe.2019.00147

Wang, Z., Gerstein, M., & Snyder, M. (2009). RNA-Seq: a revolutionary tool for transcriptomics. *Nature Reviews Genetics, 10*(1), 57–63. doi:10.1038/nrg2484

Wang, W., Xu, M., Wang, G., & Galili, G. (2017). Autophagy: An Important Biological Process That Protects Plants from Stressful Environments. *Frontiers in Plant Science, 7*. doi:10.3389/fpls.2016.02030

Weise, S. E., Kuznetsov, O. A., Hasenstein, K. H., & Kiss, J. Z. (2000). Curvature in Arabidopsis Inflorescence Stems Is Limited to the Region of Amyloplast Displacement. *Plant and Cell Physiology, 41*(6), 702–709. doi:10.1093/pcp/41.6.702

Wickham, H., François, R., Henry, L., & Müller, K. (2019). dplyr: A Grammar of Data Manipulation. R package version 0.8.3. https://CRAN.R-project.org/package=dplyr

Williams, A. (2007) *Precis Report for World Flowers: Comparative Study of Cut Roses for the British Market Produced in Kenya and the Netherlands.*

Williams, B., Njaci, I., Moghaddam, L., Long, H., Dickman, M. B., Zhang, X., & Mundree, S. (2015). Trehalose Accumulation Triggers Autophagy during Plant Desiccation. *PLOS Genetics, 11*(12), e1005705. doi:10.1371/journal.pgen.1005705

Wilson, M. (2015) Why flowers in UK vases are causing tensions in Kenya. *The Financial Times.*

Woltering, E. J. (1987). The effects of leakage of substances from mechanically wounded rose stems on bacterial growth and flower quality. *Scientia Horticulturae, 33*(1-2), 129–136. doi:10.1016/0304-4238(87)90039-2

Woltering, E. J., & Paillart, M. J. M. (2018). Effect of cold storage on stomatal functionality, water relations and flower performance in cut roses. *Postharvest Biology and Technology, 136*, 66–73. doi:10.1016/j.postharvbio.2017.10.009

Wraight, S.P., Carruthers, R.I., Jaronski, S.T., Bradley, C.A., Garza, C.J., & Galaini-Wraight, S. (2000). Evaluation of the Entomopathogenic Fungi Beauveria bassiana and Paecilomyces fumosoroseus for Microbial Control of the Silverleaf Whitefly, Bemisia argentifolii. *Biological Control, 17*(3), 203–217. doi:10.1006/bcon.1999.0799

Wyatt, S.E., Brown, D., Robertson, D. and Muday, G. (1997) The gravitropic response of the inflorescence stems of Arabidopsis (abstract No. 614). *Plant Physiology, 114(S)*, 113.

Xue, H., Wang, S., Yao, J.-L., Deng, C. H., Wang, L., Su, Y., … Yang, J. (2018). Chromosome level high-density integrated genetic maps improve the

Pyrus bretschneideri “DangshanSuli” v1.0 genome. *BMC Genomics, 19(*1). doi:10.1186/s12864-018-5224-6

Yang, X., Liu, J., Xu, J., Duan, S., Wang, Q., Li, G., & Jin, L. (2019). Transcriptome Profiling Reveals Effects of Drought Stress on Gene Expression in Diploid Potato Genotype P3-198. *International Journal of Molecular Sciences, 20*(4), 852. doi:10.3390/ijms20040852

Yarza, P., Yilmaz, P., Pruesse, E., Glöckner, F. O., Ludwig, W., Schleifer, K.-H., … Rosselló-Móra, R. (2014). Uniting the classification of cultured and uncultured bacteria and archaea using 16S rRNA gene sequences. *Nature Reviews Microbiology, 12*(9), 635–645. doi:10.1038/nrmicro3330

Ye, H., Liu, S., Tang, B., Chen, J., Xie, Z., Nolan, T. M., … Yin, Y. (2017). RD26 mediates crosstalk between drought and brassinosteroid signalling pathways. *Nature Communications, 8*(1). doi:10.1038/ncomms14573

Yoshihara, T., & Spalding, E. P. (2019). Switching the Direction of Stem Gravitropism by Altering Two Amino Acids in AtLAZY1. *Plant Physiology, 182*(2), 1039–1051. doi:10.1104/pp.19.01144

Zagory, D. (1999). Effects of post-processing handling and packaging on microbial populations. *Postharvest Biology and Technology, 15*(3), 313–321. doi:10.1016/s0925-5214(98)00093-3

Zagory, D., & Reid, M. S. (1986). Evaluation of the role of vase microorganisms in the postharvest life of cut flowers. *Acta Horticulturae,* (181), 207–218. doi:10.17660/actahortic.1986.181.25

Zamski, E., Starkman, F., & Zieslin, N. (1991). Mechanical strength and anatomical structure of the peduncles of rose (Rosa × hybrida) flowers. *Israel Journal of Botany*, 40:1, 1-6, doi: 10.1080/0021213X.1991.10677172

Zanella, M., Borghi, G. L., Pirone, C., Thalmann, M., Pazmino, D., Costa, A., … Sparla, F. (2016). β-amylase 1 (BAM1) degrades transitory starch to sustain proline biosynthesis during drought stress. *Journal of Experimental Botany, 67*(6), 1819–1826. doi:10.1093/jxb/erv572

Zhang, Y., Li, W., Dou, Y., Zhang, J., Jiang, G., Miao, L., … Zhang, Z. (2015). Transcript Quantification by RNA-Seq Reveals Differentially Expressed Genes in the Red and Yellow Fruits of *Fragaria vesca*. *PLOS ONE, 10*(12), e0144356. doi:10.1371/journal.pone.0144356

Zhang, S., Wang, L., Sun, X., Li, Y., Yao, J., Nocker, S. van., & Wang, X. (2019). Genome-Wide Analysis of the YABBY Gene Family in Grapevine and Functional Characterization of VvYABBY4. *Frontiers in Plant Science, 10*. doi:10.3389/fpls.2019.01207

Zhong, R., Lee, C., Zhou, J., McCarthy, R. L., & Ye, Z.-H. (2008). A Battery of Transcription Factors Involved in the Regulation of Secondary Cell Wall Biosynthesis in Arabidopsis. *The Plant Cell, 20*(10), 2763–2782. doi:10.1105/tpc.108.061325

Zhou, Y., Xu, Z., Zhao, K., Yang, W., Cheng, T., Wang, J., & Zhang, Q. (2016). Genome-Wide Identification, Characterization and Expression

Analysis of the TCP Gene Family in *Prunus mume*. *Frontiers in Plant Science, 7.* doi:10.3389/fpls.2016.01301

Zhuo, X., Zheng, T., Zhang, Z., Zhang, Y., Jiang, L., Ahmad, S., … Zhang, Q. (2018). Genome-Wide Analysis of the NAC Transcription Factor Gene Family Reveals Differential Expression Patterns and Cold-Stress Responses in the Woody Plant Prunus mume. *Genes, 9*(10), 494. doi:10.3390/genes9100494

Zieslin, N., Starkman, F., & Zamski, E. (1989). Growth of rose flower peduncles and effects of applied plant growth regulators. *Plant Growth Regulation, 8,* 65-76.

Appendices

1.1 qPCR supplementary figures

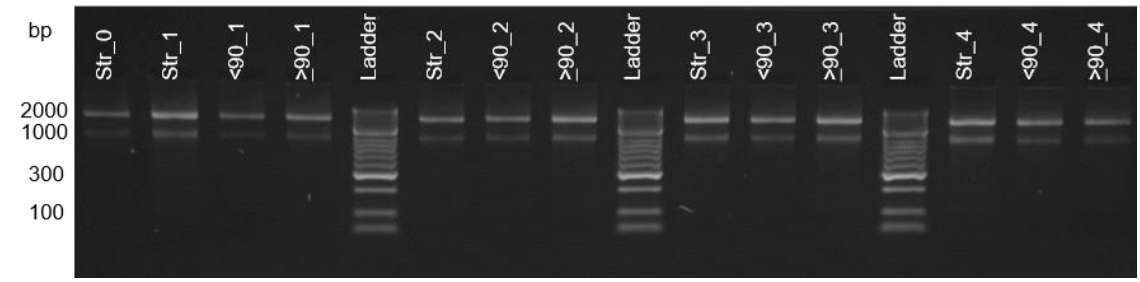

Electrophoresis gel of RNA extractions used for qPCR

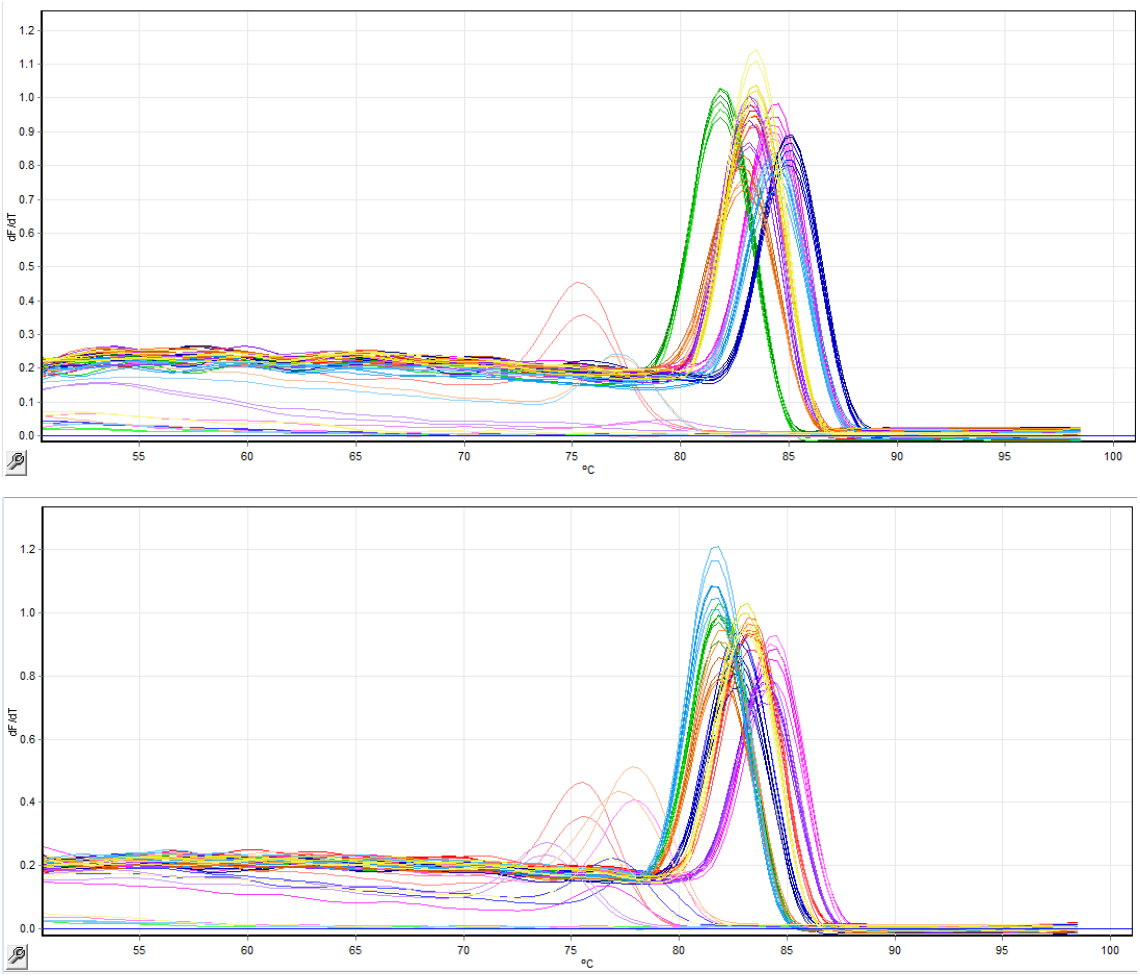

Melt curves from 21.08.2019, run 1 and 2. Showing single peaks for each of primers. Each colour represents a different primer, with lines for each of the stages and technical replicates clustered together. The smaller peaks to the left of the peak clusters were formed by the negative controls for each of the primers.

Table 24 Eurofins output for each qPCR primer and blast top hit

Primer	Sequence	Blast top hit name	E value	Ident (%)
UGE5	AAGATGTGCGGGACAGTGGATTGGGCTAGCAAGAACCCATATGGCTATGGACCTCAAGACAAAATCCCC	Rosa chinensis UDP-glucose 4-epimerase GEPI48 (LOC112179506), mRNA	9.00E-19	95.16
SIP2	TGATCATCTGGCTTCTGACGGCGAAGTTTCTTCGGAGCTTACCACTTCTCTCAGTGAGAATAGATCTTCAACTGCCACAGTCACCATCAAAACCCGT	Rosa chinensis probable galactinol--sucrose galactosyltransferase 2 (LOC112191944), transcript variant X3, mRNA	4.00E-40	100.00
DIN10	GAAGCCATGAGGTGCTGTGTAGGGACTAATGGGGTTGATTTCAGCTATGATTCGGCATCTAGGGTTGGTGACTATG	Rosa hybrid cultivar putative galactinol-sucrose galactosyltransferase 6 protein (RS6) mRNA, complete cds	2.00E-27	97.30
ATBF1	CCTTAAGAAGCTTGATTGATCACTCTATAGTGGAGAGCTTTGGTGGAGAAGGCAAGGCGTGCATAACAGCCAGGGTTTATCCGACATTGGCTGTTGATGGGGATGCCCACTTATATGCTTTCAATTAGA	Rosa chinensis beta-fructofuranosidase, insoluble isoenzyme CWINV1 (LOC112187488), mRNA	2.00E-57	99.19
PGM2	TAAAAACCTTCAAATTAGCAGAGAATCTTCAGAAGCACTTGCTCCTCTTGTTGAGGTTGCTCTTAAGCTTTCCAAGATGCAAGAATTCACTGGCCGATCTGCTA	Rosa chinensis phosphoglucomutase, cytoplasmic (LOC112197974), mRNA	9.00E-41	97.96
AGAL3	TGGGAGCACTTGGACTGCAATCCAGCATTAGTGTCTCAGTGAGAGATTTGTGGCAGCACAAACTAGTTAAGGAGGATGCCTTATCCTCATTTGGTGCTCTGGTAAGCCTGA	Rosa chinensis alpha-galactosidase 3 (LOC112185187), transcript variant X2, mRNA	4.00E-44	98.08
OMT1	CCTGTAGCACCGGACACTAGCCTCGCCACCAAGGGAGTTGTCCATATCGACGTGATCATA	Rosa chinensis caffeic acid 3-O-methyltransferase (LOC112184684), mRNA	2.00E-23	100.00
PRXPX	GAACAACTACTACAGGGAACATCCTTGGGACAACAAGGGTTTGATGATGGTGGATCACCAGCTTGCCACAGACAAGCCGACCTC	Rosa chinensis peroxidase 42 (LOC112167574), mRNA	6.00E-26	96.00
CAD9	GAATTGCCTATATTTCCATTGGTTCTGGGGAGGAAGCTCGTTGGTGGAAGCGACGTTGGAGGGATAAAAATA	Rosa chinensis probable cinnamyl alcohol dehydrogenase 9 (LOC112184982), mRNA	6.00E-27	98.55
HCT	GGGCGAACAGTTTCATGGGACGCGCTGGAATTCCAAGTGAAGGGAAGGCATACATGATACCAAGTGCAACGAATTATGGTTTATCGCTGTGCATCAATCTGCATTCTCGGCATATGAACACAG	Rosa chinensis shikimate O-hydroxycinnamoyltransferase-like (LOC112201402), mRNA	5.00E-49	95.90
GAPC2	AGGAGGAGTCCGAGGGAAGCTCAATGGTATCTTGGGTTACACCGAAGACGATGTTGTGTCAACTGACTTCATCGGTGACAACAGATCAAGCAAATGGGGG	Rosa chinensis glyceraldehyde-3-phosphate dehydrogenase, cytosolic (LOC112179622), mRNA	7.00E-38	97.85

1.2 Statistical test output

1.2.1 Physiology Chapter statistical results

1.2.1.1 Comparison of Rosa hybrida *cultivars*

Table 25. Relative fresh weight (RFW) ~ Cultivar ANOVA with Tukey post hoc test

$F_{5, 12} = 5.00, p < 0.05$					
	Akito	Fuchsiana	Furiosa	H30	Topsun
Fuchsiana	p > 0.05	-	-	-	-
Furiosa	p > 0.05	p > 0.05	-	-	-
H30	**p < 0.05**	p > 0.05	**p < 0.05**	-	-
Topsun	p > 0.05	p > 0.05	p > 0.05	p > 0.05	-
Tropical Amazon	p > 0.05	p > 0.05	p > 0.05	p > 0.05	p > 0.05

Table 26. Vase life ~ Cultivar ANOVA with Tukey post hoc test (Bunch data)

$F_{5, 12} = 22.07, p < 0.001$					
	Akito	Fuchsiana	Furiosa	H30	Topsun
Fuchsiana	**p < 0.05**	-	-	-	-
Furiosa	**p < 0.05**	p > 0.05	-	-	-
H30	p > 0.05	**p < 0.05**	**p < 0.05**	-	-
Topsun	**p < 0.05**	p > 0.05	p > 0.05	**p < 0.05**	-
Tropical Amazon	**p < 0.05**	p > 0.05	p > 0.05	**p < 0.05**	p > 0.05

Water balance data for individual stems, analysis for each day of vase life.

Table 27. Water balance ~ Cultivar (Day 1) Kruskal-Wallis and Wilcoxon tests

X^2 (5, N = 36) = 18.04, p < 0.01					
	Akito	Fuchsiana	Furiosa	H30	Topsun
Fuchsiana	p > 0.05	-	-	-	-
Furiosa	p > 0.05	p > 0.05	-	-	-
H30	p > 0.05	p > 0.05	p >0.05	-	-
Topsun	p > 0.05	p > 0.05	p > 0.05	p > 0.05	-
Tropical Amazon	**p < 0.05**	**p < 0.05**	**p < 0.05**	**p < 0.05**	**p < 0.05**

Table 28. Water balance ~ Cultivar (Day 2) Kruskal-Wallis and Wilcoxon tests

X^2 (5, N = 36) = 13.91, p < 0.05					
	Akito	Fuchsiana	Furiosa	H30	Topsun
Fuchsiana	**p < 0.05**	-	-	-	-
Furiosa	p > 0.05	**p < 0.05**	-	-	-
H30	p > 0.05	**p < 0.05**	p >0.05	-	-
Topsun	p > 0.05	p > 0.05	p > 0.05	p > 0.05	-
Tropical Amazon	p > 0.05	**p < 0.05**	p > 0.05	p > 0.05	p > 0.05

Table 29. Water balance ~ Cultivar (Day 3) Kruskal-Wallis and Wilcoxon tests

X^2 (5, N = 36) = 16.62, p < 0.01					
	Akito	Fuchsiana	Furiosa	H30	Topsun
Fuchsiana	**p < 0.05**	-	-	-	-
Furiosa	p > 0.05	**p < 0.05**	-	-	-
H30	p > 0.05	**p < 0.05**	p >0.05	-	-
Topsun	p > 0.05	p > 0.05	p > 0.05	p > 0.05	-
Tropical Amazon	**p < 0.05**	**p < 0.05**	p > 0.05	p > 0.05	p > 0.05

Table 30. Water balance ~ Cultivar (Day 4) Kruskal-Wallis and Wilcoxon tests

X^2 (5, N = 36) = 14.40, p < 0.05					
	Akito	Fuchsiana	Furiosa	H30	Topsun
Fuchsiana	p > 0.05	-	-	-	-
Furiosa	p > 0.05	p > 0.05	-	-	-
H30	p > 0.05	p > 0.05	p >0.05	-	-
Topsun	p > 0.05	p > 0.05	p > 0.05	p > 0.05	-
Tropical Amazon	p > 0.05	p > 0.05	p > 0.05	p > 0.05	p > 0.05

Table 31. Water balance ~ Cultivar (Day 5) Kruskal-Wallis and Wilcoxon tests

X^2 (5, N = 36) = 10.92, p > 0.05					
	Akito	Fuchsiana	Furiosa	H30	Topsun
Fuchsiana	p > 0.05	-	-	-	-
Furiosa	p > 0.05	p > 0.05	-	-	-
H30	p > 0.05	p > 0.05	p >0.05	-	-
Topsun	p > 0.05	p > 0.05	p > 0.05	p > 0.05	-
Tropical Amazon	p > 0.05	p > 0.05	p > 0.05	p > 0.05	p > 0.05

Table 32. Vase life (days) ~ Cultivar Kruskal-Wallis and Wilcoxon test (Individual stems)

X^2 (5, N = 36) = 16.87, p < 0.01					
	Akito	Fuchsiana	Furiosa	H30	Topsun
Fuchsiana	p > 0.05	-	-	-	-
Furiosa	p > 0.05	p > 0.05	-	-	-
H30	p > 0.05	**p < 0.05**	**p < 0.05**	-	-
Topsun	p > 0.05	p > 0.05	p > 0.05	p > 0.05	-
Tropical Amazon	p > 0.05	p > 0.05	p > 0.05	p > 0.05	p > 0.05

1.2.1.2 Relative fresh weights of flower stems

Relative fresh weight ~ Cultivar * Stage two-way unbalance ANOVA

Table 33. Results for ‘Stage’ from two-way unbalanced ANOVA with Tukey post-hoc test

$F_{2, 42} = 16.57, p < 0.001$		
	Str	<90
<90	**p < 0.05**	-
>90	**p < 0.05**	**p < 0.05**

Table 34. Results for ‘Cultivar*Stage’ from two-way unbalanced ANOVA with Tukey post-hoc test

$F_{2, 42} = 0.62, p > 0.05$						
			H30		Fuchsiana	
		Str	<90	>90	Str	<90
H30	<90	p > 0.05	-	-	-	-
	>90	**p < 0.05**	**p < 0.05**	-	-	-
Fuchsiana	Str	p > 0.05	**p < 0.05**	**p < 0.05**	-	-
	<90	**p < 0.05**	p > 0.05	**p < 0.05**	**p < 0.05**	-
	>90	**p < 0.05**	p > 0.05	p > 0.05	**p < 0.05**	p > 0.05

1.2.2 Microbial Chapter statistical results

1.2.2.1 Fungal Petrifilm audit of the Kenyan supply chain

Table 35. Mid stem fungal counts ~ Stage of supply chain Kruskal-Wallis and Wilcoxon test

X^2 (2, N = 30) = 14.77, p <0.001		
	Cold store	Harvest
Harvest	p > 0.05	-
Processing	**p < 0.05**	**p < 0.05**

Table 36. Stem end fungal counts ~ Stage of supply chain Kruskal-Wallis and Wilcoxon test

X^2 (2, N = 39) = 22.06, p <0.001		
	Cold store	Harvest
Harvest	**p < 0.05**	-
Processing	**p < 0.05**	**p < 0.05**

Table 37. Fungal counts Mid Stem vs Stem end (Cultivar data combined) paired Wilcoxon tests

	H30 + Fuchsiana counts combined
Harvest	V = 0, **p <0.05**
Cold store	V = 10, **p <0.05**
Processing	V = 0, **p <0.05**

1.2.2.2 Addition of three concentrations of Pseudomonas fluorescens *to the vase water of H30 and Fuchsiana*

Table 38. Summary of coefficients from the necking stage cumulative link model

	Estimate	Z value	P value
Condition: 10^5	2.71	2.70	<0.01
Condition: 10^6	4.33	4.03	<0.001
Condition: 10^7	5.71	4.75	<0.001
Cultivar: Fuchsiana	-4.00	-5.03	<0.001

Table 39. Necking stage cumulative link model Analysis of Deviance (type II) test

	LR Chisq	Df	P value
Condition	40.35	3	<0.001
Cultivar	42.05	1	<0.001

Table 40. Vase water condition ~ necking stage (Fuchsiana stems) Kruskal-Wallis and Wilcoxon test

$F_{3, 38} = 15.72$, $p < 0.05$			
	C	10^5	10^6
10^5	p > 0.05	-	-
10^6	p > 0.05	p > 0.05	-
10^7	**p < 0.05**	**p < 0.05**	**p < 0.05**

Table 41. Vase water condition ~ necking stage (H30 stems) Kruskal-Wallis and Wilcoxon test

$F_{3, 38} = 19.36, p < 0.05$			
	C	10^5	10^6
10^5	p > 0.05	-	-
10^6	**p < 0.05**	p > 0.05	-
10^7	**p < 0.05**	p > 0.05	p > 0.05

1.2.2.3 Addition of bacteria and fungal species to the vase water of H30 and Fuchsiana

Table 42. Summary of coefficients from the necking stage cumulative link model

	Estimate	Z value	P value
Condition: Mould	1.90	2.29	<0.05
Condition: Yeast	2.35	2.85	<0.01
Condition: Bacteria	5.36	5.25	<0.001
Cultivar: H30	2.97	4.67	<0.001

Table 43. Necking stage cumulative link model Analysis of Deviance (type II) test

	LR Chisq	Df	P value
Condition	46.34	3	<0.001
Cultivar	29.87	1	<0.001

Table 44. Vase water condition ~ necking stage (Fuchsiana stems) Kruskal-Wallis and Wilcoxon test

$F_{3, 38} = 27.17, p < 0.05$			
	Control	Bacteria	Yeast
Bacteria	**p < 0.05**	-	-
Yeast	p > 0.05	**p < 0.05**	-
Mould	p > 0.05	**p < 0.05**	p > 0.05

Table 45. Vase water condition ~ necking stage (H30 stems) Kruskal-Wallis and Wilcoxon test

$F_{3, 38} = 32.85, p < 0.05$			
	Control	Bacteria	Yeast
Bacteria	**p < 0.05**	-	-
Yeast	**p < 0.05**	**p < 0.05**	-
Mould	**p < 0.05**	**p < 0.05**	p > 0.05

1.2.3 Quantitative PCR Chapter statistical results

1.2.3.1 Galactose metabolism

Table 46. UGE5 relative expression ~ Necking stage ANOVA and Tukey post hoc test

$F_{2, 9} = 6.10$, $p < 0.05$		
	Str	<90
<90	p > 0.05	-
>90	**p < 0.05**	p > 0.05

Table 47. SIP2 relative expression ~ Necking stage ANOVA and Tukey post hoc test

$F_{2, 9} = 24.7$, $p < 0.001$		
	Str	<90
<90	**p < 0.05**	-
>90	**p < 0.001**	**p < 0.05**

Table 48. DIN10 relative expression ~ Necking stage ANOVA and Tukey post hoc test

$F_{2, 9} = 14.85$, $p < 0.01$		
	Str	<90
<90	p > 0.05	-
>90	**p < 0.01**	**p < 0.05**

Table 49. ATBF1 relative expression ~ Necking stage ANOVA and Tukey post hoc test

$F_{2, 9} = 1.66$, $p > 0.05$		
	Str	<90
<90	p > 0.05	-
>90	p > 0.05	p > 0.05

Table 50. PGM2 relative expression ~ Necking stage ANOVA and Tukey post hoc test

$F_{2, 9} = 1.06$, $p > 0.05$		
	Str	<90
<90	p > 0.05	-
>90	p > 0.05	p > 0.05

Table 51. AGAL3 relative expression ~ Necking stage ANOVA and Tukey post hoc test

$F_{2, 9} = 0.39$, $p > 0.05$		
	Str	<90
<90	p > 0.05	-
>90	p > 0.05	p > 0.05

1.2.3.2 Phenylpropanoid biosynthesis

Table 52. OMT1 relative expression ~ Necking stage ANOVA and Tukey post hoc test

$F_{2, 9} = 3.24$, $p > 0.05$		
	Str	<90
<90	p > 0.05	-
>90	p > 0.05	p > 0.05

Table 53. PRXPX relative expression ~ Necking stage ANOVA and Tukey post hoc test

$F_{2, 9} = 15.36$, $p < 0.01$		
	Str	<90
<90	**p < 0.05**	-
>90	**p < 0.01**	p > 0.05

Table 54. CAD9 relative expression ~ Necking stage ANOVA and Tukey post hoc test

$F_{2, 9} = 7.20, p < 0.05$		
	Str	<90
<90	**p < 0.05**	-
>90	**p < 0.05**	p > 0.05

Table 55. HCT relative expression ~ Necking stage ANOVA and Tukey post hoc test

$F_{2, 9} = 8.70, p < 0.01$		
	Str	<90
<90	**p < 0.05**	-
>90	**p < 0.01**	p > 0.05